Elucidating the role of SOX11 in mantle cell lymphoma

Jara Palomero Gorrindo

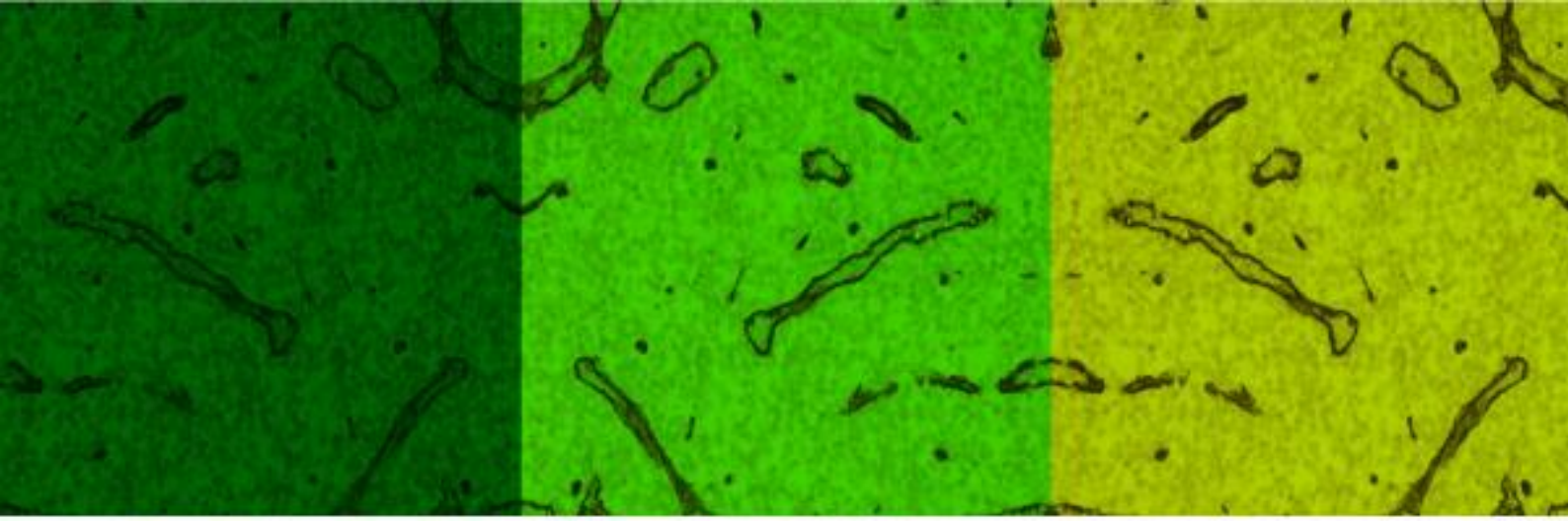

Universitat de Barcelona

Elucidating the role of SOX11 in mantle cell lymphoma

Jara Palomero Gorrindo

2014

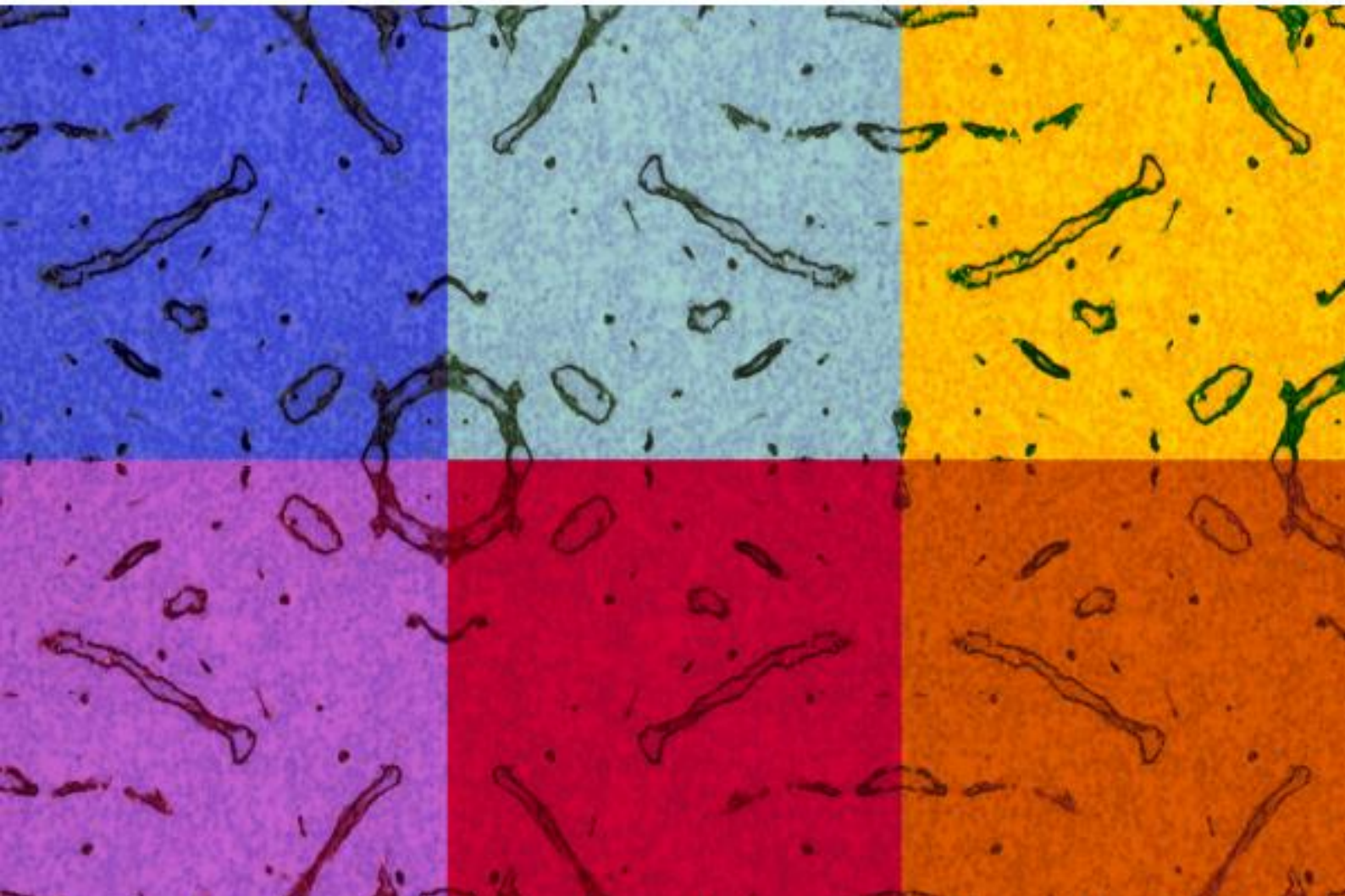

INSTITUT D'INVESTIGACIONS BIOMÈDIQUES AGUSTÍ PI I SUNYER (IDIBAPS)

DEPARTAMENT D'ANATOMIA PATOLÒGICA, FARMACOLOGIA I MICROBIOLOGIA

FACULTAT DE MEDICINA, UNIVERSITAT DE BARCELONA

HOSPITAL CLÍNIC DE BARCELONA

Elucidating the role of SOX11 in mantle cell lymphoma

Thesis presented by **Jara Palomero Gorrindo**

to obtain the degree of Doctor in Medicine

Ph.D. Program in Medicine

FACULTY OF MEDICINE

UNIVERSITY OF BARCELONA

Doctoral advisors:

Dr. **Virginia Amador**

Prof. **Elias Campo**

Barcelona, 2014

Thesis presented by:

Jara Palomero Gorrindo

Doctoral advisors:

Dr. Virginia Amador, Ph.D.

Prof. Elias Campo, M.D., Ph.D.

This work was supported by grants from the *Ministerio de Economía y Competitividad* (MINECO) (BFU2009-09235, BFU2012-30857 and RYC-2006-002110 to V.A., and SAF08/3630 to E.C.), the *Fundació La Marató de TV3* (TV3-Cancer-I3/20130110 to V.A.) and the *Instituto de Salud Carlos III* RTICC (2006RET2039, SAF2012-38432 and PIE13/00033 to E.C.), Fondo Europeo de Desarrollo Regional, Unión Europea, Una manera de hacer Europa.

a la TATI,

la humanista que millor coneix un limfòcit B,

la millor tati del món

als papes

a l'Edu

AGRAÏMENTS

Fa temps algú em va dir que escriure un article científic és com escriure un conte. Fa encara més temps em van ensenyar que la ciència i les lletres no existeixen l'una sense l'altra. I des de fa encara més temps m'ensenyen que hem de conservar el nostre món màgic infantil a mesura que ens anem fent grans. No sé si hauré aconseguit fer un conte d'algun dels meus articles científics o de la meva tesi doctoral; tant de bo.

Fa temps vaig llegir un llibre sobre la importància de que cada un de nosaltres creem el nostre propi món de color a mida que anem trobant els nostres colors. Els colors són aquelles persones que hem tingut la sort de conèixer i les quals han aportat quelcom a la nostra vida, tant siguin aportacions petites, puntuals o fugaces com contínues, dolces i duradores. Aquestes persones seran els nostres grocs, verds, blaus, liles, vermells... en funció del color que triem. Jo prefereixo pensar que aquest món és multicolor enlloc de monocromàtic. Són molts els colors que han anat omplint el meu món des de fa molt de temps, augmentant el seu cromatisme i diversitat. Per tant, només em queda donar-vos les gràcies i esperar poder mantenir aquest món multicolor que hem creat a mida que vaig descobrint nous colors...

Hi havia una vegada una porteta per on s'accedia a una món màgic ple de personetes boniques i colorides. No era una porta fàcil de localitzar i únicament uns quants afortunats eren capaços de trobar-la i endinsar-se en aquest món màgic a través d'ella. Cada una de les personetes irradiava un color diferent, mostrant així les pròpies alegries, desitjos, tristeses.... Tot i que els colors podien anar variant, sempre n'hi havia un de concret que definia millor les diferents personalitats de cada un dels integrants del món màgic.

Algunes de les personetes feia molt de temps que es coneixien i ja havien anat creant els seus móns propis. Un d'aquests móns era porpra ja que s'havia format de la barreja de diferents tonalitats de blaus i vermells, i els seus tres principals colors eren el malva, el taronja i el fúcsia. A mida que el temps anava passant, aquest món porpra havia anat captant nous colors, com ara el turquesa i el llima, que anaven augmentant la seva diversitat i riquesa. Els diferents colors compartirien experiències de tota mena, la majoria de les quals serien grans somriures, descobriments i aventures.

Una d'aquestes grans experiències, i la que comportaria la creació d'un nou món màgic multicolor, va ser possible gràcies a dos colors prioritaris, el cian i el blanc, que em van obrir les portes a una nova i enriquidora etapa. Aquests dos colors em van deixar créixer i anar adquirint diferents tonalitats a mida que m'oferien tots els recursos dels que disposaven. No era un món a començar de nou sinó que ja feia temps que estava sent creat per diferents tonalitats de granats que l'anaven enriquint a mida que s'hi incorporaven. Tot i així, altres colors van començar a formar-hi part, com els grocs, que primer no n'eren gaires, però a mida que passava el temps anaven augmentant les seves tonalitats, i augmentaven el món granat inicial. També els verds, que feia temps que enriquien el món granat inicial des d'una altra perspectiva, van començar a créixer i adquirir noves tonalitats. Més endavant, un món més extern que els altres de color orquídia, també va contribuir a fer més gran aquest món que s'estava construint.

Tots aquests colors i les seves tonalitats anaven adquirint més importància en el meu món ja que sempre estaven disposats a ajudar en el que calgués. Vam compartir moltes anècdotes, diversions, sopars, viatges, però també moments de tristesa i desmotivació. Tot i així, sempre fent pinya, érem capaços d'animar-nos els uns als altres, i trobar solucions a les preocupacions. El corall, jade, cirera, blau de cobalt, plata, taronja, or i fúcsia són colors sense els quals aquest món, així com la seva creació, haguessin estat completament diferents.

A més a més d'aquest món que se'm va obrir a través del cian i el blanc, sempre he estat acompanyada per altres colors que ja fa molt de temps anaven conformant el meu món multicolor. El grup de diferents tonalitats de rosa, el trio format d'atzur, canyella i verd oliva, el duet format per aiguamarina i carmí, i els súper compis morat i ambre. També el turquesa i el llima. Amb tots vosaltres ja fa temps que tinc la sort de compartir el meu món amb el vostre. Uns móns que no deixaran de créixer perquè ja tenim per aquí al primer mini carmí, mini rosa i un futur mini atzur. I finalment el verd, que va aparèixer en el mateix moment en què el cian i el blanc m'obrien les portetes del món que aniríem construint en els següents anys. Perquè sempre has estat donant diferents tonalitats i enfortint la construcció del meu món multicolor.

A tots i cada un de vosaltres, moltes gràcies per tot el que heu aportat al meu món; ha estat una etapa màgica. Ara toca començar-ne una de nova!

If you only read the books that everyone else is reading,
you can only think what everyone else is thinking

HARUKI MURAKAMI

ABSTRACT

Mantle cell lymphoma (MCL) is an aggressive lymphoid neoplasm derived from mature B cells genetically characterized by the presence of the t(11;14)(q13;q32) translocation causing cyclin D1 overexpression and therefore cell cycle deregulation. However, other additional secondary genetic alterations also contribute to MCL pathogenesis. Recent studies identified a distinct subgroup of tumors with an indolent clinical behavior even without chemotherapy that tend to present with non-nodal, leukemic disease instead of extensive nodal infiltration. Moreover, recent molecular studies have identified SRY (Sex determining region-Y)-like HMG box-11 (*SOX11)* as one of the best characterized discriminatory genes between these two clinical subtypes of MCL, being almost exclusively overexpressed in the aggressive presentation of the disease.

SOX11 is a high mobility group (HMG) transcription factor (TF) characterized by its critical involvement in embryonic development and neuronal cell differentiation. Although not apparently expressed in any normal cell subtype of the lymphoid system, it has been recently identified as playing a major role in several solid tumors and some subtypes of aggressive lymphomas. However, SOX11 oncogenic mechanisms contributing to the development and progression of these diseases are largely unknown. Although SOX11 function and potential target genes in lymphoid cells are poorly known, its high specific expression in aggressive MCL suggests that it may be an important element in the development and progression of this disease.

Two publications resulted from our studies and compose this thesis.

In paper I, we initiated the molecular characterization and elucidation of the SOX11-regulated transcriptional program in MCL. We performed an integrative analysis coupling data from human genome-wide promoter analysis by *SOX11* Chromatin Immunoprecipitation (ChIP)-chip experiments and gene expression profiling (GEP) upon SOX11 silencing in MCL cell lines, and identified target genes and transcriptional programs regulated by SOX11 including the block of mature B cell differentiation, modulation of cell cycle, apoptosis, and stem cell development. Paired box protein 5 (*PAX5*) stood out as one of SOX11 major direct target genes. We found that SOX11 silencing downregulated PAX5, induced B lymphocyte induced maturation protein 1 (BLIMP1) expression, and promoted the shift from a mature B cell into the initial

plasmacytic differentiation phenotype in both MCL primary tumor cells and an *in vitro* model. We also demonstrated the oncogenic implication of SOX11 expression in the aggressive behavior of MCL as SOX11-knockdown derived tumors displayed a significant reduction on tumor growth compared to SOX11-positive tumors in subcutaneous MCL xenografts. Although our results suggested that SOX11 contributed to tumor development by altering the terminal B cell differentiation program of MCL cells, the specific SOX11-regulated mechanisms promoting the oncogenic and rapid tumor growth of aggressive MCL still remained to be elucidated.

Therefore, in paper II, we further characterized the potential SOX11-regulated oncogenic mechanisms by integrating our ChIP-chip data with further analyses including GEP derived from the xenograft SOX11-positive and silenced tumors. Gene ontology analysis of SOX11 target genes and gene set enrichment analyses (GSEA) of the differentially expressed genes in xenografts, human primary tumors and MCL cell lines revealed that blood vessel development and angiogenic gene signatures were significantly enriched in SOX11-positive cells. Consequently, we performed *in vitro* angiogenic assays and observed that conditioned media derived from SOX11-positive cells induced higher tube formation, proliferation and migration of endothelial cells, corroborated by a prominent higher density of microvessels in human primary tumors and mouse xenografts. Strikingly, gene and protein expression profiling revealed that SOX11-modulation of angiogenesis in MCL was mediated by the upregulation of the pro-angiogencic factor Platelet-derived growth factor-A (PDGFA). Inhibition of the PDGFA pathway impaired angiogenesis development both *in vitro* and *in vivo*, and also MCL tumor growth *in vivo*, representing a promising novel therapeutic strategy for the treatment of aggressive MCL.

Overall, we have unraveled and characterized, for the first time, the oncogenic role of SOX11 and the tumorigenic pathways it orchestrates in MCL. Importantly, the elucidation of molecular oncogenic mechanisms that are deregulated by SOX11 in MCL will aid the management and stratification of MCL patients and lead to the development of new therapeutic strategies for this aggressive disease.

RESUM

Les neoplàsies limfoides són un grup heterogeni de tumors caracteritzats per un event genètic inicial i l'acumulació d'alteracions moleculars secundàries que condicionen la progressió tumoral. Els mecanismes genètics que condueixen a alteracions genètiques primàries són principalment les translocacions cromosòmiques que, generalment, resulten en l'activació d'un proto-oncogen que comporta l'alteració de la proliferació, l'apoptosi o la via de diferenciació de les cèl·lules B.

El limfoma de cèl·lules del mantell (LCM) és una neoplàsia limfoide caracteritzada per una proliferació alta de limfòcits B madurs, i és considerada un dels limfomes no Hodgkin (LNH) més agressius amb una supervivència mitjana de 3-4 anys. L'evolució clínica acostuma a ser molt agressiva amb poca resposta al tractament i freqüent recidiva; són pocs els pacients que es curen amb les teràpies actuals. Tot i així, observacions clíniques recents han identificat alguns LCM amb un curs clínic indolent de la malaltia i una llarga supervivència dels pacients, inclòs sense la necessitat de tractament. Estudis d'expressió gènica diferencial han identificat que *SOX11*, un factor de transcripció neuronal, és un dels gens més ben caracteritzats per diferenciar els subtipus de LCM agressius i indolents ja que se sobre-expressa en els LCM agressius però no en els indolents.

SOX11 pertany a la família dels gens *SOX* que codifiquen per possibles reguladors transcripcionals que desenvolupen funcions importants en diferents processos del desenvolupament. La funció de SOX11 i molts altres membres de la superfamília de proteïnes SOX actualment no es coneix, tot i que es creu que la funció de les proteïnes SOX és, almenys, en part estructural permetent que altres factors de transcripció s'uneixin al solc format a l'ADN i/o reunint elements reguladors, el que facilita la formació de complexes proteics.

SOX11 se sobre-expressa constantment en gairebé tots els tumors de LCM agressius, a nivells inferiors en un subgrup de limfomes de Burkitt i limfoblàstics, però no en altres neoplàsies limfoides, en cèl·lules limfoides normals ni en pacients de LCM que segueixen una llarga evolució clínica indolent. Per tant, SOX11 ha estat identificat com a biomarcador en els tumors de LCM i possible factor pronòstic.

Tot i que la funció de SOX11 i els seus possibles gens diana en cèl·lules limfoides es desconeixen, la seva alta expressió en els LCM agressius suggereix que SOX11 pot ser un element important en el desenvolupament i progressió d'aquest tumor. Per tant, els objectius d'aquest projecte de tesi doctoral són identificar, caracteritzar i validar les possibles vies oncogèniques regulades per SOX11 per obtenir un millor i major coneixement de la patogènesi del LCM, i trobar possibles candidats per a teràpies específiques per aquest tumor.

Per realitzar aquests objectius hem estudiat els gens directament regulats per SOX11 mitjançant immunoprecipitació de cromatina,així com el fenotip associat a la pèrdua de l'expressió de SOX11 en línies cel·lulars de LCM establement transduïdes (model *in vitro*). A més a més, també hem estudiat l'habilitat tumorigènica de SOX11 mitjançant el xenotransplantament subcutani de les línies cel·lulars generades *in vitro* en ratolins immunodeficients (SCID) (model *in vivo*). Un cop hem identificat els possibles gens diana i les vies oncogèniques regulades per SOX11 mitjançant els models *in vitro* i *in vivo*, els hem validat en tumors humans primaris del LCM.

S'han obtingut dos treballs d'investigació dels estudis que composen aquesta tesi doctoral, publicats a la prestigiosa revista d'hematologia Blood els anys 2013 i 2014. En ambdós treballs hem estudiat els mecanismes moleculars regulats per SOX11 responsables de la patogènesi i el desenvolupament maligne del LCM. El primer treball es centra en la caracterització del bloqueig del desenvolupament dels limfòcits B madurs degut a la sobre-expressió de SOX11 en el LCM, suggerint un diferent desenvolupament en la formació dels subtipus de LCM agressius i indolents. A més, també demostrem que SOX11 és indispensable pel creixement del LCM ja que tumors SOX11-negatius inoculats en ratolins SCID presenten un creixement menor comparat amb els tumors SOX11-positius. En el segon treball hem identificat, per primera vegada, la funció oncogènica de SOX11 en el LCM ja que regula processos angiogènics responsables del major creixement de les cèl·lules SOX11-positives. D'altra banda també mostrem noves aproximacions terapèutiques per aquest tipus de tumor que ajudarien a una millor estratificació i classificació dels pacients de LCM.

Al primer article ens hem centrat en identificar les possibles funcions biològiques de SOX11 en el LCM. Combinant anàlisis de microarray d'immunoprecipitació de cromatina i perfil d'expressió diferencial després de silenciar l'expressió de SOX11,

hem identificat gens diana i programes transcripcionals regulats per SOX11, incloent el bloqueig de la diferenciació de la cèl·lula B madura, la modulació del cicle cel·lular, l'apoptosi i el desenvolupament de cèl·lules mare. *PAX5* apareix com un dels gens diana directes més significatius de SOX11. El silenciament de SOX11 disminueix l'expressió de PAX5, indueix la de BLIMP1 i promou el canvi de fenotip de cèl·lula B madura a la diferenciació plasmacítica inicial, tant en cèl·lules tumorals primàries del LCM com en un model *in vitro*. Els nostres resultats suggereixen que SOX11 contribueix al desenvolupament tumoral mitjançant la modulació del programa de la diferenciació terminal de la cèl·lula B en el LCM. A més, hem demostrat l'habilitat tumorigènica de SOX11 *in vivo* mitjançant un model de xenotransplantament de LCM en ratolins SCID. La reducció significativa del creixement tumoral de les cèl·lules amb expressió de SOX11 silenciada comparada amb el creixement de les cèl·lules de LCM amb alts nivells d'expressió de SOX11 dels xenotransplantaments, demostra la implicació de l'expressió de SOX11 en el comportament agressiu d'aquest limfoma.

SOX11 se sobre-expressa en diferents tumors sòlids i en la majoria de LCM agressius. En el primer article constituent d'aquesta tesi doctoral hem demostrat que el silenciament de l'expressió de SOX11 redueix el creixement tumoral en un model de xenotransplantament, consistent amb el curs clínic indolent dels pacients del LCM SOX11-negatius. Tot i així, els mecanismes oncogènics directament regulats per SOX11 encara no s'han descrit. Per tant, en el segon treball ens hem centrat en la identificació i caracterització molecular de dits mecanismes. Hem observat que els tumors dels xenotransplantaments murins així com de pacients de LCM SOX11-positius estan enriquits en vies gèniques relacionades amb l'angiogènesi, i presenten una major densitat de microvasos comparada amb els tumors derivats dels xenotransplantaments i els tumors humans primaris SOX11-negatius. A més, el medi cel·lular condicionat derivat de cèl·lules SOX11-positives indueix una major proliferació, migració, formació de tubs, i activació de vies de senyalització angiogèniques en cèl·lules endotelials *in vitro*. Hem identificat el factor pro-angiogènic *PDGFA* com un gen diana directe de SOX11 en cèl·lules de LCM, la inhibició del qual elimina els efectes angiogènics accentuats en cèl·lules endotelials *in vitro*. Per altra banda, PDGFA està sobre-expressat en cèl·lules SOX11-positives tant en cultius cel·lulars de LCM, xenotransplantaments com en pacients de LCM. *In vivo*, el tractament dels xenotransplantaments SOX11-positius amb el fàrmac imatinib, un inhibidor del receptor de PDGFA, disminueix la

neo-vascularització i el creixement tumoral de dites cèl·lules, equilibrant-lo al creixement tumoral de les cèl·lules SOX11-negatives. El nostre estudi identifica, per primera vegada, que SOX11 regula senyals de supervivència angiogèniques en el LCM, demostrant la seva implicació oncogènica en el comportament i progressió agressius d'aquest tumor maligne. A més a més, recalca la via SOX11-PDGFA com una possible diana terapèutica pel subtipus agressiu del LCM, una malaltia en la que encara actualment hi ha poques opcions terapèutiques duradores i complertes.

En general, les conclusions d'aquest treball de tesi doctoral han estat les següents:

1. Identificació dels gens diana i les vies transcripcionals regulades per SOX11 en el LCM mitjançant experiments *in vitro* i *in vivo*.

2. Caracterització del bloqueig de la diferenciació dels limfòcits B madurs com a mecanisme del desenvolupament dels diferents subtipus de LCM agressius i indolents. Dit bloqueig està mediat per la sobre-expressió de PAX5 mitjançant SOX11.

3. Demostració de la implicació oncogènica de SOX11 en la patogènesi del LCM.

4. Caracterització de la regulació de processos angiogènics per part de SOX11 com a mecanisme oncogènic responsable del creixement tumoral del LCM agressiu. Dita regulació està mediada per la sobre-expressió de PDGFA mitjançant SOX11.

5. Identificació de possibles noves dianes terapèutiques en el LCM.

List of Papers

This thesis has been generated by the following papers, which are referred to in the text by the Roman numerals I and II:

I. Vegliante MC*, **Palomero J***, Pérez-Galán P, Roué G, Castellano G, Navarro A, Clot G, Moros A, Suárez-Cisneros H, Beà S, Hernández L, Enjuanes A, Jares P, Villamor N, Colomer D, Martín-Subero JI, Campo E, Amador V. SOX11 regulates PAX5 expression and blocks terminal B-cell differentiation in aggressive mantle cell lymphoma. *Blood. 2013 Mar 21;121(12):2175-85.*

* These authors contributed equally to this work.

II. **Palomero J**, Vegliante MC, Rodríguez ML, Eguileor A, Castellano G, Planas-Rigol E, Jares P, Ribera-Cortada I, Cid MC, Campo E, Amador V. SOX11 promotes tumor angiogenesis through transcriptional regulation of PDGFA in mantle cell lymphoma. *Blood. 2014 Oct 2;124(14):2235-47.*

Reprints were made with permission of the respective publishers.

Other published papers by the author associated with this thesis.

1. Vegliante MC, Royo C, **Palomero J**, Salaverria I, Balint B, Martín-Guerrero I, Agirre X, Lujambio A, Richter J, Xargay-Torrent S, Bea S, Hernandez L, Enjuanes A, Calasanz MJ, Rosenwald A, Ott G, Roman-Gomez J, Prosper F, Esteller M, Jares P, Siebert R, Campo E, Martín-Subero JI*, Amador V*. Epigenetic activation of SOX11 in lymphoid neoplasms by histone modifications. *PLoS One. 2011;6(6):e21382.*

2. Navarro A, Clot G, Royo C, Jares P, Hadzidimitriou A, Agathangelidis A, Bikos V, Darzentas N, Papadaki T, Salaverria I, Pinyol M, Puig X, **Palomero J**, Vegliante MC, Amador V, Martinez-Trillos A, Stefancikova L, Wiestner A, Wilson W, Pott C, Calasanz MJ, Trim N, Erber W, Sander B, Ott G, Rosenwald A, Colomer D, Giné E, Siebert R, Lopez-Guillermo A, Stamatopoulos K, Beà S, Campo E. Molecular subsets of mantle cell lymphoma defined by the IGHV mutational status and SOX11 expression have distinct biologic and clinical features. *Cancer Res. 2012 Oct 15;72(20):5307-16.*

TABLE OF CONTENTS

LIST OF SELECTED ABBREVIATIONS

Ab	Antibody
Ag	Antigen
AID	Activation-induced (DNA-cytosine) deaminase
ALL	Acute lymphoblastic leukemia
ANGPT	Angiopoietin
ATM	Ataxia-telangectasia mutated
BAFF	B cell activating factor
BCL	B cell lymphoma
BCR	B cell receptor
BL	Burkitt's lymphoma
BLIMP1	B lymphocyte induced maturation protein 1
BM	Bone marrow
C	Constant
CCND1	Cyclin D1
CDK	Cyclin-dependent kinase
ChIP	Chromatin Immunoprecipitation
CLL	Chronic lymphocytic leukemia
CLP	Common lymphoid progenitor
CM	Conditioned media
CSR	Class-switch recombination
CXCR	C-X-C chemokine receptor type
D	Diversity
DC	Dendritic cell
DLBCL	Diffuse large B cell lymphoma
E2A	E-box binding protein 2A
EBF1	Early B cell factor 1
EC	Endothelial cell
ECM	Extracellular matrix
ELP	Early lymphoid progenitor
FDC	Follicular dendritic cell
FGF	Fibroblast growth factor
FL	Follicular lymphoma
GC	Germinal center
GEP	Gene expression profiling
GSEA	Gene set enrichment analysis

H	Heavy
HCL	Hairy cell leukemia
HDGFRP	Hepatoma-derived growth factor related protein
HIF-1α	Hypoxia-inducible factor 1-alpha
HMG	High mobility group
HSC	Hematopoietic stem cell
HUVEC	Human umbilical vein endothelial cell
Ig	Immunoglobulin
IGL	Ig lambda
IGK	Ig kappa
IHC	Immunohistochemistry
IL	Interleukin
IRF	Interferon regulatory factor
J	Joining
L	Light
LAM	Lymphoma-associated macrophage
LBL	Lymphoblastic lymphoma
LMPP	Lymphoid-primed MPP
MALT	Mucosa-associated lymphoid tissue
MCL	Mantle cell lymphoma
MHC	Major histocompatibility complex
miR	microRNA
MM	Multiple myeloma
MMP	Matrix metalloproteinase
MPP	Multipotent progenitor
MSC	Mesenchymal stromal cell
MVD	Microvessel density
MZ	Marginal zone
MZL	Marginal zone lymphoma
NGS	Next generation sequencing
NHL	Non-Hodgkin’s lymphoma
NK	Natural killer
OS	Overall survival
PAX5	Paired box protein 5
PC	Plasma cell
PDGF	Platelet-derived growth factor
PI-3-K	Phosphoinositol-3-kinase

PlGF	Placental growth factor
pre	precursor
pro	progenitor
PTCL	Peripheral T-cell lymphoma
PU.1	Purine box factor 1
RAG	Recombination-activating gene
RB1	Retinoblastoma 1
SDF1	Stromal-cell-derived factor 1
SHM	Somatic hypermutation
SLC	Surrogate L chain
SLL	Small lymphocytic lymphoma
SMZL	Small marginal zone lymphoma
SOX	SRY (Sex determining region-Y)-like HMG box
TAD	Transactivation domain
TAM	Tumor-associated macrophage
TF	Transcription factor
TFH	T follicular helper
TGFβ	Transforming growth factor β
TLR	Toll-like receptor
TME	Tumor microenvironment
TNF	Tumor necrosis factor
T-PLL	T cell-prolymphocytic leukemia
V	Variable
VCAM1	Vascular cell adhesion molecule 1
VEGF	Vascular endotelial growth factor
vSMC	Vascular smooth muscle cell
XBP1	X-box binding protein 1

INTRODUCTION

1. B cell biology

The lymphoid system is composed of central (or primary) and peripheral (or secondary) lymphoid organs. The thymus and bone marrow (BM) comprise the primary lymphoid organs and are involved in the production and early selection of lymphocytes. Both B and T lymphocytes (or B and T cells) primarily arise in the BM, but their differentiation takes place differently. Immature B cells differentiate into mature B cells in the BM, whereas premature T cells differentiate into mature T cells in the thymus. After this initial differentiation step, mature B and T lymphocytes migrate from the BM and thymus, respectively, into the blood, and then into the peripheral lymphoid tissue. Peripheral lymphoid organs include lymph nodes and the lymphoid follicles in tonsils, Peyer's patches, spleen, adenoids and skin, among others, which are associated with the mucosa-associated lymphoid tissue (MALT). They maintain mature naïve lymphocytes and initiate an adaptive immune response as they are the sites of lymphocyte activation by antigen (Ag) (Coupland, 2011).

B cells belong to the adaptive branch of the immune system and are essential for the humoral immune response as they produce Ag-specific antibodies (Abs). Ab-complexes are recognized by other immune cell populations, which subsequently trigger an inflammatory response. The B lymphocyte population functions to provide long lasting immunity to a wide range of pathogens but B cells also act as Ag-presenting cells (APCs) (De and Barnes, 2014).

B lymphocytes represent a population of cells that express clonally diverse cell surface immunoglobulin (Ig) receptors recognizing specific antigenic epitopes. They develop in the BM from a common lymphoid progenitor (CLP) in distinct steps via progenitor (pro) and precursor (pre) B cells to immature B cells. Whereas this first differentiation phase is Ag-independent, the subsequent differentiation phase is completely Ag-dependent as B cells start to proliferate and differentiate into mature B cells, memory B cells or Ab-secreting plasma cells (PCs) upon Ag encounter and recognition by their specific receptor (LeBien and Tedder, 2008; Nescakova and Bystricky, 2011).

During their differentiation process, B cells are subjected to a selection process to avoid the development of auto or polyreactive mature B cells that may be harmful. The main selection occurs by elimination of developing B cells with high affinity for self-Ags, through mechanisms of clonal deletion, receptor editing, or induction of anergy. This

process results in a pool of B cells with limited auto or polyreactivity. Upon antigenic stimulation, Ag-specific B cells undergo affinity maturation, somatic hypermutation (SHM), class-switch recombination (CSR), and differentiation into memory B cells or Ab-secreting PCs (Giltiay et al., 2012; Nescakova and Bystricky, 2011).

In contrast to these classical B cells (B2 cells), a subset of B cells termed B1 cells is characterized by a higher degree of auto or polyreactivity and almost complete absence of memory formation. These cells produce Abs with low affinity for different Ags, and although CSR occurs in these cells, SHM is absent.

1.1. Early B cell development

The pluripotent hematopoietic stem cell (HSC) gives rise to all mature cell types in the blood (lymphoid, myeloid, and erythroid) by differentiating through intermediate stage progenitor cells. B cells, like all hematopoietic cells, are produced in a stepwise process from self-renewing HSCs in the fetal liver and postnatal BM. The earliest differentiated progeny of HSCs are multipotent progenitors (MPPs), which have lost the capacity for extensive self-renewal but retain multilineage differentiation potential. A subset of MPPs has little erythro-megakaryocytic potential but retain lymphoid and other myeloid potential leading to their designation as lymphoid-primed MPPs (LMPPs) (Adolfsson et al., 2005). The LMPP population contains early lymphoid progenitors (ELPs), which are lymphoid restricted cells and represent the precursors of BM CLPs, which give rise to B lymphocytes, natural killer (NK) cells, dendritic cells (DCs), and T lymphocytes (Balciunaite et al., 2005; Rumfelt et al., 2006) (Figure 1).

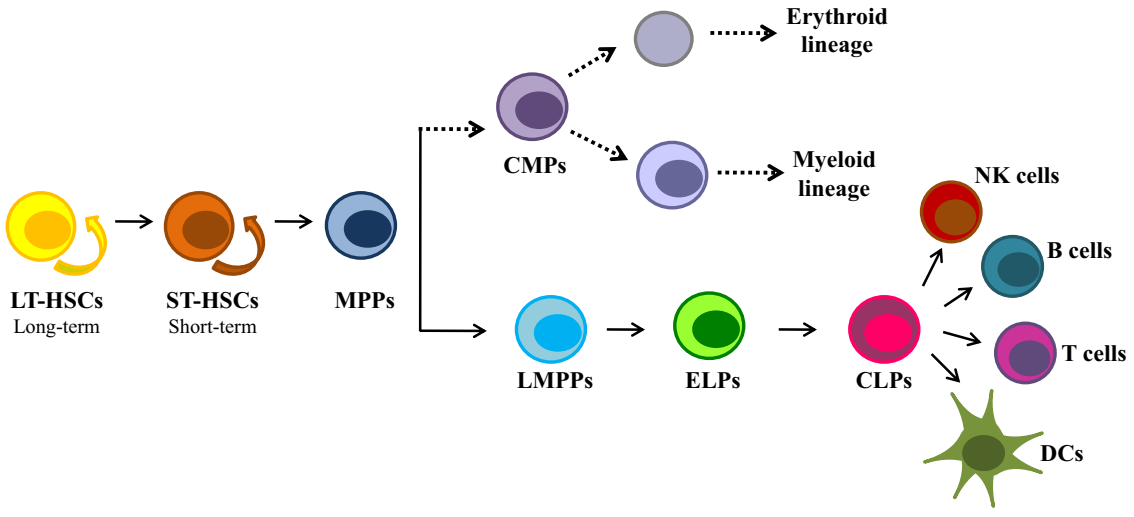

Figure 1. Model of lineage determination *in the adult human hematopoietic hierarchies.*

The first clearly identifiable B cell-specified progenitors arise from CLPs in the BM and are variously termed pre-pro B cells, which can be identified by expression of the B cell-associated marker B220 and activation of many B cell-lineage-associated genes (Gounari et al., 2002; Rumfelt et al., 2006). Generally, B cell differentiation comprises of six stages: early lymphoid stem stage, early pro-B cell, late pro-B cell, pre-B cell, immature B cell and mature B cell stage. B cell maturation starts when the lymphoid stem cell differentiates to the first B cell stage, **pro-B** cells, which proliferate and differentiate to **pre-B cells** (Figure 2) (Nescakova and Bystricky, 2011). Early B cell development is characterized by the ordered rearrangement of the *Ig* heavy (*H*) and light (*L*) chain loci, and Ig proteins themselves play an active role in regulating B cell development.

The most characteristic feature of B cell maturation is *Ig* gene segment rearrangement and expression of cell surface proteins. The functional rearrangement of the *Ig* loci occurs via an error-prone process involving the combinatorial rearrangement of the variable (*V*), diversity (*D*), and joining (*J*) gene segments in the *H* chain locus and the *V* and *J* gene segments in the *L* chain loci (LeBien, 2000; LeBien and Tedder, 2008). In mice and humans, this occurs primarily in fetal liver and adult BM, culminating in the development of a diverse repertoire of functional *VDJH* and *VJL* rearrangements encoding the B cell receptor (BCR) (LeBien and Tedder, 2008). **Pro-B** cells do not express any receptor or Ig on their surface but first carry out *DH–JH* rearrangements. In the next stage (**pre B-I**), a *VH* segment is rearranged to the *DH-JH* element. The physiological *Ig* kappa (*IGK*) and lambda (*IGL*) chain gene rearrangements start later in **pre B-II** cells (Figure 2).

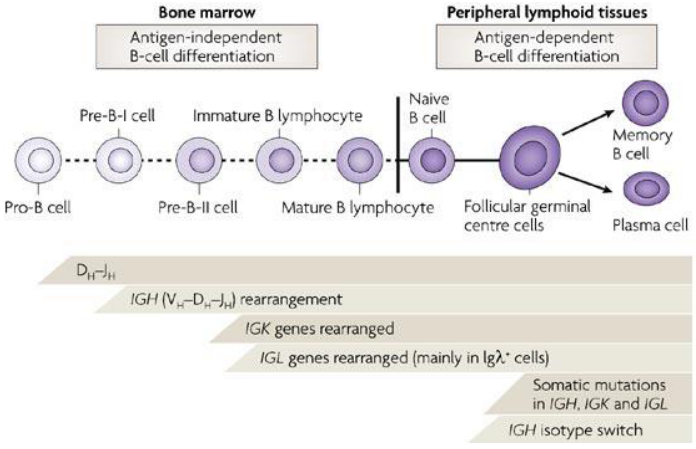

Figure 2. Different steps in the B cell differentiation process *from a pro-B cell to memory B cells or PCs. Ig gene rearrangements are also specified (Jares et al., 2007).*

Pre-B cells are the first cells to express the pre-BCR which is made up of the μ H chain, a surrogate L chain (SLC) and an Igα/Igβ signaling heterodimer. Successful expression of the pre-BCR marks the transition of the pro-B to the pre-B cell. The SLC is a heterodimer consisting of two distinct proteins, λ5 and VpreB, that pair with the H chain to constitute part of the signaling complex in murine and human pre-B cells (Figure 3). Expression of the pre-BCR by association of the newly formed IgH chains with SLC induces increased cell proliferation, resulting in clonal expansion of pre-B cells. Signaling through the pre-BCR stimulates *L* chain rearrangement, and initiates pro-survival signaling pathways (De and Barnes, 2014). Subsequently, BCR expression is a requisite for B cell development and survival in the periphery.

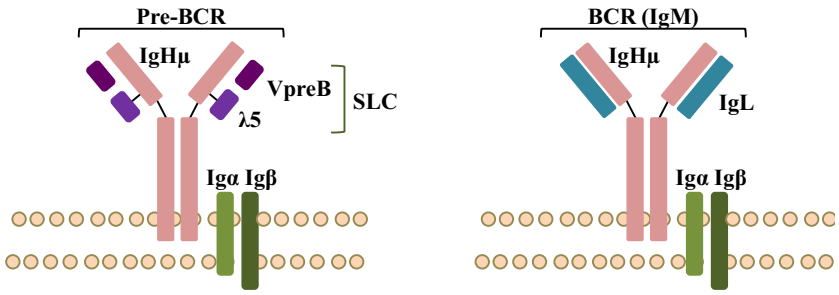

Figure 3. Composition of the pre-BCR and BCR complexes. *The pre-BCR and BCR contain a transmembrane form of the IgH that is non-covalently associated with an Igα/Igβ heterodimer and the SLC or the IgL, respectively.*

1.2. B cell activation

Newly formed B cells emigrate from the BM and home initially to the spleen where they mature via transitional stages primarily into long-lived follicular B cells, and where they also differentiate into marginal zone (MZ) B cells. Naïve follicular B cells express high levels of surface IgD and CD23 and have the ability to re-circulate, entering and exiting follicular niches in secondary lymphoid organs in search of Ag. The newly formed IgM^{low} cells that have recently left the BM and entered the circulation or spleen are also referred to as transitional B cells, which are capable of responding to Ag, and can mature into Ab-secreting PCs and undergo CSR (Giltiay et al., 2012).

1.2.1. T cell dependent or independent response

After the interaction of naïve B lymphocytes with an Ag, B cells can mature further via two pathways, the T cell dependent or independent pathways. Ag is recognized by B

cells through the BCR, which leads to structural cross-linking of the receptor. This in turn leads to activation of signaling cascades through the BCR-associated signaling molecules Igα and Igβ. BCR conjugated to Ag can be internalized and processed in endosomes, where the degraded antigenic peptides are loaded into major histocompatibility complex (MHC) class II molecules and presented on the cell surface to T cells (Harwood and Batista, 2010).

If T cell recognition of Ag occurs, a specialized T cell-dependent activation pathway leads to B cell activation. Interactions between activated B cells and helper T cells occur in lymph nodes where recognition of Ag by both cell types leads to the formation of a germinal center (GC), giving rise to either memory B cells or long-lived PCs upon successful CSR and SHM. Memory B cells are long-lived B cells which are capable of quickly proliferating and differentiating to PCs upon encounter with cognate Ag. PCs, in contrast, are responsible for secreting large amounts of Abs, and will remain in the BM and secondary lymph nodes (Yoshida et al., 2010).

An alternative pathway for B cell activation is the T cell-independent pathway. B cells which have bound Ag through the BCR can receive additional activation signals through specialized pattern recognition proteins. These pattern recognition molecules include the Toll-like receptor (TLR) family of proteins, which are capable of recognizing viral and bacterial DNA and lipids. The T cell-independent pathway leads to rapid B cell proliferation and maturation, however, the formation of a GC does not occur. Therefore, both CSR and SHM do not occur at the same levels as in the T cell-dependent pathway (Cerutti et al., 2013). Contrary to migrating into follicles to form GCs, these activated B cells migrate to extra-follicular areas where they differentiate into short-lived PCs (O'Connor et al., 2003). The predominant secreted Ab is IgM, and few memory and plasma B cells are generated from this pathway.

1.2.2. The germinal center reaction

Ag-induced B cell activation and differentiation in secondary lymphoid tissues are mediated by dynamic changes in gene expression, giving rise to the GC reaction. GCs are sites within secondary lymphoid organs where robust proliferation and differentiation of B lymphocytes occur. They are specialized microenvironments where follicular dendritic cells (FDCs), CD4 T follicular helper (TFH) cells, and B cells

interact in a coordinated fashion to exchange cognate Ag and co-stimulatory signals (Linterman et al., 2009; Nurieva et al., 2008).

The GC reaction is characterized by B cell clonal expansion, SHM of *VH* genes, CSR at the *IgH* locus and selection for increased affinity of a BCR for its unique antigenic epitope through affinity maturation (LeBien and Tedder, 2008). CSR and SHM are mediated by activation-induced (DNA-cytosine) deaminase (AID), an enzyme which is capable of introducing cytosine to uracil mutations and whose expression is induced in GCs. In conjunction with DNA damage repair machinery, these mutations are necessary for both CSR and SHM.

The process of **SHM** in the *VH* region of the *Ig* genes is characterized by the introduction of point mutations, deletions or duplications in the DNA sequence. The SHM reaction results in increased affinity to Ag through the introduced mutations in the *V* region of the BCR (Yoshida et al., 2010), changing the H chain constant (*C*) region of its Ab while keeping the same H chain *V* region and L chain intact. In this way, the specificity of Ab is identical, but the effector function is different.

The *Ig* gene **CSR** from the *C* region of IgM and IgD to IgG, IgA or IgE occurs later as a mechanism to obtain an Ab with different effector functions but the same Ag-binding domain. The CSR reaction is regulated by B and T lymphocytes contacts, type of differentiation, cytokines and site microenvironment. CSR leads to switching of the $C\mu$ to $C\gamma$, $C\alpha$, or $C\varepsilon$ exons, thereby generating IgG, IgA or IgE BCRs, respectively (Shlomchik and Weisel, 2012).

B cell selection in GCs is normally mediated by Ag acquisition from FDCs followed by Ag presentation to CD4 TFH cells. This allows that GC-B cells with high-affinity BCRs receive help and survive since they outcompete lower Ag-affinity B cells. Lack of sufficient survival signals both from FDCs and CD4 TFH cells can result in apoptosis, thereby deleting cells that have too low affinity for Ag to be competitive, or for which there is no cognate CD4 TFH cell help (Giltiay et al., 2012).

Affinity maturation reflects the process of SHM of *Ig* genes and the subsequent selection of resulting high-affinity B cells that occur in the GC. The *V*, *D* and *J* genes for Ig chains rearrange and consequently, the main mutation occurs in the hypervariable regions. The point mutations, deletions, and insertions continue with much higher

mutation speed than in regular cells. However, this random process generates not only high affinity cells and thus, all cells undergo positive high-affinity cloned selection in the light zone of the GC.

Overall, the GC reaction orchestrates in the following way. Centroblasts, which are highly proliferating B lymphocytes that lack surface Ig, migrate to the dark zone of the GC, where activated B cells undergo rapid proliferation and SHM. Large centroblasts exit the cell cycle, re-express Ig surface and change to small centrocytes that do not proliferate and migrate to the light zone of the GC. The rearrangement of *VDJ*-gene segment occurs in the process of the Ab-CSR during the centroblast/centrocyte differentiation stage (Figure 4).

In the light zone of the GC, which is rich of FDCs and Ag-specific CD4 THF cells, low-affinity centrocytes that do not recognize the specific Ag die by apoptosis. However, surviving centrocytes expressing high-affinity receptors for Ag present on FDCs enter the apical light zone, where they are selected and become memory B cells or long-lived IgG-producing PCs. During this selection process AID is expressed, both CSR and SHM are activated and B cells with increased affinity for foreign Ags are generated (Tangye and Tarlinton, 2009; Victora and Nussenzweig, 2012) (Figure 4).

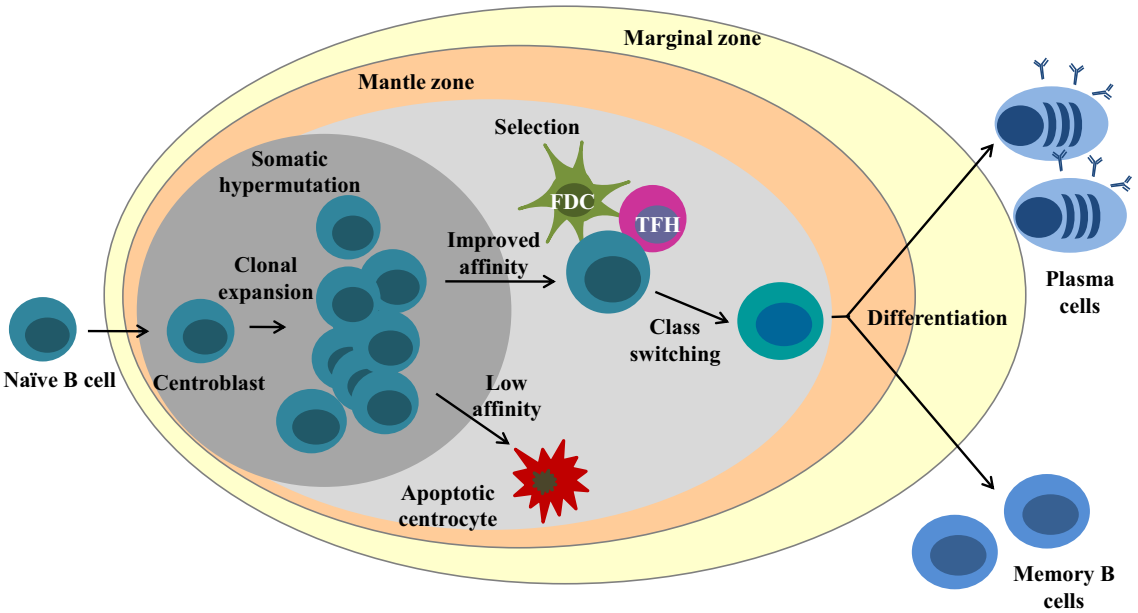

Figure 4. The B cell differentiation process. *The generation of memory B cells and long-lived PCs from a naïve B lymphocyte via the GC reaction. Dark and light grey represent the dark and light zone of the GC, respectively.*

2. Transcription factors in B cell development

The generation of B lymphocytes from hematopoietic progenitors requires lineage-specific TFs which progressively direct cell fate choices. These TFs regulate different B cell subpopulation transitions as well as subsequent effector functions, and their deregulation can lead to altered B cell biology.

The earliest stage of B cell development is the differentiation of the HSC into the ELP that can give rise to both thymic precursors of the T cell lineage, early T lineage progenitors (ETPs), or the BM CLP, from which B cells arise. The TFs E-box binding protein 2A (E2A) and early B cell factor-1 (EBF1) direct CLPs into the B cell developmental pathway. Together with PAX5 and IKAROS, these factors initiate the progressive steps of *V(D)J* recombination and expression of accessory proteins required for the display of pre- and mature BCRs. Upon commitment to the CLP stage, cells begin to express recombination-activating gene 1 (RAG1) and 2 (RAG2), which are necessary to initiate *VDJ* recombination at the *IgH* chain locus (De and Barnes, 2014; Matthias and Rolink, 2005; Ramirez et al., 2010) (Figure 5).

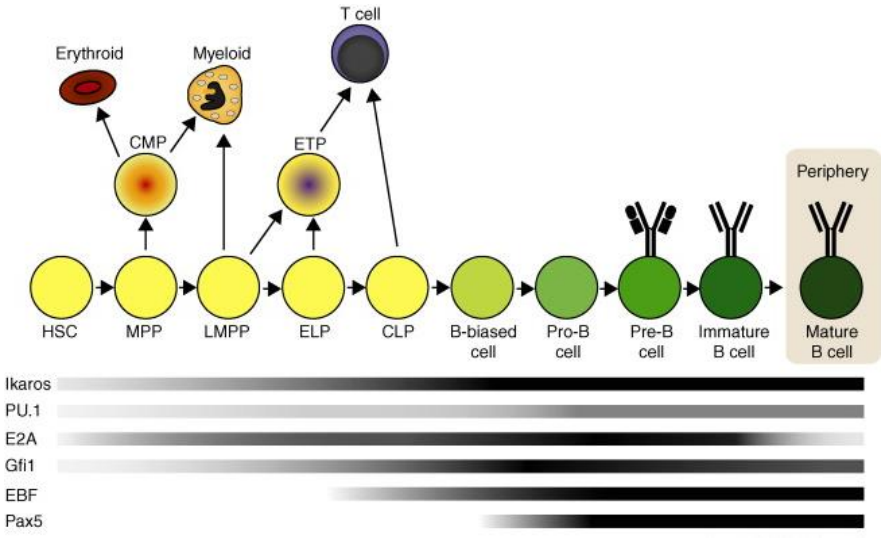

Figure 5. Important TF expression during different stages of B lymphopoiesis from HSCs. *Shaded bars represent the levels of expression of each TF during the course of differentiation; darker shading indicates increased gene expression (Ramirez et al., 2010).*

2.1. Early B cell development

The TFs IKAROS, Purine box factor 1 (PU.1) and E2A are essential for priming lineage-associated genes and restricting fates to the early B cell.

2.1.1. ETS transcription factors

At the earliest stage of lymphopoiesis, the ETS TFs characterized by a unique EYS DNA binding domain, PU.1 and SPI-B, are necessary for viability of the CLP (Busslinger, 2004; Mandel and Grosschedl, 2010). **PU.1**, encoded by *SPI1*, regulates the bifurcation between myeloid and B lymphoid development. Low concentrations of PU.1 favor the B cell fate, while higher concentrations promote myeloid differentiation. Mice lacking *Pu.1* die at embryonic age, and lack monocytes, granulocytes, B and T cells (McKercher et al., 1996). Furthermore, conditional deletion of *Pu.1* in adult mice results in the loss of the CLP population. Therefore, PU.1 is necessary for early lymphoid progenitor development. PU.1 has also been shown to function in enhancer complexes during various stages of B cell development and differentiation. Interactions between PU.1 and other B cell-associated TFs have been shown to be important for the development of PCs and Ab secretion (De and Barnes, 2014).

The other ETS family member, **SPI-B**, is highly related to PU.1 and it is expressed at all stages of B cell development (Busslinger, 2004; Matthias and Rolink, 2005). It has also been shown that SPI-B can compensate for the loss of PU.1, suggesting redundancy between the two TFs.

2.1.2. E-box transcription factors

The E-box family of TFs is characterized by their selective recognition of promoter elements containing the E-box sequence. Members of this family contain a helix-loop-helix structure, and form hetero- or homodimers to constitute active enhancer complexes. In B cell development, the two most prominent E-box TFs are EBF1 (or EBF) and E2A, which both have been shown to be involved in the maturation of the CLP to a pro-B cell.

E2A is a basic helix-loop-helix TF required for B cell development beyond the pre-pro-B cell stage, and it contributes to the maintenance of the HSC pool (Dias et al., 2008). Levels of E2A increase in pro-B cells and are subsequently maintained throughout B cell development (Herblot et al., 2002). Therefore, its deficiency strikingly affects B cell development. E2A forms homodimers to initiate a pro-B cell specific transcriptional program and targets a wide variety of genes required for pro-B cell development (Bain et al., 1994). It binds to enhancer regions of *IGH, VpreB*, and *RAG2* (Lin et al., 2010)

and it is required for initiating and maintaining expression of EBF1, PAX5 and the B cell-specific program in pro-B cells. Moreover, it is also needed for directing B cell maturation in GCs (Kwon et al., 2008).

EBF1 comprises novel DNA-binding and helix-loop-helix domains and is essential for the development of functional B cells. It has a similar role in pro-B cell development as E2A, because *Ebf1* knock-out mice have a block in B cell development at the pro-B cell stage (O'Riordan and Grosschedl, 1999). EBF1 is expressed first in CLPs and regulates many genes involved in B cell development by activating transcription of PAX5, VpreB, and Igα and Igβ, all of which are necessary for successful maturation of the pro-B cell (Gyory et al., 2012). Mice lacking *Ebf1* fail to express most B cell genes including *Cd79a* (Igα), *Cd79b* (Igβ), *Igll1* (λ5), and *VpreB1*, and do not undergo any *IgH* recombination in the BM.

Therefore, sustained expression of E2A and EBF1 is critical for full development of the pro-B cell to the mature naïve B cell stage.

2.1.3. Ikaros zinc finger transcription factors

The Ikaros zinc finger family of TFs comprises IKAROS, HELIOS and AIOLOS (encoded by *IKZF1, 2* and *3*, respectively), which contain two conserved zinc finger domains. Each member can either dimerize with itself or another member of the family to bind DNA (Busslinger, 2004; Matthias and Rolink, 2005), and are important for early pro-B cell to mature naïve B cell development. **HELIOS** is exclusively expressed in T cells, and therefore, does not play a significant role in B cell development. Both **IKAROS** and **AIOLOS** are expressed in the early pro-B cell with levels of both TFs increasing through naïve B cell development (Mandel and Grosschedl, 2010). These TFs are also important for regulating cell cycle and proliferation genes in pro- and pre-B cells (Ferreiros-Vidal et al., 2013).

IKAROS contains variable numbers of Krüppel-like zinc fingers in two domains that mediate DNA binding and formation of dimers and multimeric complexes. In *Ikaros*-deficient mice, lymphoid cell development is arrested at the LMPP stage and myeloid development is perturbed (Georgopoulos et al., 1994; Wang et al., 1996). Following the expression of E2A and EBF1, IKAROS mediates chromatin accessibility necessary for *V(D)J* recombination, and it also modulates the expression of early B cell-specific

genes, including *Igll1* (λ5), by competing with EBF1 for DNA binding (Thompson et al., 2007). Other data suggest that IKAROS promotes B cell identity because *Ikaros*-deficient pro-B cells expressing EBF1 and PAX5 are uncommitted (Reynaud et al., 2008). Thus, IKAROS restricts the self-renewal program in early hematopoiesis, while it advances the B lineage program at later stages of development.

2.2. Maintenance of B cell identity

At present, two TFs, PAX5 and B cell lymphoma (BCL)6, have been shown to play a role in inhibiting terminal B cell differentiation in the GC reaction. Both genes are considered to be master regulators during the B cell differentiation process, PAX5 of maintaining B cell identity while BCL6 of the GC reaction.

2.2.1. PAX5 transcription factor

PAX5 is a member of the PAX family of TFs and is the only one to be expressed in the hematopoietic system. All nine members of the family share their conserved paired DNA binding domain, which characterizes the PAX TFs. PAX5 was originally characterized by its capacity to bind to promoter sequences in *Ig* loci and it may be the most multifunctional TF for B cells (Cobaleda et al., 2007b). It is a transcriptional regulator stably expressed throughout the B cell lineage, from the pro-B cell stage until its downregulation in PCs (Fuxa and Busslinger, 2007). PAX5 binds to DNA through an N-terminal paired-domain motif and can both positively and negatively regulate transcription. It is important in promoting B-lineage commitment and differentiation (Nutt and Kee, 2007), and it can activate genes necessary for B cell development and repress genes that play critical roles in development of non-B-lineage cells.

Pax5-deficient mice have an arrest in B cell development at the transition from *DJ* to *VDJ* rearrangement (LeBien and Tedder, 2008). Conditional *Pax5* deletion in mature murine B cells can result in dedifferentiation to an uncommitted hematopoietic progenitor and subsequent differentiation into T-lineage cells (Cobaleda et al., 2007a). During pro-B cell development PAX5 is needed to initiate recombination of the *IgH* chain and to induce CD19 expression (Medvedovic et al., 2011). Its expression from the pro-B cell through the mature naïve B cell stage ensures to maintain B cell identity as *Pax5*-deficient pro-B cells harbor the capacity to adapt non-B-lineage fates and develop into other hematopoietic lineages (Nutt et al., 1999).

PAX5 promotes B cell differentiation by activating the transcription of Igα (CD79a), BLNK and CD19 (Nutt et al., 1998; Schebesta et al., 2002) that function in the pre-BCR-signaling pathway. Moreover, PAX5 binds to the *VpreB* and *λ5* promoters (Tian et al., 1997) and participates in the assembly of the pre-BCR complex itself, as it also activates expression of the μ chain by controlling the second *VH-DJH* recombination step of the *IGH* gene (Hesslein et al., 2003).

PAX5 is necessary for early pro-B cell development, but also for early GC-B cells. In the GC reaction, PAX5 is necessary for the induction of AID to initiate the CSR, as well as the repression of genes associated with PC fate (Revilla et al., 2012). PAX5 expression becomes downregulated during the maturation of GC-B cells to PCs (Nera et al., 2006). Among PAX5 target genes are *AID*, *CD19*, and *EBF1* but it can also regulate expression of a significant number of genes involved in B cell signaling, adhesion, and migration of mature B cells (Cobaleda et al., 2007b). Activated genes by PAX5 include those that encode a number of TFs important for various aspects of B cell differentiation, including *SPI-B*, *AIOLOS*, interferon regulator family (*IRF*)*4*, and *IRF8*, suggesting that PAX5 activity initiates a cascade that acts to reinforce B cell commitment and subsequent B cell differentiation. Interestingly, E2A and EBF1, crucial for B cell specification and thought to act upstream of PAX5, are also upregulated by this TF (Roessler et al., 2007).

An early study of the role of PAX5 in late-stage B cell development suggested that PAX5 has a role in positively regulating mature B cell proliferation as its blockade inhibited proliferation and differentiation (Wakatsuki et al., 1994). Subsequent studies showed that enforced PAX5 expression appears to prevent B cell activation-induced plasmacytic differentiation (Lin et al., 2002; Morrison et al., 1998; Usui et al., 1997), corroborated by the PAX5 repression of BLIMP1, which is required for PC development (Lin et al., 2002). In a later study Mora-López and colleagues identified that PAX5 binds to the promoter of *PRDM1* (encoding for BLIMP1), directly regulating its transcription (Mora-Lopez et al., 2007). Conditional inactivation of *Pax5* leads to the total loss of identity and function of mature murine B cells (Horcher et al., 2001), indicating that PAX5 is required to maintain B cell identity in late B cell development. *Pax5*-deficient B cells exhibited a decrease of BCL6 transcription, substantial elevated secretion of IgM and significant upregulation of the plasmacytic TFs BLIMP1 and X-box binding protein 1 (XBP1), a transcriptional activator that is strictly required for PC

development and Ab secretion (Nera et al., 2006; Reimold et al., 2001). Thus, PAX5 not only maintains the identity of B cells but also inhibits PC differentiation.

2.2.2. BCL6 transcription factor

The transcriptional repressor BCL6 is required in a B cell autonomous manner for the GC reaction and it is highly expressed in GC-B cells. BCL6 appears to modulate a very broad program in GC-B cells aiming to prevent premature activation and differentiation, and to fine tune the DNA damage response.

Microarray analyses have shown that BCL6 represses a set of genes involved in B cell activation as well as cyclin-dependent kinase (CDK) inhibitors p27 and p21, whose repression allows rapid cell proliferation (Shaffer et al., 2000). Another key BCL6 target identified in microarrays was *PRDM1*, critical for PC differentiation. Several studies confirmed that BCL6 represses plasmacytic differentiation and BLIMP1 expression in GC-B cells, thereby inhibiting terminal PC differentiation so that the GC reaction could proceed (Reljic et al., 2000). Several studies identified that BCL6 directly targets *PRDM1* via two BCL6 binding and response elements within intronic sequences of the gene, and indirectly by interfering with activator protein 1 (AP1) activation, promoting its repression (Vasanwala et al., 2002).

The regulation of BCL6 expression is complex, involving negative autoregulation and occurring at both transcriptional and post-transcriptional levels. BCL6 mRNA is expressed ubiquitously in all tissues including resting B cells and GC-B cells (Allman et al., 1996). At the transcriptional level, BCL6 represses its own transcription via regulatory elements within exon 1 and intron 1 (Kikuchi et al., 2000). At the post-translational level, BCL6 activity is regulated by the p300 co-activator via acetylation, preventing BCL6 from associating with histone deacetylase (HDAC) (Bereshchenko et al., 2002), thus inhibiting its repressive effect.

BCL6 protein stability is regulated by BCR signaling (Niu et al., 1998). Upon BCR stimulation, BCL6 is phosphorylated by mitogen-activated protein kinase (MAPK), ubiquitinated and degraded via the proteasome pathway. As GC-B cells receive multiple signals from Ag during the GC reaction when they continue to express BCL6, it may be that BCR-mediated degradation of BCL6 occurs only with high affinity BCR signaling or in combination with other signals that change as the GC reaction proceeds.

2.3. Mature B cells

2.3.1. NF-κB transcription factor family

The Nuclear factor kappa-light-chain-enhancer of activated B cells (NF-κB) TF family is composed of five subunits, p50 (NF-κB1), p52 (NF-κB2), p65 (RelA), cRel, and RelB that share a conserved Rel Homology DNA binding domain. The subunits can either homo or heterodimerize to affect gene transcription. When inactive, NF-κB is excluded from the nucleus by inhibitor proteins (IκBα, IκBβ, and IκBε) but signaling cascades initiated upon pathogen detection, cytokine signaling, or mitogen binding, lead to the activation of the IκB kinases (IKKα, IKKβ, and IKKγ), which phosphorylate the inhibitory proteins, thereby releasing NF-κB to translocate to the nucleus (Goetz and Baldwin, 2008).

NF-κB is important in the development of mature B cells as both *Nf-kb*$^{-/-}$ and *Relb*$^{-/-}$ knock-out mice have reduced levels of mature MZ B cells, and follicular B cells are decreased in *Nf-kb1*$^{-/-}$ *Relb*$^{-/-}$ double knock-out mice (Cariappa et al., 2000). NF-κB is also needed for mature B cell development to modulate expression of proliferation and survival-associated genes. NF-κB targets TFs such as c-MYC, IRF4, BCL2, and BCLXL to drive proliferation and survival in mature B cells (Sasaki et al., 2006), where CD40-CD40L interactions, BCR cross-linking, and B cell activating factor (BAFF) receptor lead to the activation of NF-κB-dependent cell survival. In addition to the maintenance of mature B cell populations, NF-κB is also involved in the maturation of GC-B cells as *Relb* and *p52* knock-out mice displayed impaired GC formation, most likely due to the rapid proliferation needed during the early stages of GC formation (Goetz and Baldwin, 2008).

2.4. Terminal B cell differentiation

Ag activation of MZ B cells causes immediate proliferation of plasmablasts and differentiation to non-dividing, Ig-secreting PCs. However, during a GC reaction, plasmacytic differentiation is inhibited to allow time for iterative rounds of mutation and selection and for CSR before terminal differentiation. BCL6-dependent repression of BLIMP1 and PAX5-dependent repression of XBP1 are probably critical for inhibiting plasmacytic differentiation in the GC (Reljic et al., 2000; Shaffer et al., 2002).

PCs are terminally differentiated end-stage B cells that do not divide and are responsible for mediating the humoral immune response by synthesizing and secreting Abs. PCs develop at three different times during an immune response: 1) following Ag activation of naïve MZ B cells located in the spleen or B1 cells located primarily in pleural and peritoneal cavities, 2) from follicular B cells that have undergone affinity maturation and isotype switching in GCs of spleen or lymph nodes, or 3) following secondary Ag stimulation of memory B cells (Calame, 2001).

2.4.1. IRF transcription factors

The IRF family of TFs consists of nine members, all of which contain a conserved N-terminal helix-turn-helix DNA binding domain composed of five tryptophan repeats. The IRFs play a role in both B cell development and activation. The roles of IRF4 and IRF8 are the best characterized in B cell development, and *Irf4*$^{-/-}$*Irf8*$^{-/-}$ double knockout mice show a block in development of pre-B cells (Lu, 2008). Among the targets of IRF4 and IRF8 in pre-B cells are AIOLOS, IKAROS, and RAG1/2 during *IgL* recombination (De and Barnes, 2014).

During B cell activation and maturation, **IRF8** is critical for the development of GC-B cells as it directly induces expression of BCL6, which is critical for the formation of the GC, and AID, involved in the CSR in the GC (Lu, 2008). **IRF4** is necessary for the development of PCs and memory B cells as evidenced by *Irf4*$^{-/-}$ knock-out mice that lack plasma B cells and have lower levels of memory B cells (Klein et al., 2006). Higher levels of IRF4 dictate development of plasma B cells, whereas lower levels lead to memory B cell development (Ochiai et al., 2013). During the late GC program, IRF4 suppresses BCL6 expression thereby allowing for differentiation of memory and plasma B cells (Klein et al., 2006).

2.4.2. BLIMP1 transcription factor

BLIMP1, encoded by *PRDM1*, is present in all PCs, in a small subset of GC-B cells with partial PC phenotype but not in memory B cells. *PRDM1* is a zinc finger transcriptional repressor containing five zinc finger motifs that confer DNA binding ability. It is required for the maturation of plasma B cells and it is a master regulator of the terminal differentiation into Ab-secreting PCs (Kallies and Nutt, 2007). Initial expression analysis of various B cell lines found that BLIMP1 expression was exclusive

to PCs. *Prdm1*$^{-/-}$ knock-out mice completely lack PC development, confirming that BLIMP1 is necessary for the differentiation of plasma B cells (Angelin-Duclos et al., 1999). Furthermore, conditional deletions of *PRDM1* further showed that expression of BLIMP1 is necessary for the viability of plasma B cells (Shapiro-Shelef et al., 2005).

BLIMP1 represses a gene expression program associated with cell proliferation and growth (Shaffer et al., 2002), including *c-MYC, RCL1, ODC, LDH-A, DHFR, E2F1*. Other genes in the proliferation program repressed by BLIMP1 are the anti-apoptotic gene *A1* (Knodel et al., 1999), and genes required for replication and mitosis such as *PCNA* and *MCM2*. In addition, BLIMP1 induces expression of CDK inhibitor p18, required for plasmacytic differentiation (Tourigny et al., 2002), and pro-apoptotic genes *GADD45* and *GADD153*.

A second set of genes indirectly regulated by BLIMP1 comprises those involved in Ig secretion, which include *Ig* genes themselves, *J chain* and *XBP1*. BLIMP1 represses *PAX5* directly by binding to its promoter, and indirectly via the repression of EBF1, which directly activates PAX5 transcription. Moreover, BLIMP1-dependent repression of *Pax5* is required for PC differentiation (Lin et al., 2002). BLIMP1 also downregulates multiple genes required for isotype switch recombination including *AID* (Muramatsu et al., 2000), *STAT6*, required for activation of some Ig region promoters, and *KU70*, *KU86* and DNA *PKC*s, required for the DNA recombination process.

Another set of genes repressed by BLIMP1 is that required for B cell identity and GC function such as *BCL6* (Shaffer et al., 2001). Genes encoding BCR signaling components, including *CD79a, BLNK, BTK, LYN, SYK, CD45, CD19, CD21* and *CD22,* are downregulated by BLIMP1 (Shaffer et al., 2002). Once the plasmacytic differentiation starts, BLIMP1 directly represses PAX5 expression and contributes to the downregulation of BCL6. This repression network acts in combination with IRF4 and XBP1 to initiate a PC development program. Also, BLIMP1 expression is upregulated by IRF4 in late GC-B cells.

2.4.3. XBP1 transcription factor

XBP1 is a TF within the CREB family and is critical in positively regulating genes associated with protein folding and secretion. As PCs secrete large amounts of Abs, XBP1 is necessary for the development of PCs (De and Barnes, 2014). *Xbp1*$^{-/-}$ murine

lymphocytes have normal B cell numbers, and B cell development is normal until the terminal PC differentiation. However, these mice are severely defective in Ig secretion and have few PCs, thus establishing a critical role for XBP1 in PC differentiation (Reimold et al., 2001).

XBP1 is ubiquitously expressed, and embryos lacking the gene have hypoplastic livers and die from anemia (Reimold et al., 2000). However, XBP1 mRNA is strongly induced in PCs (Reimold et al., 2001). One component of this induction is BLIMP1-dependent repression of PAX5, as PAX5 directly represses XBP1 transcription (Reimold et al., 1996). However, additional signals to transcriptional regulation are also important for XBP1 mRNA induction as XBP1 mRNA is also processed in response to endoplasmic reticulum (ER) stress (Yoshida et al., 2001). The unfolded protein response causes IRE1-dependent splicing of a short sequence from XBP1 mRNA, resulting in alternate reading frame usage and producing an active and stable form of the protein. In particular, the processed form of XBP1 can transactivate the promoter for BiP (*GRP78*) (Yoshida et al., 2001), suggesting that BiP and other genes induced by ER stress may be *in vivo* targets of XBP1.

3. Lymphoid neoplasms. Non-Hodgkin's lymphomas

Non-Hodgkin's lymphomas (NHLs) comprise a large, heterogeneous group of malignant lymphoproliferative disorders that represent distinct disease entities, according to their clinical, morphological, immunophenotypic and genetic features (Swerdlow, 2008). They are derived from B, T or NK cells at various stages of their differentiation, and can be divided into aggressive and indolent types, according to their clinical course. They are treated using combinations of chemotherapy, monoclonal antibodies, immunotherapy, radiation and hematopoietic stem cell transplantation.

NHLs represent the fifth most common type of cancer, and although the world health organization (WHO) recognizes a variety of well-characterized disease entities, some level of superposition criteria still prevent the adequate assignation of some tumors. GEP analyses of different types of NHLs have improved the diagnostic precision generating differential expression of several genes that could represent potential therapeutic targets (Ek et al., 2006; Leich et al., 2007).

B cell neoplasms, which comprise the majority of all lymphoid neoplasms, are a diverse group of tumors that recapitulate normal stages of B cell differentiation (LeBien and Tedder, 2008). They have typical distinctive immunophenotypes that permit classification according to their postulated cell of origin. In addition, cytogenetic profiles, genotype, and immunophenotype of the malignant cell have had considerable impact on prognostic and therapeutic stratifications of patients with B cell neoplasms.

The normal B cell developmental stage counterparts have been attributed for many of the B cell lymphomas by similarity of immunophenotype, histological appearance and GEPs. Detecting the presence of SHM allows determination that the lymphoma cell has experienced the GC. For example, the majority of MCLs are mostly reminiscent of naïve B cells; however, 15-40% of cases show SHM, indicating that they have experienced the GC reaction (Jares et al., 2012). Burkitt's lymphomas (BLs), follicular lymphomas (FLs) and GC-B cell-like diffuse large B cell lymphomas (GCB-DLBCLs) show features that are consistent with GC-B cell derivation (Figure 6). The majority of these lymphomas have GEP that are most similar to B cells within the GC light zone, although a proportion of BLs have profiles that more closely resemble cells from the dark zone. Activated B cell-like DLBCLs (ABC-DLBCLs) have experienced the GC and have a putative cell of origin that is reminiscent of the plasmablast stage of B cell

development (Shaffer et al., 2012). Marginal zone lymphomas (MZLs) cells have a microscopic appearance and immunophenotype that is reminiscent of B cells from the MZ, the area that forms the outer layer of B cell follicles (Figure 6). The idea of the cell of origin does not determine that the key oncogenic events were necessarily acquired solely at that stage of B cell development but rather that genetic events accumulated prior to or at that stage of B cell development contribute to block further maturation.

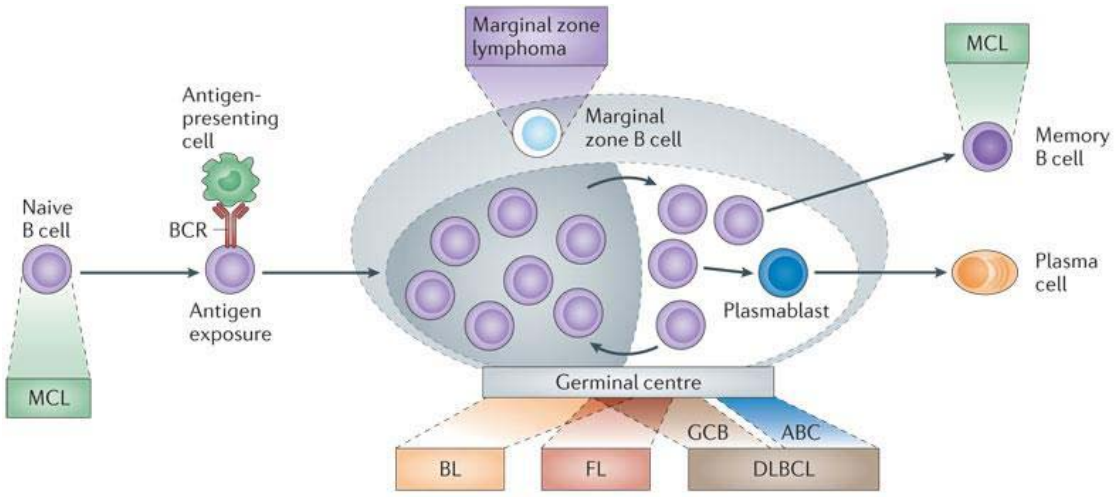

Figure 6. Cell of origin and normal cellular counterpart of the different NHLs *(Scott and Gascoyne, 2014).*

Chromosomal translocations are the main genetic mechanisms driving primary genetic alterations in NHLs, and some of them have been identified and associated to specific types of lymphoma and/or histological subgroups. However, the detection of these translocations in healthy individuals supports the idea that such alterations are required for tumor development but additional secondary alterations are necessary for neoplastic transformation. The spectrum of such secondary events linked to tumor progression is complex and includes genetic and epigenetic alterations that have an important impact in the clinical evolution of the patients, and comprises specific genes critical for disease (Swerdlow, 2008).

In general, these translocations result in the activation of a proto-oncogene promoting the pathogenic mechanisms by deregulating key cellular processes such as alteration of cellular proliferation, apoptosis or cellular differentiation blockade, or disruption of DNA damage responses, among others. For instance, in FL the anti-apoptotic *BCL2* gene was discovered as the translocation partner with the *IgH* locus in the t(14;18)(q32;q21) translocation, and in MCL, the proto-oncogene cyclin D1 (*CCND1*)

is under the control of the promoter of the *IgH* locus due to the t(11;14)(q13;q32) translocation (Jares et al., 2007; LeBien and Tedder, 2008). In BL, translocation of the *c-MYC* oncogene, involved in cell cycle regulation and apoptosis, takes place into the *IgH* or *IgL* chain (Boxer and Dang, 2001). All these gene juxtapositions promote cell cycle deregulation and thus, uncontrolled proliferation and growth of the malignant cells.

3.1. Mantle cell lymphoma

MCL is a type of malignant NHL analogous to a subset of pre-GC cells localized to the primary B lymphocyte follicles and the mantle zones of secondary lymphoid follicles. MCL is one of the most aggressive NHL with a median survival of 3-5 years and it is generally considered to be an incurable disease. Its clinical evolution is usually very aggressive with short responses to treatment and frequent relapses, only a small percentage of the patients get cured with current therapies.

MCL accounts for approximately 6% of NHLs and it characteristically occurs in adults with a median age of presentation of 60 years and a male predominance. It is a lymphoid neoplasia characterized by a high proliferation of mature B lymphocytes with a striking tendency to disseminate throughout the body (Swerdlow, 2008). Patients usually present with lymphadenopathy and advanced stage disease.

Extranodal involvement is frequent and 30-50% of the patients present two or more affected extranodal sites (Jares and Campo, 2008). Hepatosplenomegaly is common as well as involvement of the gastrointestinal tract, peripheral blood, BM and spleen (Angelopoulou et al., 2002; Jares et al., 2007). Central nervous system involvement occurs in 10-20% of the patients, and usually appears as a late event associated with resistant disease or generalized relapse (Ferrer et al., 2008; Montserrat et al., 1996).

3.1.1. Primary oncogenic event and cyclin D1 deregulation

The primary oncogenic event in MCL is the t(11;14)(q13;q32) translocation that juxtaposes the proto-oncogene *CCND1* locus on a region at 11q13 designated BCL1 under the control of the *IgH* chain joining region enhancer localized at 14q32 (Figure 7).

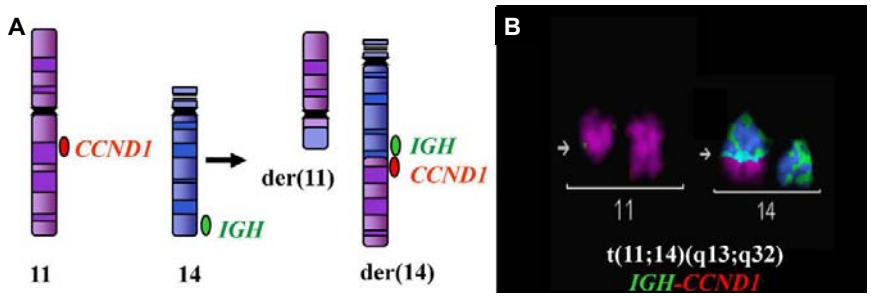

***Figure** 7. **Primary chromosomal translocations in MCL.** (A) Schematic representation of the classic translocation of CCND1 gene (red) with IGH (green). After the rearrangement, both derivative chromosomes are shown with the fusion signal (green and red colocalization) in the derivative chromosome 14. (B) t(11:14)(q13;q32) translocation detected by M-FISH technique, pseudocolored chromosomes 11 (pink) and 14 (green) and the fusion signal (arrow) (Royo et al., 2011).*

This results in aberrant overexpression of cyclin D1, which is not expressed in B lymphocytes under normal conditions and plays an important role in cell cycle regulation inducing G1 to S phase transition by binding to CDKs (Jares et al., 2007). The majority of breakpoint sites at 11q13 happen at the major translocation cluster (MTC) region (30-50%) but 10-20% of the breaks occur outside the MTC closer to *CCND1*. *CCND1* is the closest gene located 120kb downstream of the MTC locus and its expression is deregulated by the translocation (Jares and Campo, 2008) (Figure 8).

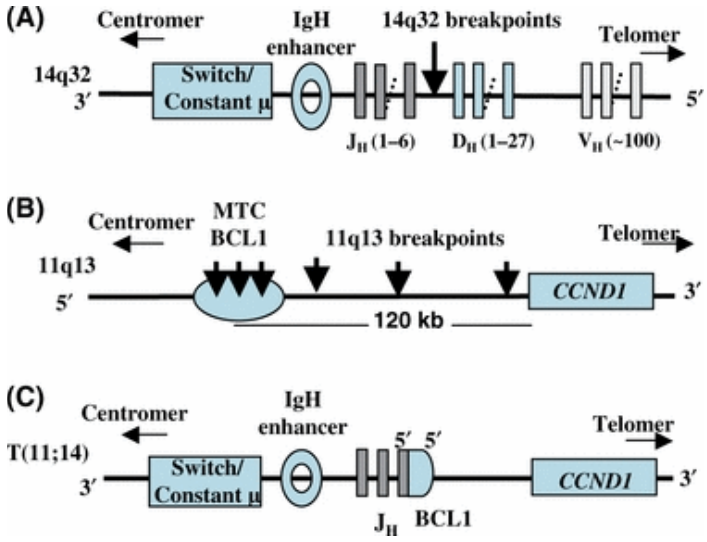

***Figure 8. The translocation t(11;14)(q13;q32) in MCL.** (A) Schematic representation of the germline IgH locus (IGH@) on chromosome 14q32 displaying the genomic organization of the V, D, J and the C region (only the Cl gene is shown). The breakpoint in IgH seems to occur between the D and J joining regions during the early steps of the V(D)J recombination. (B) Genomic organization of the BCL-1 locus on chromosome 11q13. (C) The translocation leads to a 5'-5' fusion of the BCL-1 locus with sequences from the IGH@ locus and CCND1, brought under the control of the IgH enhancer (Jares and Campo, 2008).*

Additionally to the t(11;14) translocation, other mechanisms promoting an overexpression of CCND1 are frequent in MCL. Some of these comprise secondary chromosomal rearrangements at 3' of the *CCND1* locus (Bosch et al., 1994; de Boer et al., 1997), or point mutations or genomic deletions in the 3'untranslated region (UTR) causing the expression of truncated cyclin D1 transcripts (Chen et al., 2008; Wiestner et al., 2007).

CCND1 encodes for two transcripts of 4.5 and 1.5 kb which contain the whole coding region that codifies for the resulting 36kD polypeptide, representing **isoform a**. However, these two shorter transcripts differ in the length of the 3'UTR that contains an AU-rich element involved in transcript stability. They lack the destabilizing AU-rich elements present in the long mRNA transcript, and the binding sites for different microRNAs (miR-16, miR-503, miR-15a, miR-34a, miR-195, miR-424) that negatively regulate cyclin D1 expression (Chen et al., 2008; Jiang et al., 2009). About 4-10% of MCLs lack the 4.5kb transcript and instead express aberrant mRNAs with shorter 3'UTR.

Although the function of these shorter transcripts is not clear, they have an extended half-life and their expression correlates with high levels of CCND1 mRNA, increased proliferation and more aggressive clinical behavior (Sander et al., 2005). Furthermore, amplifications of the translocated t(11;14) allel have also been detected and can contribute to cyclin D1 overexpression (Bea et al., 2009).

CCND1 also encodes for a less abundant isoform than the canonical protein, **isoform b**, which lacks the C-terminal region. Cyclin D1 isoform b is generated by alternative splicing producing a transcript lacking whole exon 5 which contains important regulatory motifs for the nuclear export of phosphorylated cyclin (Alt et al., 2000). Although cyclin D1b isoform seems to have a tumorigenic effect (Solomon et al., 2003), its implication in MCL is still not clear as MCL tumor cells mostly express the canonical isoform a but low levels of cyclin D1b mRNA (Marzec et al., 2006).

3.1.2. Cyclin D1 involvement in MCL lymphomagenesis

Cyclin D1 plays an important role in cell cycle regulation of G1-S transition following mitotic growth factor signaling, and its role in promoting MCL lymphomagenesis is related to its function in cell cycle regulating CDK4 and CDK6. Cyclin D1 binds to

CDK4 and CDK6 to form a CDK/cyclin complex that phosphorylates retinoblastoma 1 (RB1) facilitating cell cycle progression. RB1 plays a master role in G1-S transition by sequestering and inactivating E2F TFs that transactivate essential genes required for S phase entry and DNA replication, including cyclin E (Harbour and Dean, 2000).

RB1 phosphorylation by cyclin D1/CDK4-6 initiates the release of E2F promoting the accumulation of cyclin E/CDK2 complexes that irreversibly inactivate RB1 and promote the subsequent progression into the S phase (Jares et al., 2007) (Figure 9). Thus, cyclin D1 overexpression would contribute to lymphomagenesis in MCL by overcoming the suppressor effect of RB1 in the G1/S transition. RB1 seems to be normally expressed in most MCL and its protein appears hyperphosphorylated, especially in highly proliferative MCL blastoid variants (Jares et al., 1996). However, recent studies identified intragenic deletions of *RB1* which lead to a total lack of protein expression in some cases of MCL (Pinyol et al., 2007), suggesting that cyclin D1 may also have an oncogenic role independently of RB1 in these tumors.

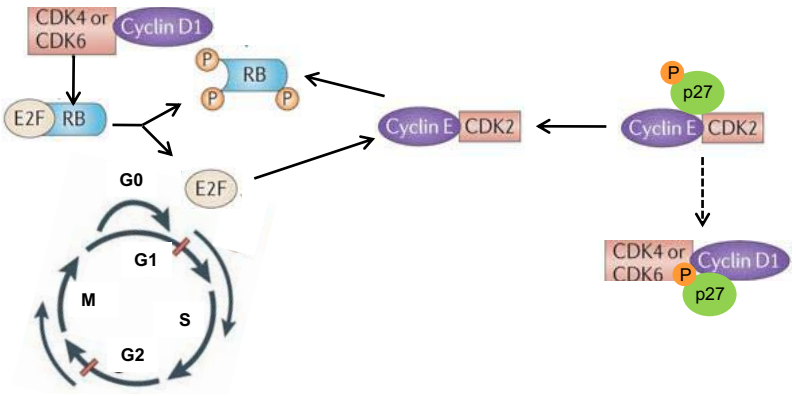

Figure 9. Potential role of cyclin D1 in G1/S phase transition. *Modified from (Jares and Campo, 2008).*

MCL may also have an impaired control of late G1 phase and G1-S phase transition, a step that is regulated by the cyclin E-CDK2 complex and the CDK inhibitor p27. Cyclin D1 binds to CDK4 and controls the G1/S-phase transition by initiating the hyperphosphorylation of RB1 allowing the accumulation of cyclin E. In addition, the titration of p27 into cyclin D1/CDK4 complexes will promote the raising of active cyclin E/CDK2 complexes that will enhance p27 degradation and further phosphorylation of RB1 allowing the cell to progress into S phase (Chiarle et al., 2000) (Figure 9).

Cyclin D1 has additional oncogenic effects besides its role in cell cycle as it participates in the regulation of several TFs and transcription co-regulators such as Signal transducer and activation of transcription (STAT)3, CCAAt/enhancer binding protein β (C/EBP), MYB and members of the nuclear receptor family, among others (Fu et al., 2004).

Cyclin D1 may also promote chromosome instability by binding to genes that regulate chromosome segregation and chromatin reorganization (Casimiro et al., 2012), and promote DNA repair by binding to RAG1 and homologous DNA recombination (Jirawatnotai et al., 2011). Although these non-cell cycle-related functions of cyclin D1 have not been properly investigated in MCL, the complete inactivation of *RB1* by mutations and deletions in some MCL (Pinyol et al., 2007) makes cyclin D1 dispensable for cell cycle functions, and would support the idea that cyclin D1 may play additional oncogenic roles in this disease. The recent observation that cyclin D1 promotes cell survival in MCL by sequestering the pro-apoptotic BAX protein reinforces this idea (Beltran et al., 2011).

Several observations suggest that cyclin D1 deregulation is not sufficient to trigger the complete neoplastic transformation or to explain the aggressiveness of MCL. Some studies have described the presence of low level monoclonal B cells with an *IGH@-CCND1* fusion in healthy individuals without evidence of disease (Hirt et al., 2004). Moreover, the development of cyclin D1 transgenic mouse models failed to generate MCL as mice overexpressing cyclin D1 did not develop spontaneous lymphoma. However, the cooperation with other oncogenes like *MYC* was required for lymphomagenesis (Lovec et al., 1994). These results suggest that cyclin D1 is important for MCL initiation, but additional oncogenic events are necessary for the complete neoplastic transformation and maintenance of the tumor. Secondary chromosome alterations that influence MCL pathogenesis include target genes involved in molecular pathways such as cell cycle control (such as *ARF-MDM2-TP53*, and *INK4a-CDK4-RB1*), DNA damage response (*ATM*, *CHK1* and *CHK2*), and cell survival pathways (*BCL2* and *BIM*), that are frequently found in aggressive MCL.

3.1.3. Secondary molecular events contributing to MCL pathogenesis

Genetic studies have revealed that MCL is one of the malignant lymphoid neoplasms with the highest level of genomic instability. Indeed, various studies have revealed a high number of such secondary chromosomal alterations in MCL, including gains in 3q, 6p, 7p, 8q, 10p, 12q, and 18q as well as losses of 1p, 6q, 8p, 9p, 9q, 11q, and 13q (Salaverria et al., 2007) (Figure 10). Crucial target genes such as $p16^{INK4a}$ in 9p21 (Pinyol et al., 1998), *BMI-1* in 10p12 (Bea et al., 2001), *ATM* in 11q22.3 (Camacho et al., 2002), *CDK4* in 12q14 (Hernandez et al., 2005), and *p53* in 17p13 (Greiner et al., 1996; Hernandez et al., 1996) have been identified.

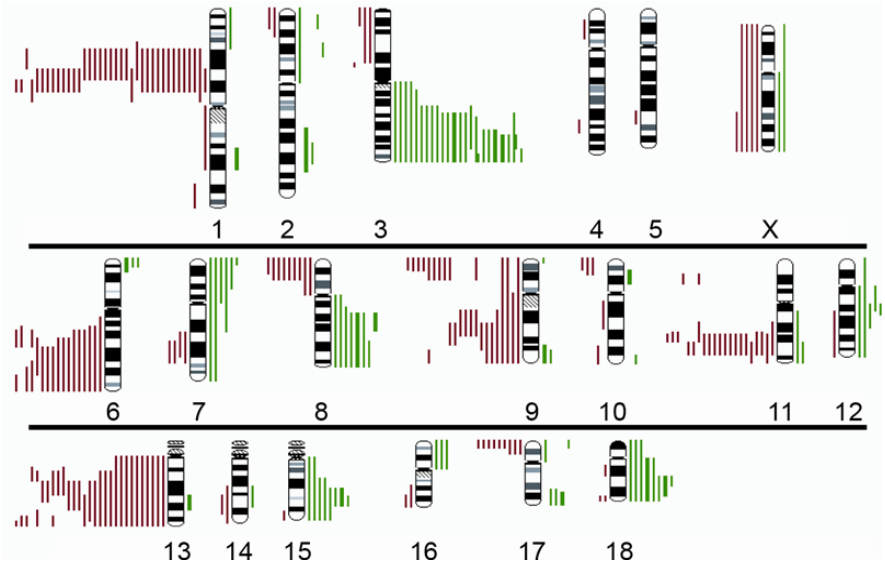

Figure 10. Ideogram of the distribution of gains and losses *of genetic material detected by comparative genomic hybridization in cyclin D1-positive MCL. Red bars on the left side correspond to genetic losses; green bars on the right side indicate genetic gains. Bold bars indicate amplifications (Salaverria et al., 2007).*

In addition, alterations in a number of chromosomal regions show a clear association with the clinical course of MCL patients (Salaverria et al., 2007), with very aggressive MCL blastoid variants having more complex karyotypes. Additionally to chromosomal imbalances, the two highly aggressive presentations of MCL, the blastoid and pleomorphic variants, also present frequently tetraploidy, which comprises more centrosome anomalies and overexpression of centrosome-associated genes (Ott et al., 1997). Uniparental disomies (UPD) have been identified in regions similar to the ones commonly deleted, supporting an alternative mechanism to inactivate tumor suppressor genes (Fitzgibbon et al., 2005).

Secondary genetic alterations involved in cell cycle pathways very frequently target the INK4a/CDK4/RB1 and ARF/MDM2/p53 cell cycle pathways which are connected by the *CDKN2A* locus at 9p21. This locus encodes for INK4 and ARF and is deleted in MCL (Jares et al., 2012). *TP53* and *RB1* are also commonly inactivated by point mutations or gene deletions, and inactivations of *RB1* by intragenic homozygous deletions have been identified in MCL cell lines and primary MCL tumors (Hernandez et al., 1996; Pinyol et al., 2007). Furthermore, gene amplifications deregulate *CDK4*, *BM1* and *MDM2* (Hernandez et al., 2005; Pinyol et al., 2007) (Figure 11).

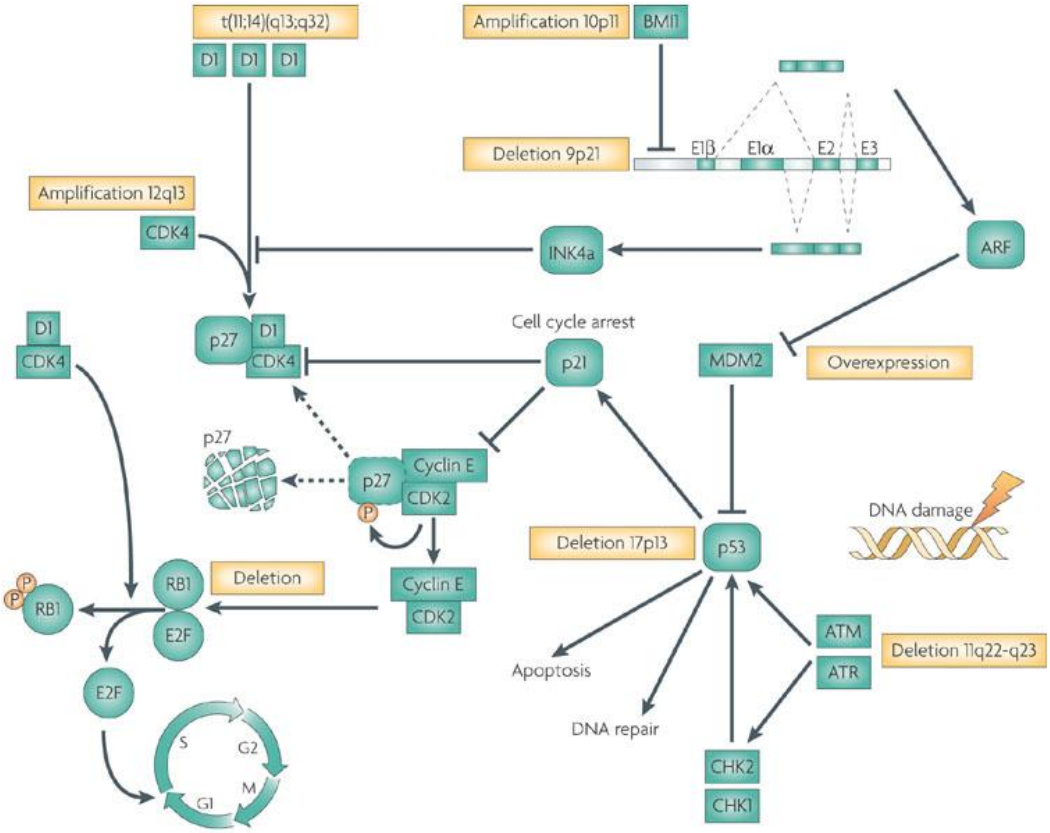

Figure 11. Cell cycle and DNA damage response pathways deregulation in MCL *(Jares et al., 2007).*

Chromosome aberrations in MCL are also consistent with an important role of deregulation of the DNA damage response in this disease (Royo et al., 2011). Ataxia-telangectasia mutated *(ATM)* is frequently deleted and mutated in MCL with increased genomic instability (Camacho et al., 2002), and additional downstream elements of this pathway, including *CHK1* and *CHK2*, have also been found deregulated in MCL, suggesting that mutations of DNA damage response elements contribute to oncogenesis (Jares et al., 2007) (Figure 11).

Recent studies have also shown that genes involved in cell survival are targets of recurrent genetic alterations in MCL such as amplifications and overexpression of the anti-apoptotic gene *BCL2* located at 18q21, and homozygous deletions of the pro-apoptotic gene *BCL2L11* located at 2q13 (Bea et al., 2009).

Concordant with these secondary genetic alterations, GEP studies revealed an imbalance between pro-apoptotic and survival signaling pathways in MCL as evidenced by a downregulation of pro-apoptotic genes (*FADD, DAXX, RAIDD*) and an upregulation of cell cycle-related genes, growth factors and their receptors (Hofmann et al., 2001). Martínez and colleagues also identified a homogeneous GEP for MCL consisting of genes participating in apoptosis regulation, cell cycle control and signal transduction. In particular, many genes involved in the tumor necrosis factor (TNF) and NF-kB pathways were deregulated (Martinez et al., 2003). Concordant with these results, another study observed an aberrant expression of genes of the transforming growth factor β (TGFβ) superfamily, and upregulation of genes involved in the WNT and phosphatidylinositol-3-kinase (PI-3-K)/AKT signaling pathways in leukemic MCL (Rizzatti et al., 2005).

The use of next generation sequencing (NGS) technologies in B cell lymphomas is also revealing more secondary oncogenic events involved in the pathogenesis of these diseases. A recent study based on whole transcriptome sequencing showed that 12% MCL present mutations in the PEST domain of *NOTCH1* which is associated with poor survival. This gene encodes for a transmembrane protein that functions as a ligand-activated TF and those mutations generated a truncated, more stable and transcriptionally active protein. Moreover, the inhibition of this pathway reduced proliferation and induced apoptosis in MCL cell lines (Kridel et al., 2012).

Another recent work on whole-genome and/or whole-exome sequencing in MCL by Beà and colleagues identified recurrent mutated genes by targeted sequencing. They found known drivers such as *ATM*, *CCND1*, and the tumor suppressor *TP53*, but also novel mutated genes encoding the anti-apoptotic protein *BIRC3* and *TLR2*; and the chromatin modifiers *WHSC1*, *MLL2*, and *MEF2B*. They also found *NOTCH2* mutations as an alternative phenomenon to *NOTCH1* mutations in aggressive tumors with a dismal prognosis (Bea et al., 2013).

3.1.4. Heterogeneity in mantle cell lymphoma

Although MCL is one of the most aggressive NHLs, the characterization and approach to this tumor is evolving. Different subtypes of the disease have been recognized, increasing the biological complexion of this malignancy, both from a prognostic as a therapeutical perspective.

3.1.4.1. Morphological, phenotypic and clinical features of MCL

MCL in the lymph nodes adopt a mantle zone, nodular or diffuse growth pattern which might represent different stages of tumor infiltration. The mantle zone growth pattern is characterized by an expansion of the follicular mantle area by neoplastic cells surrounding reactive GCs (Jares and Campo, 2008). The observation of the mantle zone growth pattern in lymph nodes from some indolent clinical course patients (Espinet et al., 2005; Nodit et al., 2003) indicates that it represents the initial tumor infiltration of the follicle. Frequently, these tumor cells also infiltrate the GC of the follicles and replace the lymphoid follicle completely, developing a nodular pattern. In a later stage of disease development, neoplastic cells invade and obliterate the internodular areas resulting in a diffuse growth pattern which is the most common in MCL (Jares and Campo, 2008).

The **classical cytological variant** of MCL occurs in 80-90% of patients and is characterized by a monotonous proliferation of small or medium-sized cells with irregular nuclear contours, moderately dispersed chromatin and inconspicuous nucleoli (Swerdlow, 2008).

Some tumors may present with small cells with round nuclei but absence of the central nucleoli. This **small-cell variant** has been associated with a leukemic and splenomegalic presentation of MCL without lymphadenopathy and a more indolent clinical course of the patients (Angelopoulou et al., 2002; Orchard et al., 2003). Their MCL proliferation activity is usually low with 15-30% Ki-67-positive cells.

Two more cytological variants have been described, the blastoid and pleomorphic MCLs which have higher proliferation rates, complex karyotypes, tetraploidization, and are associated with more aggressive clinical behavior and poorer prognosis.

Blastoid MCLs show extremely high proliferative activity with numerous mitotic figures, high percentage of Ki-67 index-positive cells (>40%) and a histology that has been associated with unfavorable prognosis and high expression of p53 (Greiner et al., 1996; Hernandez et al., 1996). Blastoid variants occur usually *de novo* and less frequently in patients with previous diagnosis of classical MCL. Some observations support the idea that blastoid MCL in patients with previous diagnosed classical MCL represent histological transformation of the initial neoplastic clone rather than a *de novo* tumor (Yin et al., 2007).

Pleomorphic MCLs comprise a more heterogeneous population of larger cells, and although the proliferation activity is also high, it is usually lower than in the blastoid variant. The tumors are frequently tetraploid with mitotic figures highly hyperchromatic with an apparent high number of chromosomes (Ott et al., 1997).

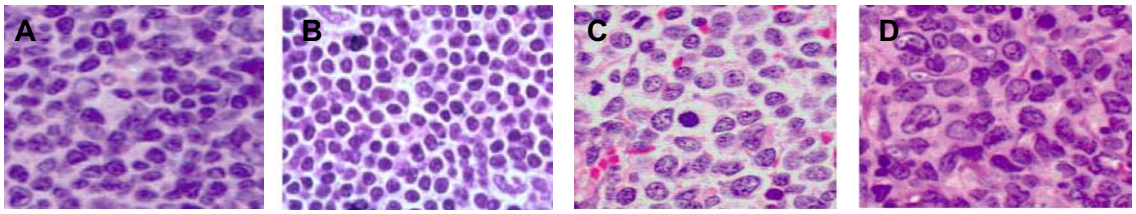

Figure 12. MCL histological variants *displaying haematoxilin and eosin (H&E) staining of tissue sections from (A) classical, (B) small-cell, (C) blastoid, and (D) pleomorphic MCL. Modified from (Jares et al., 2007).*

These cytological variants represent the ends of a morphological spectrum, and transitional forms between them may be observed in some tumors making its classification difficult. Some tumors may even present a discordant morphology with areas of pleomorphic cells intermingled with others with classical morphology.

The phenotype of MCL is characterized by the expression of mature B cell Ags with moderate to strong expression of surface Igs (IgM or IgD which are usually associated with the *L* chain), B cell associated Ags such as CD20, CD22, CD79, and co-expression of the T cell associated Ag CD5. Expression of CD23, a key cell surface molecule for B cell activation and growth, CD10, a transmembrane endopeptidase encoding for the GC-associated Ag, and BCL6, involved in lymphoid follicle GC formation and maintenance, are usually negative (Jares et al., 2007).

Although this immunophenotype is quite common in MCL, some variants have also been described, making the diagnosis more complicated. Some tumors may be CD5

negative, especially blastoid variants, and express CD23 (Gong et al., 2001). Others may express CD8 and CD7 (Hoffman et al., 1998) or BCL6, CD10 or MUM1 (Camacho et al., 2004), whose its expression is usually negative in MCL.

3.1.4.2. Cyclin D1 negative MCL

In 2003 Rosenwald and colleagues performed a GEP study on MCL and found a characteristic and unique gene expression-based proliferation signature that comprised the gene expression levels of 20 different genes, and constituted a powerful predictor of survival of MCL patients at the time of diagnosis. It allowed for the stratification of MCL patients into prognostic subgroups in which survival time differed by more than 5 years. Interestingly, they identified a cyclin D1-negative subset of MCL that demonstrated identical morphological, immunophenotypic, gene expression features and secondary genetic alterations in comparison to cyclin D1-positive MCL tumors (Figure 13). In the absence of cyclin D1, these cases overexpressed cyclin D2 or D3, but with no evidence of chromosomal aberrations affecting these loci (Rosenwald et al., 2003).

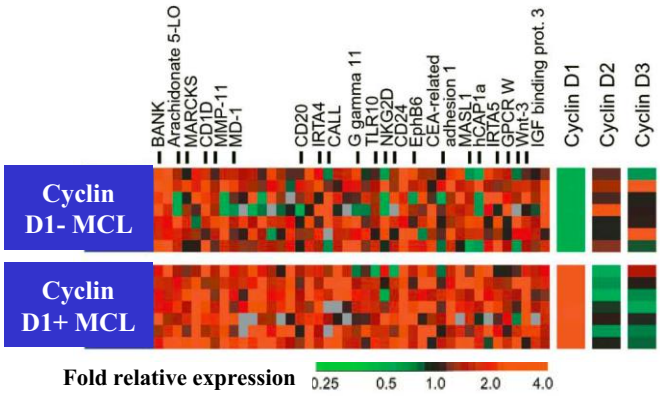

Figure 13. Expression of MCL signature genes in seven cyclin D1-positive and seven cyclin D1-negative lymphoma tumors. *Cyclin D1-negative tumors had MCL morphology and immunophenotype and were classified as MCL based on their GEP. Shown on the right is the relative gene expression of cyclin D1, D2 and D3. Modified from* (*Rosenwald et al., 2003*).

Although the t(11;14) translocation is considered the hallmark of MCL causing an overexpression of cyclin D1, other studies also identified these uncommon cyclin D1-negative MCL patients with indistinguishable morphology, phenotype, global GEP and secondary genetic alterations, suggesting that they comprise the same disease entity (Fu et al., 2005; Salaverria et al., 2007). Strikingly, these MCLs overexpress CCND2 or CCND3, demonstrating the importance of the oncogenic deregulation of cell cycle G1

phase in the pathogenesis of the disease. However, the mechanisms deregulating these cyclins are not well understood.

Interestingly, subsequent studies were able to detect MCL cases with high levels of cyclin D2 due to chromosomal translocations involving *CCND2* and *Ig* genes such as the t(2;12)(p11;p13) fusing the *CCND2* gene to the *IGK* locus (Gesk et al., 2006), the t(12;22)(p13;q21) with the fusion *IGL-CCND2* (Shiller et al., 2011), and the t(12;14)(p13;q32) fusing *IGH-CCND2* (Herens et al., 2008). Additionally, two *CCND2* translocations with an unidentified partner have also been described (Mozos et al., 2009; Quintanilla-Martinez et al., 2009), both cases with high levels of cyclin D2. Only one MCL case with translocation of *IGH* with *CCND3* has been reported so far (Wlodarska et al., 2008).

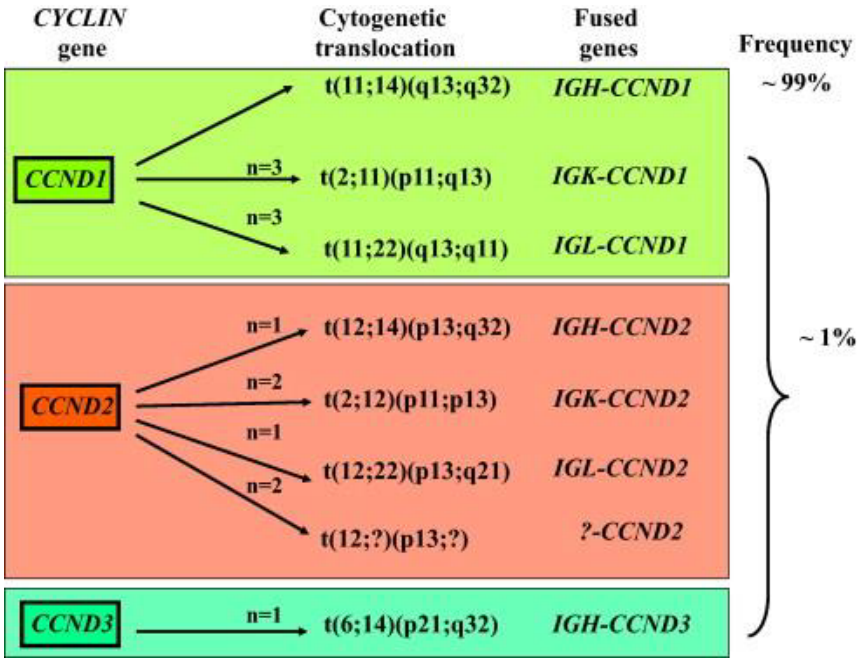

***Figure 14. Variant primary chromosomal translocations in MCL**. Virtually all MCL tumors have the conventional t(11;14). However, six patients have been reported with variant translocations of CCND1 and IGL chain genes, six with breaks in CCND2 and one with translocation in CCND3 (Royo et al., 2011).*

In a subsequent work by Salaverria and colleagues, the authors studied the largest series of well-defined CCND1-negative MCL patients with similar pathologic and genetic characteristics, clinical presentation and evolution to the conventional CCND1-positive MCL. They observed that the most frequent genetic events in cyclin D1-negative MCLs are *CCND2* rearrangements since more than half of CCND1-negative patients presented *CCND2* rearrangements with *Ig* genes. Interestingly, they also found two patients with

CCND2 breaks with normal *IGH*, *IGK* and *IGL* genes, suggesting a novel translocation partner (Salaverria et al., 2013).

The recognition of these cyclin D1-negative MCL can be challenging as some small B-cell lymphomas (MZL, FL, Small lymphocytic lymphoma (SLL)) may mimic MCL morphologically and phenotypically. Moreover, immunohistochemical staining of CCND2/D3 in routine diagnosis may not be sensitive enough to clearly identify cyclin D1-negative MCL because these cyclins are also expressed in other B cell lymphomas at lower levels (Mozos et al., 2009; Quintanilla-Martinez et al., 2009).

Further, the absence of any *CCND* gene alteration in a subset of conventional MCL triggers the investigation of the initial drivers for MCL pathogenesis in these patients. SOX11, a neural TF overexpressed in virtually all conventional MCLs but not in other mature lymphoid neoplasms and normal lymphocytes at any stage of development, is highly expressed in both cyclin D1-positive and -negative MCL tumors, suggesting that it may represent a valuable diagnostic biomarker as well as an important factor for pathogenesis in MCL (Jares et al., 2012; Mozos et al., 2009).

3.1.4.3. Indolent, non-nodal MCL

Recent clinical observations have identified a group of patients with a more indolent course of the disease and longer survival even without treatment, suggesting that the biological features of this disease are more heterogeneous than initially thought (Espinet et al., 2005; Nodit et al., 2003; Orchard et al., 2003). There is immunological and genomic evidence that aggressive and indolent patients represent two distinct subgroups of MCL varying in their distinct clinical course of the disease (Fernandez et al., 2010; Vizcarra et al., 2001). Over the last decade several groups have identified these two subtypes of MCL, resulting in the term **indolent MCL**.

In 2002 Angelopolou and colleagues described a distinct clinical group of patients fulfilling MCL diagnostic criteria that presented with a more indolent clinical course characterized by splenomegaly, leukemic presentation and absence of lymphadenopathy as compared to classical MCLs (Angelopoulou et al., 2002). In a subsequent study, Orchard and colleagues studied a series of MCL patients harboring the t(11;14), and divided the patients in nodal or non-nodal MCL. They observed that **non-nodal MCLs**, contrary to conventional nodal MCLs, presented with less complex karyotypes, no

lymphadenopathy, and followed an indolent clinical course of the disease without the need for treatment. Furthermore, the median overall survival (OS) of non-nodal patients was much larger than nodal MCLs (Orchard et al., 2003).

Concordant with these observations, Martin and colleagues performed a retrospective cohort study to evaluate the results of deferred initial therapy and noted that a significant number of patients could go months to years before requiring treatment pointing to a more indolent course of MCL (Martin et al., 2009). In another study, Ondreijka and colleagues also reported a series of indolent MCL patients with leukemic presentation that were asymptomatic, had simple karyotypes, low level lymphocytosis without lymphadenopathy or splenomegaly and hardly any BM involvement (Ondrejka et al., 2011).

Furher studies over the last 10 years have identified more indolent MCL subtypes with a non-nodal presentation, some with disease location primarily in the BM and/or spleen. Leukemic presentation is also common and not related to negative prognosis, as opposed to conventional, nodal MCL. The prognosis of non-nodal MCL is better than that of typical, nodal MCL, and the tumors express the characteristic immunophenotype of MCL with expression of CD19, CD20, CD5 and surface IgL chain expression. Moreover, the classical t(11;14)(q13;q32) is also present in this group of patients (Hsi and Martin, 2014).

In 2010 Fernàndez and colleagues performed a GEP study in order to elucidate putative biomarkers distinguishing aggressive from indolent MCL. The authors performed a comparison of clinicopathologic features, gene expression and genomic profiles between conventional and indolent MCL. A first unsupervised analysis showed that both subtypes of the disease clustered together compared to other lymphoid neoplasms analyzed (chronic lymphocytic leukemia (CLL), FL, small marginal zone lymphoma (SMZL), hairy cell leukemia (HCL) and HCL variant (HCLv), implying that they belong to the same disease entity (Fernandez et al., 2010).

Interestingly, a supervised analysis showed that indolent MCLs lack the expression of a 13-gene signature that belongs to the protein family of the HMG and hepatoma-derived growth factor related protein (HDGFRP) which comprises genes involved in B cell proliferation and lymphomagenesis. Among the most differentially expressed genes the study identified *SOX11*, *HDGFRP3* and HMG-BOX3 (*HMGB3*) as being overexpressed

in aggressive MCL and absent in indolent MCL and other NHLs (Fernandez et al., 2010) (Figure 15). These data suggested that these genes could represent candidates directly involved in the aggressive behavior of MCL.

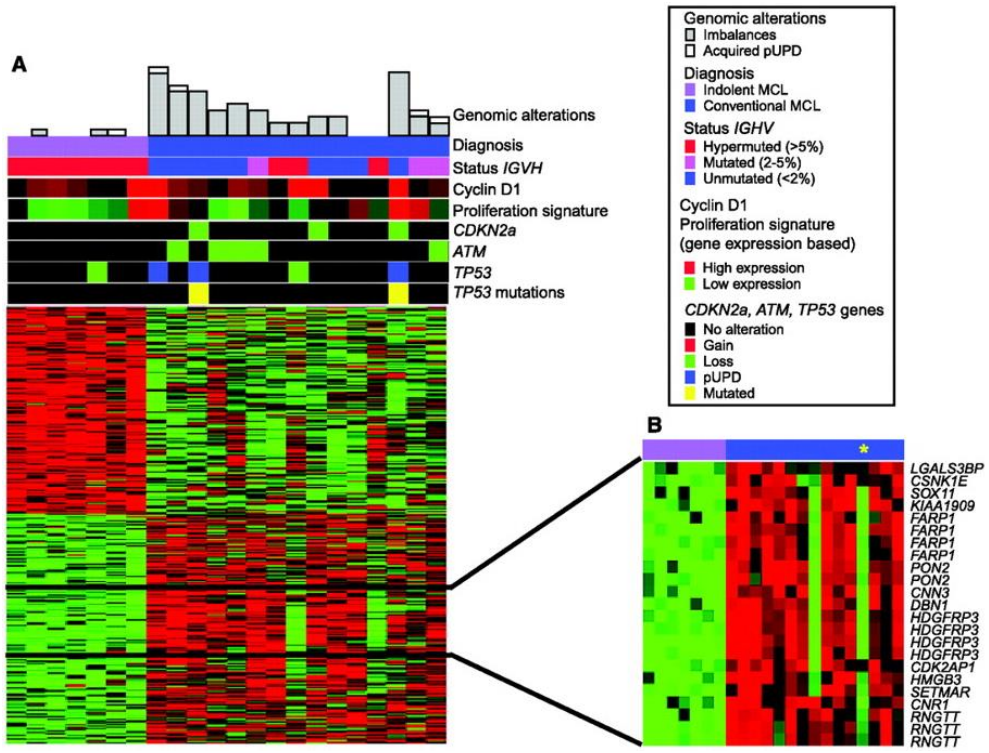

Figure 15. GEP of several B cell lymphomas. *(A) Characterization of indolent MCL according to their genetic and molecular features. The genomic complexity is illustrated in the bar plots at the top of the panels, reflecting the number of alterations for each case. The plot below indicates the diagnosis of the cases. Violet, iMCL; blue, cMCL. IGVH gene status of all MCL cases is indicated by color (red, >5% mutations; pink, 3–5% mutations; blue, 0–2%). Bright red, high expression; green, low expression. (B) Differential signature between indolent and conventional MCL. Probe sets that showed a highly significant differential expression between indolent and conventional MCL are highlighted (Fernandez et al., 2010).*

In a subsequent study in 2012, Royo and colleagues interrogated whether a three-gene signature comprising the expression of *SOX11, HDGFRP3* and drebrin 1 *(DBN1*) could discriminate conventional from indolent, non-nodal MCL patients. This signature was derived from the 13-gene signature previously identified by Fernàndez and colleagues. They performed an unsupervised hierarchical clustering analysis of the tumors according to the expression of this three-gene signature and identified two clusters of MCL with relatively high or low expression of the three genes. These two subgroups of MCL had significant differences in clinical and biological features. Lymphadenopathy and chemotherapy treatment were more frequent in patients carrying tumors with high than low expression signature. Also, the clinical outcome was significantly different in

these two subgroups of patients with a strikingly lower 5-year OS rate for the group with high expression signature compared to patients with low expression signature (Royo et al., 2012).

Adding to MCL heterogeneity, there is an emerging interest in another form of indolent MCL or precursor to MCL different from indolent non-nodal MCL that has recently appeared in the literature designated as ***in situ* MCL** (Adam et al., 2012; Bassarova et al., 2008). It is associated with a low tumor burden and a lack of symptoms related to a lymphoproliferative disorder. It presents monoclonal CCDN1-positive lymphocytes and the hallmark t(11;14) translocation. These CCND1-positive B cells are restrictively found in the mantle zones of reactive lymphoid follicles which are not usually expanded, and no tumor cells spread into interfollicular areas (Carvajal-Cuenca et al., 2012; Richard et al., 2006). The clinical course is indolent with leukemic involvement and no need for treatment. The incidence of this very early or precursor form of MCL is uncertain and an *in situ* MCL in tissue is quite rare (Hsi and Martin, 2014). Although the evidence that these *in situ* MCLs progress to overt lymphoma is limited, they may represent a very early event in MCL lymphomagenesis and may correspond to the tissue counterpart of the circulating cells with the t(11;14) (Carvajal-Cuenca et al., 2012).

3.1.5. Cell of origin and normal cellular counterpart

Sequencing the V region of the *IGVH* genes has provided new insights into the clonal origin of chronic B cell malignancies. An absence of somatic mutations is consistent with an origin from a pre-GC B cell, whereas tumors that show SHM arise either from GC-B cells or from post-GC memory cells. Some B cell malignancies typically arise from one or other of these groups.

In MCL, sequence analyses of the t(11;14) breakpoint regions have shown that this chromosomal translocation arises early in B cell ontogeny in the BM, at the pre-B cell stage of differentiation when the cell is undergoing recombination of the V(D)J segments of the *IGHV* region (Jares and Campo, 2008; Jares et al., 2012; Orchard et al., 2003; Welzel et al., 2001).

The topographic distribution of the tumor cells surrounding GCs and their co-expression of IgM/IgD and CD5 resemble the phenotype and topographic distribution of normal CD5-positive naïve B cells which produce low affinity polyreactive antibodies and

colonize the normal mantle zone of the lymphoid follicles and tend to recirculate. Therefore, MCL has been considered to derive from this naïve B lymphocyte population. Although the initial t(11;14) translocation takes place at an immature stage of B cell development, all these observations suggest that the selective advantage of the translocation and thus, the complete neoplastic phenotype occurs in later stages of development, specifically at the mature naïve pre-GC B lymphocyte (Jares and Campo, 2008; Welzel et al., 2001).

Nonetheless, recent studies analyzing the BCR diversity have changed this concept to a more complex oncogenic developmental model where Ag selection is important for MCL pathogenesis. Studies on *IGHV* mutational status have revealed that 15-40% MCLs present *IGHV* hypermutations, suggesting that these tumors derive from cells that have experienced and undergone the microenvironment and mutational machinery of the GC (Jares and Campo, 2008; Jares et al., 2012). However, the mutational rate in MCL is lower compared to other B cell neoplasms suggesting a weaker influence of the GC microenvironment (Jares and Campo, 2008).

Several studies showing a strong bias in the *IGHV* gene repertoire such as the use of *IGHV3-21, IGHV3-23* and *IGHV4-34* (Hadzidimitriou et al., 2011; Thorselius et al., 2002; Walsh et al., 2003) indicate that these tumors may originate from specific populations of B lymphocytes. Tumors with *IGHV3-21* mainly occur in unmutated MCLs with longer survival and less genomic instability (Camacho et al., 2003; Thelander et al., 2005).

Notably, MCL tumor cells with non-nodal, leukemic presentation, better survival and clinical presentation present more frequently mutated *IGHV* genes (Navarro et al., 2012; Ondrejka et al., 2011; Royo et al., 2011), indicating that these cells may have undergone the GC reaction. In previous studies, Nodit and colleagues had also identified MCLs with indolent clinical course harboring the classical t(11;14) with leukemic involvement, no lymphadenopathy and mutated *IGHV* genes (Nodit et al., 2003). Orchard and colleagues also identified that non-nodal MCL patients harboring the t(11;14) presented with *IGHV* genes and a median OS much larger than nodal MCLs (Orchard et al., 2003). Moreover, 10% MCLs present with stereotyped heavy complementarity-determining region 3 (VH CDR3) sequences, suggesting a role of Ag-driven selection in the clonogenic expansion of MCL tumor cells (Jares et al., 2012).

All these results shift the historical developmental model of MCL towards a more complex scenario with possibly several cell types dominating in different subtypes of MCL. First, MCLs with no mutations in their *IGHV* genes may derive from naïve B lymphocytes whereas MCLs with low number of somatic mutations may derive from intermediate cells between naïve and GC-cells or transitional B cells from the MZ. These tumors are genetically unstable and tend to accumulate alterations in genes deregulating cell cycle, DNA damage response pathways, and cell survival mechanisms.

Alternatively, MCL with stereotyped BCR and high mutational load on their *IGHV* may be Ag-selected and have originated from cells which have experienced the GC reaction microenvironment. These tumor cells tend to spread to the peripheral blood and spleen more than to lymph nodes, and the disease seems to be stable for long periods of time (Figure 16).

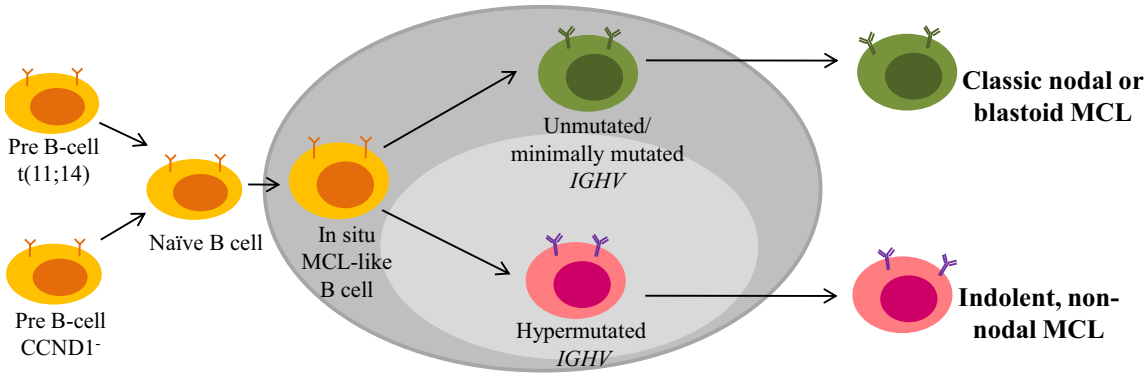

Figure 16. Hypothetical model of the development of different molecular subtypes of MCL. *The naïve B cell carrying the t(11;14) colonizes the mantle zone (dark grey) of the lymphoid follicle and generates an in situ MCL lesion. Most MCLs evolve from these cells or cells in the MZ with no or limited IGHV somatic mutations (green). Alternatively, some genetically stable cells with the t(11;14) may enter the GC (light grey) and undergo IGHV SHM (pink).*

4. The *SOX* gene family of transcription factors

SOX genes encode TFs belonging to the HMG superfamily. Members of the *SOX* gene family were first identified through homology of the HMG domain to the testis-determining factor, SRY. Located on the Y chromosome of mouse and human, *Sry* is a decisive factor for male sex determination in mammals.

The HMG protein family comprises architectural non-histone proteins thought to be involved in gene regulation and maintenance of chromatin structure. One of the common characteristics of HMG proteins is the presence of a DNA-binding domain called the HMG domain, consisting of approximately 80 residues. They have a twisted L-shape structure that presents a concave surface made up of three alpha helices and the N- and C-terminal strands (Bewley et al., 1998) (Figure 17).

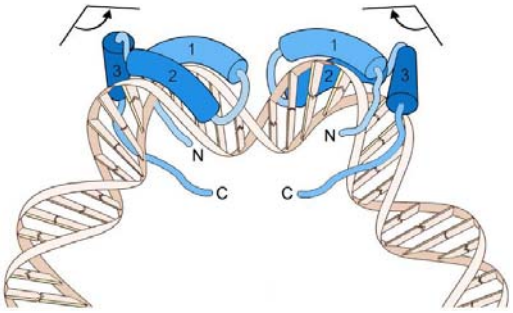

Figure 17. Unique structural and functional features of the SOX HMG box domain*. This domain is folded into an L-shape composed of three alpha helices. It contacts the DNA double helix in the minor groove and forces it to bend to an angle varying between 30º and 110º. Two HMG box domains are shown, binding in opposite orientation on DNA. Their alpha helices are shown as cylinders. Sequences N-terminal and C-terminal to the HMG box domains and sequences linking the helices are shown as thin rods. The DNA bending angle is schematized above the HMG box domains (Lefebvre et al., 2007).*

While most other types of DNA-binding proteins contact the DNA major groove and only induce minor changes of the DNA conformation, the two arms of the L-shaped HMG domain bind DNA in the minor groove, intercalate amino acid side chains between DNA base pairs, and induce a significant bend of the DNA helix. The minor groove is widened and the major groove compressed. HMG domain proteins are thus unique in their ability to alter the conformation of DNA and to increase its protein accessibility and plasticity. They thereby facilitate the formation of enhanceosomes, functionally active complexes of TFs on gene enhancer sequences (Lefebvre et al., 2007).

Two groups of HMG domains have been classified on the basis of their DNA-binding properties: HMG1 and related proteins bind to distorted DNA structures in a sequence unspecific manner, whereas TFs such as SOX proteins recognize and bind to specific DNA sequences (Bewley et al., 1998). Like the HMG class of proteins, SOX factors contain a 79-amino-acid, DNA-binding HMG domain and regulate gene transcription (Wegner, 1999), recognizing the consensus motif, 5'-(A/T)(A/T)CAA(A/T)G-3' in the minor group of the DNA, inducing large conformational changes. When bound to DNA, the structure of SOX proteins is not significantly altered. However, the DNA strand bends and the minor groove widens (Werner et al., 1995).

It is suggested that the role of SOX proteins is partly architectural, allowing other TFs to bind the major groove, and/or bringing together regulatory elements and thereby facilitating the formation of protein complexes. In addition, it has been shown that sequences outside the HMG box may facilitate interactions and influence the specificity of SOX proteins (Wilson and Koopman, 2002). There have been described different classes of SOX partners, co-factors and protein-protein interactions that can be divided in three main groups: 1) DNA-binding proteins that partner with SOX proteins to regulate gene expression; 2) adaptor proteins that link SOX factors to other proteins, and 3) importins that are required for the nuclear import of SOX proteins (Figure 18).

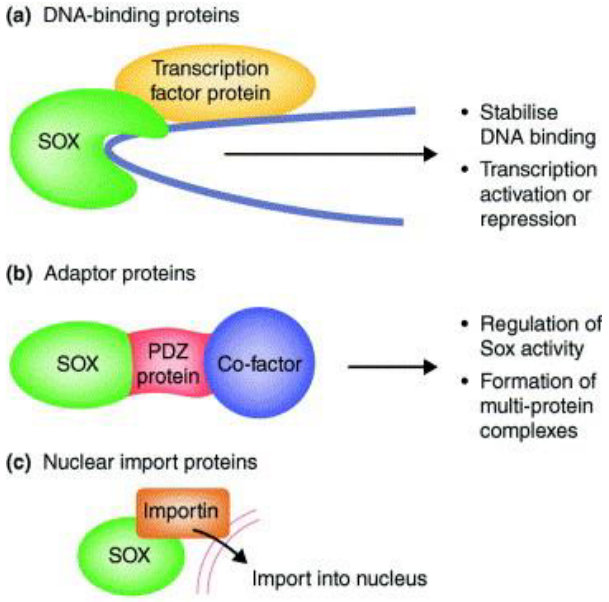

Figure 18. SOX protein-protein interactions *(Wilson and Koopman, 2002).*

SOX genes are conserved across species and show tissue-specific expression patterns. Knock-out experiments demonstrated that these genes play key roles in embryonic

development. As a whole, the SOX family controls cell fate and differentiation in a multitude of processes, such as male differentiation, stemness, neurogenesis, and skeletogenesis (Lefebvre et al., 2007). There are more than 20 gene members of the SOX family that have been identified in several species, and can be divided in eight groups (from A to H, with two B subgroups, B1 and B2) depending on their homology degree inside or outside the HMG domain. Most feature a transactivation or transrepression domain and thereby also act as typical TFs.

SOX proteins within the same group share a high degree of identity (generally 70-95%) both within and outside the HMG box, whereas SOX proteins from different groups share partial identity (≥46%) in the HMG box domain and none outside this domain (Lefebvre et al., 2007). Furthermore, members of the same group of SOX proteins tend to have similar genomic organizations in mammals. For example, SOX proteins belonging to groups B and C are intronless, whereas members of groups D-G possess an exon-intron structure (Wegner, 1999).

Each *SOX* gene has distinct expression patterns and molecular properties, often redundant with those in the same group and overlapping with those in other groups. For example, SOX proteins belonging to the subgroup B (SOX1, SOX2 and SOX3) can perform similar functions in the developing nervous system and can be functionally redundant. Group C proteins SOX4, SOX11 and SOX12 also show overlapping expression in the developing central and peripheral nervous systems (Kuhlbrodt et al., 1998a).

Most SOX proteins also feature one or several other functional domains outside the HMG box. These domains have generally been highly conserved among orthologues as well as among members of the same group, and they are totally different between proteins from distinct groups. They include transactivation, transrepression and dimerization domains (Lefebvre et al., 2007). Additionally, the SOX HMG box domain contains two nuclear localization domains that are independent of each other and that have been highly conserved in all SOX proteins.

4.1. Cancer involvement of *SOX* genes

In addition to sex differentiation, *SOX* genes regulate a number of processes including germ layer formation and nervous system development (Wegner, 1999). Many studies suggest a role for many of the SOX factors in cell-type specification and cellular differentiation. For example, SOX9 is implicated in chondrocyte differentiation (Bi et al., 1999), SOX10 in neural crest specification (Kuhlbrodt et al., 1998b), SOX17 in endoderm specification (Hudson et al., 1997), and SOX18 in endothelial cell (EC) differentiation (Pennisi et al., 2000).

Regarding cancer biology, overexpression and/or amplification of *SOX* genes have been associated with a large number of tumor types *in vivo*. SOX1, SOX2, SOX3 and SOX21 are significantly downregulated in adult tissues (Gure et al., 2000), but are upregulated in lung carcinoids and lung squamous cell carcinomas (Dong et al., 2004a). *In vitro* studies showed that ectopic Sox3 expression induced oncogenic transformation of chicken embryonic fibroblasts, and this effect was shown to depend upon both the HMG and transactivation domains (TADs) of the gene (Xia et al., 2000). In addition, *Sox3* was identified, amongst several known proto-oncogenes in a genome-based analysis of retroviral insertion sites in mouse T cell lymphomas, further suggesting that this *Sox* gene may play a role in tumorigenesis (Kim et al., 2003).

SOX4 and SOX11 are of interest in respect to neurological cancers, and both are strongly expressed in most medulloblastomas (Lee et al., 2002). In addition to neurological cancers, SOX4 has been implicated in several tumor types. Its expression is increased in malignancies of the pancreas and ovary, and its expression has been associated with oncogenic transformation in adenoid cystic carcinoma (Frierson et al., 2002). Furthermore, SOX4 is also highly expressed in subcutaneous human hepatocarcinoma mouse xenografts. Expression of SOX4 mRNA is upregulated in breast cancer cell lines, indicating that SOX4 may also be involved in oncogenic transformation in the breast (Graham et al., 1999). In line with these studies, SOX4 has also been identified as a potential regulator of the human breast cancer oncogene, *HER2/neu* (*c-ErbB2*) (Chang et al., 1997).

SOX8 and SOX9 are both also potential genetic markers for cancer. Although *SOX9* is considered a master regulator gene for cartilage differentiation, a study indicates that it is expressed in mesenchymal chondrosarcomas, but not in other small cell malignancies,

lymphomas and leukemias (Wehrli et al., 2003). Sox8 is expressed in the immature glia of developing chick cerebellum as well as cells scattered throughout medulloblastomas, providing a useful marker for these tumors (Cheng et al., 2001).

SOX10 is overexpressed in melanoma tumors as compared to normal tissue (Khong and Rosenberg, 2002), and is critical for regulation of melanocyte development as a transactivator of micropthalmia-associated transcription factor (*MITF*), a master gene for development and postnatal survival of melanocytes (Bondurand et al., 2000). In addition to melanomas, further analyses revealed expression of SOX10 in anaplastic oligodendroglioma and mammary adenocarcinoma cell lines (Dong et al., 2004a).

Other studies revealed higher expression levels of SOX18 mRNA in gastric cancer cell lines, pancreatic cell lines and embryonic tumor cell lines compared to other tissues (Saitoh and Katoh, 2002). Additional analyses showed that SOX18 mRNA is expressed in a number of cancers including melanotic melanomas, neuroblastoma cells, pancreatic carcinomas and a number of ovarian and uterine cancers (Dong et al., 2004a).

4.2. SOXC subgroup of transcription factors

SOX4, SOX11 and SOX12 constitute the group C of SOX proteins. They are single-exon genes highly conserved through vertebrates that are co-expressed in embryonic neuronal progenitors and in mesenchymal cells in many developing organs. They feature two functional domains: a SOX DNA-binding domain and a TAD, located at the N- and C-terminal of the protein, respectively (Dy et al., 2008) (Figure 19).

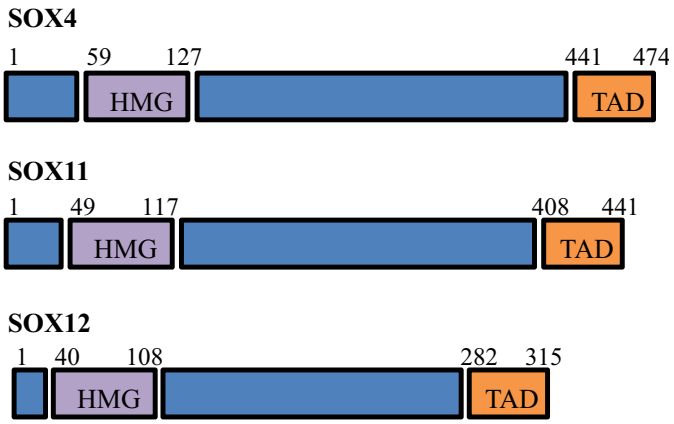

Figure 19. Schematic representations of human SOXC group proteins. *SOX4 (474 aa), SOX11 (441 aa) and SOX12 (315 aa). Adapted from (Penzo-Mendez, 2010).*

The HMG box is 84% identical across all vertebrate SOXC proteins. SOX4 binds DNA more efficiently than SOX12, whereas SOX11 binds it very weakly (Dy et al., 2008; Wiebe et al., 2003). Removal of the C-terminus increases the binding efficiency of SOX11 and SOX12, suggesting that the TAD may be inhibitory. Two acidic domains in SOX11 also inhibit DNA binding, perhaps by providing a hinge that facilitates masking of the HMG box by the TAD (Penzo-Mendez, 2010).

The TAD is only 66% identical across all vertebrate SOXC proteins, but it is 97% identical amongst SOX4 and SOX11 orthologues, and 79% identical amongst SOX12 orthologues (Dy et al., 2008). This 33-residue domain is predicted to form a 20-residue long alpha helix that would be continuous in SOX11, but interrupted by three and seven residues in SOX4 and SOX12, respectively. Consistent with the notion that this configuration may be essential for the strength of the TAD, SOX11 is the most potent and SOX12 the least potent of the three proteins in activating transiently transfected reporter genes (Dy et al., 2008; Hoser et al., 2008; Wiebe et al., 2003).

SOXC proteins are able to cooperate with protein partners and some reports indicate that protein interactions may also be used by the SOXC proteins to regulate non-transcriptional targets. SOX4 was found to bind to *TP53* and thereby prevent p53 degradation in lung non-small cell carcinoma cells (Pan et al., 2009). Protein interaction occurred both between the SOX4 and p53 DNA-binding domains and the SOX4 TAD and p53 regulatory domain.

SoxC expression studies in vertebrates suggest that SoxC functions have been conserved through evolution. Expression of Sox4 and Sox11 in chick embryos was reported to be very similar to that in mice (Maschhoff et al., 2003). The two *Sox11* genes of the zebrafish have distinct expression patterns, but their combined expression is similar to that in chick and mouse embryos, further suggesting that Sox11 functions have been conserved (de Martino et al., 2000).

The expression pattern of the *SOXC* genes and the molecular properties of their proteins strongly suggest that these genes could play critical roles in development. *Sox4*-null mice die at embryonic day 14 (Schilham et al., 1996) showing severe malformation of the heart outflow tract, which leads to circulatory failure. *Sox11*-null mice die immediately after birth from similar but less severe heart outflow tract malformations

(Sock et al., 2004). On the contrary, *Sox12*-null mice have no obvious malformations and a normal lifespan and fertility (Hoser et al., 2008).

Other studies have started to reveal critical roles for SOX4 and SOX11 in multiple major developmental processes. For example, RNA knockdown of Sox4 and Sox11 in neural tubes of chick embryo blocked neuronal gene expression while forced expression of Sox4, Sox11 or Sox12 resulted in neuronal gene upregulation. Other studies showed that forced expression of Sox4 resulted in impaired oligodendrocyte differentiation in mice (Potzner et al., 2007), suggesting that the *SoxC* genes may both promote differentiation of progenitor cells into neurons and prevent differentiation into glia.

SOX4 is very widely expressed during embryogenesis in brain, gonads, lung, heart and thymus, and is also a very prominent TF in lymphocytes of the B and T cell lineages (van de Wetering et al., 1993). Studies of SOX4 on B lymphocyte differentiation showed that it is required for this process as its targeted deletion in the mouse led to a block in early B cell development at the pro-B cell stage (Schilham et al., 1996), similar to that observed for PAX5. Although T cells also express SOX4, there was only a mild effect of SOX4 deletion on T cell development (Schilham et al., 1997), suggesting that it is essential for B cell development, but only of minor importance for T cell development.

Other studies have suggested that the *SOXC* genes may also be important in specific cell lineages to promote cell proliferation or survival. *Sox4* heterozygous adult mice develop osteopenia, with low osteoblast numbers and low-level expression of osteoblast markers, and Sox4 knockdown impaired proliferation and differentiation of osteoblasts *in vitro* (Nissen-Meyer et al., 2007). Similarly, *Sox4*-null pancreatic explants displayed severely reduced numbers of insulin-producing beta cells (Wilson et al., 2005), and knockdown of the Sox4b in zebrafish embryos resulted in loss of glucagon-producing cells (Mavropoulos et al., 2005). Taken together, these data strongly support the notion that *SOXC* genes regulate differentiation in multiple cell lineages.

4.3. SOX11

Human *SOX11* gene is mapped at chromosome 2p25.3 and it is homolog to *SOX4* with a 55% identity homology in the C-terminal TAD and 86% identity in the HMG domain (Wegner, 1999). It functions as a TF involved in embryonic tissue remodeling and neurogenesis, and among the SOXC group it is the best analyzed gene for its expression in the nervous system. SOX11 is normally expressed throughout the developing nervous system of human embryos and is required for neuron survival and neurite growth.

In the central nervous system, it is co-expressed in the neuroepithelium with SOX1, SOX2 and SOX3 on a low level and transiently upregulated in cells that leave the neuroepithelium. As these cells simultaneously downregulate SOX2 and SOX3, a model was postulated in which neural differentiation is characterized by an ordered switch from one group of SOX proteins to the next.

Another interesting aspect of SOX11 concerns its expression in a subset of differentiating brain regions during late embryonic development, indicating that SOX11 is not only important for the development of early neural precursors, but might also be involved in the differentiation of distinct neuronal subpopulations (Kuhlbrodt et al., 1998a). A murine study showed that survival and growth of primary cultures established from normal neurons were dependent on SOX11 (Jankowski et al., 2006), and a knock-out mouse model of several malformations showed that *Sox11* is important for tissue remodeling and that mutated *SOX11* in humans could be associated with malformation syndromes (Sock et al., 2004).

Outside the nervous system, SOX11 seems to be primarily expressed at places of epithelio-mesenchymal interactions including somites, branchial arches, developing face and limbs (Hargrave et al., 1997).

4.3.1. SOX11 in cancer

The function of SOX and other members of the family are still ill-defined. However, the relevance of the *SOXC* genes has risen to a high level in recent years as numerous reports have suggested that the *SOXC* genes may contribute to tumor prognosis. SOX4 and SOX11 have been shown to be highly expressed in most medulloblastomas (Lee et al., 2002). Increased SOX4 expression is also associated with bladder (Aaboe et al., 2006), prostate (Liu et al., 2006), colon (Andersen et al., 2009), and non-small cell lung

tumors (Medina et al., 2009). High expression of SOX11 is associated with gliomas (Weigle et al., 2005), NH-B cell lymphomas (Wang et al., 2008) and epithelial ovarian tumors (Brennan et al., 2009; Sernbo et al., 2011). Recently, SOX11 was found highly expressed in breast cancer (Lopez et al., 2012), and in a subsequent study by Zvelebil and colleagues it was observed that breast cancer patients expressing higher levels of SOX11 showed a worse OS than did those with tumors expressing lower levels (Zvelebil et al., 2013).

4.3.2. SOX11 in mantle cell lymphoma

Since the last decade, studies in MCL started to point to a complex role of SOX11 in the pathogenesis of the disease. Although its expression has not been detected in any normal hematopoietic cells, SOX11 is expressed at high levels in virtually all MCL cells compared to naïve B cells and other B cell lymphomas except for some BLs, lymphoblastic lymphomas (LBLs) and T cell-prolymphocytic leukemias (T-PLLs) (Dictor et al., 2009; Ek et al., 2008; Mozos et al., 2009). Strikingly, it is highly expressed in both cyclin D1-positive and -negative MCL tumors, suggesting that it may represent a valuable diagnostic biomarker as well as an important factor for pathogenesis in MCL (Jares et al., 2012; Mozos et al., 2009) (Figure 20).

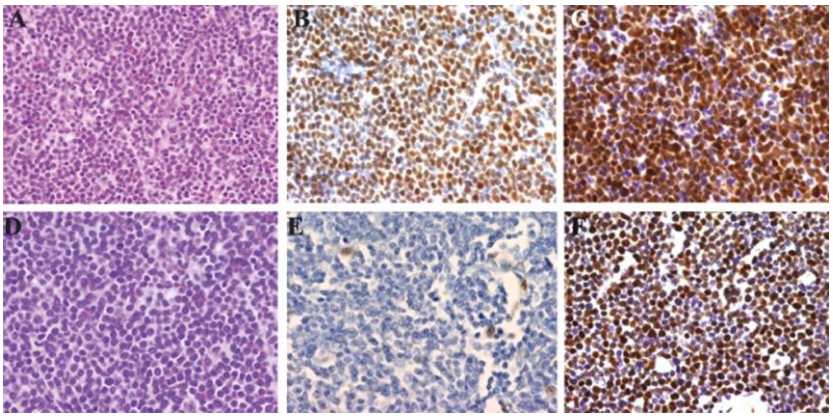

Figure 20. SOX11 protein expression in conventional and cyclin D1-negative MCL*. (A,D) H&E staining in conventional and cyclin D1-negative MCL, respectively; (B, E) Cyclin D1 and (C, F) SOX11 expression in conventional and cyclin D1-negative MCL, respectively (Mozos et al., 2009).*

The GEP study performed by Fernàndez and colleagues in 2010 was one of the first works elucidating biomarkers distinguishing aggressive from indolent MCL. The 13-gene signature downregulated in the indolent MCL group of patients showed that *SOX11* was one of the genes that best discriminated indolent versus aggressive

presentation of the disease (Fernandez et al., 2010), suggesting that SOX11 could represent a candidate directly involved in the aggressive behavior of MCL.

Subsequently, a study by Ondreijka and colleagues showed that a series of asymptomatic, indolent non-nodal MCL patients lacked SOX11 expression compared to patients with the aggressive clinical presentation of the disease and SOX11-positivity (Ondrejka et al., 2011). The detection of SOX11 by immunohistochemistry (IHC) or quantitative PCR in a larger series of patients confirmed the relationship between SOX11 lack of expression, hypermutated *IGHV*, low karyotype complexity, non-nodal leukemic disease, and longer survival with stable disease in independent cohorts of patients (Navarro et al., 2012; Royo et al., 2012).

However, the role of SOX11 predicting MCL survival and pathogenesis remains controversial. Contrary to the reported findings, Nygren and colleagues found that low SOX11 expression was associated with a predicted worse OS in a large group of MCL patients. They found that SOX11-negativity was associated with a higher frequency of lymphocytosis, elevated lactate dehydrogenase (LDH) and TP53-positivity (Nygren et al., 2012). Nevertheless, further studies have shown that the aggressive behavior of SOX11-negative MCL seems related to an extensive nodal disease, blastoid morphology, complex karyotypes and 17p/*TP53* alterations (Navarro et al., 2012; Royo et al., 2012). One explanation would be that SOX11-negative tumors with aggressive disease could correspond to a progressed or transformed stage with generalized lymphadenopathy, suggesting that this phenotype may have an indolent phase and eventually some of the tumors could progress with a generalized lymphadenopathy and aggressive behavior associated with acquisition of *TP53* mutations or other genetics events (Jares et al., 2012). In fact, most SOX11-negative MCLs in the Nygren study had *TP53* alterations (Nordstrom et al., 2014).

SOX11 is not expressed in any hematopoietic cell or in any of the normal B cell differentiation stages. Likewise, little is known about the molecular mechanisms driving SOX11 expression in MCL cells. A study by Gustavsson and colleagues described for the first time a strong correlation between promoter methylation status and SOX11 mRNA and protein levels both in B cell lymphoma cell lines and primary tumors (Gustavsson et al., 2010). Subsequent studies have also interrogated the mechanisms by which SOX11 becomes activated in aggressive neoplasms, and shown that SOX11

expression in normal and neoplastic lymphoid cells is regulated by epigenetic changes rather than promoter methylation, mainly by a change from inactive to activating histone marks (Vegliante et al., 2011; Wasik et al., 2013).

Although SOX11 is a reliable biomarker of a subtype of MCL, its prognostic impact still has to be evaluated. The identification of alterations in potent oncogenes seems to be clarifying the discrepancies observed in the indolent versus aggressive clinical presentation of the SOX11-negative MCL patients. However, SOX11-regulated target genes and transcriptional programs contributing to MCL pathogenesis still remain to be elucidated.

5. Tumor microenvironment

Cancers develop in complex tissue environments which they depend upon for sustained growth, invasion and metastasis. Interactions between malignant and non-transformed cells create the tumor microenvironment (TME) in which the non-malignant cells have a dynamic and often tumor-promoting function at all stages of carcinogenesis (Hanahan and Coussens, 2012). The TME comprises innate and adaptive immune cells, stromal cells, extracellular matrix (ECM), and blood and lymphatic vascular networks, which collectively have critical modulatory functions in tumor development and metastasis (Figure 21). Intercellular communication is driven by a complex and dynamic network of cytokines, chemokines, growth factors, and inflammatory and matrix remodeling enzymes (Balkwill et al., 2012).

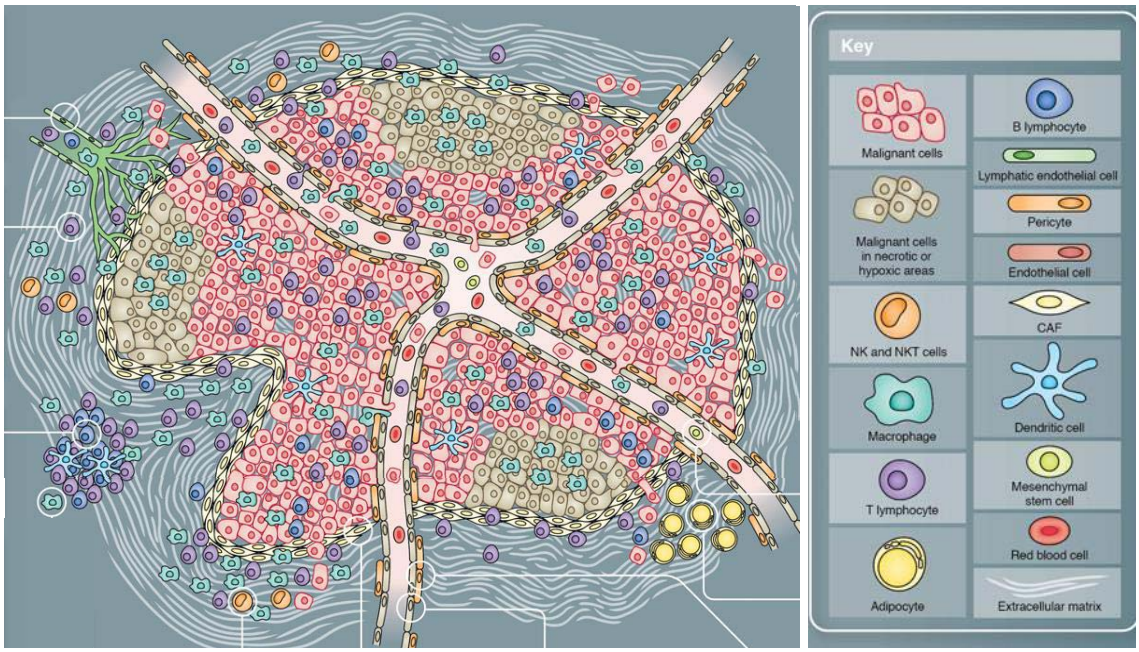

Figure 21. Cellular landscape involved in the TME *(Balkwill et al., 2012).*

5.1. Tumor microenvironment in B cell malignancies

As with other malignancies, it has been demonstrated that the development and progression of B cell lymphomas involve complex interactions between the neoplastic B cells and the surrounding microenvironment, including stromal cells that favor the survival of malignant cells, various subsets of T cells that may support the disease progression, overcoming the antitumor effect exerted by still other specific T cell subsets, ECs that organize neoangiogenetic microvessels as well as various types of macrophages (Burger et al., 2009). In lymphomas, it appears that this network of

stromal cells creates a microenvironment that initially attracts cancer cells, allowing their early survival, and subsequently contributes to tumor growth (Gascoyne et al., 2010).

Recent gene expression array data have emphasized the roles of the various components of the microenvironment, demonstrating the importance of the microenvironment in B-NHLs. Compelling evidence suggests that cross-talk with accessory stromal cells in specialized tissue microenvironments, such as the BM and secondary lymphoid organs, favors disease progression by promoting malignant B cell growth and drug resistance (Burger et al., 2009; Burger and Kipps, 2002).

Many cytokines, chemokines and adhesion molecules are implicated in cross-talk between stromal cells and neoplastic lymphocytes. The balance between specific ligands and their receptors determines whether there is tumor cell growth promotion or inhibition (Coupland, 2011). The role of cytokine, chemokine and adhesion molecules has been extensively demonstrated in multiple myeloma (MM), some forms of B-NHLs, including FL and DLBCL, and classical Hodgkin lymphoma (cHL). However, it is considerably less explored in MCL. Soluble mediators, including interleukin (IL)6, IL7, IL4, IL8, vascular endothelial growth factor (VEGF), C-X-C chemokine receptor type (CXCR)4, MIP1, Jagged 1 and insulin growth factor 1 (IGF1), appear to play a role in the communications between the accompanying stroma and the tumor cells (Aldinucci et al., 2010; Calvo et al., 2008; Gascoyne et al., 2010).

In MM, BM stromal cells secrete IL6 and VEGF, leading to activation of tumor proliferation pathways (Bisping et al., 2003; Ria et al., 2003). Furthermore, osteoclast-mediated bone destruction in MM appears to be modulated by RANKL production by BM stromal cells (Pearse et al., 2001). *In vitro* studies with B-lineage leukemic cell lines have shown that BM stromal cells protect the leukemic cells via the PI-3K/Akt-BCL2 anti-apoptotic pathway (Fortney et al., 2002; Wang et al., 2004). In CLL, nurse-like stromal cells prevent spontaneous apoptosis of CLL cells by the secretion of stromal-cell-derived factor 1 (SDF1) (Burger et al., 2000).

Furthermore, Ag stimulation and the molecules involved in lymphocyte trafficking are more specifically operating in the microenvironments of B cell tumors, and evidence is growing that malignant B cells exploit the physiological mechanisms of tissue-specific lymphocyte migration and homing to access supportive microenvironmental niches

(Burger et al., 2009). Just as tumor derived substances can be used as prognostic markers, stromal elements can be used as biomarkers to identify tumors associated with favorable or unfavorable outcomes; or even therapeutic targets within the microenvironment itself.

5.1.1. Tumor microenvironment in mantle cell lymphoma

There is growing evidence suggesting that cross-talk between MCL cells and stromal cells in tissue microenvironments, such as the BM and secondary lymphoid organs, causes disease progression by promoting lymphoma cell survival, growth, and drug resistance. Although the intrinsic growth-promoting t(11;14) disrupts normal cell cycle regulation, extrinsic signals from the microenvironment also contribute to MCL growth and dissemination (Burger et al., 2009; Perez-Galan et al., 2011a). Some of the key molecular pathways of B cell cross-talk with the microenvironment are BCR signaling, activation of CD40 and other members of the TNF receptor superfamily, activation via TLRs and various cytokines, chemokine receptors and adhesion molecules. Data from various B cell lymphomas including limited data in MCL suggest that these pathways are also functional in malignant B cells and contribute to lymphoma progression and drug resistance (Kurtova et al., 2009; Pighi et al., 2011).

Clinical features suggest that MCL cells have a high propensity for dissemination and homing to different tissue compartments, allowing the MCL cells to interact with accessory stromal cells, such as mesenchymal stromal cells (MSCs) and lymphoma-associated macrophages (LAMs). LAMs and MSCs attract MCL cells via G protein coupled chemokine receptors CXCR4, CXCR5 (Kurtova et al., 2009) that are highly expressed on MCL cells. Very late antigen-4 (VLA4) integrin (CD49d) co-operates with chemokine receptors in adhesion and tissue retention through binding to respective stromal ligands vascular cell adhesion molecule 1 (VCAM1) and fibronectin. LAMs can also express the TNF family members BAFF and APRIL, providing survival signals to MCL cells via corresponding receptors (BCMA, TACI, BAFF-R) (Nakamura et al., 2005; Rodig et al., 2005) (Figure 22).

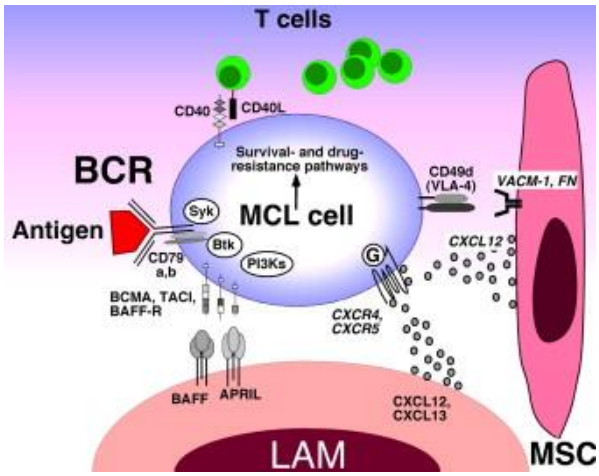

Figure 22. Cellular and molecular interactions between MCL cells and their microenvironment*. Contact between MCL cells and LAMs or MSCs is established and maintained by chemokine receptors and adhesion molecules (Burger and Ford, 2011).*

Besides the aspect of lymphoma cell trafficking and homing, interactions with the microenvironment also provide survival and drug-resistance signals to the neoplastic B cells. In stroma co-cultures, MCL become resistant to conventional cytotoxic agents via cell adhesion mediated drug resistance (CAM-DR) (Damiano et al., 1999; Kurtova et al., 2009). Such MCL-stroma interactions likely contribute to drug resistance *in vivo* and the development of (minimal) residual disease after conventional therapy, which paves the way to relapses.

Also, stimulation of the BCR complex (BCR and CD79a and b) induces downstream signaling by recruitment and activation of SYK, BTK and PI-3-K (Pighi et al., 2011; Rinaldi et al., 2006; Rudelius et al., 2006). Collectively, this cross-talk between MCL cells and accessory cells results in activation of survival and drug-resistance-pathways (Burger and Ford, 2011).

5.2. Angiogenesis

Angiogenesis is also a major player in the TME, and interactions between tumor cells and ECs play critical roles in tumor progression and maintenance. Many soluble factors present in the TME, such as VEGFs, fibroblast growth factors (FGFs), PDGFs and chemokines stimulate ECs and their associated pericytes during the neovascularization that is needed for cancer growth. When a quiescent blood vessel senses an angiogenic signal from malignant or inflammatory cells or owing to hypoxic conditions in the

TME, angiogenesis is stimulated and new vessels sprout from the existing vasculature (Balkwill et al., 2012; Carmeliet and Jain, 2011).

During embryogenesis, the development of the vasculature involves vasculogenesis and angiogenesis. While the first comprises the development of new ECs from angioblasts and their assembly into tubes, the latter represents the sprouting of new vessels from existing ones (Carmeliet and Jain, 2011). Following this morphogenesis, the normal vasculature becomes largely quiescent in the adult. During normal physiological angiogenesis, new vessels rapidly mature and become stable. By contrast, tumors, described as wounds that never heal, have lost the appropriate balances between positive and negative controls. One characteristic feature of tumor blood vessels is that they fail to become quiescent, enabling the constant growth of new tumor blood vessels. Consequently, the tumor vasculature develops unique characteristics and becomes quite distinct from the normal blood supply system (Bergers and Benjamin, 2003).

Tumor blood vessels are architecturally different from their normal counterparts; they are irregularly shaped, dilated, and tortuous, are not organized into definitive venules, arterioles and capillaries like their normal counterparts, but rather share chaotic features of all of them. The vascular network that forms in tumors is often leaky and hemorrhagic, partly due to the overproduction of VEGF (Bergers and Benjamin, 2003). Perivascular cells, which are usually in close contact with the endothelium, often become more loosely associated or less abundant.

Tumor vessels have also been reported to have cancer cells integrated into the vessel wall (Folberg et al., 2000; McDonald et al., 2000), and some tumors rely heavily on vasculogenesis, recruiting endothelial precursor cells from the BM (Lyden et al., 2001). Endothelial precursor cells can be mobilized from the BM and transported through the bloodstream to become incorporated into the walls of growing blood vessels. Factors that stimulate angiogenesis, such as VEGFA, placental growth factor (PlGF) and angiopoietin 1 (ANGPT1) have been shown to stimulate this process (Hattori et al., 2001; Hattori et al., 2002).

5.2.1. The angiogenic switch

In the adult, as part of physiological processes such as wound healing, angiogenesis is turned on but only transiently. However, during the multistage development of invasive

cancers both in animal models and in humans, angiogenesis is induced surprisingly early. Moreover, during tumor progression, an angiogenic switch is almost always activated and remains on, causing normally quiescent vasculature to continually sprout new vessels that help sustain expanding neoplastic growths (Hanahan and Folkman, 1996).

The angiogenic switch activates quiescent ECs, causing them to enter into a cell biological program that allows them to construct new blood vessels (Hanahan and Weinberg, 2011). A compelling body of evidence indicates that the angiogenic switch is governed by countervailing factors that either induce or oppose angiogenesis, the pro- and anti-angiogenic factors (Baeriswyl and Christofori, 2009; Bergers and Benjamin, 2003). Some of these angiogenic regulators are signaling proteins that bind to stimulatory or inhibitory cell surface receptors displayed by vascular ECs. The angiogenic switch can occur at different stages of the tumor-progression pathway, depending on the tumor type and the environment. It has been shown that dormant lesions, and, in some instances, pre-malignant lesions, also initiate neovascularization, which allows them to progress (Hanahan and Folkman, 1996) (Figure 23).

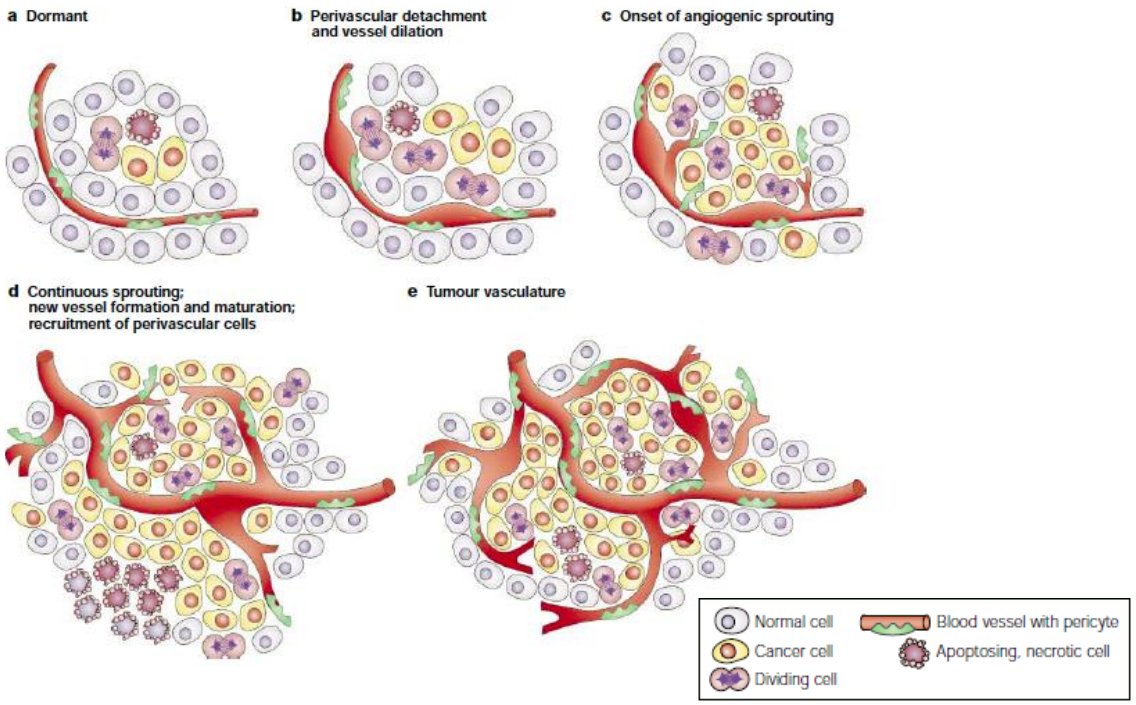

Figure 23. The classical angiogenic switch. *Most tumors start growing as dormant, avascular nodules (a) until they reach a steady-state level of proliferating and apoptosing cells. The initiation of angiogenesis, or the angiogenic switch, has to occur to ensure exponential tumor growth. The switch begins with perivascular detachment and vessel dilation (b), followed by angiogenic sprouting (c), new vessel formation and maturation, and the recruitment of perivascular cells (d). Blood vessel formation*

will continue as long as the tumor grows, and the blood vessels specifically feed hypoxic and necrotic areas of the tumor to provide it with essential nutrients and oxygen (e) (Bergers and Benjamin, 2003).

5.2.2. Molecular mechanisms of vessel branching

The molecular mechanisms of vessel branching comprise three different steps represented by i) selection of tip cell, ii) stalk elongation and tip guidance, and iii) quiescent phalanx resolution.

During the **selection of the tip cell**, when a quiescent vessel senses an angiogenic signal such as VEGF, VEGFC, ANG2, FGFs or chemokines, released by a hypoxic, inflammatory or tumor cells, proteolytic degradation by matrix metalloproteinases (MMPs) detach pericytes from the vessel wall and the basement membrane. ECs loosen their junctions, and the nascent vessel dilates. VEGF increases the permeability of the EC layer, causing extravasation of plasma proteins and formation of a provisional ECM into which ECs migrate in response to integrin signaling. Proteases liberate angiogenic molecules stored in the ECM, and remodel it into an angio-competent milieu. Then, a type of EC denominated tip cell is selected to lead the tip and build a perfused tube (Figure 24).

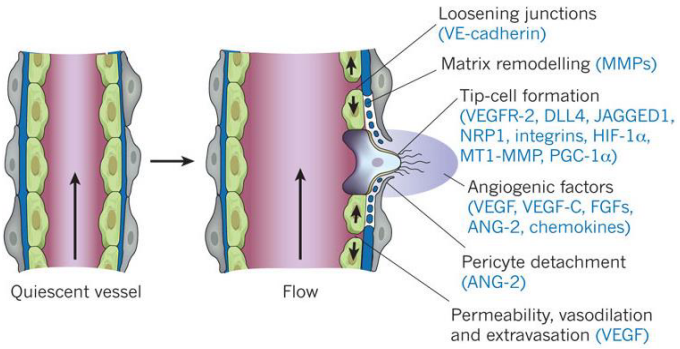

Figure 24. Selection of tip cell. *After stimulation with angiogenic factors, the quiescent vessel dilates and the tip cell is selected in the presence of different factors to ensure branch formation (Carmeliet and Jain, 2011).*

In the next step, the **stalk elongation and tip guidance,** the stalk cells, which are neighboring cells of the tip cell, divide to elongate the stalk stimulated by NOTCH, NOTCH-regulated ankyrin repeat protein (NRARP), WNTs, PlGF and FGFs and establish the lumen by VE-cadherin, CD34, sialomucins, VEGF and hedgehog. Tip cells present filopodia to sense environmental guidance signals such as ephrins and semaphorins, whereas stalk cells release molecules such as EGFL7 into the ECM to convey spatial information about the position of their neighbours, so that the stalk

elongates. A hypoxia-inducible program, driven by hypoxia-induced factor (HIF)-1α, renders ECs responsive to angiogenic signals. Myeloid bridge cells aid fusion with another vessel branch, allowing the initiation of blood flow (Figure 25).

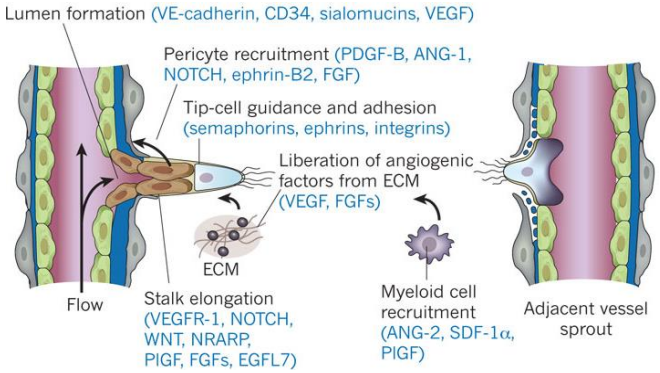

Figure 25. Stalk elongation and tip guidance. *In response to sempahorins and ephrins tip cells navigate and adhere to the ECM to migrate. Stalk cells behind the tip cell proliferate, elongate and form a lumen, and sprouts fuse to establish a perfused neovessel. Proliferating stalk cells attract pericytes and deposit basement membranes to become stabilized. Recruited myeloid cells can produce pro-angiogenic factors or proteolytically liberate angiogenic growth factors from the ECM (Carmeliet and Jain, 2011).*

The last step of the process is the **quiescent phalanx resolution**. For a vessel to become functional, it must become mature and stable. ECs resume their quiescent phalanx state, and signals such as PDGFB, ANGPT1, TGFβ, ephrin-B2 and NOTCH cause the cells to become covered by pericytes. Tissue inhibitors of metalloproteinases (TIMPs) and plasminogen activator inhibitor 1 (PAI1) are protease inhibitors that cause the deposition of a basement membrane. Then, junctions are re-established to ensure optimal flow distribution (Figure 26).

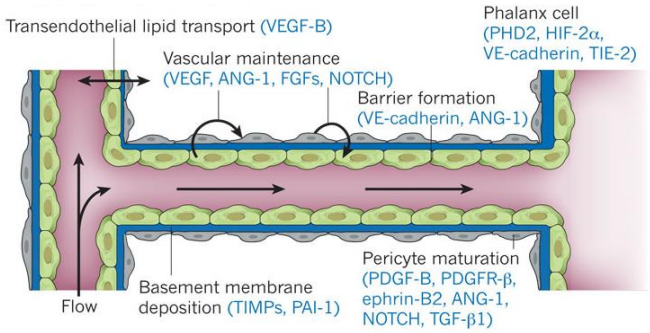

Figure 26. Quiescent phalanx resolution. *After fusion of neighboring branches, lumen formation allows perfusion of the neovessel, which resumes quiescence by promoting a phalanx phenotype, re-establishment of junctions, deposition of basement membrane, maturation of pericytes and production of vascular maintenance signals. Other factors promote transendothelial lipid transport (Carmeliet and Jain, 2011).*

5.3. Angiogenic signaling pathways

Angiogenesis is a complex process controlled by the balance of a large number of regulating factors, the pro- and anti-angiogenic factors. Although many mechanisms contribute to its induction, several signaling pathways involved in this process have been characterized.

5.3.1. VEGF family

The most important and best described molecular pathway involved in angiogenesis is the one based on VEGF/VEGFRs signal transduction. There are, to date, five growth factors in the VEGF family: VEGFA, -B, -C, -D and PlGF that do not have redundant roles. Moreover, VEGFA, VEGFB and PlGF can suffer alternative splicing, and VEGFA, VEGFC and VEGFD further processing.

VEGFRs comprise an extracellular component and an intracellular domain with a consensus tyrosine kinase sequence and each of the members of the VEGF family bind these receptors with different affinities. VEGFR1 and VEGFR2 were found to be predominantly expressed in ECs whilst VEGFR3 is primarily associated with lymphangiogenesis (Grothey and Galanis, 2009). VEGFR1 is the main receptor for VEGFB and PIGF, and during pathologic conditions such as tumorigenesis, it is a potent and positive regulator of angiogenesis (Schwartz et al., 2010). VEGFR2 mediates most of the cellular effects of VEGFA during angiogenesis, including microvascular permeability, EC proliferation, migration, and invasion (Ferrara et al., 2003). VEGFR3 binds with the highest affinities to VEGFC and VEGFD and is necessary for the formation of the blood vasculature during early embryogenesis, but later becomes a key regulator of lymphangiogenesis (Tammela and Alitalo, 2010) (Figure 27). Like VEGFR2, VEGFR3 signaling can contribute to angiogenesis in tumors in which the receptor is expressed on tumor blood vessels as well as on lymphatics (Sakurai and Kudo, 2011).

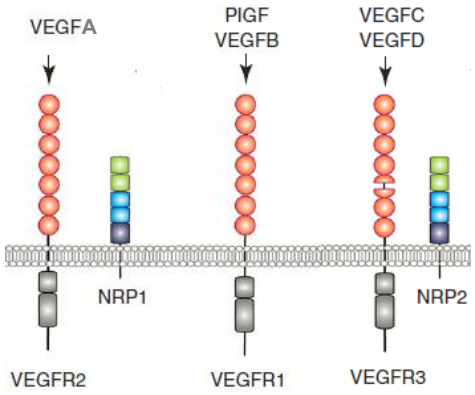

Figure 27. **VEGF family of ligands and their receptors.** Modified from (Saharinen et al., 2010).

VEGFA (or VEGF) is the predominant angiogenic factor in the TME and is produced by both malignant cells and inflammatory leukocytes; however, advanced tumors can produce a range of other angiogenic factors that can substitute for VEGFA (Carmeliet and Jain, 2011). The *VEGFA* gene encodes ligands that are involved in orchestrating new blood vessel growth during embryonic and postnatal development, and then in homeostatic survival of ECs, as well as in physiological and pathological situations in the adult (Ferrara, 2009; Nagy et al., 2007).

VEGFA is upregulated by HIF-1α, PDGFB or oncogenic signaling, and it can also be released from the ECM by MMP9 to initiate the angiogenic switch (Ferrara, 2009; Sakurai and Kudo, 2011). VEGFA upregulation mainly occurs through VEGFR2, which is expressed at elevated levels by ECs engaged in angiogenesis and by circulating BM-derived endothelial progenitor cells (Kerbel, 2008). Whereas soluble VEGFA isoforms promote vessel enlargement, matrix-bound isoforms stimulate branching. VEGFA can act both in a paracrine and an autocrine way. When released by tumors, myeloid or other stromal cells, paracrine VEGFA increases vessel branching and renders tumor vessels abnormal (Stockmann et al., 2008). However, autocrine VEGFA released by ECs maintains vascular homeostasis (Lee et al., 2007).

5.3.2. FGF family

The FGF superfamily includes 18 ligands which are among the earliest angiogenic factors reported. FGFs and their four main receptors control a wide range of biological functions, and are involved in promoting the proliferation, migration, and differentiation of vascular ECs. FGF2 (or bFGF) was among the first discovered angiogenic factors and, like FGF1 (or aFGF) it has angiogenic and arteriogenic properties. FGFs activate

FGFRs on ECs or indirectly stimulate angiogenesis by inducing the release of angiogenic factors from other cell types (Beenken and Mohammadi, 2009). Low levels of FGFs are required for the maintenance of vascular integrity, as inhibition of FGFR signaling in quiescent ECs causes vessel disintegration (Murakami et al., 2008).

FGFs have been reported to promote angiogenesis independently of VEGF (Cao et al., 2008), and FGF2 in particular has been shown to possess potent angiogenic activity (Lindner et al., 1990). Aberrant FGF signaling promotes tumor angiogenesis and mediates the escape of tumor vascularization from VEGF- or epidermal growth factor receptor (EGFR)-inhibitor treatment (Bergers and Hanahan, 2008). FGFRs are often overexpressed in tumors, and mutations of the *FGFR* genes have been found in human cancers, making it particularly significant that FGFR activation in EC culture and animal models leads to angiogenesis (Cao et al., 2008; Korc and Friesel, 2009). Moreover, overexpression of various FGF ligands has been demonstrated in different types of tumors (Korc and Friesel, 2009).

5.3.3. PDGF family

PDGF was originally isolated because of its ability to promote proliferation of mesenchymal cells but it can also initiate additional cellular responses such as cell migration and survival. It was identified as a disulfide-linked dimer of two different polypeptide chains, A and B, and the PDGF family was thought of consisting of the three proteins PDGFAA (or PDGFA), PDGFAB, and PDGFBB (or PDGFB), encoded by two genes, *PDGFA* and *PDGFB*. Later, two additional *PDGF* genes and proteins were identified, PDGFC and PDGFD. The members of the PDGF family act as mitogens for many cell types of mesenchymal or neuro-ectodermal origin. However, in angiogenesis, the main role of the PDGF family is to ensure a correct maturation of blood vessels, and their coverage by mural cells (Jain, 2003). PDGF signaling promotes cell migration, survival, and proliferation, and regulates angiogenesis indirectly by inducing VEGF transcription and secretion (Wang et al., 1999).

PDGFs act via two receptor tyrosine kinases (RTKs), PDGFRα and PDGFRβ, with common domain structures, including five extracellular Ig loops and a split intracellular TK domain. Ligand binding promotes receptor dimerization, which initiates signaling. Depending on ligand configuration and the pattern of receptor expression, different receptor dimers may form (Heldin and Westermark, 1999). The dimerization is a key

event in activation since it brings the intracellular parts of the receptors close to each other promoting autophosphorylation between the receptors. Furthermore, it changes the conformation of the intracellular part of the receptor so that the kinase is activated and it creates docking sites for SH2-domain-containing signaling molecules. PDGFs bind to the receptors with different affinities. Thus, PDGFA, -AB, -B and -C induce αα receptor homodimers, PDGFB and PDGFD ββ receptor homodimers, and PDGFAB, -B, -C and -D αβ receptor heterodimers (Andrae et al., 2008) (Figure 28).

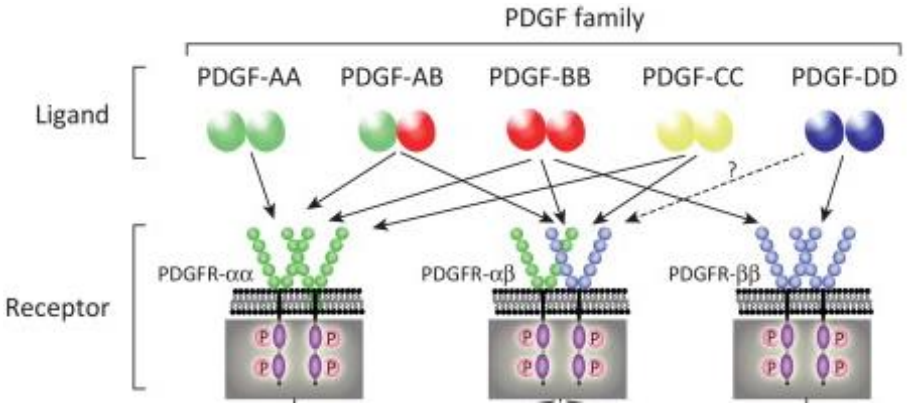

Figure 28. **Interactions between PDGF ligands and their receptors** (Cao, 2013).

The role of PDGFB/PDGFRβ signaling during embryonic development is the promotion of the proliferation of vascular smooth muscle cells (vSMCs) or perycite progenitors during their recruitment to new vessels (Hellstrom et al., 1999). PDGFB is involved in vessel maturation and the recruitment of pericytes; it is expressed by ECs and generally acts in a paracrine manner, recruiting PDGFR-expressing cells, particularly pericytes and vSMCs, to the developing vessels (Andrae et al., 2008; Hellberg et al., 2010). Moreover, PDGFB also induces VEGF expression in the endothelium and subsequently promotes pericyte recruitment to tumor vessels (Guo et al., 2003).

The involvement of PDGFs in angiogenesis involves cross-talk with other angiogenic factors. PDGFs can promote neovascularization by recruiting BM-derived endothelial progenitor cells to angiogenic vessels, and they can regulate expression levels of FGFRs and VEGFRs to amplify angiogenic signals mediated by their corresponding ligands (Li et al., 2005; Nissen et al., 2007). Other angiogenic factors such as FGF2 can induce PDGFR expression in ECs, which become susceptible to PDGF stimulation (Cao et al., 2003; Nissen et al., 2007). PDGFB can also upregulate TGFβ expression in vSMCs

(Nishishita and Lin, 2004) and TGFβ under certain circumstances stimulates tumor angiogenesis (Pardali and ten Dijke, 2009).

Whereas PDGFB and PDGFRβ are essential for the development of support cells in the vasculature, PDGFA and PDGFRα are more broadly required during embryogenesis with essential roles in numerous contexts, including central nervous system, neural crest and organ development (Gnessi et al., 2000; Karlsson et al., 2000). PDGFRα functions in early and late stages of embryonic development, wound healing, angiogenesis, and modulating interstitial fluid pressure (Ostman, 2004). However, it also plays roles in angiogenesis as evidenced by a study with *VEGF*-null tumorigenic cells, where PDGFA was identified as the major stromal fibroblast chemotactic factor produced by the tumor cells that lead to recruitment of VEGF-producing stromal fibroblasts for tumor angiogenesis and growth (Dong et al., 2004b). In tumor stroma, the PDGF-PDGFRα axis functions in fibroblast activation, aberrant epithelial-stromal interactions, modulation of tumor interstitial pressure, and production and secretion of VEGF (Bauman et al., 2007; Dong et al., 2004b).

When expressed on cancer cells, PDGFRα has been implicated in the development and progression of several malignancies (Pietras et al., 2003). Co-expression of PDGF and PDGFRα has been reported in various cancer types, consistent with autocrine-mediated growth (Ostman and Heldin, 2001). In lung cancer, expression of PDGF and/or PDGFRα is associated with more aggressive tumor biology and worse prognosis (Donnem et al., 2008). Activating mutations in the intracellular domain of *PDGFRα* occur in gastrointestinal stromal tumors (Heinrich et al., 2003), and *PDGFRα* amplifications in non-small cell lung cancer (NSCLC) (Ramos et al., 2009). Moreover, peripheral T-cell lymphomas (PTCLs) are known to express high levels of PDGFRα (Piccaluga et al., 2007; Piccaluga et al., 2005).

5.3.4. TGFβ

TGFβ and the corresponding receptors are produced by nearly every cell type, although the three isoforms TGFβ1, 2 and 3 demonstrate a different tissue expression pattern. TGFβ participates in angiogenesis, cell regulation and differentiation, embryonic development, wound healing and also has potent growth inhibition properties (Blobe et al., 2000). TGFβ receptors are classified as type I, II, or III. Type I and II receptors contain serine/threonine kinase domains in their intracellular protein regions, whereas

type III does not possess kinase activity but is believed to participate in transferring TGFβ ligands to type II receptors. TGFβ ligands bind to and stimulate type II receptors that recruit, bind, and phosphorylate type I receptors, activating downstream signaling proteins known as SMADs (Sakurai and Kudo, 2011).

TGFβ is believed to have both pro-angiogenic and anti-angiogenic properties, depending on the levels present. Low levels of TGFβ contribute to angiogenesis by upregulating angiogenic factors and proteases, whereas high doses of TGFβ stimulate basement membrane reformation, recruit SMCs, and inhibit EC growth (Carmeliet, 2003).

5.3.5. ANGPTs and TIE receptors family

ANGPTs are important angiogenic molecules that have been identified as ligands for TIE2 receptors. The ANGPT-TIE family is a binary system that ensures that healthy vessels maintain quiescence, while remaining able to respond to angiogenic stimuli. The human ANGPT family consists of two receptors, TIE1 and TIE2, and four ligands, ANGPT1, ANGPT2 ANGPT3 and ANGPT4 (Carmeliet, 2003).

ANGPT1 is expressed by mural and tumor cells, whereas ANGPT2 is released from angiogenic tip cells. ANGPT1 is a vasculogenic factor which signals through the endothelial and BM cell-specific TIE2 receptor tyrosine kinase, promoting EC survival and vascular maturation by increasing EC-pericyte interaction. It also activates EC migration and survival through the PI-3-K-AKT signaling pathway (Augustin et al., 2009; Saharinen et al., 2010).

The ANGPT2-TIE2 axis promotes angiogenesis in tumors by destabilizing the blood vessels and sensitizing ECs to proliferation signals mediated by other pro-angiogenic factors such as VEGF (Augustin et al., 2009; Saharinen et al., 2010). ANGPT2 targeting reduced tumor angiogenesis and delayed the growth of subcutaneous tumors in different studies (Brown et al., 2010; Hashizume et al., 2010; Oliner et al., 2004). In accordance, *Tie2* deficiency in mice causes vascular defects, and activating germline and somatic *TIE2* mutations in humans result in venous malformations. Tumor-derived ANGPT2 also promotes angiogenesis by recruiting pro-angiogenic TIE2-expressing monocytes (De Palma et al., 2003; DeNardo et al., 2009) which have features of M2-polarized

tumor associated macrophages (TAMs) that promote tumor angiogenesis and are required for the formation of tumor blood vessels.

5.4. Angiogenesis in B cell lymphomas

Angiogenesis has been widely studied in tumor malignancies where it has been associated with tumor progression for many decades (Folkman, 1985). Although its role in B cell tumors is less well defined compared to solid tumors, an increasing body of literature demonstrates that it is also important in hematological malignancies of both the myeloid and lymphoid origin (Koster and Raemaekers, 2005; Ribatti et al., 2013). Specifically, several studies have recently started to focus on angiogenesis in B cell-NHL, and results suggest that increased microvessel density (MVD) and angiogenic markers correlate with poor prognosis (Cardesa-Salzmann et al., 2011; Farinha et al., 2010; Ganjoo et al., 2008; Mezei et al., 2012; Negaard et al., 2009; Vacca et al., 1999).

Angiogenesis in B cell lymphomas is highly determined by the surrounding TME. On the one hand, tumor cells produce VEGFA and other angiogenic factors such as FGF2, PlGF and VEGFC which promote neo-angiogenesis via at least two mechanisms: sprouting angiogenesis of mature resident EC, and vasculogenesis from recruitment of BM-derived progenitor cells (Burger et al., 2009). VEGFA also supports the survival, proliferation and migration of lymphoma cells which express VEGFR1 and VEGFR2 in an autocrine fashion. Additionally, tumor cells may also release stromal cell-recruitment factors, such as PDGFA.

On the other hand, the malignant stroma composed of fibroblasts, inflammatory and immune cells provides additional angiogenic factors. Tumor-associated fibroblasts produce chemokines such as SDF1 which recruit BM-derived angiogenic cells, and TAMs produce VEGFA, VEGFC, and MMP9, among others, to support EC proliferation. Moreover, ECs produce PDGFB which promotes recruitment of pericytes via activation of PDGFRβ (Ruan et al., 2009) (Figure 29).

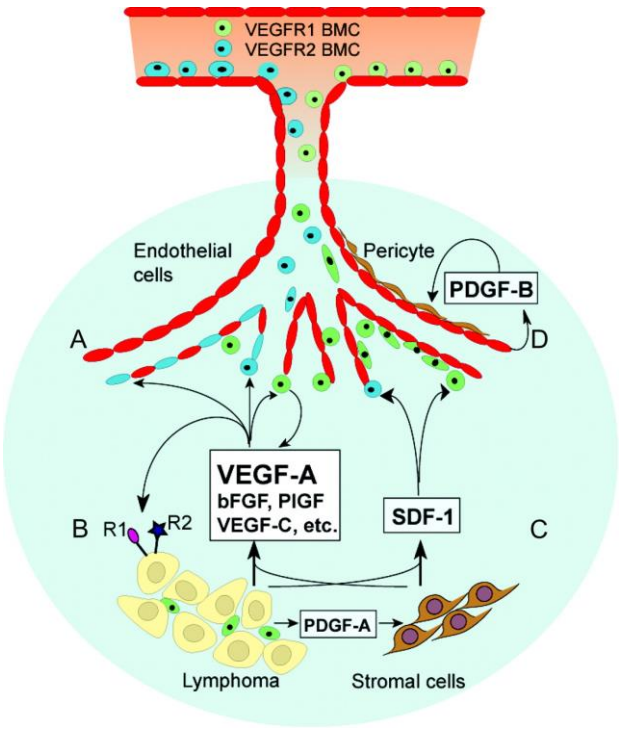

Figure 29. Overview of the B cell lymphoma vascular microenvironment*. B cell lymphoma growth is enhanced by at least two angiogenic mechanisms i) autocrine stimulation of tumor cells via expression of VEGF and VEGFRs by lymphoma cells, as well as ii) paracrine effects on local neovascularization and recruitment of circulating endothelial progenitors (Ruan et al., 2009).*

Several studies have addressed the prognostic value of serum VEGF and other angiotropic molecules in lymphomas. In a large study comprising 200 patients with malignant lymphoma, Salven and colleagues reported that high pretreatment levels of both serum VEGF and FGF2 were prognostic factors for survival (Salven et al., 2000). Similar results were observed in another study with aggressive lymphomas of B or T cell lineage patients (Niitsu et al., 2002). Pazgal and colleagues also found that increased tumor tissue expression of FGF2 was associated with worse progression-free and OS (Pazgal et al., 2002).

Adverse outcome associated with an increased VEGF tissue expression in aggressive and indolent lymphomas of B cell and T cell origin was also reported by Kuramoto and colleagues (Kuramoto et al., 2002). Ho and colleagues compared VEGFA expression in indolent lymphomas with that in aggressive lymphomas and found that only a minority of the patients with indolent form of the disease expressed VEGFA in contrast to aggressive lymphomas, which all expressed this protein. Remarkably, most of the indolent lymphomas expressing VEGFA showed histologic transformation to aggressive lymphoma (Ho et al., 2002).

Another angiogenic feature investigated in lymphomas has been the presence of circulating endothelial cells (CECs). Several evidences indicate that BM-derived CE-progenitor cells contribute to tumor growth and angiogenesis (Ribatti, 2007). In a study in immunodeficient mice engrafted with BL cells, Monestiroli and colleagues found a significant increase of CECs that was significantly correlated with the tumor volume and tumor-generated VEGF. When phenotyped, most CECs in healthy control mice seemed to be apoptotic, in contrast to the CECs observed in tumor-bearing mice, which may be due to the anti-apoptotic effect of VEGF on ECs (Monestiroli et al., 2001). The same authors also reported an increase in CECs in humans with breast cancer and lymphoma, in comparison with control individuals, which significantly correlated with plasma levels of VCAM1 and VEGF (Mancuso et al., 2001).

Therefore, clinical trials with many different agents are being explored to test for the efficacy of anti-angiogenic treatment approaches in mature B cell malignancies (Burger et al., 2009; Ribatti et al., 2013; Ruan et al., 2009).

Despite not being substantially explored, there is growing evidence suggesting that cross-talk between MCL cells and stromal cells in tissue microenvironments, such as the BM and secondary lymphoid organs, causes disease progression by promoting lymphoma cell survival, growth, and drug resistance. The majority of MCL patients present with advanced stage disease, and more than 90% of patients have extranodal manifestations, with a high prevalence of circulating MCL cells, BM, and gastrointestinal involvement. These clinical features suggest that MCL cells have a high propensity for dissemination and homing to different tissue compartments. Angiogenesis is part of the TME and its involvement in tumor progression has been vastly studied and corroborated in solid tumors. Although its implication in MCL has been poorly investigated, it could be an important mechanism responsible for the aggressive behavior of such B cell malignancy.

AIMS OF THE PRESENT STUDY

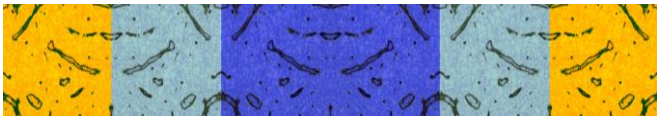

The overall aims of the present study were:

I. To identify and characterize SOX11 target genes and transcriptional pathways using different strategies, aiming for a better understanding of the pathogenesis of aggressive MCL, and to find potential candidates for targeted therapies.

II. To elucidate the oncogenic mechanisms regulated by SOX11 contributing to MCL pathogenesis and aggressive development.

Hypothesis I

SOX11 is a neuronal TF that has no known function in lymphoid cells and is not expressed in any cell of the lymphoid system. However, its overexpression has been observed in several types of human solid tumors, in virtually all aggressive MCLs, and at lower levels in some BLs and LBLs but not in other types of lymphoid malignancies.

Recent studies have shown that SOX11 is one of the best genes to discriminate between conventional and indolent MCL tumors both by GEP as well as mRNA and protein expression. The observation that SOX11-negativity is associated with an indolent, non-nodal clinical presentation, long-term survival and better outcome of MCL patients compared to its higher expression in aggressive, nodal MCL suggests that this TF might be playing a role in the pathogenesis of the disease.

Therefore, the goal of our first study was to identify and characterize the spectrum of genes and molecular pathways regulated by SOX11 in malignant lymphoid cells and decipher how the overexpression of SOX11 contributes to a more aggressive and tumorigenic manifestation of the disease.

<u>The specific aims rose for paper I were:</u>

a) To identify SOX11 direct target genes and transcriptional programs using a combined approach of ChIP-chip and GEP upon gene silencing in MCL cell lines.

b) To validate and molecularly characterize SOX11 direct genes and transcriptional programs in MCL cell lines.

c) To confirm SOX11 direct target genes and molecular pathways in human MCL primary tumors.

d) To interrogate SOX11 putative oncogenic function in MCL using a subcutaneous murine xenotransplant model.

Hypothesis II

In paper I we demonstrated the oncogenic implication of SOX11 expression in the aggressive behavior of MCL as SOX11-knockdown derived tumors displayed a significant reduction on tumor growth compared to SOX11-control tumors in subcutaneous MCL xenograft experiments. To uncover SOX11 target genes and transcriptional programs in MCL, we performed an integrative analysis coupling data from human genome-wide promoter analysis by SOX11 ChIP-chip experiments and GEP upon SOX11 silencing in MCL cell lines. In these studies we initially identified the role of SOX11 in blocking the terminal B-cell differentiation by the direct positive regulation of PAX5. However, SOX11-regulated oncogenic mechanisms that could explain an enhanced tumor growth still remained to be elucidated.

Therefore, we have integrated our ChIP-chip data with further analyses including GEP derived from the xenograft SOX11-positive and silenced tumors to further characterize the potential oncogenic mechanisms regulated by SOX11.

Thus, the goal of our second study was to shed light on the oncogenic mechanisms promoting a strikingly more prominent growth of the SOX11-positive xenograft tumors compared to their SOX11-negative counterparts which would explain the more aggressive manifestation of the human disease.

<u>The specific aims rose for paper II were:</u>

a) To investigate the oncogenic mechanisms regulating the strikingly prominent growth of the SOX11-positive xenograft tumors.

b) To study and molecularly characterize the oncogenic mechanisms regulated by SOX11 in *in vitro* settings.

c) To validate the oncogenic pathways and their associated target genes regulated by SOX11 in human primary MCL samples.

d) To find new therapeutic strategies for the treatment of MCL.

RESULTS

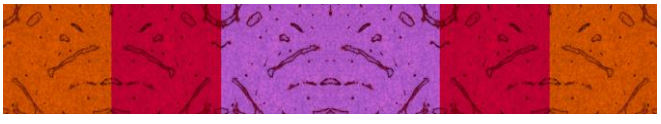

Paper I

SOX11 regulates PAX5 expression and blocks terminal B-cell differentiation in aggressive mantle cell lymphoma.

Abstract

Mantle cell lymphoma (MCL) is one of the most aggressive lymphoid neoplasms whose pathogenesis is not fully understood. The neural transcription factor SOX11 is overexpressed in most MCL but is not detected in other mature B-cell lymphomas or normal lymphoid cells. The specific expression of SOX11 in MCL suggests that it may be an important element in the development of this tumor, but its potential function is not known. Here, we show that SOX11 promotes tumor growth in a MCL-xenotransplant mouse model. Using chromatin immunoprecipitation microarray analysis combined with gene expression profiling upon SOX11 knockdown, we identify target genes and transcriptional programs regulated by SOX11 including the block of mature B-cell differentiation, modulation of cell cycle, apoptosis, and stem cell development. *PAX5* emerges as one of the major SOX11 direct targets. SOX11 silencing downregulates PAX5, induces BLIMP1 expression, and promotes the shift from a mature B cell into the initial plasmacytic differentiation phenotype in both primary tumor cells and an in vitro model. Our results suggest that SOX11 contributes to tumor development by altering the terminal B-cell differentiation program of MCL and provide perspectives that may have clinical implications in the diagnosis and design of new therapeutic strategies.

Plenary Paper

SOX11 regulates PAX5 expression and blocks terminal B-cell differentiation in aggressive mantle cell lymphoma

Maria Carmela Vegliante,[1] Jara Palomero,[1] Patricia Pérez-Galán,[1] Gaël Roué,[1] Giancarlo Castellano,[1] Alba Navarro,[1] Guillem Clot,[1] Alexandra Moros,[1] Helena Suárez-Cisneros,[1] Sílvia Beà,[1] Luis Hernández,[1] Anna Enjuanes,[1] Pedro Jares,[1] Neus Villamor,[1] Dolors Colomer,[1] José Ignacio Martín-Subero,[2] Elias Campo,[1,2] and Virginia Amador[1]

[1]Hematopathology Unit, Pathology Department, Hospital Clínic, Institut d'Investigacions Biomèdiques August Pi i Sunyer; and [2]Department of Anatomic Pathology, Pharmacology and Microbiology, University of Barcelona, Barcelona, Spain

Key Points

- SOX11 silencing promotes the shift from a mature B cell into the initial plasmacytic differentiation phenotype in MCL.
- SOX11 promotes tumor growth of MCL cells in vivo, highlighting its implication in the aggressive behavior of conventional MCL.

Mantle cell lymphoma (MCL) is one of the most aggressive lymphoid neoplasms whose pathogenesis is not fully understood. The neural transcription factor SOX11 is overexpressed in most MCL but is not detected in other mature B-cell lymphomas or normal lymphoid cells. The specific expression of SOX11 in MCL suggests that it may be an important element in the development of this tumor, but its potential function is not known. Here, we show that SOX11 promotes tumor growth in a MCL-xenotransplant mouse model. Using chromatin immunoprecipitation microarray analysis combined with gene expression profiling upon SOX11 knockdown, we identify target genes and transcriptional programs regulated by SOX11 including the block of mature B-cell differentiation, modulation of cell cycle, apoptosis, and stem cell development. *PAX5* emerges as one of the major SOX11 direct targets. SOX11 silencing downregulates PAX5, induces BLIMP1 expression, and promotes the shift from a mature B cell into the initial plasmacytic differentiation phenotype in both primary tumor cells and an in vitro model. Our results suggest that SOX11 contributes to tumor development by altering the terminal B-cell differentiation program of MCL and provide perspectives that may have clinical implications in the diagnosis and design of new therapeutic strategies. (*Blood*. 2013;121(12):2175-2185)

Introduction

Mantle cell lymphoma (MCL) is one of the most aggressive lymphoid neoplasms.[1] This biological behavior has been attributed to the molecular mechanisms involved in its pathogenesis combining the deregulation of cell proliferation, disruption of the DNA-damage–response pathways, and the activation of cell-survival mechanisms.[2] Recent studies have identified a subgroup of patients with MCL that have an indolent clinical behavior and long survival even without chemotherapy. These tumors have very stable karyotypes and frequently carry hypermutated *IGHV*, indicating an origin in cells that have experienced the follicular germinal center microenvironment.[3-7] A gene expression profiling (GEP) study has shown that these indolent MCL differ from conventional MCL in a particular gene signature that lacks the expression of some transcription factors of the high-mobility group (HMG). One of the best discriminatory genes between these 2 subtypes of tumors is *SOX11* (SRY [sex-determining region-Y]-box11),[4,6] a neural transcription factor whose function in normal and neoplastic B-cell development is unknown.

SOX11 belongs to the *SOX* gene family encoding for transcription factors that play a critical role in the regulation of cell fate and differentiation in major developmental processes. In mice, Sox11 is important in organ development and neurogenesis.[8,9] SOX11 upregulation has been detected in various types of human solid tumors.[10,11] SOX4, the SOX family member with the highest homology to SOX11, is a prominent transcription factor in lymphocytes of both B- and T-cell lineage[12] and is crucial for B-cell lymphopoiesis.[13] In contrast, SOX11 has no known lymphopoietic function and it is not expressed in lymphoid progenitors or in mature normal B-cells. However, it is expressed in virtually all aggressive MCL and at lower levels in a subgroup of Burkitt and acute lymphoblastic lymphomas, but not in other lymphoid neoplasms.[14-16] These findings suggest that SOX11 plays a relevant role in the pathogenesis of these tumors. However, the function of SOX11 and its potential target genes in lymphoid cells remain unknown.

To identify direct target genes, transcriptional programs, and oncogenic pathways regulated by SOX11 in malignant lymphoid cells, we have used genome-wide promoter analysis and GEP after SOX11 silencing in MCL cell lines, followed by the validation in an in vivo murine model and in primary MCL tumors.

Submitted June 24, 2012; accepted December 10, 2012. Prepublished online as *Blood* First Edition paper, January 15, 2013; DOI 10.1182/blood-2012-06-438937.

M.C.V. and J.P. contributed equally to this study.

All microarray data are available in the Gene Expression Omnibus (accession numbers GSE34763 and GSE3502 for the gene expression array and the ChIP-chip array, respectively).

The online version of this article contains a data supplement.

There is an Inside *Blood* commentary on this article in this issue.

The publication costs of this article were defrayed in part by page charge payment. Therefore, and solely to indicate this fact, this article is hereby marked "advertisement" in accordance with 18 USC section 1734.

Materials and methods

Cell lines and patient samples

A total of 6 MCL cell lines, 5 SOX11 positive (Z138, GRANTA519, REC1, HBL2, and JEKO1) and 1 SOX11 negative (JVM2),[17] were used for chromatin immunoprecipitation (ChIP) microarray (ChIP-chip) and/or ChIP quantitative polymerase chain reaction (qPCR) experiments, gene expression analysis after SOX11 silencing, and western blot (WB) experiments. Human embryonic kidney 293 (HEK293) cells were used for luciferase assays.

Microarray GEP data previously generated in 38 primary MCL (16 SOX11-positive and 22 SOX11-negative) were used for gene set enrichment analysis (GSEA) (GSE36000).[7] Immunophenotypic surface markers were investigated in 6 of these primary MCL (3 SOX11 positive and 3 SOX11 negative) by flow cytometry.

Details on cell culture and primary tumor's information are provided in "supplemental Materials and methods."

ChIP

Z138, GRANTA519, and JVM2 cell lines were used for ChIP-chip and/or ChIP-qPCR analysis. Cells were crosslinked with 1% of formaldehyde for 10 minutes and chromatin sonicated using Branson Sonifer 250 followed by Biorupter sonicator from Diagenode. SOX11 antibody (sc-17347; Santa Cruz Biotechnology, Santa Cruz, CA) was used to immunoprecipitate protein-DNA complexes. Immunocomplexes were amplified in 2 steps using a GenomePlex Whole Genome Amplification WGA Kit (Sigma, St Louis, MO), following the manufacturer's instructions, and used for ChIP-chip analysis and/or ChIP-qPCR. We performed ChIP assays in triplicate from Z138-SOX11-positive cells and in a single experiment from JVM2 cell line as negative control (supplemental Materials and methods).

ChIP-qPCR

Primers for the qPCR analysis of the SOX11 ChIP-enriched genomic DNA regions were designed using Primer3 (http://frodo.wi.mit.edu/) (supplemental Table 1). Amplified SOX11-ChIP DNA and 1:100 diluted input samples were analyzed in triplicate by qPCR using Fast SYBR Green Master Mix in a StepOnePlus PCR detection system (Applied Biosystems, Foster City, CA).

Reporter plasmid constructs and luciferase assay

The SOX11-binding site from the regulatory region of *PAX5* gene (ChIP-peak region from 2435 bp to −1884 bp) was amplified by PCR using GRANTA519 genomic DNA and primers are listed in supplemental Table 1. Subsequently, the PCR fragment was cloned in front of a minimal promoter luciferase reporter vector pGL4.23[*luc2*/minP] (Promega, Leiden, The Netherlands). Constructs were sequenced using internal primers prior to use.

Lipofectamine 2000 system (Invitrogen, Life Technologies, Carlsbad, CA) was used for transient cotransfection experiments in HEK293 cells following the manufacturer's instructions. Cotransfected HEK293 cells were harvested and luciferase activity was measured 24 hours after transfection with Dual-Glo Luciferase Assay System (Promega) and a Modulus microplate luminometer (Turner BioSystems, Sunnyvale, CA). All assays were performed in triplicate on separated days.

Gene expression profiling

Total RNA of Z138 cells stably transduced with short hairpins targeting SOX11 and control short hairpin was extracted with the TRIzol reagent following the manufacturer's recommendations (Invitrogen). RNA integrity was examined with the Agilent 2100 Bioanalyser (Agilent Technologies, Palo Alto, CA) and hybridized to HG-U133plus2.0 GeneChips (Affymetrix) according to Affymetrix standard protocols. The analysis of the GEP is detailed in "supplemental Materials and methods."

GSEA

We performed GSEA[18] on 2 preranked lists of genes derived from in vitro SOX11 silencing microarray data and from our series of 38 purified primary MCL data. To generate these preranked lists, we analyzed the GEP of our in vitro cell line model as well as the GEP of 38 primary MCL according to their SOX11 expression levels. Details on GSEA are provided in "supplemental Materials and methods."

SOX11 silencing by lentiviral infection

SOX11 shRNA lentiviral particles (shRNASOX11.1, clone ID NM_003108.3-982s1c1; shRNASOX11.2, clone ID NM_003108.3-1235s1c1; and shRNASOX11.3, clone ID NM_003108.3-454s1c1) were purchased from Sigma-Aldrich. Control shRNA lentiviral particle (Clone ID sc-108080) was purchased from Santa Cruz Biotechnology.

SOX11 knockdown stable MCL cell lines were generated by lentiviral transduction of PLKO1-puro–shSOX11 and PLKO1-puro–scramble constructs in 3 MCL cell lines (Z138, GRANTA519, and JEKO1). Details on SOX11 silencing are provided in "supplemental Materials and methods."

WB analysis

Protein extract preparation and WB experiments were performed as previously described[19] using antibodies against hemagglutinin (Roche Applied Science, Indianapolis, IN; 12CA5), SOX11 (Atlas Antibodies, Stockholm, Sweden [HPA000536]; Santa Cruz Biotechnology [H-290 and C-20]), PAX5 (Santa Cruz Biotechnology; C-20), BLIMP1 (CNIO, Madrid, Spain; Ros 195G/G5), IRF4 (Santa Cruz Biotechnology; M-17), GAPDH (Santa Cruz Biotechnology; A-3), and α-tubulin (Oncogene, Uniondale, NY; CP06-100UG). Membranes were developed with chemiluminescence substrate Pierce ELC WB substrate (Thermo Fisher Scientific, South Logan, UT) and visualized on a LAS4000 device (Fujifilm, Tokyo, Japan). Protein quantification was done with Image Gauge software (Fujifilm).

qRT-PCR

qRT-PCR was performed as described before[19] using a designed primer set and TaqMan MGB probe for SOX11 using Primer Express Software Version 2.0 (Applied Biosystems) (primers used are shown in supplemental Table 1). Inventoried TaqMan Gene Expression Assays were used for *HSPD1* (Hs01941522_u1), *SUV39H2* (Hs00226595_m1), *SEPT2* (Hs00189358_m1), *MSI2* (Hs-00292670_m1), *PAX5* (Hs00277134_m1), *VPREB3* (Hs00429452_m1), *SPIB* (Hs0062150_m1), *EBF1* (Hs00365513_m1), *CD19* (Hs00174333_m1), *IKZF3* (Hs00232635_m1), *LEF1* (Hs01547250_m1), and *LCK* (Hs00178427_m1). Relative quantification of gene expression was analyzed with the $2^{-\Delta\Delta Ct}$ method using *GUS* (Hs00939627_m1) as the endogenous control.

Flow cytometry studies

For immunophenotype analysis, 500 000 cells of interest were collected in 1.5-mL tubes, washed once in phosphate-buffered saline 0.5% bovine serum albumin (BSA), and stained with 5 μL of antibody against CD20 (2H7), CD24 (ML5), immunoglobulin (Ig) M (G20-127), IgD (IA6-2), CD5 (UCHT2), CD19 (HIB19), CD38 (HIT2) (all from BD Pharmingen, San Diego, CA), and CD138 (B-A38; Beckman Coulter, Carlsbad, CA) for 30 minutes at 4°C in the dark. Cells were then washed 3 times in phosphate-buffered saline 0.5% BSA and acquired and analyzed using the Attune Acoustic Focusing Cytometer and Software (Applied Biosystems). For the analysis, 10 000 events were collected in the lymphocyte gate. Details on proliferation assay, cell-cycle analysis, and apoptosis assay are provided in "supplemental Materials and methods."

Xenograft mouse model and tumor phenotyping

CB17 severe combined immunodeficient (CB17-SCID) mice (Charles River Laboratory, Wilmington, MA) were housed in the animal care facility under

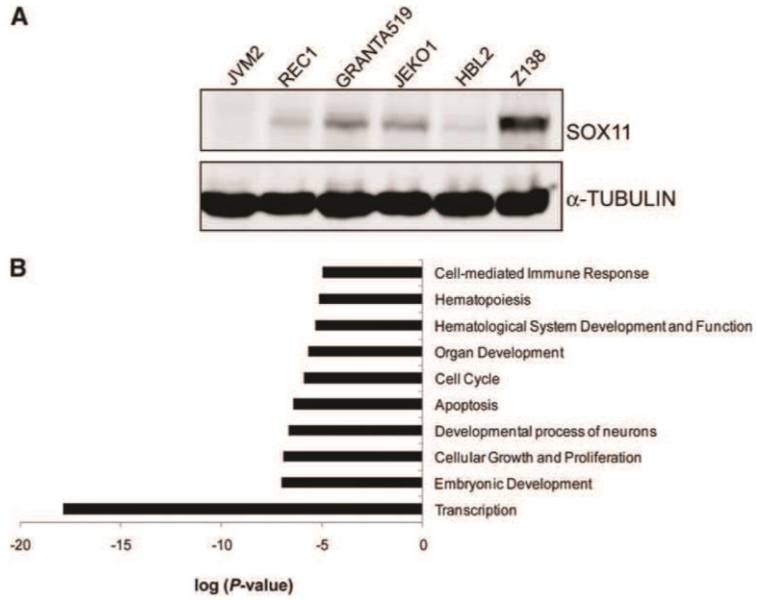

Figure 1. ChIP-chip screening of SOX11-bound target genes in MCL cell lines. (A) The expression levels of SOX11 protein in different MCL cell lines (JVM2, REC1, GRANTA519, JEKO1, HBL2, and Z138) were detected by WB using an anti-SOX11 antibody (H-290). α-Tubulin was used as a loading control. (B) IPA functional annotation tool related to the high-confidence SOX11-bound genes. The 10 most significant biological-process GO terms and their log *P* values are shown.

a 12/12-hour light/dark cycle at 22°C, and they received a standard diet and acidified water ad libitum. With the use of a protocol approved by the animal testing Ethical Committee of the University of Barcelona, mice were subcutaneously inoculated into their lower dorsum with 1×10^7 Z138shSOX11.1 (n = 8), shSOX11.3 (n = 6), shControl (n = 7), JEKOshSOX11.3 (n = 5), JEKOshControl (n = 5), GRANTA519shSOX11.3 (n = 5), and GRANTA519shControl (n = 5) in Matrigel basement membrane matrix (Becton Dickinson, San Jose, CA). The shortest and longest diameters of the tumor were measured with external calipers every 3 days, and tumor volume (in mm^3) was calculated with the use of the following standard formula: (the shortest diameter)^2 × (the longest diameter) × 0.5. Animals were sacrificed according to institutional guidelines, and tumor xenografts were paraffin embedded on silane-coated slides in a fully automated immunostainer (Bond Max; Vision Biosystems, Mount Waverley, Australia).

Immunohistochemical staining

Immunohistochemical studies were performed as previously described[16,20] using antibodies against human Ki67, kappa, lambda, and IgM (ready to use; Dako, Glostrup, Denmark), anti-phosphohistone H3 (Epitomics, Burlingame, CA; polyclonal), anti–caspase-3 cleaved (Cell Signaling Technology, Danvers, MA; 5A1E), SOX11 (Atlas Antibodies; HPA000536), cyclin D1 (Thermo Fisher Scientific; EPR2241IHC), PAX5 (Santa Cruz Biotechnology; sc-1974), and BLIMP1 (CNIO; Ros 195G/G5).

Necrotic areas were quantified using the digitalized images of the activated caspase-3 immunohistochemical staining acquired with an Olympus BX51 microscope at original magnification ×4 and analyzed with an Olympus Cell B Basic Imaging Software. Necrotic areas were delineated by cleaved caspase-3–positive staining and quantified as the sum of all necrotic areas (μm^2) divided by the total area of the core analyzed (μm^2).

Statistical analysis

Data are represented as mean ± standard deviation (SD) of 3 independent experiments. Statistical tests were performed using SPSS v16.0 software. Comparison between 2 groups of samples was evaluated by independent-sample *t* test, and results were considered statistically significant when $P < .05$.

Results

Genome-wide promoter analysis of SOX11 in MCL

We first investigated the direct target genes of SOX11 using ChIP and DNA microarrays (ChIP-chip). We used a MCL cell line with high SOX11 expression (Z138) and one negative for SOX11 (JVM2) (Figure 1A). ChIP was performed using a SOX11 specific antibody (supplemental Figure 1). ChIP-enriched DNA sequences were amplified and hybridized to a high-resolution DNA tiling array spanning promoter regions of the whole human genome. These experiments identified 5842 significant enriched peaks belonging to 1133 unique genes (SOX11-bound genes) that were consistently enriched in immunoprecipitated material across all 3 independent Z138 replicates after subtracting the corresponding nonspecific immunoprecipitated material in JVM2 (supplemental Table 2).

The promoter region of SOX11 was not identified in this analysis. We have reported that SOX11 expression is associated with active histone marks.[19] We have now observed a significant reduction in the enrichment of the activating histone mark H3K4me3 at the SOX11 promoter upon SOX11 silencing (supplemental Figure 2), suggesting that SOX11 may indirectly regulate its own expression by epigenetic mechanisms.

Gene ontology (GO) term enrichment analysis showed several biological processes overrepresented in the SOX11-bound genes, including transcription, embryonic and neuronal development, cell growth and proliferation, cell death and apoptosis, cell cycle, hematopoiesis, and hematological system development and function (Figure 1B).

Differential gene expression profiling after SOX11 silencing

To determine the transcriptional programs regulated by SOX11, we generated a MCL cellular model by silencing SOX11 expression (Figure 2A). We then compared the GEP of stably transduced shSOX11 and shControl Z138 cells (Figure 2B and

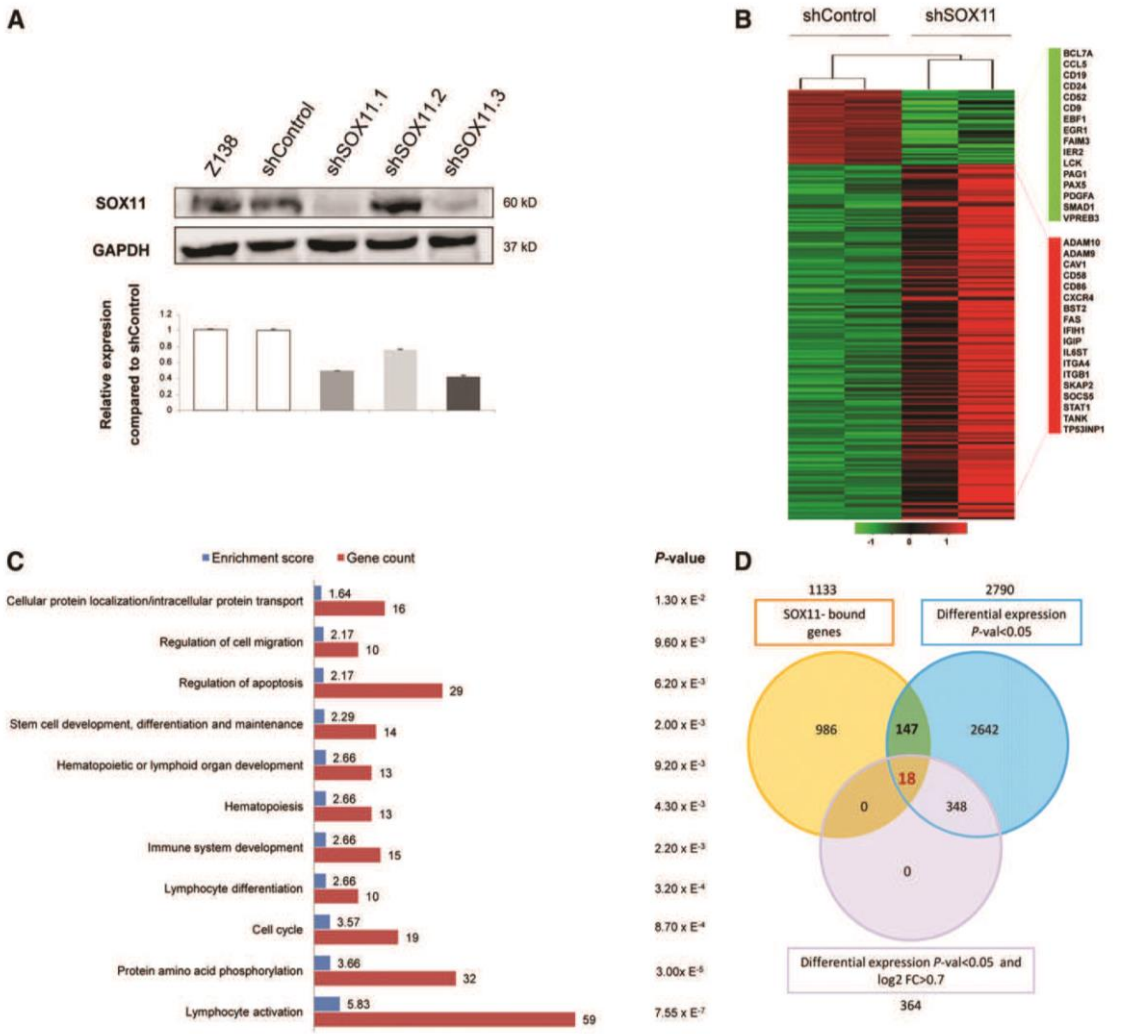

Figure 2. GEP upon SOX11 silencing. (A) SOX11 silencing in Z138 stably transduced with shSOX11.1, shSOX11.2, and shSOX11.3 was verified (upper panel) at the protein level by WB using GAPDH as a loading control and (lower panel) at the transcriptional level by qRT-PCR. A scramble shControl and untransduced cells (Z138) are also shown. Bar plot represents the mean ± SD of 3 independent experiments. (B) Heat map illustrating 366 significant differentially expressed genes (adjusted $P < .05$ and log2 FC > 0.7) in Z138 shSOX11.1 and shSOX11.3 compared with 2 Z138-shControl cells. Red indicates increased expression and green decreased expression relative to the median expression level according to the color scale shown. (C) DAVID functional annotation of the 366 differentially expressed genes. The 11 most significant ($P < .05$) biological process GO terms, their *P* value, enrichment score, and gene count are shown. (D) Venn diagram depicting the overlap of 1133 SOX11-bound genes (orange circle), 2790 significant differentially expressed genes ($P < .05$) upon SOX11 silencing (blue circle), and differentially expressed genes using more stringent statistical criteria ($P < .05$ and log2 FC > 0.7) (purple circle).

supplemental Table 3). The top annotated functions of the differentially expressed genes included lymphocyte activation and differentiation, phosphorylation, cell cycle, immune system development, and hematopoiesis (Figure 2C). A GSEA using the genes differentially expressed in primary SOX11-positive and SOX11-negative MCL confirmed that the GEP observed in our in vitro model was representative of that observed in these primary MCL (supplemental Table 4 and supplemental Figure 3).

Interestingly, among the significant differentially expressed genes between shSOX11 and shControl cells, we observed upregulation of key regulators of plasma cell differentiation and pronounced downregulation of B-cell genes. To further characterize the significance of these changes, we performed a GSEA using well-defined gene signatures related to the different steps of the mature B-cell and plasma cell differentiation programs (supplemental Table 4).[21-24] These analyses showed that the GEP of Z138shControl cells was enriched for gene signatures related to the mature B-cell program whereas Z138shSOX11 cells were enriched in gene signatures related to the plasma cell differentiation program (supplemental Table 5 and supplemental Figure 4). These findings indicate that SOX11 silencing triggers a shift from the mature B cell to a plasmacytic gene expression program in MCL cells.

SOX11 directly regulates the transcription of *PAX5*

To determine the direct targets transcriptionally regulated by SOX11, we overlaid the list of SOX11-bound genes and those with differential expression upon SOX11 knockdown and found 147

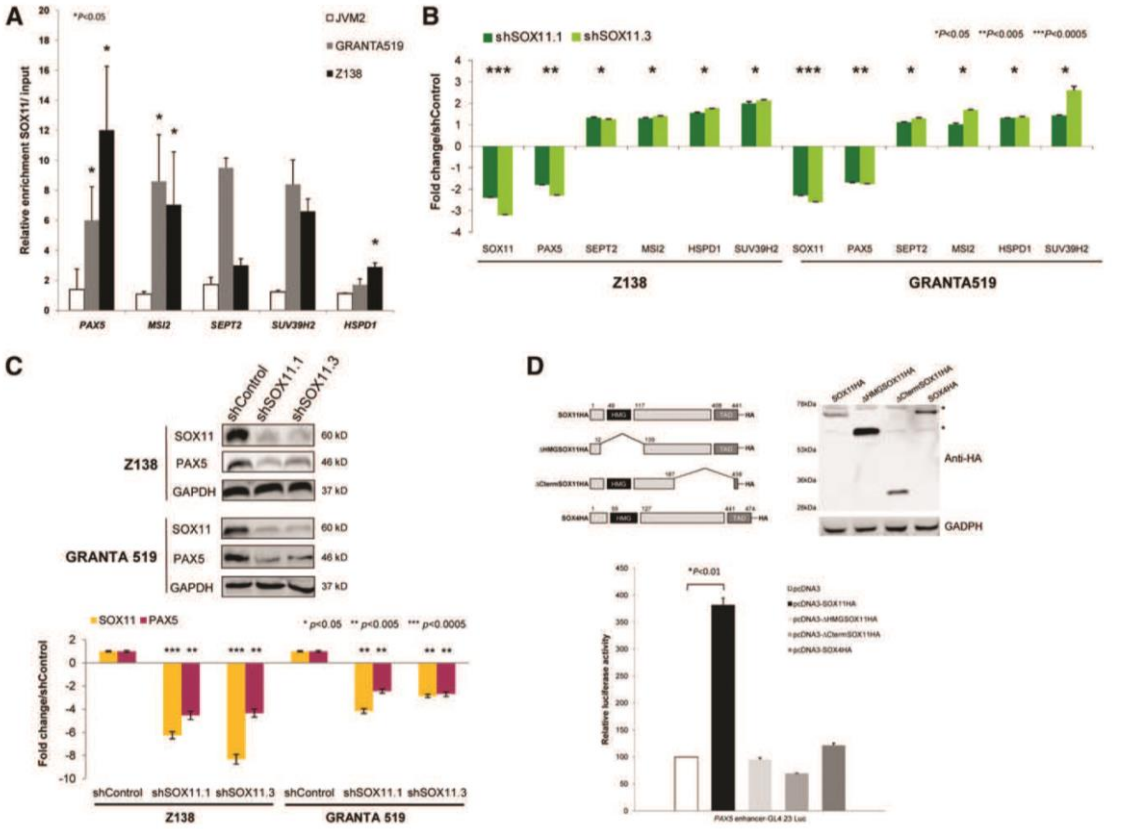

Figure 3. SOX11 directly regulates *PAX5* transcription. (A) Binding of SOX11 to regulatory regions of *PAX5*, *MSI2*, *SEPT2*, *SUV39H2*, and *HSPD1* was confirmed by ChIP-qPCR in different MCL cell lines. Results are shown as enrichment relative to input. (B) Levels of the indicated transcripts in Z138 and GRANTA519 quantified by qRT-PCR after SOX11 silencing. Fold-change differences compared with control cells are shown. (C) Upper panel: Levels of SOX11 and PAX5 in Z138 and GRANTA519 cell lines stably transduced with shControl, shSOX11.1, or shSOX11.3 determined by WB, using GAPDH as a loading control. Lower panel: Fold-change differences of SOX11 and PAX5 protein expression levels between control and silenced cells. SOX11 and PAX5 expression levels were corrected by quantification of GAPDH expression levels. (D) Luciferase assays in transient cotransfections of *PAX5* enhancer-GL4.23 Luc with SOX11 full-length, the truncated SOX11 proteins (SOX11ΔHMG and SOX11ΔCtermTAD), or SOX4 full-length expression vectors, in HEK293 cells. Upper panel: Schematic representation of the constructs and results of the WB experiment of SOX11 mutants are shown. *Nonspecific bands. Bottom panel: Results are shown as fold induction relative to luciferase activity in cotransfection with the empty vector (pcDNA3). Bar plot represents the mean ± SD of 3 independent experiments. The significance of difference was determined by paired *t* test. HA, hemagglutinin.

genes in common. From these 147 genes, 18 genes still overlapped using more stringent statistical criteria ($P < .05$ and log2 fold change > 0.7) (Figure 2D and supplemental Table 6).

Interestingly, among these 18 genes we identified PAX5, an essential transcription factor regulating B-cell identity in early B-cell development[25] and late B-cell differentiation,[26] as one of the highest-confident SOX11-bound genes (false discovery rate [FDR] < 0.1 and peak score ≥ 0.5). We also found genes that can contribute to SOX11 hematopoietic and B-cell activation functions (MSI2 and HSPD1, respectively).

We then verified the direct binding of SOX11 to the regulatory regions of the most significantly overlaid genes by ChIP-qPCR in Z138 and GRANTA519 MCL cell lines. As expected, no binding within these regulatory regions was detected in the SOX11-negative JVM2 (Figure 3A). Downregulation of PAX5 in stable SOX11-knockdown MCL cell lines was confirmed by qRT-PCR and WB (Figure 3B-C, respectively). Upregulation of MSI2, HSPD1, SUV39H2, and SEPT2 was also observed but to a much lesser extent than PAX5, prompting us to focus on the SOX11-PAX5 relationship.

To verify the transcriptional effect of SOX11 on the *PAX5* promoter, the amplified SOX11 ChIPed-*PAX5* fragment (supplemental Figure 5) was cloned in front of a minimal promoter luciferase reporter and tested in transient cotransfections with SOX11 expression vector. The induction in luciferase activity was detected in the coexpression with SOX11 but not with SOX4 or truncated SOX11 proteins lacking the HMG domain (ΔHMGSOX11) or the C-terminal TAD domain (ΔTADSOX11) (Figure 3D), both of which are required for its transcriptional activity.[27,28] These findings demonstrate the specificity of SOX11 in regulating the transcription of *PAX5*.

SOX11-knockdown MCL cell lines display early plasmacytic differentiation

PAX5 is the critical transcription factor that determines and maintains B-cell identity by activating the expression of B-cell–specific genes and simultaneously repressing genes that promote plasma cell differentiation.[25,26] The significant shift from a mature B cell to a plasmacytic gene expression program identified by GSEA in our SOX11-knockdown cells was highly suggestive of

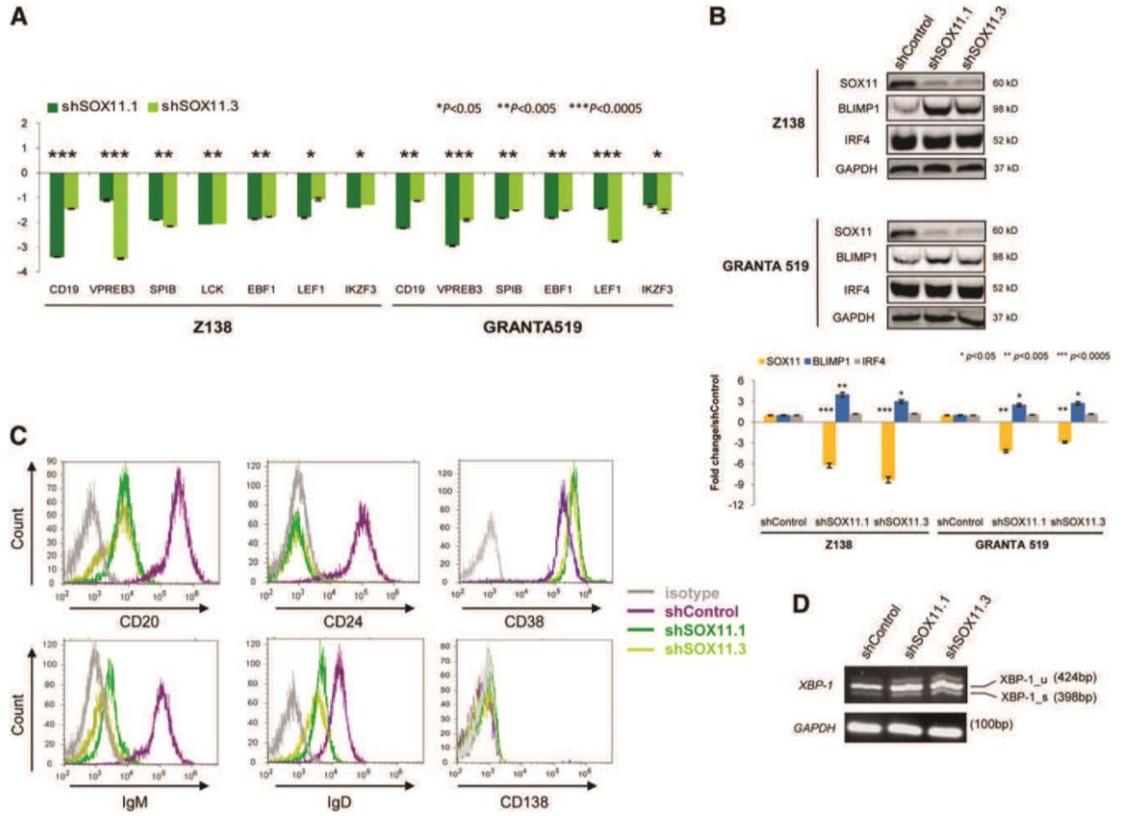

Figure 4. SOX11 activates B-cell–specific genes and represses plasma cell gene program. (A) Messenger RNA expression levels of the indicated genes were analyzed by qRT-PCR in Z138 and GRANTA519 stably transduced with shSOX11.1 or shSOX11.3. Figure shows the fold differences compared with the corresponding control cells (±SD; n = 3 technical replicates). *P* values are shown. The significance of difference was determined by independent-samples *t* test. (B) Upper panel: BLIMP1 and IRF4 expression levels in Z138 and GRANTA519 stably transduced with shControl, shSOX11.1, or shSOX11.3 assessed by WB, using GAPDH as a loading control. Lower panel: Fold-change differences of SOX11, BLIMP1, and IRF4 protein expression levels between control and silenced cells. SOX11, BLIMP1, and IRF4 expression levels were corrected by quantification of GAPDH expression levels. (C) Histograms showing the expression of B-cell and plasma cell surface markers (CD20, CD24, CD38, and CD138) and surface IgM and IgD measured by flow cytometry in shControl, shSOX11.1, and shSOX11.3 Z138 cell lines. Isotype control is shown in gray. (D) XBP1 mRNA expression levels by RT-PCR in Z138shControl, shSOX11.1, or shSOX11.3. GADPH was used for the loading control.

a major effect of the direct modulation of PAX5 by SOX11 in these tumor cells. These observations prompted us to further investigate the expression of genes regulated by PAX5 in SOX11-knockdown cells. As expected, several B-cell genes were downregulated (CD19, VPREB3, SPIB, LCK, EBF1, LEF1, and IKZF3) in SOX11 knockdown cells compared with control cells (Figure 4A).

The transcription factors BLIMP1, XBP1, and IRF4 are critical regulators promoting plasma cell differentiation whereas PAX5 inhibits plasma cell development by repressing BLIMP1 and XBP1 expression.[26,29] We next examined the modulation of these transcription factors in SOX11-knockdown MCL cells. IRF4 was already expressed in control cells and SOX11 silencing did not modify its expression levels. On the contrary, SOX11 knockdown resulted in a marked increase of BLIMP1 protein levels compared with control cells (Figure 4B and supplemental Figure 6C). Consistent with BLIMP1 function as a repressor of the B-cell program during plasma cell differentiation,[30] we found decreased or undetectable expression of B-cell surface markers CD20, CD24, IgD, and IgM in SOX11-silenced cells compared with control cells. The plasma cell marker CD38 was already expressed in control cells and only marginally upregulated in SOX11 knockdown whereas expression of CD138 was undetected in both control and silenced cell lines (Figure 4C).

Full plasma cell differentiation includes synthesis and secretion of immunoglobulins, and this secretory program is controlled by the activated splicing form of XBP1. SOX11 knockdown slightly increased the levels of XBP1(u) but the levels of the spliced form of XBP1(s) did not change (Figure 4D).

Altogether, these findings indicate that SOX11 silencing in MCL cell lines promotes the initial steps into plasmacytic differentiation with downregulation of mature B-cell markers and increasing levels of BLIMP1. However, the absence of XBP1 splicing and CD138 expression indicates that the full plasma cell program is not completed.[31,32]

SOX11 promotes tumor growth of MCL in vivo

To investigate the potential tumorigenic ability of SOX11 in vivo, we studied the effect of SOX11 downregulation in a MCL-xenotransplant model by inoculating CB17-SCID mice with stably transduced Z138shSOX11 and shControl cell lines. Tumor

RESULTS

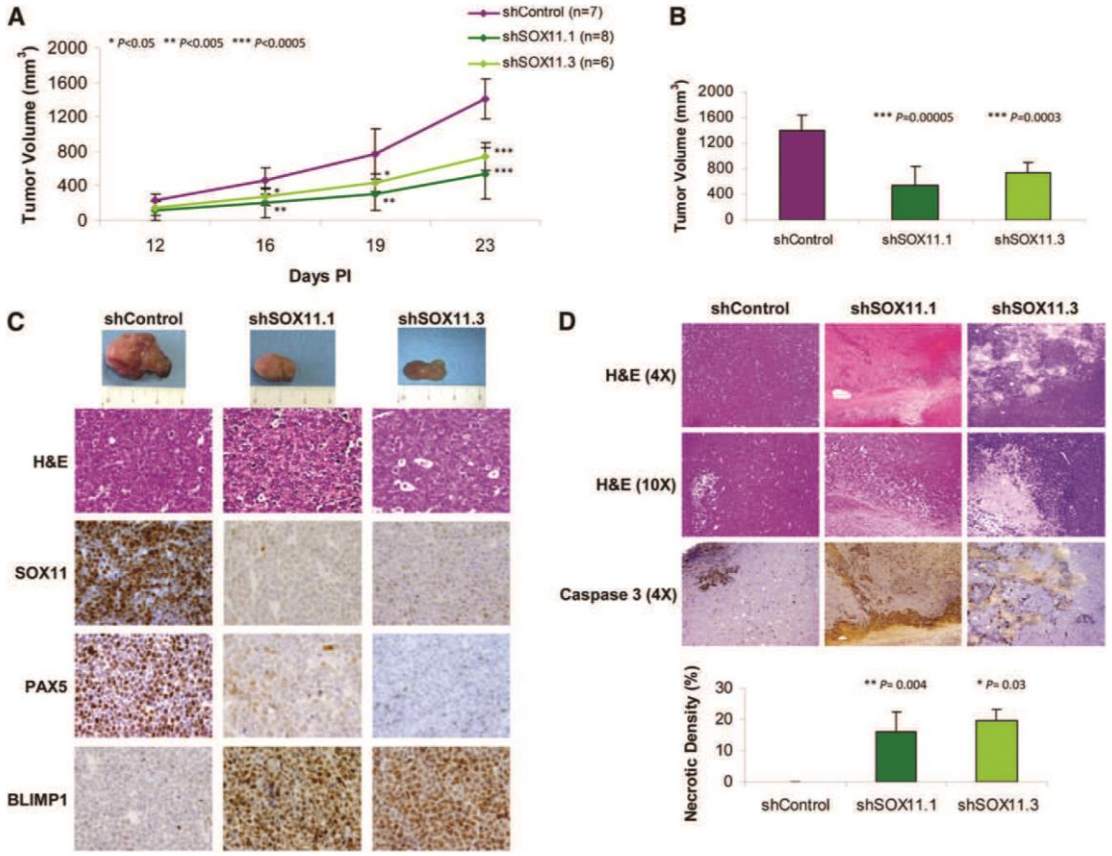

Figure 5. SOX11 silencing inhibits the growth of MCL tumors in SCID mice. (A) Z138 stably transduced with shSOX11.1, shSOX11.3, and shControl (10^7cells/mouse) were subcutaneously inoculated into the right flank of CB17-SCID mice. Tumor growth was measured using a caliper at the indicated days PI. Bar plot represents the mean ± SD. (B) Tumor volume (mm^3) of Z138shSOX11.1 (n = 8), Z138shSOX11.3 (n = 6), and Z138shControl (n = 7) cells at day 23 PI into the lower dorsum of CB17-SCID mice. (C) Macroscopic appearance (upper panel) and consecutive histological sections from representative shSOX11 and shControl tumors stained with hematoxylin and eosin (H&E) and specific antibodies anti-human SOX11, PAX5, and BLIMP1 (×40). (D) Histologic sections of representative shSOX11 and shControl tumors (upper panels, H&E ×4 and ×10). shSOX11 tumors show extensive necrotic areas that are minimal in shControl tumors. Necrotic areas are highlighted by the immunostaining for activated caspase-3 (×4). Lower panel: Density (percentage of necrotic areas vs total area of the histologic section) of necrotic areas in control and SOX11-silenced tumors delineated by the presence of activated caspase-3–positive areas. Bar plot represents the mean percentage ± SD. *P* values are shown. The significance of difference was determined by independent-samples *t* test.

growth was followed up, and at 23 days postinoculation (PI) tumor size in control mice reached 8.8% of the body weight. SOX11 silencing reduced tumor growth compared with SOX11-positive control tumors, and significant differences in tumor size were already achieved at day 16 PI (Figure 5A). Tumors isolated from mice bearing shSOX11.1- and shSOX11.3-silenced cells showed 73.1% and 54.9% reduction in tumor burden, respectively, compared with SOX11-positive tumors (Figure 5B). We also observed a similar significant reduction in tumor growth and size, at day 23 PI, of the tumors derived from JEKO1shSOX11 and GRANTA519shSOX11 compared with their SOX11-positive tumor counterparts, JEKO1shControl and GRANTA519shControl (supplemental Figure 6A-B).

Concordant with the in vitro results, the in vivo SOX11-silenced tumors showed SOX11 and PAX5 downregulation and BLIMP1 upregulation compared with SOX11-positive tumors (Figure 5C and supplemental Figure 6D). The Ki-67 proliferation index and phosphohistone H3 were similar in control and silenced tumors (supplemental Figure 7A). We did not observe significant changes in cell density, proliferation, cycle phases, or viability after SOX11 silencing in cell lines in culture (supplemental Figure 7B-E). However, in vivo SOX11-silenced tumors had large necrotic areas with high levels of activated cleaved caspase-3 that were minimal or not observed in SOX11-positive tumors (Figure 5D and supplemental Figure 6D). These results suggest that SOX11 sustains the B-cell differentiation program and tumor cell survival in vivo and support the implication of SOX11 expression in the aggressive behavior of these tumors.

SOX11 expression and B-cell differentiation program in primary tumors

We next investigated whether SOX11 modulation of the mature B-cell and early plasmacytic differentiation programs observed in vitro also occurred in primary cells from SOX11-positive and SOX11-negative MCL tumors.

We first investigated whether the expression of the SOX11-bound genes was modulated in MCL. GSEA analysis showed

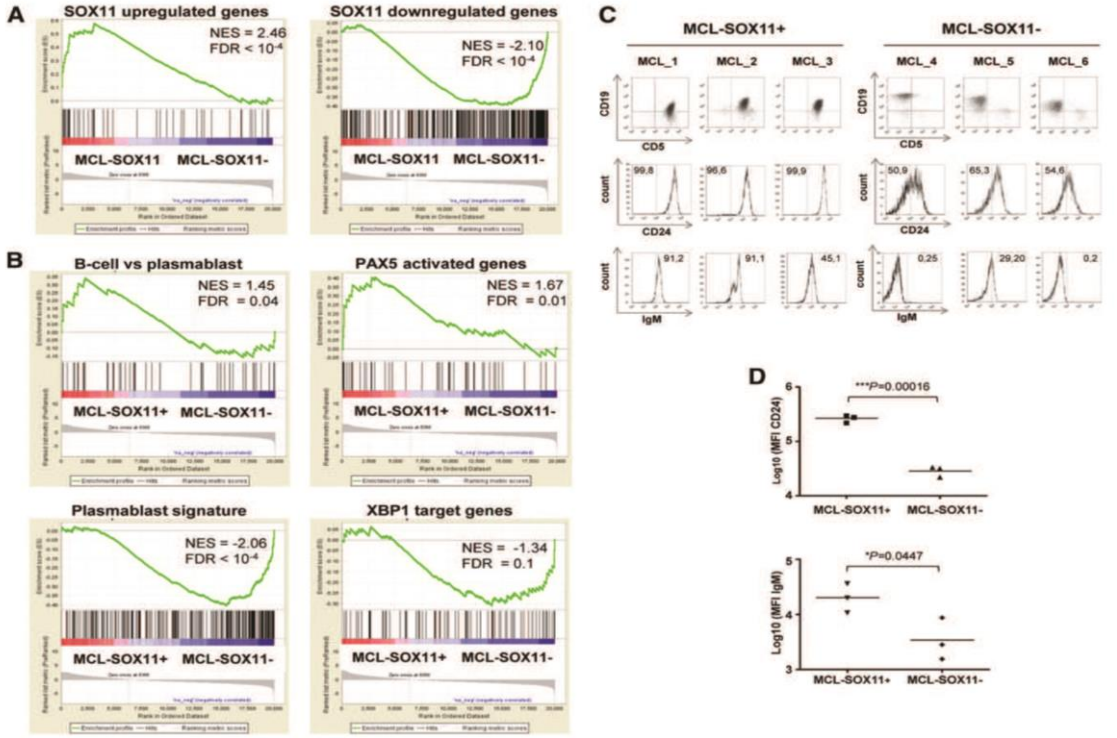

Figure 6. MCL SOX11-negative primary tumors lose B-cell identity and gain in a plasmablast gene signature. (A-B) GSEA analysis on preranked lists. (A) Using our customized gene sets described in "supplemental Materials and methods," SOX11 upregulated and downregulated genes and primary MCL-SOX11$^+$ tumors are enriched for SOX11-upregulated genes whereas primary MCL-SOX11$^-$ tumors are enriched in SOX11-downregulated genes. (B) MCL-SOX11$^+$ tumors are enriched in B-cell vs plasmablast and PAX5 activated genes gene sets whereas MCL-SOX11$^-$ tumors are enriched in plasmablast signature and XBP1 target genes. NES and FDR are shown. Statistical significance is considered when FDR < 0.1. (C) Analysis of CD24 and surface IgM expression in CD19+ CD5+ cells (MCL-SOX11$^+$) or CD19+ CD5$^-$ cells (MCL-SOX11$^-$). Numbers inside the histograms indicate the percentage of positive cells above the isotype control. (D) Mean fluorescence intensity (MFI) of surface CD24 and IgM expression in primary MCL tumors.

a statistically significant enrichment of SOX11 high-confident bound genes identified by ChIP-chip (supplemental Table 2) in both Z138shControl and primary SOX11-positive MCL (supplemental Figure 8), indicating that in these models SOX11 significantly activates the expression of its target genes.

We then defined 2 gene sets related to SOX11 transcriptional program extracted from our in vitro microarray data: SOX11-upregulated genes (genes downregulated upon SOX11 silencing) and SOX11-downregulated genes (upregulated upon knockdown) (supplemental Table 4). Notably, we found that SOX11-positive primary MCL had a GEP significantly enriched in SOX11-upregulated genes (normalized enrichment score [NES] = 2.46, FDR $< 10^{-4}$). Conversely, SOX11-negative primary MCL presented an enrichment in SOX11-downregulated genes (NES = -2.10, FDR $< 10^{-4}$) (Figure 6A).

These results suggest that the SOX11 transcriptional program derived from our knockdown experiments is also observed in primary tumors, prompting us to evaluate whether the modulation of B-cell and plasmacytic differentiation programs also occurs in these primary tumors.

We thus performed a GSEA with gene signatures of the different steps of the mature B-cell and plasma cell differentiation programs used in our previous analysis (supplemental Table 4). In line with the in vitro observations, this analysis revealed that SOX11-positive MCL were significantly enriched in B-cell vs plasmablast and PAX5 activated genes gene sets (NES = 1.45, FDR = 0.04 and NES = 1.67, FDR = 0.01, respectively) whereas SOX11-negative MCL showed statistical significance in the plasmablast signature[23] and XBP1 target genes (NES = -2.06, FDR $< 10^{-4}$ and NES = -1.34, FDR = 0.1, respectively) (Figure 6B).

We then studied the same panel of surface B-cell markers in the primary MCL cohort by flow cytometry. Concordant with the in vitro studies, SOX11-positive tumors had stronger expression of the mature B-cell marker CD24 and brighter IgM than SOX11-negative MCL (Figure 6C-D).

SOX11-silenced tumors in xenografted experiments showed increased apoptotic cells. We performed a GSEA using gene signatures related to apoptotic pathways and observed that SOX11-knockdown MCL cell lines were enriched in several apoptotic gene signatures (Fas, apoptosis, and caspase pathways). The

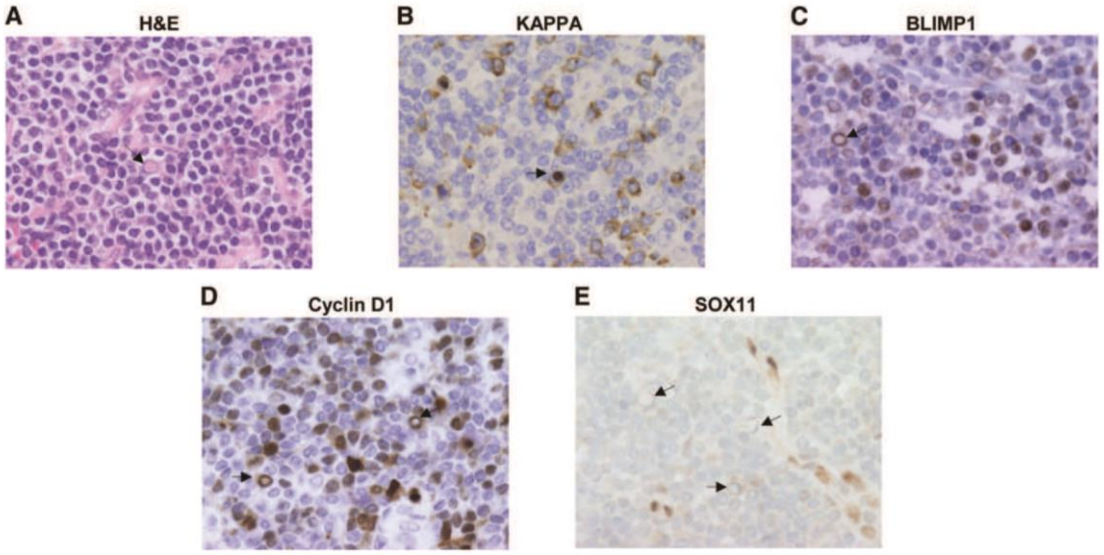

Figure 7. Plasma cells in MCL tumors are SOX11 negative. (A) MCL with focal plasmacytic differentiation. Some cells show Dutcher bodies corresponding to the accumulation of restricted immunoglobulins (arrow) (H&E; ×60). (B-C) Tumor cells expressing restricted kappa light chain and BLIMP1 (×60). (D) Tumor cells expressing cyclin D1 (×60). (E) SOX11 expression is negative in the tumor cells but positive in internal controls such as endothelial and histiocytic cells (×60). Arrows point to tumor cells with Dutcher bodies.

caspase-pathway gene signature was also significantly enriched in SOX11-negative primary MCL (supplemental Figure 9). These results suggest that SOX11 may regulate cell survival by controlling the expression of apoptotic genes in MCL cells.

Primary MCL have a monotonous cell morphology lacking the modulation toward plasmacytic differentiation observed in other types of B-cell lymphomas.[1] Intriguingly, some rare cases of MCL may show plasmacytic differentiation.[33] We postulated that this differentiation would occur in SOX11-negative MCL. In a review of our files, we found 2 MCL with plasmacytic differentiation expressing IgM, kappa, and BLIMP1 (Figure 7A-C). All tumor cells, including the cells with plasmacytic differentiation, expressed strong cyclin D1 but were SOX11 negative (Figure 7D-E). These results reinforce the idea that SOX11-negative MCL may modulate the mature B-cell and early plasma cell differentiation programs in primary tumors whereas the strong expression of SOX11 in conventional MCL may block the cells in a mature B-cell stage, preventing their further progress into differentiation.

Discussion

In this study, we have used a ChIP-chip approach to reveal the first human genome-wide promoter analysis of SOX11 and identified 1133 unique genes as putative targets of this transcription factor in MCL. Using GEP, we have also identified 366 genes whose expression was modulated by silencing SOX11 in MCL cell lines. GO analyses identified that genes regulated by SOX11 in these lymphoid cells were involved in lymphocyte activation and differentiation, phosphorylation, cell cycle, immune system development, hematopoiesis, and lymphoid organ development as the top annotated functions, but also in stem cell development, apoptosis, and cell migration.

The role of different members of the *SOX* gene family, including *SOX11*, as direct regulators of an expression program of early neural lineage development has been recently recognized in a murine model.[34] Our ChIP-chip study confirmed SOX11 binding to regulatory regions of similar genes involved in neuronal development (*BTG2, MEIS1,* and *NR2E1),* but these genes were not expressed in our lymphoid model, indicating the tissue-specific regulation of the SOX11-bound genes. In our study, the main target genes modulated by SOX11 were involved in immune system development and hematopoiesis, and *PAX5*, *MSI2*, and *HSPD1* were among the most significant genes directly regulated by SOX11.

The significant shift from a mature B cell to a plasmacytic gene expression program identified by GSEA in our SOX11 knockdown cells was highly suggestive of a major effect of the direct modulation of PAX5 by SOX11 in these tumor cells. We have demonstrated here that PAX5 is a direct target gene regulated by SOX11 and the constitutional expression of SOX11 in these tumors maintains the downstream PAX5 program. Thus, several B-cell–specific genes directly activated by PAX5 were downregulated in SOX11-knockdown MCL cell lines whereas BLIMP1 was upregulated upon SOX11 repression. The slight upregulation of XBP1(u) variant and the surface phenotype of Z138shSOX11 cells confirmed that SOX11 downregulation is able to initiate the terminal B-cell differentiation process but is not sufficient to drive the full plasma cell program.

SOX11 is constitutively overexpressed in the vast majority of MCL.[14-16] However, recent studies have identified a subset of SOX11-negative MCL[4] that differ from conventional SOX11-positive tumors in their frequent hypermutated *IGHV*, leukemic, nonnodal presentation and more indolent clinical behavior.[3-5,7] The significant reduction on tumor growth of the SOX11-silenced cells in the xenograft experiments is consistent with the indolent clinical course of the nonnodal SOX11-negative primary MCL and highlights the implication of SOX11 expression in the aggressive behavior of conventional MCL. Some studies have identified

SOX11-negative MCL with aggressive behavior but virtually all these cases have *TP53* alterations.[6,7,35] In our study, we confirmed that the gene signatures modulated upon SOX11 silencing in vitro were also enriched in primary MCL, indicating that our cell line model closely reflects the in vivo situation. Similarly, primary SOX11-positive MCL showed a GEP characteristic of mature B cells whereas negative tumors exhibited a relative shift to genes distinctive of early plasmacytic differentiation steps. However, the downregulation of SOX11 in both the in vitro model and primary tumors is not sufficient to trigger a mature plasma cell program. These results, together with our finding that the uncommon plasmacytic differentiation in MCL appears to occur in SOX11-negative tumors, reinforce the idea that these tumors may modulate the mature B-cell and plasmacytic differentiation programs. Conversely, SOX11 overexpression in aggressive MCL may block the cells in a mature B-cell stage, preventing their further differentiation. The resistance of MCL to new treatments with proteasome inhibitors has been linked to the development of plasmacytic differentiation, suggesting that the findings in our study may also have implications in the design of new therapeutic strategies.[36]

The significance of blocking plasma cell differentiation program as a relevant oncogenic mechanism in lymphoid neoplasias has been previously observed. The impairment of terminal B-cell differentiation caused by SOX11 overexpression in MCL may parallel the forced expression of *PAX5* by the t(9;14)(p13;q32) translocation identified in some B-cell lymphomas,[37-39] and the inactivating mutations of *PRDM1* in diffuse large B-cell lymphomas.[40-42]

In summary, our study reveals the global transcriptional network and direct target genes regulated by SOX11 in MCL that may contribute to the development and aggressive behavior of this tumor. Our findings provide an improved understanding of the molecular mechanisms contributing to the pathogenesis of MCL and may have clinical implications in the diagnosis of patients and selection of therapeutic strategies more adapted to the molecular diversity of this tumor.

Acknowledgments

This work was supported by grants from the Ministerio de Economía y Competitividad (MINECO) (BFU2009-09235 and RYC-2006-002110) (V.A.), (RYC-2009-05134) (P.P.-G.), (SAF08/3630) (E.C.), and the Instituto de Salud Carlos III RTICC (2006RET2039) (E.C.), (PS09/00060) (G.R.), Fondo Europeo de Desarrollo Regional, Unión Europea, Una manera de hacer Europa.

Authorship

Contribution: M.C.V. performed the ChIP experiments; J.P. performed all in vitro experiments; P.P.-G. performed experiments with the MCL primary cases; G.R. performed the in vivo study supervising; A.M. and J.P. performed in vivo experiments; A.N. generated microarray data from MCL primary tumors; G.C. performed statistical analysis; S.B. provided information of the MCL patients; A.E. and H.S.-C. helped with the ChIP-chip experiments; P.J., G.C., and J.I.M.-S. helped with microarray data; L.H. and D.C. helped with the discussion; N.V. performed fold-change analysis; E.C. performed immunohistochemistry experiments, identified morphologically MCL tumors with PC differentiation, analyzed data, and supervised experiments; V.A. designed, performed, and supervised experiments, analyzed data, and wrote the manuscript; and all authors discussed the results and commented on the manuscript.

Conflict-of-interest disclosure: The authors declare no competing financial interests.

Correspondence: Virginia Amador, Centre Esther Koplowitz (CEK), C/Rosselló 153, Barcelona 08036, Spain; e-mail: vamador@clinic.ub.es.

References

1. Swerdlow S, Campo E, Harris N, et al, eds. WHO Classification of Tumours of Haematopoietic and Lymphoid Tissues. Lyon, France: International Agency for Research on Cancer; 2008.
2. Jares P, Colomer D, Campo E. Genetic and molecular pathogenesis of mantle cell lymphoma: perspectives for new targeted therapeutics. *Nat Rev Cancer.* 2007;7(10):750-762.
3. Orchard J, Garand R, Davis Z, et al. A subset of t(11;14) lymphoma with mantle cell features displays mutated IgVH genes and includes patients with good prognosis, nonnodal disease. *Blood.* 2003;101(12):4975-4981.
4. Fernàndez V, Salamero O, Espinet B, et al. Genomic and gene expression profiling defines indolent forms of mantle cell lymphoma. *Cancer Res.* 2010;70(4):1408-1418.
5. Ondrejka SL, Lai R, Smith SD, et al. Indolent mantle cell leukemia: a clinicopathological variant characterized by isolated lymphocytosis, interstitial bone marrow involvement, kappa light chain restriction, and good prognosis. *Haematologica.* 2011;96(8):1121-1127.
6. Royo C, Navarro A, Clot G, et al. Non-nodal type of mantle cell lymphoma is a specific biological and clinical subgroup of the disease. *Leukemia.* 2012;26(8):1895-1898.
7. Navarro A, Clot G, Royo C, et al. Molecular subsets of mantle cell lymphoma defined by the IGHV mutational status and SOX11 expression have distinct biologic and clinical features. *Cancer Res.* 2012;72(20):5307-5316.
8. Sock E, Rettig SD, Enderich J, et al. Gene targeting reveals a widespread role for the high-mobility-group transcription factor Sox11 in tissue remodeling. *Mol Cell Biol.* 2004;24(15):6635-6644.
9. Haslinger A, Schwarz TJ, Covic M, et al. Expression of Sox11 in adult neurogenic niches suggests a stage-specific role in adult neurogenesis. *Eur J Neurosci.* 2009;29(11):2103-2114.
10. Weigle B, Ebner R, Temme A, et al. Highly specific overexpression of the transcription factor SOX11 in human malignant gliomas. *Oncol Rep.* 2005;13(1):139-144.
11. de Bont JM, Kros JM, Passier MM, et al. Differential expression and prognostic significance of SOX genes in pediatric medulloblastoma and ependymoma identified by microarray analysis. *Neuro-oncol.* 2008;10(5):648-660.
12. van de Wetering M, Oosterwegel M, van Norren K, et al. Sox-4, an Sry-like HMG box protein, is a transcriptional activator in lymphocytes. *EMBO J.* 1993;12(10):3847-3854.
13. Smith E, Sigvardsson M. The roles of transcription factors in B lymphocyte commitment, development, and transformation. *J Leukoc Biol.* 2004;75(6):973-981.
14. Dictor M, Ek S, Sundberg M, et al. Strong lymphoid nuclear expression of SOX11 transcription factor defines lymphoblastic neoplasms, mantle cell lymphoma and Burkitt's lymphoma. *Haematologica.* 2009;94(11):1563-1568.
15. Ek S, Dictor M, Jerkeman M, et al. Nuclear expression of the non B-cell lineage Sox11 transcription factor identifies mantle cell lymphoma. *Blood.* 2008;111(2):800-805.
16. Mozos A, Royo C, Hartmann E, et al. SOX11 expression is highly specific for mantle cell lymphoma and identifies the cyclin D1-negative subtype. *Haematologica.* 2009;94(11):1555-1562.
17. Salaverria I, Perez-Galan P, Colomer D, et al. Mantle cell lymphoma: from pathology and molecular pathogenesis to new therapeutic perspectives. *Haematologica.* 2006;91(1):11-16.
18. Subramanian A, Tamayo P, Mootha VK, et al. Gene set enrichment analysis: a knowledge-based approach for interpreting genome-wide expression profiles. *Proc Natl Acad Sci USA.* 2005;102(43):15545-15550.
19. Vegliante MC, Royo C, Palomero J, et al. Epigenetic activation of SOX11 in lymphoid neoplasms by histone modifications. *PLoS ONE.* 2011;6(6):e21382.
20. Roué G, Pérez-Galán P, Mozos A, et al. The Hsp90 inhibitor IPI-504 overcomes bortezomib resistance in mantle cell lymphoma in vitro and in vivo by down-regulation of the prosurvival ER chaperone BiP/Grp78. *Blood.* 2011;117(4):1270-1279.

21. Tarte K, Zhan F, De Vos J, et al. Gene expression profiling of plasma cells and plasmablasts: toward a better understanding of the late stages of B-cell differentiation. *Blood.* 2003;102(2):592-600.

22. Shaffer AL, Wright G, Yang L, et al. A library of gene expression signatures to illuminate normal and pathological lymphoid biology. *Immunol Rev.* 2006;210:67-85.

23. Jourdan M, Caraux A, Caron G, et al. Characterization of a transitional preplasmablast population in the process of human B cell to plasma cell differentiation. *J Immunol.* 2011; 187(8):3931-3941.

24. McManus S, Ebert A, Salvagiotto G, et al. The transcription factor Pax5 regulates its target genes by recruiting chromatin-modifying proteins in committed B cells. *EMBO J.* 2011;30(12): 2388-2404.

25. Cobaleda C, Jochum W, Busslinger M. Conversion of mature B cells into T cells by dedifferentiation to uncommitted progenitors. *Nature.* 2007;449(7161):473-477.

26. Nera KP, Kohonen P, Narvi E, et al. Loss of Pax5 promotes plasma cell differentiation. *Immunity.* 2006;24(3):283-293.

27. Dy P, Penzo-Méndez A, Wang H, et al. The three SoxC proteins—Sox4, Sox11 and Sox12—exhibit overlapping expression patterns and molecular properties. *Nucleic Acids Res.* 2008;36(9): 3101-3117.

28. Wiebe MS, Nowling TK, Rizzino A. Identification of novel domains within Sox-2 and Sox-11 involved in autoinhibition of DNA binding and partnership specificity. *J Biol Chem.* 2003; 278(20):17901-17911.

29. Tarlinton D, Radbruch A, Hiepe F, et al. Plasma cell differentiation and survival. *Curr Opin Immunol.* 2008;20(2):162-169.

30. Shaffer AL, Lin KI, Kuo TC, et al. Blimp-1 orchestrates plasma cell differentiation by extinguishing the mature B cell gene expression program. *Immunity.* 2002;17(1):51-62.

31. Kallies A, Hasbold J, Fairfax K, et al. Initiation of plasma-cell differentiation is independent of the transcription factor Blimp-1. *Immunity.* 2007; 26(5):555-566.

32. Nutt SL, Tarlinton DM. Germinal center B and follicular helper T cells: siblings, cousins or just good friends? *Nat Immunol.* 2011;12(6):472-477.

33. Visco C, Hoeller S, Malik JT, et al. Molecular characteristics of mantle cell lymphoma presenting with clonal plasma cell component. *Am J Surg Pathol.* 2011;35(2):177-189.

34. Bergsland M, Ramsköld D, Zaouter C, et al. Sequentially acting Sox transcription factors in neural lineage development. *Genes Dev.* 2011; 25(23):2453-2464.

35. Nygren L, Baumgartner Wennerholm S, Klimkowska M, et al. Prognostic role of SOX11 in a population-based cohort of mantle cell lymphoma. *Blood.* 2012;119(18):4215-4223.

36. Pérez-Galán P, Mora-Jensen H, Weniger MA, et al. Bortezomib resistance in mantle cell lymphoma is associated with plasmacytic differentiation. *Blood.* 2011;117(2):542-552.

37. Busslinger M, Klix N, Pfeffer P, et al. Deregulation of PAX-5 by translocation of the Emu enhancer of the IgH locus adjacent to two alternative PAX-5 promoters in a diffuse large-cell lymphoma. *Proc Natl Acad Sci USA.* 1996;93(12): 6129-6134.

38. Iida S, Rao PH, Nallasivam P, et al. The t(9;14) (p13;q32) chromosomal translocation associated with lymphoplasmacytoid lymphoma involves the PAX-5 gene. *Blood.* 1996;88(11):4110-4117.

39. Morrison AM, Jäger U, Chott A, et al. Deregulated PAX-5 transcription from a translocated IgH promoter in marginal zone lymphoma. *Blood.* 1998;92(10):3865-3878.

40. Mandelbaum J, Bhagat G, Tang H, et al. BLIMP1 is a tumor suppressor gene frequently disrupted in activated B cell-like diffuse large B cell lymphoma. *Cancer Cell.* 2010;18(6):568-579.

41. Tam W, Gomez M, Chadburn A, et al. Mutational analysis of PRDM1 indicates a tumor-suppressor role in diffuse large B-cell lymphomas. *Blood.* 2006;107(10):4090-4100.

42. Pasqualucci L, Compagno M, Houldsworth J, et al. Inactivation of the PRDM1/BLIMP1 gene in diffuse large B cell lymphoma. *J Exp Med.* 2006; 203(2):311-317.

SUPPLEMENTAL INFORMATION

SOX11 REGULATES PAX5 EXPRESSION AND BLOCKS TERMINAL B-CELL DIFFERENTIATION IN AGGRESSIVE MANTLE CELL LYMPHOMA

Vegliante et al.

I. SUPPLEMENTAL MATERIALS AND METHODS

Cell lines and primary tumors

MCL cell lines Z138 (CRL-3001, ATCC), JEKO1 (CRL-3006, ATCC), REC1 (ACC-584, DSMZ), HBL2 (kindly provided by Prof. M. Dreyling) and JVM2 (CRL-3002, ATCC) were cultured in RPMI 1640 medium, supplemented with 10% fetal bovine serum (FBS; Sigma Chemical, Co. St Louis, Mo), 2µM L-glutamine, 100U/mL penicillin, and 100µg/mL streptomycin (GIBCO, Grand Island, NY). All these cell lines carry the t(11;14) translocation and express high levels of cyclin D1. GRANTA519 (ACC-342, DSMZ) and human embryonic kidney 293 cells (HEK293) (CRL-1573; ATCC) were cultured in DMEM medium, supplemented with 10% FBS, 2 µM L-glutamine, 100 U/mL penicillin, and 100 µg/mL streptomycin.

The tumor samples of the 38 primary MCL used in the GEP and the six used for flow cytometry analysis were highly purified leukemic MCL cells (>95% as determined by flow cytometry). All cases had the t(11;14) and/or overexpressed cyclin D1. These cases were diagnosed according to previous defined criteria[1,2] and their SOX11 expression levels were quantified by qRT-PCR.[3] The study was approved by the Institutional Review Board of the Hospital Clínic, Barcelona, Spain.

Written informed consent was obtained from all participants and the Ethics Committees approved this consent procedure in accordance with the principles of the Declaration of Helsinki.

Immunoprecipitation (IP)

Protein extracts were obtained from Z138 and JVM2 cells or from HEK293 cells transiently transfected with pcDNA3-SOX11HA or pcDNA3-SOX4HA expression plasmids using Triton buffer as previously described.[4] 5mg of protein extracts were used for IP using specific antibodies against SOX11 (rabbit H-290 (sc-20096); goat C-20 (sc-17347), Santa Cruz Biotechnology). IP was performed overnight (O/N) at 4ºC with slow rotation. Lysates were then rotated with Dynabeads Protein G (Invitrogen) for 2h at 4ºC, after which the supernatant was separated from the beads, washed three times with triton buffer and SOX11 protein eluted with Laemmli buffer 1h at room temperature (RT). Immunoprecipitated proteins were analyzed by WB using the HA antibody (12CA5, Roche Applied Science, Indianapolis, IN) for IP experiments done in the HEK293 cell; and the antibody (HPA000536, Atlas Antibodies, Stockholm, Sweden) that detects SOX11 and SOX4 proteins for IPs done in the MCL cell lines.

Chromatin Immunoprecipitation

Z138, GRANTA519 and JVM2 cell lines ($5x10^7$ cells) were fixed with 1% formaldehyde in culture medium for 10min at RT followed by quenching with 0.125M glycine for 5min. Cells were washed twice with ice-cold PBS and nuclei were isolated by incubation with ChIP buffer (25mM HEPES pH 8.0, 1.5mM $MgCl_2$, 10mM KCl, 0.1% Nonidet-P40, and 1mM DTT) for 10min at 4°C. Nuclei were resuspended in 1mL of lysis buffer (50mM HEPES, 140mM NaCl, 1mM EDTA, 1% Triton X-100, 0.1% SDS and 0.1% Na-deoxycholate) and sonicated on ice with a Branson Sonifier 250 (20 X 20 seconds, duty 20%, output control 7, hold on ice 1min between pulses) followed by sonication using Biorupter™ sonicator from Diagenode (20 cycles of [40 seconds "ON"/ 20 seconds "OFF"]). Sonicated fragments ranged in size from 200-1000bp. After a spinning step to reduce debris, 10µg of anti-SOX11 antibody (goat C-20; sc-17347;

Santa Cruz Biotechnology, Santa Cruz, CA) were used to immunoprecipitate protein-DNA complexes O/N at 4°C and collected using DNA-saturated Protein G Sepharose™ 4 Fast Flow (GE Healthcare, Little Chalfont, United Kingdom) for 2h. After incubation, the immunocomplexes were washed sequentially with low-salt wash buffer (0.1% SDS, 1% Triton X-100, 2mM EDTA, 20mM Tris-HCl, at pH 8.0 and 150mM NaCl), high-salt wash buffer (0.1% SDS, 1% Triton X-100, 2mM EDTA, 20mM Tris-HCl, at pH 8.0, and 500mM NaCl), LiCl wash buffer (0.25M LiCl, 1% NP-40, 1% Na-deoxycholate, 1mM EDTA and 10mM Tris-HCl, at pH 8.0) and TE buffer (10mM Tris-HCl, at pH 8.0, and 1mM EDTA). Immunocomplexes were eluted in ChIP elution buffer (1%SDS and 0.1M $NaHCO_3$), crosslinking was reverted by addition of 5M NaCl and incubation at 65°C for at least 4h, and DNA was precipitated with ethanol O/N at -20°C. Samples were then treated with Proteinase K solution (1M Tris-HCl at pH 6.5, 0.5M EDTA and proteinase K 10mg/mL) at 45°C for 2h and DNA purified using QIAquick® PCR Purification Kit (QIAGEN, Hilden, Germany). 10ng purified DNA (SOX11-ChIP and Input from Z138, GRANTA519 and JVM2 cells) were amplified in two steps using a GenomePlex® Whole Genome Amplification WGA Kit (Sigma), following the manufacturer's instructions and used for ChIP-chip analysis and/or ChIP-qPCR. We performed ChIP assays in triplicate from Z138 cell line expressing SOX11 and in a single experiment from JVM2 cell line as negative control.

ChIP-chip analysis

Amplified immunoprecipitated and input DNA (9.5µg) from Z138 and JVM2 cell lines were quality controlled, quantified, and sent to NimbleGen System for probe labeling and hybridization to NimbleGen Human ChIP-chip 2.1M Deluxe Promoter array (Roche NimbleGen, Iceland)

(http://www.nimblegen.com/products/chip/index.html). Raw data were analyzed for peaks (significant regions of SOX11 enrichment) using NimbleScan v2.4 software and data were visualized in SignalMap v1.9 software. Nimblegen software detects peaks using default parameters, by searching for four probes using a 500bp sliding window.

Genomic fragments that overlapped across three independent replicates in Z138 SOX11 ChIP-chip experiments and were not present in the JVM2 SOX11 ChIP-chip experiment were considered SOX11-bound regions. This analysis yielded high confidence genes bound by SOX11 (FDR<0.1 and Peak Score>0.5), which were used to perform GO analysis using Ingenuity Pathway analysis (IPA, Ingenuity® Systems) and DAVID (The Databse for Annotation, Visualization and Integrated Discovery) Bioinformatic Resources (http://david.abcc.ncifcrf.gov/).

Vector constructs

The expression plasmids pcDNA$_3$-SOX11HA and pcDNA$_3$-SOX4HA were generated as previously described.[4] Deletion mutants of SOX11 protein lacking HMG domain (ΔHMGSOX11HA) or C-terminal TAD motif (ΔCtermSOX11HA) were generated by PCR using the QuikChange Kit (Stratagene, La Jolla, CA) reagents and following the manufacturer's instructions with some modifications. pcDNA$_3$-SOX11HA was used as a DNA template and the PCR primers were modified on the 5'-end with a phosphate group: for pcDNA3-ΔHMGSOX11HA, 5'-TCCCGGGGCAGGTTGCTCT-3' (Forward primer) and 5'-GAAAAAGCCCAAAATGGACC-3' (Reverse primer) and for pcDNA3-ΔCtermSOX11HA were 5'-GGTCCATTTTGGGCTTTTTC-3' (Forward primer) and 5'-AACTTCTCCGACCTGGTGTT-3' (Reverse primer). PCR products were treated with DpnI (Stratagene) to degrade the vector template, and purified using QIAquick®

PCR Purification Kit (QIAGEN), following manufacturer's instructions. Cleaned PCR fragments were religated with T4 ligase (Promega, Leiden, The Netherlands), following the manufacturer's instructions. All expression plasmids were sequenced prior to use. Expression plasmids were transiently transfected in HEK293 cell line using Lipofectamine 2000 system (Invitrogen, Carlsbad, CA), following the manufacturer's instructions. The efficiency of expression was assayed by WB experiments using mouse monoclonal anti-HA antibody (12CA5).

SOX11 silencing by lentiviral infection

For lentiviral infections, $1.5x10^6$ exponentially growing MCL target cells (Z138, GRANTA519 and JEKO1), cultured in their corresponding mediums with 10% of FBS and without antibiotics, were mixed with $1x10^5$ infectious units (IFU) of the lentiviral particles and plated on 6 well plates at $0.5x10^6$ cells/mL. Cells were spined for 150min at 2500rpm and 32ºC. After centrifugation, 6mL of complete medium were added to the cells and incubated at 37ºC and 5%CO_2. Infected MCL cells were resuspended in new complete medium with puromycin selection at a final concentration of 0.25mg/mL. The efficiency of the knockdown was assayed by qRT-PCR and WB experiments.

Gene expression profiling analysis

The hybridized arrays were scanned. The analysis of the scanned images and the determination of the signal value for each probe set of the array were obtained with GeneChip® Command Console® Software (AGCC) (Affymetrix). Raw data were imported to R Statistical Package (http://www.r-project.org/) for analysis and data were normalized using the Robust Multichip Analysis (RMA) algorithm of the BioConductor affy Package and genes with *P*-val>0.05 were excluded. Differential gene expression

between Z138shSOX11.1 and shSOX11.3 and Z138shControl.1 and shControl.2 was determined using moderated t-statistics with empirical Bayes shrinkage of the standard errors implemented in the BioConductor limma Package.[5] The FDR controlling method of Benjamini and Hochberg was used to adjust the *P*-val for each gene based on a significance level of 0.05 and log2 FC>0.7. The signatures in these two independent SOX11 silenced MCL cell lines were highly similar (r2= 0.95 taking all the genes covered in the array, and r2=0.99, within the differentially expressed genes).

Gene Set Enrichment Analysis (GSEA)

We performed GSEA on two pre-ranked lists of genes derived from *in vitro* SOX11 silencing microarray data and from our series of 38 purified primary MCL dataset. To generate these pre-ranked lists we analyzed the GEP of our *in vitro* cell line model as well as the GEP of 38 primary MCL according to their SOX11 expression levels.

The top 26,000 genes selected with a greatest InterQuartile Range (IQR) were first ranked with respect to the phenotype, shControl vs shSOX11 and SOX11-positive vs -negative primary tumors, by using *t*-statistic value. With this approach, the final position in the ranked gene lists depended only on the strength of the gene in discriminating between phenotypes. We used 1,000 permutations and a weighted statistic to assess statistical significance.

The query gene sets included gene signatures related to B-cell and plasma cell differentiation programs and apoptotic pathways. The well-defined gene signatures related to the different steps of the mature B-cell and plasma cell differentiation programs, and signatures of genes modulated by PAX5, IRF4, BLIMP1, and XBP1

were obtained from different publications (Table S4 and Table S5), whereas the apoptotic signatures (KEGG_Apoptosis, Biocarta_Fas pathway and caspase 3 pathway) were downloaded from the MSigDB, Molecular Signature Database of Broad Institute.

Additionally, we customized two gene sets derived from our knockdown experiments, SOX11 upregulated and downregulated genes. For this purpose, we considered genes regulated by SOX11 knockdown with log2 FC>0.7 and FDR *P*-val<0.05 for components of SOX11 gene expression signature (Table S3). We also customized two more gene sets derived from microarray data from our series of 38 purified primary MCL, MCL-SOX11+ and MCL-SOX11- genes (Table S4). To generate these gene sets we considered differentially expressed genes between SOX11-positive and negative MCL-primary tumors with log2 FC>0.7 and FDR *P*-val<0.05.

Furthermore, GSEA was also performed on microarray data of MCL patients and SOX11 knockdown experiments dataset to test the enrichment of high confidence SOX11 target genes (PS>0.5 and FDR<0.1, Table S2) among phenotypes. Difference of classes and *t*-Test were used as metric method for ranking genes from SOX11 silencing and MCL patient's dataset respectively and a weighted statistic to assess statistical significance.

XBP-1 splicing

XBP-1 mRNA spliced and unspliced forms were detected by RT-PCR using the protocol and primers previously described.[6] PCR products representing spliced [*XBP1(s)*, 398 base pairs) and unspliced (*XBP1(u)*, 424 base pairs)] were detected on agarose gel.

Cell density assay

Cells of interest were cultured at 0.2 x10^6 cells/mL in complete RPMI or DMEM medium and every 24h cell density was measured in a TC10 System Sample Slide Dual Chamber using the BIO-RAD TC10 Automated Cell Counter (Bio-rad, Hercules, CA).

Proliferation assay

Cells of interest were resuspended in PBS-0.1% BSA at a final concentration of 1x10^6 cells/mL and incubated with serial doubling concentrations of CFSE FITC (CellTrace CFSE Cell Proliferation Kit, Invitrogen) (2.5, 5, 10µM) at 37ºC for 10min. The staining was quenched by adding 5 volumes of ice-cold RPMI to the cells on ice for 5min. Cells were then washed three times in fresh RPMI, and cultured for five days at 37ºC under a 5%CO_2 atmosphere at a cell density of 0.2 x10^6 cells/mL. Every 24h, 500,000 cells were collected and analyzed using the Attune Accoustic Focusing Cytometer and Software (Applied Biosystems, Foster City, CA). For the analysis, 10,000 events were collected in the lymphocyte gate.

Cell cycle

Cells of interest at a final concentration of 1x10^6 cells/mL were stained with DyeCycle Violet (Invitrogen) for 30min at 37ºC in the dark and acquired and analyzed using the Attune Acoustic Focusing Cytometer and Software (Applied Biosystems). For the analysis, 10,000 events were collected in the lymphocyte gate, and cell cycle was analyzed every 24h.

Apoptosis assay

Cells were cultured at 0.2 x10^6 cells/mL in complete RPMI or DMEM medium for five days, and every 24h cell viability was analyzed. Cells of interest were resuspended in annexinV-binding buffer at a final concentration of 1x10^6 cells/mL and stained with annexin-V-FITC (eBioscience, San Diego, CA) for 15min at 4ºC in the dark. After washing the cells twice with annexinV-binding buffer, Propidium Iodide (PI) was added to the cell suspension, and cells were acquired and analyzed using the Attune Acoustic Focusing Cytometer and Software (Applied Biosystems). For the analysis, 10.000 events were collected in the lymphocyte gate.

Quantitative chromatin immunoprecipitation of histone marks

Chromatin immunoprecipitation (ChIP) experiments were performed as previously described [4] using LowCell ChIP kit (Diagenode; Liege, Belgium) according to manufacturer's instructions with the following antibodies: H3K9/14Ac, H3K4me3 (Diagenode). A rabbit IgG (Diagenode) was used as a negative control.

Immunoprecipitated DNA and 1:100 diluted input samples were analyzed in triplicate by quantitative real-time PCR analyses using Fast SYBR ®Green Master Mix in a StepOnePlus PCR detection system (Applied Biosystems). The primers for the *SOX11* gene promoter region are: SOX11prom_Forward: 5'-GAGAGCTTGGAAGCGGAGA-3' and SOX11prom_Reverse: 5'-AGTCTGGGTCGCTCTCGTC-3'.

II. SUPPLEMENTAL FIGURES

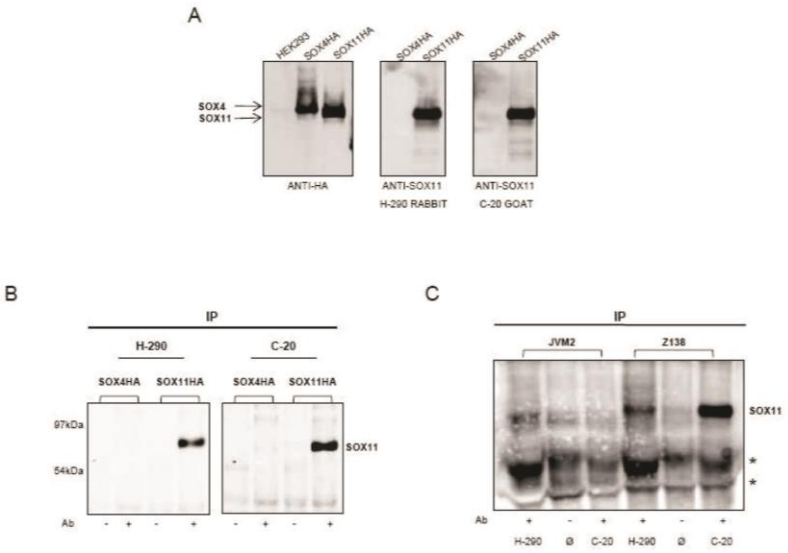

Figure S1. SOX11 antibody for Chromatin Immunoprecipitation (ChIP).

(A) The specificity of different polyclonal antibodies against SOX11 was tested by WB analysis in HEK293 cells transfected with vectors encoding for SOX4HA, SOX11HA proteins and with the empty vector pcDNA3.1 as a control (HEK293). 24h after transfection, cells were collected and protein extracts were subjected to immunoblotting with the indicated antibodies: (left panels) against Hemagglutinin epitope tagged (HA) (mouse monoclonal anti-HA, 12CA5) to detect SOX4HA and SOX11HA proteins and (right panel) against SOX11 (the polyclonal rabbit H-290 and the polyclonal goat C-20 anti-SOX11 antibodies).

(B) Immunoprecipitation (IP) of SOX11 protein was performed using HEK293 cells expressing SOX4HA or SOX11HA proteins and two different antibodies (H-290 and C-20 anti-SOX11 antibodies) (+). Control rabbit IgG was used as a negative control (-).

The efficiency and specificity of these antibodies to immunoprecipitate SOX11 were tested by WB using the anti-HA antibody.

(C) The efficiency of the indicated SOX11 antibodies H-290 and C-20 (+) to IP SOX11 in MCL cell lines was tested by IP-WB experiments in Z138 and JVM2 cell lines. Control rabbit IgG was used as a negative control (Ø) (-). The presence of immunoprecipitated SOX11 was determined by WB using the rabbit polyclonal anti-SOX11 antibody (HPA000536), that detects SOX4 and SOX11 proteins. * Non-specific bands.

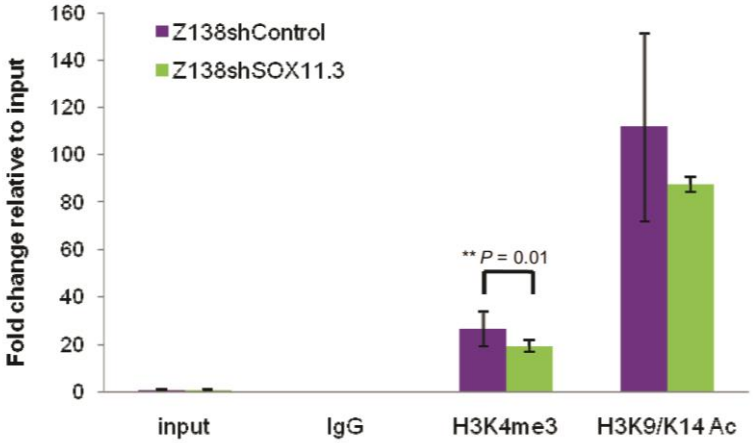

Figure S2. Enrichment of activating chromatin marks in *SOX11* promoter after SOX11-silencing in MCL Z138 cell line. Enrichment of H3K4me3 and H3K9/K14Ac active chromatin marks in *SOX11* promoter in Z138shControl and Z138shSOX11.3 MCL cell lines. A rabbit IgG was used as a ChIP negative control. The values are relative to 1:100 diluted input samples.

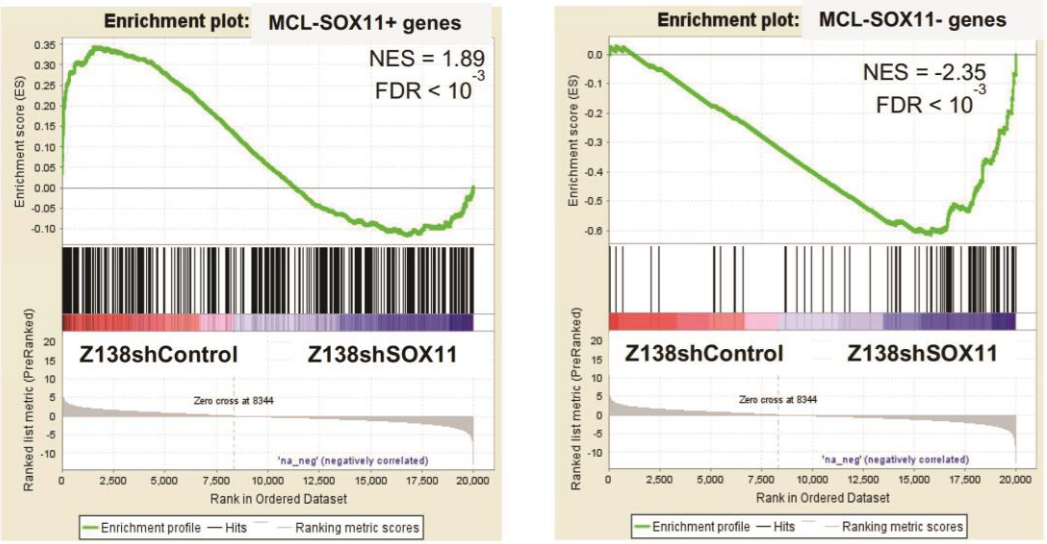

Figure S3. Z138shControl and Z138shSOX11 *in vitro* model cell lines show a significant enrichment in the clinical MCL GE markers. We generated two gene sets derived from the microarray expression data of SOX11-positive and negative MCL primary tumors (MCL-SOX11+ and MCL-SOX11- genes) (Table S4) and performed a GSEA on the *in vitro* pre-ranked list showing that (Left) Z138shControl had a GEP significantly enriched in SOX11-positive primary MCL genes whereas (Right) Z138shSOX11 presented a GEP enriched in SOX11-negative primary MCL genes. NES and FDR *P*-values are shown. Statistical significance is considered when FDR<0.05.

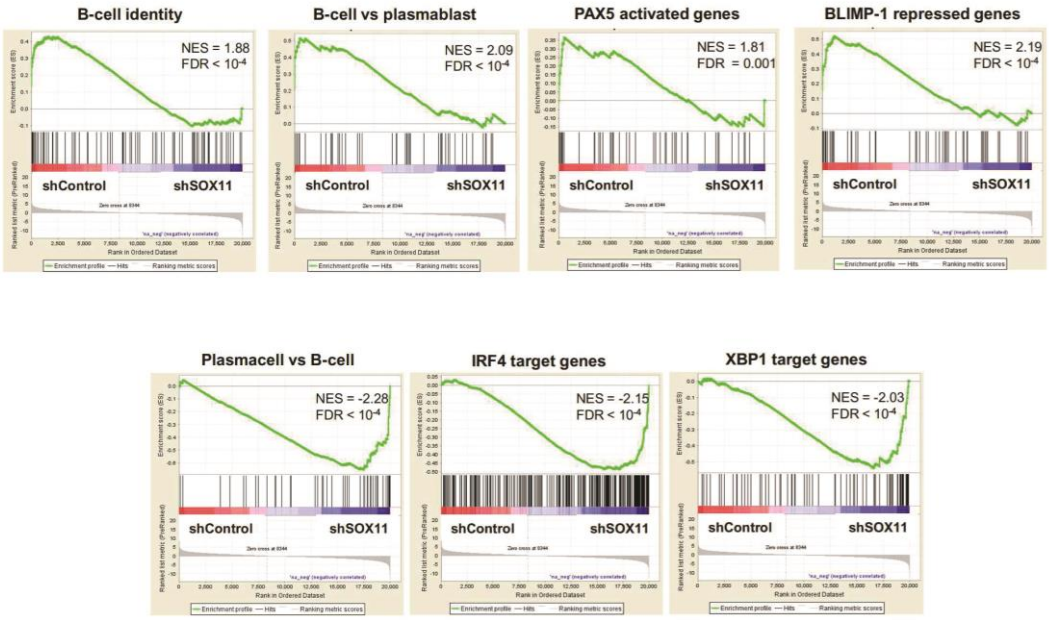

Figure S4. Shift from a mature B-cell to a plasmacytic gene expression program in SOX11-knockdown MCL cells. GSEA on the *in vitro* pre-ranked list showing that Z138shControl cells were significantly enriched in gene signatures related to the B-cell program (B-cell identity, B-cell vs plasmablast, PAX5 activated genes and BLIMP1 repressed genes) whereas gene signatures related to the plasma cell program (Plasmacell vs B-cell, IRF4 target genes and XBP1 target genes) were significantly enriched in shSOX11 cells. NES and FDR *P*-values are shown. Statistical significance is considered when FDR<0.05.

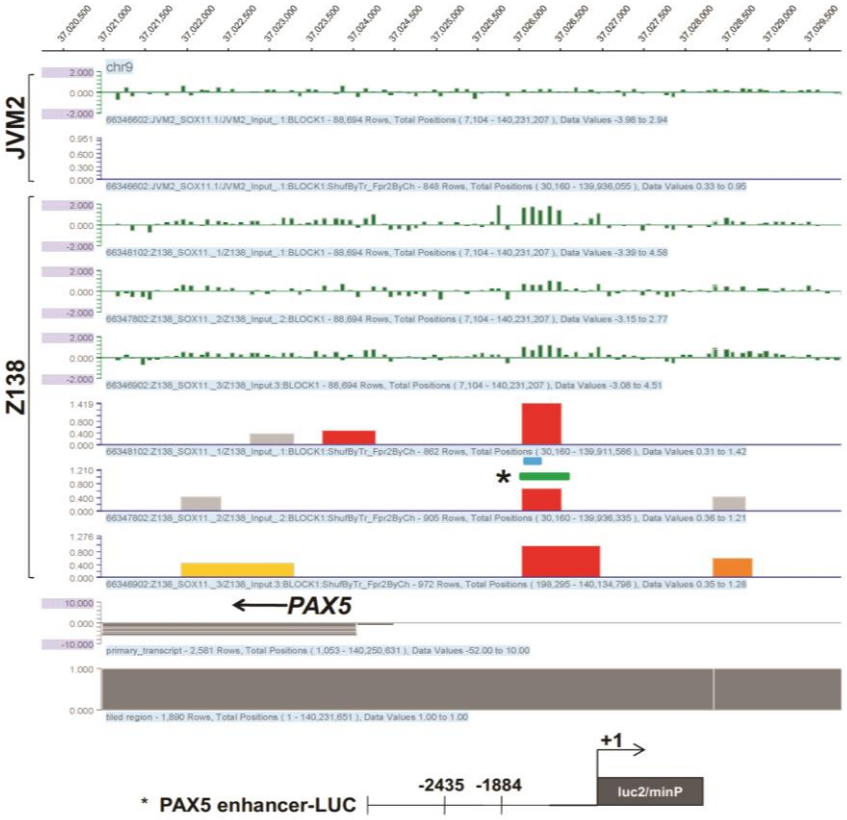

Figure S5. SignalMap representation of SOX11 binding at the *PAX5* promoter-enhancer site. SOX11 binding site at the promoter of *PAX5* by triplicates in Z138 MCL cell line. Green bars represent fluorescent intensity of probe around *PAX5* promoter region expressed as log2 ratio and red bars show high confidence peaks using Nimblescan peak finding algorithm. Position of gene transcripts and the region tiled on the array (from 5kb upstream to 1kb downstream of the TSS) are indicated at the bottom panels, in grey. The blue bar below the red peak indicates the SOX11 binding region validated by ChIP-qPCR, and the green asterisked bar identifies high confidence peaks within sequences of *PAX5* cloned at the luciferase reporter construct. The scale at the top of the panel indicates the base pair position on chromosome 9. No peaks at the promoter-enhancer site of *PAX5* in JVM2 MCL cell line were observed.

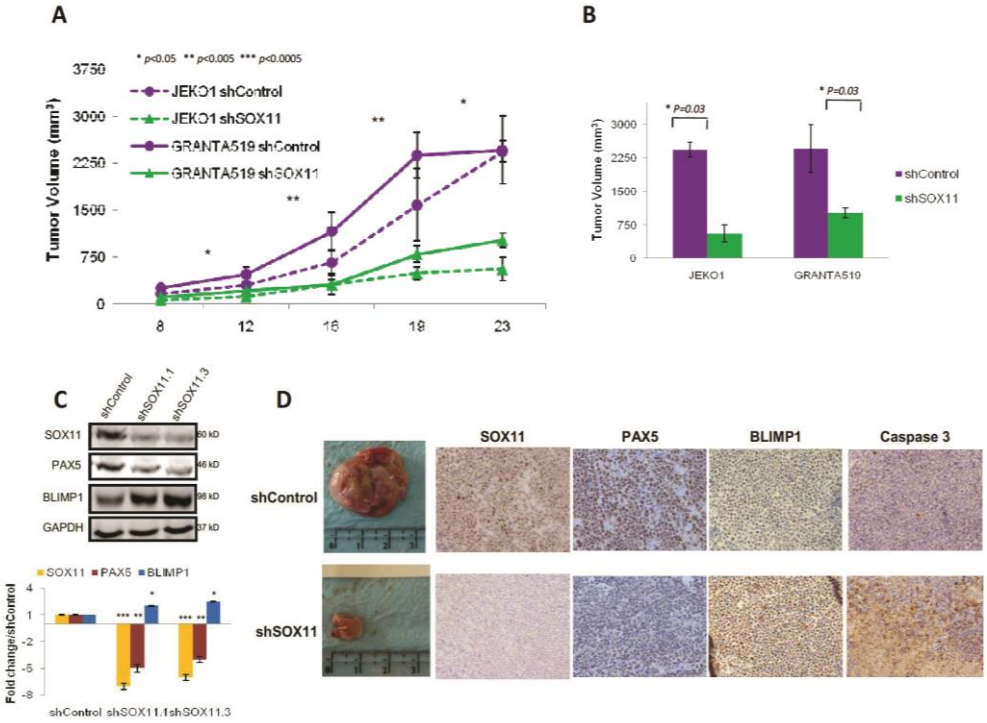

Figure S6. SOX11 inhibits the growth of MCL cell lines-derived tumors in SCID mice.

(A) JEKO1 and GRANTA519 stably transduced with shSOX11.3 and shControl (10^7cells/mouse) were subcutaneously inoculated into the right flank of CB17-SCID mice. Tumor growth was measured using a caliper at the indicated days Post Inoculation (PI).

(B) Tumor volume (mm^3) of JEKO1shSOX11.3 (n=5), GRANTA519shSOX11.3 (n=5), JEKO1shControl (n=5) and GRANTA519shControl (n=5) cells at day 23 PI into the lower dorsum of CB17-SCID mice.

(C) (Upper panel) SOX11, PAX5 and BLIMP1 expression levels in JEKO1 stably transduced with shControl, shSOX11.1 or shSOX11.3 assessed by WB, using GAPDH

as a loading control. (Lower panel) Fold differences compared to control cells are shown of SOX11, PAX5 and BLIMP1 protein expression levels. Protein quantification was done with Image Gauge software, and SOX11, PAX5 and BLIMP1 expression levels were corrected by quantification of GAPDH expression levels.

(D) Macroscopic appearance and consecutive histological sections from representative shSOX11 and shControl derived tumors stained with specific antibodies anti-human SOX11, PAX5, BLIMP1 and activated caspase-3 (x20). shSOX11 tumors show extensive necrotic areas that are minimal in shControl tumors. Necrotic areas are highlighted by the immunostaining for activated caspase-3 (x20).

Bar plot represents the mean percentage ±SD. *P*-val are shown. The significance of difference was determined by independent samples *t*-test.

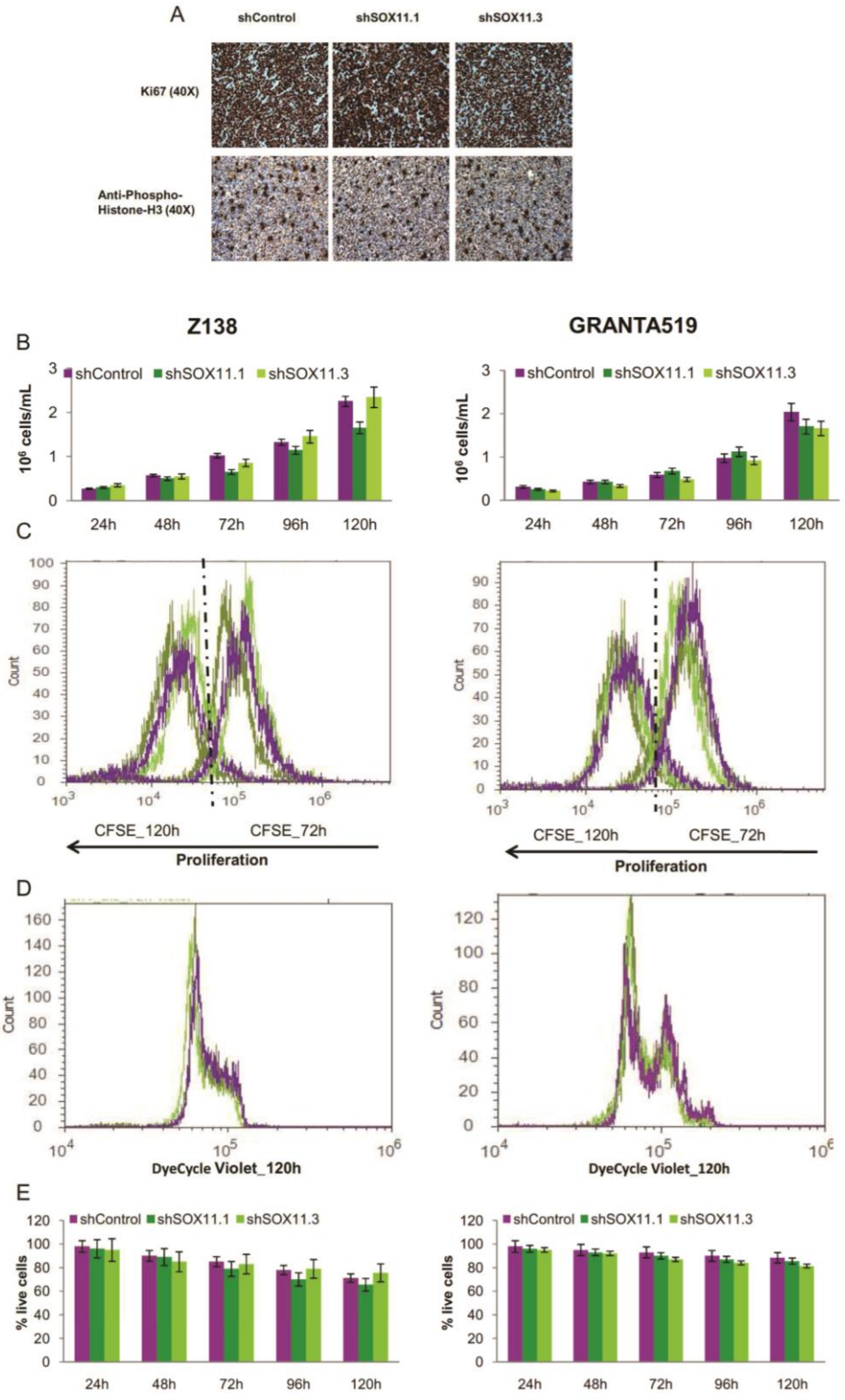
A
shControl
shSOX11.1
shSOX11.3
Ki67 (40X)
Anti-Phospho-Histone-H3 (40X)
Z138
GRANTA519
B
shControl shSOX11.1 shSOX11.3
10⁶ cells/mL
24h 48h 72h 96h 120h
C
Count
CFSE_120h
CFSE_72h
Proliferation
D
Count
DyeCycle Violet_120h
E
% live cells

Figure S7. SOX11 knockdown has no effect on cell proliferation, cell cycle and cell viability in MCL.

(A) Consecutive histological sections from representative shSOX11 and shControl tumors stained with human specific antibodies anti-Ki67 and phospho-histone-H3 (x40). No differences in proliferation index were observed.

(B) Cell density of Z138 and GRANTA519 growing cells stably transduced with shSOX11.1, shSOX11.3 or shControl every 24h at the indicated time points.

(C-E) Flow cytometry analysis on growing Z138 and GRANTA519 cells stably transduced with shSOX11.1, shSOX11.3 or shControl (C) stained with doubling concentrations of CFSE measuring cell proliferation at 72 and 120h (D) stained with DyeCycle Violet measuring cell cycle at 120h, and (E) stained with annexin-V analyzing cell viability at the indicated time points.

No differences in cell proliferation, cell cycle phases or cell viability were seen between the samples.

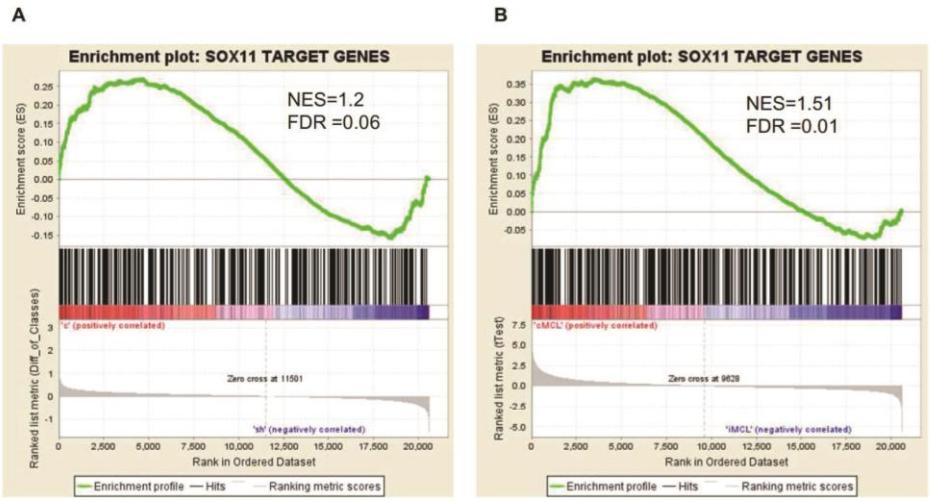

Figure S8. SOX11-bound high confidence genes are significantly enriched in the SOX11-positive MCL primary cases and Z138shControl MCL cell lines microarray data. GSEA on the primary tumors and MCL cell line dataset was performed using the SOX11 high confidence target genes derived from ChIP-chip as a gene signature. Enrichment of SOX11-bound genes was shown in both Z138shControl (A) and SOX11 positive MCL primary cases (B). NES and FDR *P*-values are shown. Statistical significance is considered when FDR<0.1.

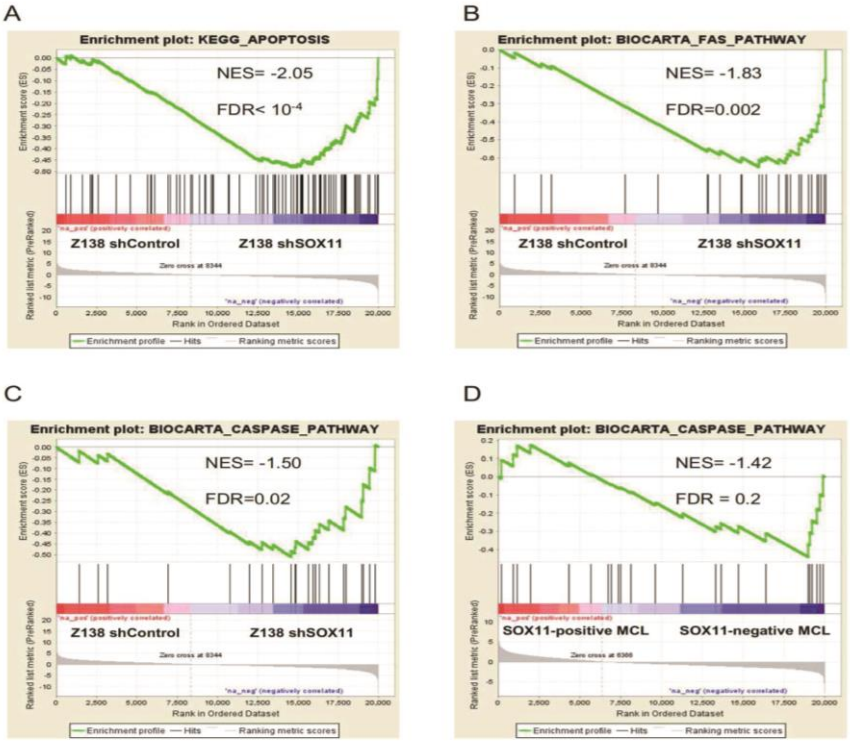

Figure S9. SOX11 regulates the expression of pro-apoptotic genes in MCL cell lines and primary cases. GSEA analysis performed on pre-ranked lists derived from the microarray expression data of SOX11-positive and negative MCL primary tumors and of SOX11-modulated Z138 cell lines. Graphs show a significant enrichment of (A – C) Fas, apoptosis and caspase pathway on Z138shSOX11cell lines and of (D) caspase pathway on SOX11-negative MCL tumors. Gene sets were downloaded from the MSigDB (Molecular Signature Database of Broad Institute). NES and FDR *P*-values are shown. Statistical significance is considered when FDR≤0.2.

III. SUPPLEMENTAL TABLES

Table S1. Oligonucleotides used for ChIP-qPCR, luciferase assay and qRT-PCR experiments.

Gene	Primer sequence	Annealing temperature	Expected size	Experiment
PAX5	Forward 5'-TAATCCTCTGCCCTTCATGG-3'	63.9 °C	247bp	ChIP-qPCR
	Reverse 5'-TGTTGCCTTAGGGAATTTCG-3'	63.7 °C		
MSI2	Forward 5'-CAAAAACAAAACAGAATAACAACAGA-3'	61.9 °C	232bp	ChIP-qPCR
	Reverse 5'-GACAAAATCCAGAAGGGAATG-3'	62.2 °C		
SEPT-2	Forward 5'-AGCAGGGGGTAGGGTATAGG-3'	62.9 °C	123bp	ChIP-qPCR
	Reverse 5'- GGTTTGTCTGGGCCAGTAGG-3'	65.6 °C		
SUV39H2	Forward 5'-GTCAGTGAAATCTTTTTCTGCAT-3'	61.1 °C	129bp	ChIP-qPCR
	Reverse 5'-GCAAAGGAAATGCTCTTTGAA-3'	63.1 °C		
HSPD1	Forward 5'-CGCGGTGAAAGATTAACTCG-3'	64.5 °C	130bp	ChIP-qPCR
	Reverse 5'-AGCCACTAGCGCAAGCTAAA-3'	63.9 °C		
PAX5	Forward 5'-CCGCTCGAGTAATCCTCTGCCCTTCATGG-3´	76.1 °C	552bp	Luciferase assay
	Reverse 5'-CCCAAGCTTTGTTTCCATTTAGAGGGCTTG-3'	72.3 °C		
SOX11	Forward 5'-CATGTAGACTAATGCAGCCATTGG-3´	62.9 °C	87bp	qRT-PCR
	Reverse 5'-CACGGAGCACGTGTCAATTG-3´	63.7 °C		

Table S2. SOX11-bound genes

	Z138.1		Z138.2		Z138.3	
Gene Name	**PEAK_SCORE**	**PEAK_FDR**	**PEAK_SCORE**	**PEAK_FDR**	**PEAK_SCORE**	**PEAK_FDR**
AANAT	0.542484	0.01588	0.526241	0.12084	0.576247	0.06777
ABCA1	0.647087	0.00232	0.508007	0.14672	0.448938	0.13502
ABCC12	0.46583	0.05078	0.501408	0.14672	0.428169	0.16693
ABCG2	0.649976	0.00462	0.524316	0.14672	0.848306	0.00287
ABT1	0.547067	0.023	0.38951	0.1565	0.640747	0.00764
ACAA2	0.367901	0.13555	0.49685	0.08005	0.761159	0.00471
ACOT1	0.460775	0.05942	0.551733	0.09619	0.767168	0.00471
ACPT	0.632137	0.003	0.678784	0.06407	0.389119	0.18703
ACSS2	0.38131	0.09315	0.588507	0.08274	0.645064	0.05558
ACTG1	0.876321	0	0.837202	0.004	0.912391	0.00153
ACVRL1	0.529323	0.03147	0.415837	0.19063	0.698189	0.01824
ADAMTS10	0.800707	0.00034	0.460603	0.07182	0.753918	0.01005
ADAMTS13	0.60534	0.00462	0.508007	0.14672	0.496195	0.13433
ADAR	0.974867	0	0.647538	0.03938	0.96131	0.0004
ADCK2	0.40754	0.13719	0.482054	0.17949	0.539108	0.08735
ADORA1	0.445048	0.0798	0.527624	0.12084	0.562718	0.06777
AFG3L2	0.519389	0.01404	0.49685	0.14672	0.50744	0.10837
AGMAT	0.466241	0.05942	0.671521	0.02999	0.562718	0.06777
AHNAK	0.503453	0.03147	0.490274	0.17949	0.599322	0.05287
AHR	1,051,025	0	0.964108	0.00094	0.609426	0.04211
AK1	0.480097	0.02176	0.677343	0.02999	0.803363	0.00384
ALK	0.452757	0.0798	0.463763	0.03644	0.567579	0.06777
ALOX12B	0.438161	0.06849	0.717602	0.04075	0.768329	0.02547
AMIGO2	0.396992	0.17587	0.513681	0.14672	0.505585	0.13433
AMZ2	0.47989	0.04302	0.526241	0.10562	0.888381	0.16
ANK1	0.512111	0.03147	0.5123	0.08005	0.449553	0.19866
ANKRD15	0.521845	0.023	0.459626	0.14849	0.496195	0.13433
ANKRD20A1	0.480097	0.04302	0.60477	0.0636	0.614336	0.04211

ANKRD20A3	0.375728	0.17587	0.628961	0.04899	0.590708	0.02929
ANKRD53	0.517436	0.01404	0.707849	0.02218	0.591228	0.05287
ANP32A	0.759332	0.00044	0.503218	0.14672	0.586613	0.05287
ANXA2	0.569499	0.00292	0.455292	0.12597	0.7274	0.0012
AOF2	0.487434	0.04302	0.503641	0.14672	0.586165	0.02929
AP1M2	0.358211	0.13555	0.53333	0.12084	0.437759	0.16693
AP4B1	0.38147	0.12426	0.479658	0.17949	0.515825	0.10837
APBB2	0.515498	0.02176	0.574251	0.04939	1,017,968	0.00047
APBB3	0.690571	0.00159	0.507962	0.14672	0.959727	0.0004
APCDD1	0.584313	0.00292	0.733445	0.01098	0.599701	0.04211
APEX1	1,193,827	0	0.59971	0.0636	1,348,356	0
APOA2	0.339084	0.14501	0.575589	0.07797	0.515825	0.10837
APOB	0.883953	0	0.707849	0.02218	0.80407	0.00384
AQP3	0.375728	0.12426	0.653152	0.03938	0.519823	0.10837
ARHGAP17	0.708871	0.00062	0.549161	0.09619	0.547104	0.08735
ARHGAP9	0.529323	0.03147	0.684908	0.02999	0.577812	0.06777
ARHGEF18	0.463567	0.05942	0.484845	0.17949	0.462079	0.19866
ARHGEF2	1,207,988	0	0.647538	0.01536	1,219,222	0
ARHGEF5	0.772182	0.00044	0.843594	0.004	0.632866	0.03233
ARID3B	1,202,276	0	0.575106	0.07797	1,032,439	0.00069
ARID5B	0.857061	0	0.514658	0.14672	0.357267	0.10793
ARL16	0.47989	0.04302	0.502321	0.14672	0.528226	0.10837
ARL3	0.942767	0	0.49015	0.17949	0.762171	0.00693
ARNTL2	0.81604	0.00049	0.464759	0.07182	0.553736	0.09489
ARPC2	0.668355	0.00232	0.488172	0.10098	0.733122	0.01005
ARPM1	0.835632	0	0.481594	0.17949	0.445738	0.08849
ATF3	0.720554	0.00087	0.503641	0.14672	0.679951	0.01824
ATG4C	0.99606	0	0.671521	0.02999	0.726844	0.0012
ATP12A	0.39629	0.17587	0.443214	0.15876	0.544573	0.08735
ATP1A2	0.339084	0.15404	0.575589	0.07797	0.539271	0.08735
ATP1B1	0.529819	0.023	0.359743	0.19837	0.539271	0.08735

ATP2B4	0.656976	0.00232	0.647538	0.03938	0.750291	0.00693
ATP5G2	0.419048	0.09315	0.415837	0.19063	0.457434	0.19866
ATP5J2	0.750732	0.11016	0.482054	0.17949	0.468789	0.10845
ATP6V1G1	1,043,689	0	0.677343	0.02999	1,086,903	0
ATP6V1G2	0.612715	0.00745	0.438199	0.16507	0.545821	0.08735
ATXN2L	0.668364	0.00134	0.573037	0.07797	0.523317	0.10837
AUTS2	0.536237	0.023	0.506157	0.14672	0.468789	0.16574
AVPR1B	0.656976	0.00232	0.791435	0.00608	0.586165	0.05287
AXIN2	0.667673	0.00159	0.526241	0.12084	0.600257	0.05287
AZI1	0.438161	0.0798	0.621922	0.04899	0.576247	0.06777
B3GALNT2	1,229,180	0	0.671521	0.02999	0.89097	0.00153
B3GALT3	0.642794	0.003	0.529753	0.06249	0.633417	0.03233
B3GNT4	0.352882	0.15404	0.660447	0.06484	0.505585	0.12085
B4GALNT1	0.463158	0.06849	0.807213	0.00608	0.457434	0.14113
BAG5	0.649274	0.00232	0.575722	0.07797	0.627683	0.03233
BAT4	0.700246	0.00159	0.413854	0.19063	0.498359	0.08288
BAT5	0.547067	0.00206	0.511232	0.08005	0.640747	0.03233
BCL2	1,038,779	0	0.615148	0.06839	1,199,403	0
BCL6	0.66422	0.00232	0.650152	0.03938	0.656877	0.01041
BCORL1	0.723885	0.00087	0.568632	0.09619	0.404421	0.10578
BIN2	0.595489	0.0242	0.587064	0.07797	0.74634	0.01005
BLOC1S1	0.485213	0.05942	0.415837	0.1824	0.650038	0.03233
BLVRA	0.664934	0.00232	0.578465	0.00957	0.468789	0.01215
BMF	0.527314	0.00932	0.575106	0.03811	0.703936	0.00474
BNC2	0.626213	0.003	0.556389	0.09619	0.543451	0.08735
BRAF	1,308,419	0	0.819492	0.00481	0.867261	0.00193
BRD2	1,466,141	0	0.657298	0.01536	1,281,494	0
BRI3	0.42899	0.10476	0.506157	0.14672	0.609426	0.0666
BRP44	1,080,831	0	0.695504	0.02218	0.844077	0.00196
BRUNOL4	0.389542	0.12426	0.567829	0.03811	0.55357	0.06777
BSG	0.842849	0	0.727268	0.01656	0.632319	0.04211

BTG2	0.720554	0.00087	0.74347	0.01098	0.914417	0.00149
BYSL	0.56895	0.01588	0.438199	0.16507	0.640747	0.03233
BZRAP1	0.938915	0	0.598001	0.0292	0.81635	0.00384
C10orf77	0.621369	0.00462	0.514658	0.01263	0.476357	0.16574
C12orf22	0.749875	0.00087	0.73383	0.01656	0.650038	0.03233
C12orf24	0.419048	0.09315	0.562603	0.09456	0.409283	0.17011
C12orf30	0.77193	0	0.366915	0.19837	0.770416	0.00079
C12orf47	0.86015	0	0.758291	0.01098	0.818566	0.00384
C12orf5	0.396992	0.17587	0.366915	0.19837	0.505585	0.13433
C12orf52	0.948371	0	0.587064	0.07797	0.866717	0
C12orf62	0.705764	0.00159	0.48922	0.17949	0.577812	0.06777
C13orf18	1,034,758	0	1,108,035	0	1,018,114	0.00057
C14orf132	0.376998	0.17587	0.383815	0.11173	0.46495	0.16574
C14orf159	0.397942	0.13719	0.479768	0.10098	0.418455	0.16693
C14orf166B	0.607386	0.00462	0.671675	0.06407	0.581188	0.05287
C15orf20	0.421851	0.10476	0.575106	0.07797	0.492755	0.13433
C15orf23	0.569499	0.00292	0.503218	0.14672	0.539684	0.05038
C15orf27	0.421851	0.10476	0.527181	0.12084	0.469291	0.16574
C15orf38	0.548407	0.01588	0.527181	0.12084	0.868188	0.00193
C16orf47	0.364562	0.17587	0.573037	0.08746	0.451956	0.19866
C17orf49	0.938915	0	0.478401	0.17949	0.86437	0.00196
C17orf81	0.500755	0.03147	0.406641	0.19063	0.504216	0.13433
C18orf21	0.865649	0	0.544169	0.04939	0.55357	0.06777
C18orf4	1,514,886	0	1,372,253	0	1,568,450	0
C19orf18	1,137,846	0	0.775753	0.00771	1,240,317	0
C19orf2	0.442496	0.0798	0.557572	0.09619	0.583679	0.06777
C19orf37	0.674279	0.00159	0.53333	0.06249	0.705279	0.01824
C1orf115	0.529819	0.00932	0.671521	0.01102	0.586165	0.05287
C1orf131	0.466241	0.05942	0.407709	0.19063	0.656504	0.0234
C1orf14	0.360277	0.13555	0.527624	0.12084	0.445485	0.19866
C1orf174	0.61459	0.00462	0.503641	0.08005	0.468932	0.10845

C1orf38	0.402663	0.10286	0.695504	0.02218	0.703397	0.01325
C1orf66	0.953675	0	0.527624	0.12084	0.703397	0.01325
C20orf18	0.782689	0	0.635588	0.03938	0.529874	0.05038
C20orf91	0.461586	0.04302	0.635588	0.00642	0.437722	0.19866
C21orf124	0.53275	0.01588	0.414706	0.12725	0.421054	0.15516
C2orf10	0.409637	0.09315	0.414946	0.19063	0.614877	0.04211
C2orf31	0.409637	0.13719	0.536989	0.12084	0.709473	0.01325
C3orf60	0.407103	0.13719	0.577913	0.07797	0.492658	0.13433
C6orf21	0.547067	0.00206	0.511232	0.08005	0.640747	0.03233
C6orf32	0.634598	0.00462	0.486887	0.17949	0.640747	0.0152
C6orf47	0.700246	0.00159	0.413854	0.19063	0.498359	0.08288
C7orf24	0.471889	0.05942	0.506157	0.14672	0.656305	0.0234
C7orf34	0.471889	0.05942	0.602567	0.0636	0.656305	0.0234
C8orf33	0.405421	0.13719	0.609882	0.0636	0.662499	0.0234
C9orf100	0.396602	0.13719	0.508007	0.14672	0.56708	0.06777
C9orf66	0.313107	0.18102	0.483816	0.10098	0.448938	0.13502
C9orf76	1,419,417	0	0.846679	0.004	1,228,672	0
CABIN1	0.747756	0.00034	0.536373	0.09619	0.664005	0.01824
CABP1	0.573434	0.18827	0.464759	0.12597	0.577812	0.06777
CACNA1S	0.508626	0.03147	0.503641	0.14672	0.445485	0.19866
CACNB4	0.452757	0.0798	0.585806	0.03811	0.567579	0.06777
CALB1	0.384084	0.17587	0.5123	0.14672	0.70982	0.01325
CALCA	0.356612	0.15726	0.612842	0.0636	0.575349	0.01664
CALM2	0.883953	0	0.488172	0.17949	0.591228	0.0129
CAMK2D	1,008,584	0	0.649153	0.04899	0.751357	0.01005
CANT1	0.396431	0.13719	0.574081	0.07797	0.456195	0.19866
CASC1	0.926316	0	0.587064	0.07797	0.625963	0.04211
CBWD1	1,034,872	0	0.805484	0.00608	0.779734	0.00471
CBWD2	1,034,872	0	0.805484	0.00608	0.614877	0.00796
CBWD3	1,001,941	0	0.556389	0.09619	0.779734	0.00471
CBWD5	0.709709	0	0.725725	0.01656	0.779734	0

CBX4	0.459025	0.01721	0.478401	0.05974	0.792339	0.00101
CCBL1	1,127,184	0	0.628961	0.04899	1,275,929	0
CCDC47	0.709403	0.00087	0.478401	0.17949	0.648278	0.03233
CCDC50	1,114,176	0	0.577913	0.07797	0.844556	0.00196
CCDC63	0.485213	0.03375	0.48922	0.17949	0.529661	0.10837
CCDC97	1,432,844	0	0.921206	0.00121	1,215,998	0
CCM2	0.750732	0.00672	0.433849	0.16507	0.562547	0.06777
CCNA1	0.462338	0.0798	0.664821	0	0.56825	0.06777
CCR6	0.415771	0.13719	0.511232	0.14672	0.569553	0.06777
CD109	0.56895	0.00477	0.632953	0.01902	0.593284	0.02929
CD1D	0.805325	0.00034	0.479658	0.17949	0.609611	0.04211
CD300E	0.52162	0.023	0.526241	0.03306	0.528226	0.10837
CD302	0.668355	0.00064	0.536989	0.06249	0.52028	0.06541
CD37	0.695351	0.00134	0.630299	0.06839	0.462079	0.19866
CD46	0.529819	0.023	0.623555	0.04899	0.797184	0.00384
CD86	0.814206	0	0.481594	0.17949	0.516118	0.06541
CDC37L1	0.960194	0	0.508007	0.14672	0.779734	0.00471
CDC42SE1	0.868903	0	0.527624	0.06249	0.867523	0
CDC6	1,105,834	0	0.478401	0.17949	0.696298	0.01824
CDCP1	0.514235	0.01404	0.481594	0.17949	0.539578	0.08735
CDH6	0.474768	0.05942	0.507962	0.14672	0.538383	0.08735
CDH7	0.71416	0.00134	0.851743	0.00257	0.853421	0
CDK5RAP2	0.563592	0.00292	0.435435	0.15876	0.543451	0.08735
CDK6	0.85798	0	0.506157	0.14672	0.679745	0.01824
CDKN1B	1,323,308	0	1,027,362	0	1,227,850	0
CENPF	0.76294	0.00044	0.551606	0.09619	0.562718	0.03751
CENTA2	0.375566	0.12426	0.526241	0.12084	0.624267	0.04211
CEP68	0.862394	0	0.488172	0.10098	0.591228	0.05287
CHD3	0.688538	0.00134	0.574081	0.03811	0.528226	0.00544
CHD9	0.607604	0.003	0.477531	0.17949	0.761189	0.00693
CHIT1	0.529819	0.0031	0.551606	0.02276	0.586165	0.05287

CHRM2	0.450439	0.02839	0.506157	0.08005	0.492229	0.08288
CITED1	0.85163	0	0.420293	0.19063	0.808843	0.00384
CLDN7	0.375566	0.12426	0.454481	0.12597	0.456195	0.19866
CLEC4C	0.485213	0.05942	0.587064	0.07797	0.674114	0.05558
CLIC1	1,028,487	0	0.77902	0.00771	0.972986	0.0004
CLK2	0.635783	0.003	0.599572	0.0636	0.492378	0.08288
CLNS1A	0.713225	0.00087	0.563815	0.09619	0.527403	0.10837
CLYBL	0.726532	0.00134	0.517083	0.08005	0.544573	0.09489
CMPK	0.699361	0.00134	0.503641	0.14672	0.679951	0.01824
CMTM1	0.364562	0.17587	0.405901	0.12725	0.689827	0.00711
CNOT6L	0.739628	0	0.524316	0.14672	0.557458	0.08735
CNTN2	0.551012	0.01588	0.575589	0	0.445485	0.13502
CNTNAP2	0.579136	0.00292	0.482054	0.10098	0.468789	0.16574
CNTNAP3	0.60534	0.00462	0.725725	0.01656	0.590708	0.05287
COG1	0.563349	0.011	0.430561	0.15876	0.792339	0.00471
COL18A1	0.430298	0.0798	0.658651	0.03938	0.467838	0.16574
COL1A2	0.536237	0.0031	0.62667	0.00965	0.421911	0.07991
COL23A1	0.496348	0.04302	0.55634	0.09619	0.444751	0.19866
COL27A1	1,064,563	0	0.991824	0	0.850619	0.00196
COL5A3	1,032,490	0	1,042,418	0	1,191,678	0
COPZ1	0.595489	0.011	0.562603	0.09456	0.553736	0.08735
COQ10A	0.573434	0.18827	0.415837	0.1824	0.409283	0.17011
COX4I1	0.364562	0.17587	0.405901	0.19063	0.451956	0.19866
CPNE2	0.445576	0.00805	0.358148	0.14041	0.49953	0.08288
CR1L	0.61459	0.00462	0.695504	0.02218	0.468932	0.10845
CREB3	0.730582	0.00062	0.459626	0.12597	0.685221	0.01824
CREB3L3	0.358211	0.13555	0.581815	0.08746	0.486399	0.16574
CRH	0.426759	0.06808	0.683067	0.02999	0.591517	0.05287
CRIP2	0.607386	0.00462	0.359826	0.14041	0.65093	0.01041
CRK	0.438161	0.06849	0.478401	0.17949	0.384165	0.18703
CROP	0.52162	0.00932	0.406641	0.1824	0.504216	0.13433

CS	0.330827	0.18102	0.48922	0.10098	0.577812	0.06777
CSNK2B	0.700246	0.00159	0.413854	0.19063	0.498359	0.08288
CSPG4LYP1	0.491299	0.04302	0.428276	0.1565	0.592043	0.06777
CTHRC1	0.405421	0.13719	0.536696	0.03091	0.520535	0.03168
CTNNA1	0.668991	0.01019	0.435396	0.16507	0.514975	0.10837
CUEDC1	0.47989	0.05078	0.526241	0.10562	0.792339	0.0269
CUTA	0.80966	0	0.681642	0.02999	0.735672	0.01005
CX36	0.485129	0.02176	0.69492	0.02218	0.539684	0.08735
CXCR4	0.754594	0	0.366129	0.19837	0.709473	0.00474
CYB5D1	0.417296	0.10476	0.526241	0.12084	0.720309	0.01325
CYB5R3	0.413233	0.0798	0.559694	0.07797	0.641109	0.0234
CYFIP1	0.400759	0.13719	0.599069	0.0292	0.469291	0.10845
DARC	0.317892	0.18102	0.695504	0.02218	0.468932	0.10845
DAXX	1,181,666	0	0.77902	0.00771	1,044,180	0.00069
DBNDD2	0.602069	0.03147	0.423725	0.16507	0.437722	0.19866
DCXR	0.605079	0.00462	0.526241	0.12084	0.576247	0.06777
DDX23	0.793985	0.00044	0.758291	0.01098	0.987095	0.0004
DDX42	0.709403	0.00087	0.478401	0.17949	0.648278	0.03233
DDX54	0.948371	0	0.587064	0.07797	0.866717	0
DEFB1	0.490773	0.04302	0.414719	0.19063	0.520535	0.10837
DEK	0.56895	0	0.511232	0.14672	0.68821	0.00711
DENND2A	0.922328	0	0.506157	0.08005	0.867261	0.00193
DEPDC2	0.917533	0	0.707463	0.02218	0.70982	0.00474
DFNB31	0.396602	0.06393	0.435435	0.15876	0.590708	0.05287
DHH	0.441103	0.10476	0.48922	0.17949	0.625963	0.04211
DHX32	0.707075	0.00134	0.49015	0.17949	0.500174	0.08288
DIDO1	0.822827	0	0.541427	0.09619	0.829368	0.00196
DIRC2	0.578514	0.0242	0.529753	0.12084	0.516118	0.06541
DKFZP434A0131	0.750732	0	0.650773	0.06484	0.679745	0.01824
DKFZP434B0335	0.729283	0.00087	0.433849	0.15876	0.515668	0.03168
DKFZp779O175	0.653208	0.00232	0.436361	0.09521	0.729599	0.01325

DLEU1	0.968709	0	0.590952	0.01477	0.899729	0
DLEU2	0.968709	0	0.590952	0.01477	0.899729	0
DLEU8	0.638467	0	0.517083	0.14672	0.852374	0.00196
DLG4	0.438161	0.0798	0.550161	0.09619	0.504216	0.04471
DLL3	1,264,274	0	0.872722	0.00257	0.753918	0.01005
DMTF1	0.600586	0.00745	0.433849	0.15876	0.44535	0.19866
DNAJC6	0.572205	0.011	0.695504	0.00658	0.609611	0.04211
DNAJC7	0.375566	0.1193	0.406641	0.1824	0.456195	0.19866
DNM1L	0.551378	0.03321	0.48922	0.13676	0.457434	0.13502
DOCK8	0.563592	0.011	0.532198	0.12084	0.448938	0.13502
DOK2	0.384084	0.17587	0.5123	0.04338	0.449553	0.06293
DPEP2	0.324055	0.15404	0.429778	0.16507	0.475743	0.13266
DPF2	0.943974	0	0.441246	0.16507	0.527403	0.06541
DPP6	0.579136	0.011	0.602567	0.0636	0.515668	0.06541
DPYS	0.469435	0.05942	0.46351	0.14849	0.449553	0.13502
DPYSL2	0.426759	0.01602	0.414719	0.08664	0.591517	0.05287
DRD1IP	0.385678	0.17587	0.637195	0.00965	0.523992	0.10837
DRG1	0.491944	0.0031	0.489732	0.14672	0.526625	0.01517
DSC2	0.649237	0.003	0.449531	0.07182	0.55357	0.03751
DSCR1L1	0.634598	0.00462	0.438199	0.07139	0.593284	0.05287
DTX2	0.557687	0.01588	0.578465	0.07797	0.656305	0.0234
DULLARD	0.500755	0.03147	0.406641	0.19063	0.504216	0.13433
DUOX2	0.674962	0.00159	0.623032	0.00965	0.7274	0.01005
DYDC1	0.407104	0.09315	0.68621	0.02999	0.619264	0.04211
DYNLT1	0.459537	0.04765	0.657298	0.03938	0.52209	0.06541
E2F7	0.970426	0	0.48922	0.17949	0.529661	0.10837
ECRG4	0.517436	0.03147	0.51258	0.14672	0.591228	0.05287
EDEM3	0.572205	0.011	0.479658	0.17949	0.703397	0.00474
EDNRA	0.470672	0.02839	0.499349	0.02037	0.484747	0.16574
EEF1G	0.482476	0.04302	0.367705	0.19837	0.407539	0.10578
EFCBP1	0.490773	0.02176	0.658672	0.03938	0.496874	0.08288

EFNA4	0.445048	0.0798	0.503641	0.12138	0.398592	0.17011
EGLN1	0.656976	0.00232	0.479658	0.17949	0.539271	0.08735
EHD1	0.776156	0.00478	0.539301	0.10562	0.767132	0.02547
EIF2AK2	0.474317	0.05942	0.561398	0.09619	0.472982	0.16574
EIF3S6IP	0.413233	0.06849	0.466412	0.13676	0.526625	0.09489
EIF3S9	0.707833	0.12782	0.506157	0.14672	0.585987	0.05287
ELAVL1	0.969277	0	0.387876	0.1565	0.535039	0.02786
EN1	0.431197	0.10476	0.488172	0.17949	0.472982	0.16574
EN2	0.450439	0.0798	0.482054	0.10098	0.609426	0.04211
ENAH	0.551012	0.01588	0.719487	0.04075	0.562718	0.08618
ENPP7	0.312972	0.17381	0.598001	0.08274	0.456195	0.19866
ENTPD6	0.421448	0.0798	0.470806	0.10098	0.414684	0.10931
EP400NL	0.683709	0.01019	0.587064	0.08746	0.818566	0.02105
EPHA1	0.386091	0.12426	0.457951	0.07182	0.562547	0.06777
EPN1	0.842849	0	0.387876	0.1565	0.778238	0.00693
ERN1	0.584214	0.00745	0.478401	0.17949	0.528226	0.10837
ESPL1	0.463158	0.0798	0.587064	0.07797	0.674114	0.0234
EZH2	0.579136	0.011	0.457951	0.14849	0.515668	0.10837
F11R	0.402663	0.13719	0.527624	0.12084	0.656504	0.00413
FAM102A	0.500971	0.03147	0.508007	0.14672	0.519823	0.10837
FAM107B	0.792782	0	0.514658	0.14672	0.809806	0.00384
FAM112A	0.501724	0.00932	0.494346	0.12138	0.437722	0.13502
FAM35A	0.664222	0	0.637195	0.04899	0.476357	0.16574
FAM54B	0.38147	0.17587	0.623555	0.04899	0.679951	0.01824
FAM70B	0.484355	0.05942	0.467837	0.07182	0.615604	0.04211
FAM96A	0.696055	0.00134	0.742845	0.01098	0.703936	0.00474
FANCD2	0.321397	0.17381	0.433434	0.16507	0.398818	0.17011
FBXL10	0.661654	0.003	0.48922	0.10098	0.674114	0.01041
FBXL2	0.407103	0.09315	0.577913	0.07797	0.469198	0.10845
FBXO17	0.632137	0.01225	0.509088	0.14672	0.583679	0.06777
FBXO21	0.529323	0.00324	0.635986	0.04899	0.553736	0.08735

FBXO31	0.546844	0.00292	0.405901	0.19063	0.451956	0.08849
FGF20	0.725491	0.00087	0.756253	0.01098	0.662499	0.0234
FGFR1	0.405421	0.13719	0.658672	0.03938	0.473213	0.10845
FKBP14	0.729283	0	0.530259	0.06249	0.562547	0.06777
FLAD1	0.847711	0	0.599572	0.08274	0.468932	0.10845
FLII	0.417296	0.08279	0.502321	0.14672	0.480206	0.13266
FLJ10081	0.323398	0.18102	0.414946	0.1824	0.496631	0.13433
FLJ10154	1,122,822	0	0.566329	0.09619	0.686635	0.01824
FLJ10986	0.487434	0.04302	0.431692	0.15876	0.468932	0.10845
FLJ14154	0.425323	0.0798	0.596914	0.0636	0.808763	0.00384
FLJ14768	0.653208	0.00232	0.824237	0.00481	0.437759	0.16693
FLJ14803	1,008,126	0	0.698978	0.02218	1,054,776	0
FLJ14834	0.484355	0.05942	0.566329	0.09619	0.449864	0.08849
FLJ20366	0.469435	0.05942	0.634277	0.04899	0.591517	0.05287
FLJ20433	0.417476	0.10476	0.628961	0.00965	0.519823	0.06541
FLJ20489	0.904261	0	0.587064	0.07797	0.650038	0.03233
FLJ21767	0.686384	0	0.506157	0.08005	0.656305	0.00413
FLJ21908	0.529323	0.03147	0.538142	0.12084	0.625963	0.04211
FLJ25415	0.797714	0.00049	0.488172	0.17949	0.638526	0.03233
FLJ25801	0.403433	0.17587	0.574251	0.09619	0.508984	0.08288
FLJ30707	0.484355	0.03375	0.467837	0.07182	0.615604	0.04211
FLJ32679	0.548407	0.01588	0.503218	0.14672	0.492755	0.13433
FLJ35784	0.463567	0.05942	0.436361	0.15876	0.462079	0.19866
FLJ36749	0.376998	0.17587	0.503757	0.14672	0.604435	0.04211
FLJ39005	0.463567	0.05768	0.53333	0.10562	0.413439	0.17011
FLJ39739	1,229,180	0	0.695504	0.00658	0.844077	0.00196
FLJ41131	0.568923	0.011	0.53333	0.12084	0.729599	0.01325
FLJ41841	0.459537	0.04765	0.77902	0.00771	0.450896	0.19866
FLJ42562	1,142,672	0	0.561398	0.09619	0.969614	0.0004
FLJ43692	0.750732	0.00062	0.698978	0	0.750063	0.00693
FLJ45079	0.459025	0.01721	0.574081	0.01477	0.456195	0.19866

FLJ45187	1,499,857	0	0.857763	4	1,262,345	0
FLJ45983	0.471384	0.05942	0.833255	0.00481	0.523992	0.10837
FLJ46385	0.674279	0.00842	0.557572	0.02081	0.851198	0.02068
FLJ90231	0.419544	0.10476	0.612842	0.08274	0.599322	0.05287
FLVCR	0.635783	0.003	0.503641	0.14672	0.539271	0.08735
FN3K	0.375566	0.1193	0.430561	0.16507	0.408175	0.17011
FN3KRP	0.584214	0.00745	0.574081	0.07797	0.456195	0.19866
FNDC3A	0.6825	0.00232	0.615575	0.0636	0.947083	0.00103
FOXA3	0.674279	0.00159	0.484845	0.17949	0.486399	0.16574
FOXC1	0.459537	0.04765	0.584265	0.07797	1,067,911	0
FOXD1	0.517929	0.00699	0.628906	0.04899	0.538383	0.01517
FOXJ1	0.563349	0.011	0.358801	0.10812	0.600257	0.05287
FOXK2	0.417296	0.01602	0.502321	0.14672	0.528226	0.06541
FRMD3	0.375728	0.12426	0.411244	0.12725	0.826991	0.00287
FUT5	0.568923	0.0242	0.460603	0.14849	0.389119	0.18703
FZD7	0.409637	0.13719	0.488172	0.17949	0.685824	0.01824
GAB1	0.784454	0.00062	0.574251	0.09619	0.63017	0.02429
GABRA2	0.515498	0.04302	0.773991	0.01098	1,090,680	0
GAD1	0.495876	0.04302	0.561398	0.09619	0.80407	0.00384
GALR1	0.454466	0.0798	0.591488	0.0636	0.668898	0.00711
GAPDH	0.595489	0.011	0.611525	0.01089	0.529661	0.03168
GATA3	0.471384	0.05942	0.833255	0.00481	0.523992	0.10837
GBA	0.868903	0	0.767452	0.00771	0.937863	0.00103
GCAT	0.491944	0.023	0.466412	0.17949	0.480832	0.08288
GHRHR	0.514788	0.03147	0.433849	0.15876	0.515668	0.10837
GLDC	0.93932	0	0.459626	0.14849	0.56708	0.03751
GLT25D2	0.699361	0.00134	0.551606	0.09619	0.867523	0.00193
GLT8D3	0.551378	0.023	0.513681	0.14672	0.457434	0.19866
GNA12	0.42899	0.10476	0.506157	0.08005	0.515668	0.10837
GNB2L1	0.539509	0.023	0.580528	0.07797	0.725647	0.01005
GNG12	0.445048	0.04765	0.575589	0.07797	0.562718	0.06777

GNG4	0.508626	0.01404	0.551606	0.04939	1,008,203	0.00057
GNPTG	0.688618	0.00087	0.501408	0.14672	0.49953	0.13433
GOLGA8E	0.506222	0.03147	0.646994	0.06484	0.445826	0.19866
GOLGA8F	0.548407	0.01588	0.503218	0.14672	0.422362	0.16693
GOLPH3	0.561089	0.01588	0.507962	0.12138	0.585199	0.05287
GP6	0.316068	0.17381	0.509088	0.08005	0.559359	0.08735
GPC5	0.418306	0.13719	0.541706	0.12084	0.520895	0.10837
GPR132	0.397942	0.13719	0.59971	0.0636	0.55794	0.06777
GPR148	0.517436	0.03147	0.781075	0.00771	0.449333	0.19866
GPR81	0.463158	0.0798	0.48922	0.10098	0.505585	0.13433
GPSM3	0.547067	0.023	0.413854	0.19063	0.68821	0.01824
GRB10	0.386091	0.1193	0.62667	0.00965	0.515668	0.06541
GRP	0.497748	0.04302	0.686126	0.02218	0.576636	0.05287
H19	0.419544	0.06808	0.661869	0.01536	0.527403	0.03168
H1F0	0.590333	0.14267	0.466412	0.17949	0.480832	0.08288
H3F3A	1,250,373	0	0.767452	0.00771	1,289,562	0
H6PD	0.339084	0.15404	0.479658	0.13676	0.468932	0.16574
HAVCR1	0.431607	0.10476	0.580528	0.07797	0.468159	0.16574
HCN3	0.635783	0.003	0.599572	0.0636	0.492378	0.08288
HELZ	0.605079	0.00462	0.478401	0.17949	0.696298	0.01824
HES7	0.688538	0.00134	0.645842	0.03938	0.648278	0.0152
HGS	0.47989	0.04302	0.621922	0.04899	0.528226	0.10837
HHAT	0.61459	0.00462	0.719487	0.01656	0.422038	0.16693
HIC2	0.688722	0.00062	0.443091	0.14849	0.549522	0.08618
HIP1	0.622035	0.00462	0.650773	0.03938	0.492229	0.13433
HIP1R	0.904261	0	0.48922	0.17949	0.842642	0.00287
HIPK1	0.593397	0.00745	0.479658	0.17949	0.633058	0.03233
HIPK3	1,006,906	0	0.637356	0.04899	0.671241	0.0234
HIST1H2AM	1,247,314	0	0.584265	0.01477	1,328,956	0
HIST1H3E	0.56895	0.01588	0.681642	0.01102	0.498359	0.13433
HIST1H3J	1,247,314	0	0.584265	0.01477	1,328,956	0

HIST3H2A	0.635783	0.003	0.695504	0.02218	0.445485	0.19866
HIST3H2BB	0.635783	0.003	0.695504	0.02218	0.445485	0.19866
HIVEP3	0.826518	0	0.599572	0.0636	0.609611	0.02429
HK1	0.449957	0.04765	0.539165	0.12084	0.690717	0.0501
HLRC1	0.589994	0.16499	0.484845	0.17949	0.437759	0.15516
HMG20B	0.526781	0.00932	0.557572	0.09619	0.559359	0.05038
HMGCR	0.798473	0.00049	0.411208	0.19063	0.538383	0.08735
HMGN4	0.634598	0.01637	0.438199	0.15876	0.498359	0.13433
HMX1	0.511089	0.011	0.489475	0.14672	0.593733	0.05287
HMX2	0.535663	0.023	0.68621	0.02999	0.785988	0.00471
HNF4A	0.38131	0.13719	0.423725	0.15876	0.506836	0.10837
HNRPD	1,299,952	0	0.699088	0.00451	1,066,442	0.00069
HNRPK	1,419,417	0	0.846679	4	1,228,672	0
HNRPL	1,137,846	0	0.872722	0.00257	0.559359	0.08735
HNRPU	0.61459	0.00462	0.479658	0.17949	0.633058	0.03233
HOOK3	0.917533	0	0.414719	0.19063	0.496874	0.13433
HOXA4	0.579136	0.011	0.62667	0.01902	0.773503	0.00101
HOXA7	0.40754	0.13719	0.530259	0.12084	0.539108	0.08735
HOXB13	0.667673	0.00159	0.526241	0.03091	0.81635	0.00384
HOXB4	0.47989	0.02176	0.741522	0.01098	0.624267	0.04211
HOXB7	0.396431	0.13719	0.358801	0.10812	0.576247	0.0108
HS2ST1	0.784132	0.00049	0.527624	0.06249	0.586165	0.02929
HSPC049	0.42899	0.10476	0.530259	0.10562	0.539108	0.08735
HSPC159	0.538996	0.00932	0.561398	0.09619	0.567579	0.01664
HSPD1	1,013,313	0	0.707849	0.02218	0.969614	0.0004
HSPE1	1,013,313	0	0.707849	0.02218	0.969614	0.0004
ID1	0.541862	0.011	0.470806	0.17949	0.552912	0.06777
IFITM1	0.755179	0.00044	0.637356	0.04899	0.719186	0.01325
IFT20	0.375566	0.17587	0.406641	0.19063	0.504216	0.08288
IFT80	1,071,323	0	0.698311	0.02218	0.985316	0.00047
IGF2BP1	1,356,211	0	0.645842	0.03938	0.984422	0

IL17RD	0.535662	0.023	0.553833	0.09619	0.469198	0.10845
IL4I1	0.948205	0	0.581815	0.03811	0.583679	0.06777
ILDR1	0.685647	0	0.481594	0.05974	0.633417	0.03233
ILF2	0.99606	0	0.863384	0.00257	0.726844	0.01005
IMPA2	0.649237	0.003	0.733445	0.01098	0.738094	0.00693
IMPACT	0.411183	0.09315	0.591488	0.0636	0.80729	0.00287
ING4	0.617544	0.00745	0.587064	0.07797	0.505585	0.13433
INOC1	0.316389	0.17381	0.838696	4	0.703936	0.01325
INTS5	0.461498	0.05768	0.441246	0.16507	0.479458	0.13266
IPF1	0.330242	0.18102	0.369345	0.10812	0.449864	0.13502
IQWD1	1,080,831	0	0.695504	0.02218	0.844077	0.00196
IRAK4	0.529323	0.03147	0.48922	0.17949	0.433359	0.10931
IRF2	0.403433	0.04197	0.474381	0.07182	0.557458	0.02378
IRF2BP2	1,631,843	0	1,199,144	0	1,875,726	0
IRF5	0.536237	0.00932	0.602567	0.0292	0.609426	0.04211
IRF8	0.506337	0.023	0.549161	0.09619	0.880125	0.00193
ITGB2	0.471278	0.05078	0.658651	0.03938	0.725149	0.03171
ITGB8	0.42899	0.10476	0.674875	0.02999	0.726624	0.01005
IXL	0.379282	0.17587	0.436361	0.16507	0.656639	0.03233
JUNB	0.695351	0.00134	0.53333	0.12084	0.729599	0.01325
KAZALD1	0.599943	0.00249	0.857763	0.004	0.666899	0.0234
KCNA6	0.419048	0.09315	0.635986	0.04899	0.505585	0.00526
KCNH1	0.61459	0.00462	0.479658	0.17949	0.726844	0.0012
KCNH6	0.667673	0.00159	0.980722	0	1,152,494	0
KCNN4	0.758564	0	0.557572	0.09456	0.729599	0
KCNS3	0.452757	0.0798	0.488172	0.17949	0.449333	0.13502
KDELC1	0.726532	0.00134	0.664821	0.06484	0.520895	0.10837
KIAA0195	0.625944	0.003	0.526241	0.12084	0.456195	0.19866
KIAA0703	0.384816	0.09315	0.644667	0.06484	0.404382	0.10578
KIAA0907	0.656976	0.00064	0.479658	0.17949	0.726844	0.01005
KIAA1212	0.819274	0	0.634623	0.04899	0.80407	0.00384

KIAA1383	0.339084	0.07974	0.719487	0.01656	0.492378	0.13433
KIAA1430	1,053,410	0	0.449414	0.09521	0.848306	0.00287
KIAA1545	0.330827	0.18102	0.391376	0.11173	0.457434	0.19866
KIAA1683	0.421425	0.08279	0.606057	0.08274	0.535039	0.10968
KIAA1688	0.426759	0.10476	0.439115	0.16507	0.496874	0.13433
KIAA1729	0.918932	0	0.749023	0.01656	0.872544	0.00196
KIAA1754L	0.646795	0.003	0.585806	0.07797	0.52028	0.10837
KIAA1772	0.411183	0.13719	0.544169	0.09619	0.369047	0.18703
KIAA1794	1,138,999	0	0.69492	0.02218	1,220,156	0
KIAA1822	0.439831	0.0798	0.671675	0.02999	0.418455	0.16693
KLF10	0.554787	0.01588	0.487905	0.17949	0.520535	0.10837
KLF4	0.500971	0.03147	0.508007	0.08005	0.519823	0.03168
KLHDC5	0.639599	0.00193	0.660447	0.03938	0.794491	0.00471
KRT18	0.683709	0.00232	0.660447	0.03938	0.987095	0.00478
LA16c-360B4.1	0.506337	0.023	0.62079	0.04899	0.475743	0.16574
LBR	0.572205	0.011	0.527624	0.12084	0.679951	0.01824
LBX1	0.449957	0.0798	0.710718	0.02218	0.619264	0.02429
LDLRAP1	0.38147	0.17587	0.551606	0.04939	0.609611	0.04211
LECT1	0.528387	0.03147	0.714067	0	0.544573	0.00789
LEMD3	0.419048	0.13719	0.513681	0.14672	0.529661	0.00544
LEO1	0.801518	0.00034	0.503218	0.14672	0.7274	0.01005
LGR5	0.419048	0.13719	0.48922	0.17949	0.722265	0.01325
LHX2	0.354854	0.06096	0.532198	0.06249	0.519823	0.10837
LILRA5	0.400353	0.13719	0.557572	0.09619	0.705279	0.00711
LIM2	0.316068	0.17381	0.412119	0.19063	0.486399	0.16574
LIME1	0.521793	0.00477	0.588507	0.0636	0.506836	0.03168
LIMS3	0.388077	0.17587	0.732258	0.01656	0.449333	0.19866
LIN9	0.360277	0.11338	0.479658	0.17949	0.726844	0.01005
LITAF	0.830392	0	0.501408	0.14672	0.594679	0.05287
LMAN2	0.453187	0.0798	0.459585	0.07182	0.468159	0.16574
LMO3	0.705764	0.00159	0.415837	0.19063	0.529661	0.10837

LOC126860	0.741747	0.00062	0.719487	0.01656	0.562718	0.06777
LOC129138	0.413233	0.06849	0.466412	0.13676	0.526625	0.09489
LOC136263	1,008,126	0	0.698978	0.02218	1,054,776	0
LOC138046	0.490773	0.04302	0.561091	0.04939	0.567856	0.03751
LOC144363	0.926316	0	0.587064	0.07797	0.625963	0.04211
LOC146439	0.729125	0.11842	0.549161	0.09456	0.523317	0.10837
LOC148696	0.360277	0.15726	0.407709	0.19063	0.633058	0.03233
LOC152586	0.627563	0.00249	0.674121	0.03938	0.436272	0.0386
LOC161527	0.632777	0.003	0.599069	0.08274	0.469291	0.13266
LOC201895	0.963758	0	0.798958	0.00771	1,017,968	0.00047
LOC283340	0.449957	0.0798	0.514658	0.08005	0.476357	0.10845
LOC283392	0.595489	0.011	0.73383	0.01656	0.625963	0.02429
LOC285148	0.409637	0.13719	0.51258	0.12138	0.54393	0.08735
LOC285989	0.600586	0.00745	0.482054	0.17949	0.468789	0.10845
LOC286334	0.396602	0.13719	0.556389	0.09619	0.543451	0.01517
LOC338799	1,124,812	0	0.464759	0.12597	1,107,472	0
LOC339123	0.445576	0.05942	0.525284	0.06249	0.523317	0.06541
LOC339229	0.500755	0.01404	0.550161	0.09456	0.648278	0.03233
LOC375133	0.629689	0	0.489732	0.14672	0.480832	0.13433
LOC388152	0.632777	0.003	0.599069	0.08274	0.680471	0.01824
LOC388558	0.463567	0.05942	0.484845	0.13676	0.413439	0.17011
LOC389199	0.537911	0.03147	0.574251	0.09619	0.508984	0.13433
LOC390811	0.47989	0.04302	0.478401	0.17949	0.528226	0.10837
LOC392331	0.480097	0.04302	0.60477	0.0636	0.614336	0.04211
LOC400713	0.568923	0.00063	0.775753	0.00771	0.559359	0.08735
LOC400948	0.452757	0.0798	0.414946	0.19063	0.472982	0.16574
LOC402670	0.364641	0.13555	0.433849	0.16507	0.468789	0.13266
LOC402682	0.40754	0.13719	0.457951	0.14849	0.375032	0.18703
LOC405753	0.485129	0.04302	0.910585	0.00121	0.492755	0.08288
LOC440093	0.507268	0.05078	0.415837	0.1824	0.457434	0.14113
LOC440330	0.445576	0.05942	0.525284	0.06249	0.523317	0.06541

LOC440345	0.607604	0.003	0.549161	0.09456	0.547104	0.08735
LOC441426	0.375728	0.12426	0.628961	0.04899	0.590708	0.02929
LOC441548	0.449957	0.0798	0.661703	0.03938	0.666899	0.0234
LOC442578	0.750732	0	0.650773	0.06484	0.679745	0.01824
LOC442582	0.750732	0	0.650773	0.06484	0.679745	0.01824
LOC51136	0.52162	0.023	0.430561	0.09521	0.480206	0.13266
LOC541473	0.450439	0.0798	0.674875	0.02999	0.539108	0.08735
LOC641702	0.421425	0.10476	0.654541	0.01536	0.535039	0.10837
LOC642423	0.611684	0.00462	0.383404	0.1565	0.680471	0.01824
LOC642431	0.405856	0.13719	0.883318	0.00608	0.715385	0.00711
LOC642432	0.611684	0.00462	0.383404	0.1565	0.680471	0.01824
LOC642491	0.590833	0.011	0.535576	0.12084	0.498359	0.13433
LOC642586	0.448577	0.0798	0.722715	0.03938	0.567375	0.05038
LOC642620	0.579136	0.011	0.62667	0.04899	0.468789	0.10845
LOC642693	0.696673	0.00087	0.414706	0.19063	0.514622	0.06541
LOC642781	0.431607	0.06808	0.55634	0.04939	0.655423	0.00413
LOC643305	582	0.00086	0.353104	0.10812	0.57595	0.05287
LOC643647	0.776154	0.11842	0.561398	0.09619	0.496631	0.08288
LOC643664	0.396431	0.06393	0.358801	0.04737	0.528226	0.10837
LOC643749	0.612715	0.00077	0.486887	0.17949	0.593284	0.00679
LOC644241	0.503302	0.01084	0.486887	0.17949	0.617015	0.00796
LOC644349	0.445576	0.00805	0.358148	0.14041	0.49953	0.08288
LOC644368	0.517929	0.00699	0.628906	0.04899	0.538383	0.01517
LOC644558	0.480097	0.04302	0.60477	0.0636	0.614336	0.04211
LOC644605	0.99606	0	0.863384	0.00257	0.937863	0.00103
LOC644912	0.536237	0.023	0.506157	0.14672	0.468789	0.16574
LOC645052	1,229,180	0	0.695504	0.00658	0.844077	0.00196
LOC645215	0.965227	0	0.771286	0.03047	0.609426	0.0666
LOC645248	0.686384	0	0.530259	0.12084	0.656305	0.0234
LOC645370	0.388446	0.17587	0.55634	0.09619	0.655423	0.0234
LOC645444	0.403433	0.12426	0.574251	0.02276	0.533221	0.06541

LOC645562	1,419,417	0	0.846679	0.004	1,228,672	0
LOC645580	0.445048	0.0798	0.503641	0.14672	0.703397	0.01325
LOC645722	0.52162	0.023	0.885042	0.00103	0.672288	0.0234
LOC645856	0.667961	0.00159	0.919251	0.00121	0.897876	0.00153
LOC646073	0.409637	0.13719	0.536989	0.12084	0.709473	0.01325
LOC646098	0.632137	0.003	0.678784	0.06407	0.389119	0.18703
LOC646365	0.364562	0.17587	0.405901	0.19063	0.451956	0.19866
LOC646471	0.38147	0.17587	0.623555	0.04899	0.679951	0.01824
LOC646484	0.627563	0.00249	0.674121	0.03938	0.436272	0.0386
LOC646590	0.356054	0.15726	0.503757	0.14672	0.441703	0.19866
LOC646765	0.607386	0.00462	0.671675	0.06407	0.581188	0.05287
LOC647135	0.99606	0	0.863384	0.00257	0.937863	0.00103
LOC647219	0.508626	0.03147	0.503641	0.14672	0.445485	0.19866
LOC647251	0.48172	0.04302	0.791617	0.00608	0.627683	0.03233
LOC649897	0.544553	0.02747	0.407803	0.1824	0.395208	0.17011
LOC653033	0.547067	0.023	0.632953	0.04899	0.68821	0.01824
LOC653091	0.611684	0.00462	0.383404	0.1565	0.680471	0.01824
LOC653148	0.548407	0.01588	0.527181	0.12084	0.868188	0.00193
LOC653168	0.405856	0.09315	0.829784	0.01098	0.616711	0.02929
LOC653178	0.448577	0.0798	0.722715	0.03938	0.567375	0.05038
LOC653277	0.548407	0.01588	0.503218	0.14672	0.422362	0.16693
LOC653301	1,499,857	0	0.857763	0.004	1,262,345	0
LOC653344	0.464037	0.03375	0.527181	0.03306	0.445826	0.19866
LOC653361	0.579136	0.011	0.602567	0.0636	0.679745	0.01824
LOC653392	0.622035	0.00462	0.650773	0.03938	0.492229	0.13433
LOC653456	0.653208	0.00232	0.436361	0.09521	0.729599	0.01325
LOC653550	0.425323	0.0798	0.525284	0.06249	0.49953	0.13433
LOC653648	0.417476	0.06808	0.508007	0.14672	0.732478	0.01005
LOC653688	0.674279	0	0.53333	0.12084	0.778238	0.00693
LOC653709	0.379282	0.12426	0.557572	0.09456	0.656639	0.03233
LOC653748	0.579136	0.011	0.602567	0.0636	0.44535	0.19866

LOC653749	0.506222	0.03147	0.646994	0.06484	0.445826	0.19866
LOC653759	0.474317	0.05942	0.536989	0.12084	0.425684	0.16693
LOC653840	0.579136	0.011	0.602567	0.0636	0.679745	0.01824
LOC91664	0.33714	0.15404	0.509088	0.12138	0.413439	0.17011
LRIG1	0.535662	0.00932	0.650152	0.03938	0.609957	0.02429
LRRC45	0.396431	0.13719	0.358801	0.19837	0.480206	0.16574
LRRFIP1	0.668355	0.00232	0.561398	0.09619	0.567579	0.06777
LTA	0.437654	0.10476	0.55992	0.04939	0.474627	0.10845
LUZP5	0.343192	0.14501	0.482054	0.17949	0.609426	0.04211
LYSMD1	0.466241	0.03375	0.551606	0.09456	0.468932	0.16574
MAFK	0.40754	0.13719	0.530259	0.12084	0.539108	0.05038
MAGEF1	0.385676	0.17587	0.505674	0.08005	0.445738	0.19866
MANEAL	0.445048	0.0798	0.359743	0.19837	0.515825	0.10837
MAP1LC3A	0.481655	0.01404	0.706209	0.01656	0.737216	0.00693
MAP1LC3C	0.423855	0.10476	0.503641	0.12138	0.375145	0.18703
MAP3K12	0.551378	0.00932	0.415837	0.19063	0.698189	0.01824
MAP3K8	0.642796	0.003	0.465643	0.14849	0.762171	0.00693
MAP4	0.535662	0.00932	0.529753	0.12084	0.797637	0.00384
MAPBPIP	0.551012	0.01588	0.503641	0.14672	0.726844	0.0012
MAPK1	0.747756	0.00034	0.652976	0.02999	1,007,457	0
MAPKAPK5	0.86015	0	0.758291	0.01098	0.818566	0.00384
MAPT	0.375566	0.1193	0.454481	0.03644	0.456195	0.08849
MARCH4	0.495876	0.04302	0.585806	0.07797	0.54393	0.08735
MARCKS	1,794,381	0	1,046,808	0	0.854329	0.00196
MARS	0.529323	0.03147	0.684908	0.02999	0.601887	0.05287
MATN2	0.384084	0.17587	0.536696	0.12084	0.496874	0.13433
MATR3	0.820054	0	0.55634	0.09619	1,053,359	0
MAZ	0.749378	0.00049	0.573037	0.07797	0.737402	0.01005
MBD3	0.653208	0.00232	0.509088	0.14672	1,094,398	0
MCC	0.517929	0.03147	0.653094	0.03938	0.538383	0.08735
MCM10	0.471384	0.05942	0.661703	0.03938	0.666899	0.0234

MED11	0.605079	0.01637	0.430561	0.16507	0.384165	0.18703
MED12L	0.449956	0.0798	0.553833	0.09456	0.516118	0.10968
MEF2C	0.388446	0.17587	0.55634	0.09619	0.655423	0.0234
MEIS1	0.668355	0.00232	0.707849	0.02218	0.567579	0.03751
MEIS2	0.864795	0	0.43133	0.09521	0.891652	0.00153
METTL5	0.776154	0.11842	0.561398	0.09619	0.496631	0.08288
MGC12760	0.551012	0.18827	0.431692	0.16507	0.492378	0.13433
MGC14289	0.493338	0.04302	0.482054	0.10098	0.585987	0.05287
MGC16186	0.407104	0.09315	0.68621	0.02999	0.619264	0.04211
MGC16597	0.500755	0.01404	0.550161	0.09456	0.648278	0.03233
MGC16824	0.58735	0.00462	0.62079	0.04899	0.475743	0.16574
MGC23270	0.544553	0.02747	0.407803	0.12725	0.743921	0.02547
MGC24125	0.874106	0	0.574251	0.09619	0.581696	0.06777
MGC24381	0.688618	0.00087	0.477531	0.17949	0.475743	0.16574
MGC26694	0.379282	0.17587	0.484845	0.17949	0.729599	0.01325
MGC3265	0.690571	0	0.435396	0.04947	0.468159	0.10845
MGC39633	0.690571	0.00159	0.507962	0.14672	0.608607	0.04211
MGC4093	0.379282	0.17587	0.509088	0.14672	0.559359	0.08735
MICAL-L2	0.386091	0.17587	0.650773	0.03938	0.773503	0.00471
MIF4GD	0.500755	0.03147	0.478401	0.17949	0.624267	0.04211
MIXL1	0.529819	0.023	0.719487	0.01656	0.586165	0.02929
MKL1	0.3542	0.17587	0.41977	0.15876	0.480832	0.13433
MLLT11	0.868903	0	0.527624	0.06249	0.867523	0
MLLT6	0.834591	0	0.406641	0.19063	0.81635	0.00384
MLSTD2	0.818111	0	0.539301	0.12084	0.599322	0.05287
MMP17	0.441103	0.08279	0.538142	0.12084	0.48151	0.16574
MOBKL2A	0.632137	0.003	0.53333	0.06249	0.729599	0.01325
MORC2	0.787111	0	0.489732	0.14672	0.961663	0.00047
MOSC2	0.466241	0.05942	0.599572	0.0636	0.773737	0.00471
MOSPD3	0.364641	0.13555	0.433849	0.16507	0.375032	0.18703
MPPE1	1,168,626	0	0.638807	0.06484	0.599701	0.02429

MPPED2	0.67127	0.00159	0.686383	0.02999	0.719186	0.01325
MPZ	0.572205	0.011	0.479658	0.17949	0.539271	0.05038
MPZL1	0.784132	0.00049	0.479658	0.17949	0.492378	0.08288
MRPL12	0.542484	0.01588	0.645842	0.03938	0.648278	0.0152
MRPL17	0.398567	0.06393	0.490274	0.17949	0.647268	0.03233
MRPL24	0.720554	0.00087	0.479658	0.17949	0.914417	0
MRPS18B	1,203,548	0	0.876397	0.00257	0.996717	0.00047
MSH5	1,028,487	0	0.77902	0.00771	0.972986	0.0004
MSI2	0.813727	0	0.502321	0.04162	1,032,442	0.00057
MSRB3	0.573434	0.01588	0.440298	0.15876	0.529661	0.06541
MTA1	0.397942	0.13719	0.551733	0.09619	0.511445	0.06541
MTERFD1	1,173,588	0	0.561091	0.09619	0.567856	0.06777
MTG1	0.535663	0.023	0.563673	0.09619	0.619264	0.04211
MTRF1L	0.459537	0.0798	0.511232	0.14672	0.569553	0.06777
MUTYH	0.678169	0.00159	0.503641	0.12138	0.797184	0.02105
MVP	0.749378	0.00049	0.573037	0.07797	0.737402	0.01005
MX1	0.409807	0.10476	0.536678	0.06249	0.538014	0.05038
MX2	0.368827	0.17587	0.4391	0.15876	0.421054	0.10931
MXRA7	0.563349	0.011	0.669762	0.02999	0.576247	0.06777
MYBPH	0.76294	0.00044	0.431692	0.09521	0.89097	0.00153
MYCBP2	1,122,822	0	0.812559	0.00608	0.639281	0.00764
MYCL1	0.317892	0.17381	0.671521	0.06407	0.609611	0.0666
MYL2	0.419048	0.13719	0.611525	0.0636	0.698189	0.01824
MYL6	0.639599	0.01637	0.635986	0.04899	0.698189	0.0501
MYLPF	0.344309	0.11338	0.429778	0.15876	0.618466	0.02429
MYNN	0.835632	0	0.481594	0.17949	0.445738	0.08849
MYO10	0.539509	0.00932	0.55634	0.09619	0.538383	0.05038
MYO5B	0.389542	0.17587	0.473191	0.05121	0.55357	0.06777
MYO9B	0.547852	0.01588	0.654541	0.03938	0.680959	0.0234
NAG8	0.471889	0.05942	0.578465	0.07797	0.562547	0.06777
NAGK	0.733035	0	0.414946	0.19063	0.709473	0.01325

NALP1	0.605079	0.01637	0.621922	0.04899	0.576247	0.03751
NANOS2	0.463567	0.05942	0.727268	0.01656	0.559359	0.05038
NBPF11	0.699361	0.00134	0.599572	0.0636	0.586165	0.05287
NCF1	0.686384	0.13158	0.554362	0.09619	0.843821	0.16978
NCLN	0.758564	0.00044	0.824237	0.00481	0.705279	0.01824
NCOA7	0.590833	0.011	0.511232	0.14672	0.498359	0.12085
NCOR2	0.441103	0.10476	0.611525	0.0636	0.529661	0.10837
NDRG4	0.405069	0.10476	0.501408	0.14672	0.451956	0.19866
NEK5	0.616451	0.00745	0.590952	0.03811	0.639281	0.01053
NEUROD1	0.582116	0.011	0.488172	0.17949	0.638526	0.03233
NFATC3	0.52659	0.00111	0.69242	0.02218	0.856337	0.00196
NFE2L2	0.474317	0.05942	0.585806	0.07797	0.472982	0.16574
NFKBIE	0.612715	0.00745	0.632953	0.04899	0.640747	0.03233
NIP	0.358574	0.15726	0.718883	0.01656	0.539684	0.08735
NIPSNAP1	0.3542	0.17587	0.489732	0.12138	0.480832	0.08288
NLN	0.949536	0	0.725661	0.01656	0.538383	0.08735
NME1	1,043,239	0	0.669762	0.01102	0.696298	0.01824
NME1-NME2	1,043,239	0	0.669762	0.01102	0.696298	0.01824
NMI	0.819274	0.00034	0.488172	0.13676	0.662175	0.0234
NOL1	0.661654	0.01225	0.635986	0.04899	0.577812	0.06777
NOP5/NOP58	0.344957	0.15404	0.488172	0.17949	0.496631	0.13433
NOS1	0.595489	0.00292	1,027,362	0	0.74634	0.0012
NOVA2	0.589994	0.00745	0.727268	0.01656	0.729599	0.00175
NOX5	0.400759	0.13719	0.623032	0.04899	0.680471	0.01824
NPAS4	0.629316	0.00114	0.514787	0.14672	0.647268	0.0152
NPHS2	0.678169	0	0.767452	0.00351	0.867523	0
NPR1	0.720554	0	0.647538	0.01536	0.726844	0
NPR3	0.388446	0.17587	0.55634	0.04939	0.397936	0.07315
NPY5R	0.470672	0.0099	0.549284	0.06249	0.557458	0.01517
NR2F2	0.379666	0.17587	0.43133	0.15876	0.469291	0.10845
NRN1	0.56895	0.01588	0.413854	0.19063	0.617015	0.02429

NRXN2	0.629316	0.003	0.759924	0.01098	0.575349	0.06777
NTE	0.379282	0.17587	0.412119	0.19063	0.972798	0.00103
NTNG2	0.459223	0.05942	0.60477	0.0636	0.496195	0.00526
NTRK2	0.417476	0.06808	0.508007	0.14672	0.732478	0.01005
NTSR2	0.819274	0.00034	0.488172	0.10098	0.52028	0.06541
NUMA1	0.67127	0.00159	0.490274	0.10098	0.743159	0.01005
NUMBL	0.547852	0.01588	0.606057	0.0636	0.632319	0.04211
NXPH1	0.42899	0.04164	0.650773	0.03938	0.632866	0.03233
NXPH2	0.862394	0	1,025,161	0	0.969614	0
NY-SAR-48	0.632137	0.003	0.509088	0.14672	0.753918	0.01005
OAS3	0.595489	0.011	0.562603	0.09619	0.529661	0.10837
ODF2L	0.38147	0.1193	0.431692	0.16507	0.562718	0.06777
OGT	0.915502	0	0.568632	0.09619	0.642316	0.0152
OLFML2B	0.445048	0.0798	0.551606	0.09619	0.562718	0.06777
ONECUT2	0.627596	0.00193	0.49685	0.04162	0.784225	0
OR2A20P	0.772182	0.00044	0.843594	0.004	0.632866	0.03233
ORC6L	0.627857	0.00232	0.549161	0.09619	0.761189	0.00693
OSBPL1A	0.735802	0.00087	0.638807	0.01536	0.761159	0.00471
OSGEP	1,193,827	0	0.59971	0.0636	1,348,356	0
OSM	0.432911	0.03375	0.513053	0.12084	0.549522	0.06777
OTOA	0.384816	0.13719	0.573037	0.01477	0.547104	0.08735
OXT	0.421448	0.0798	0.447266	0.12597	0.598988	0.00796
P2RX7	0.749875	0.00726	0.660447	0.06484	0.48151	0.13266
PAF1	0.379282	0.17587	0.436361	0.16507	0.656639	0.03233
PALM2	0.751456	0.00044	0.435435	0.15876	0.637965	0.03233
PANK2	0.561931	0.00745	0.517886	0.10562	0.437722	0.19866
PAPSS2	0.514237	0.03147	0.58818	0.07797	0.785988	0.00471
PARD6A	0.364562	0.17587	0.596914	0.0636	0.49953	0.13433
PARVB	0.550978	0.00249	0.466412	0.17949	0.732696	0.00693
PAX5	1,398,543	0	0.628961	0.04899	0.945133	0
PCDH8	0.946693	0	0.615575	0.0636	0.686635	0.01824

PCDHA6	0.366866	0.13555	0.507962	0.12138	0.514975	0.10837
PCDHB15	0.388446	0.12426	0.55634	0.09619	0.468159	0.16574
PCDHB3	0.561089	0.02747	0.628906	0.06839	0.632015	0.06151
PCDHGA9	0.668991	0.00232	0.55634	0.04939	0.561791	0.03751
PCF11	0.482476	0.01084	0.73541	0.01656	0.623295	0.04211
PCNA	0.903103	0	0.753289	0.00771	1,221,014	0
PDAP1	0.664934	0.00232	0.674875	0.02999	0.656305	0.0234
PDCD1	0.431197	0.06808	0.463763	0.07182	0.449333	0.13502
PDE4D	0.431607	0.10476	0.55634	0.04939	0.655423	0.00413
PDXP	0.373878	0.13719	0.583014	0.0636	0.480832	0.12085
PELP1	0.667673	0.00159	0.502321	0.08005	0.480206	0.10845
PEO1	0.514237	0.03147	0.58818	0.03811	0.452539	0.13502
PERP	0.590833	0.011	0.705987	0.02218	0.854329	0.00196
PFKL	0.53275	0.02747	0.512284	0.12138	0.678365	0.0501
PFKM	0.793985	0.00044	0.48922	0.17949	0.457434	0.19866
PFN1	0.730268	0.00062	0.430561	0.15876	0.696298	0.00711
PFTK1	0.643485	0.003	0.433849	0.15876	0.609426	0.04211
PHF19	0.730582	0.00062	0.749915	0.01098	0.56708	0.06777
PHF23	0.709403	0	0.406641	0.19063	0.504216	0.13433
PIGN	0.476107	0.05942	0.473191	0.17949	0.668898	0.01824
PIK3R5	0.438161	0.0798	0.574081	0.07797	0.504216	0.13433
PIM2	0.830339	0	0.815863	0.00608	0.832632	0.00287
PKD1L2	0.405069	0.10476	0.501408	0.14672	0.428169	0.10931
PKD1L3	0.324055	0.14501	0.477531	0.17949	0.451956	0.19866
PLAUR	0.400353	0.09315	0.53333	0.03091	0.632319	0.0666
PLB1	0.366517	0.15726	0.439355	0.16507	0.685824	0.01824
PLCD3	0.563349	0.011	0.454481	0.12597	0.672288	0.0234
PLD1	0.36425	0.15726	0.577913	0.07797	0.539578	0.08735
PLEK2	0.376998	0.17587	0.59971	0.0636	0.441703	0.19866
PLEKHA8	0.729283	0	0.530259	0.06249	0.562547	0.06777
PLEKHG5	0.423855	0.10476	0.407709	0.19063	0.539271	0.08735

PLEKHG6	0.419048	0.09315	0.684908	0.01102	0.529661	0.10837
PLEKHO1	1,080,831	0	0.503641	0.14672	0.797184	0.00384
PLEKHQ1	0.569499	0.011	0.670957	0.02999	0.657007	0.0234
PLK1	0.506337	0.023	0.501408	0.14672	0.570892	0.06777
PLXDC2	0.55709	0.01588	0.465643	0.12597	0.738353	0.0012
PLXNA4A	0.386091	0.17587	0.530259	0.12084	0.609426	0.04211
PNKP	0.358211	0.06096	0.484845	0.17949	0.607999	0.02929
POFUT1	0.622138	0.00232	0.447266	0.12597	0.368608	0.18303
POLA2	0.776156	0.00049	0.637356	0.04899	0.647268	0.03233
POLDIP3	0.3542	0.17587	0.559694	0.07797	0.549522	0.06777
POP5	0.749875	0.00087	0.587064	0.07797	0.625963	0.04211
PPAPDC2	0.438349	0.0798	0.508007	0.14672	0.472566	0.16574
PPCDC	0.358574	0.15726	0.479255	0.17949	0.657007	0.0234
PPL	0.344309	0.13555	0.549161	0.09456	0.404382	0.17011
PPP1R10	1,203,548	0	0.876397	0.00257	0.996717	0.00047
PPP1R14A	0.484638	0.04302	0.606057	0.0636	0.437759	0.15516
PPP2CA	0.62583	0.00462	0.483774	0.10098	0.772463	0.00471
PPT2	0.547067	0.023	0.632953	0.04899	0.68821	0.01824
PRDM13	0.437654	0.10476	0.705987	0.02218	0.569553	0.06777
PRDM8	0.403433	0.17587	0.674121	0.03938	0.557458	0.08735
PRIC285	0.461586	0.04302	0.470806	0.17949	1,036,710	0
PRKAG1	0.573434	0.01588	0.587064	0.07797	0.48151	0.16574
PRKCG	0.800707	0.00034	0.727268	0	0.656639	0.00764
PRKCH	0.397942	0.09315	0.935548	0.00159	0.488198	0.08288
PRLR	0.431607	0.06808	0.459585	0.12597	0.585199	0.05287
PRO1073	0.755179	0	0.539301	0.06249	0.623295	0.04211
ProSAPiP1	0.38131	0.10286	0.659128	0.02999	0.57595	0.07582
PROX1	0.529819	0.00932	0.647538	0.03938	0.562718	0.0108
PRR5	0.373878	0.13719	0.699617	0.04075	0.549522	0.06777
PRR6	0.646808	0.00232	0.598001	0.08274	0.504216	0.12085
PRR8	0.493338	0.01084	0.554362	0.09619	0.750063	0.00079

PRRT1	0.547067	0.023	0.632953	0.04899	0.68821	0.01824
PRRT2	0.749378	0.00049	0.573037	0.07797	0.737402	0.01005
PRUNE	0.61459	0.00462	0.503641	0.14672	0.726844	0.01005
PSEN1	0.733052	0.00062	0.479768	0.17949	0.55794	0.03751
PSMA8	0.519389	0.03147	0.473191	0.10098	0.576636	0.05287
PSMD3	0.584214	0.00745	0.621922	0.04899	0.504216	0.08288
PTDSS1	1,173,588	0	0.561091	0.09619	0.567856	0.06777
PTGER2	0.418887	0.04164	0.575722	0.07797	0.697426	0.01325
PTGER4	0.820054	0.00034	0.628906	0.04899	0.983135	0
PTK2	0.618801	0	0.536696	0.12084	0.520535	0.10837
PTPRN	0.409637	0.10286	0.488172	0.13676	0.402035	0.17011
PTPRN2	0.386091	0.17587	0.530259	0.12084	0.44535	0.19866
PTPRO	0.705764	0.00159	0.611525	0.01089	0.650038	0.03233
PTPRU	0.99606	0	0.623555	0.04899	1,219,222	0
PUM1	1,186,795	0	0.599572	0.0636	1,008,203	0.00057
PURB	0.707833	0	0.506157	0.08005	0.632866	0.03233
PUS7L	0.529323	0.03147	0.48922	0.17949	0.433359	0.10931
PXMP4	0.401379	0.10476	0.564967	0.07797	0.483798	0.13433
RAB30	1,048,860	0	0.588328	0.07797	0.695213	0.00257
RAB34	1,105,834	0	0.526241	0.12084	1,176,504	0
RAB3IL1	0.398567	0.13719	0.514787	0.14672	0.479458	0.10845
RAB5C	0.563349	0.00292	0.550161	0.09619	0.576247	0.06777
RAB6B	0.492809	0.04302	0.553833	0.09619	0.563038	0.06777
RAD52	0.551378	0.03321	0.709369	0.05409	0.48151	0.16574
RAFTLIN	0.642794	0.00114	0.361195	0.19837	0.539578	0.05038
RAI16	0.405421	0.10286	0.658672	0.06484	0.638838	0.06151
RANBP9	0.765894	0.00062	0.657298	0.03938	0.68821	0.01824
RASA1	0.453187	0.0798	0.532151	0.12084	0.983135	0.00047
RASA3	0.440322	0.10476	0.418591	0.08664	0.56825	0.01664
RASA4	0.42899	0.10476	0.62667	0.06839	0.656305	0.05558
RASAL2	0.529819	0.0031	0.551606	0.09619	0.703397	0.01325

RASGEF1A	0.49281	0.01084	0.58818	0.07797	0.428721	0.16693
RASGRP4	0.547852	0.01588	0.509088	0.08005	0.486399	0.16574
RASSF2	0.582116	0.00086	0.447266	0.14849	0.368608	0.18703
RAX	0.389542	0.17587	0.686126	0.02218	0.438243	0.19866
RBM4	0.650293	0.00232	0.416732	0.1824	0.719186	0.01325
RBMX	0.638722	0.003	0.815863	0.00608	1,094,317	0
RBMY1A1	0.427216	0.10476	0.856551	0.00351	0.592043	0.06777
RBMY1B	0.320412	0.10341	0.749482	0.02999	0.468701	0.06293
RBMY1D	0.384495	0.12426	0.776249	0.00658	0.419364	0.14277
RBMY1E	0.427216	0.10476	0.66918	0.01089	0.592043	0.06777
RBMY1F	0.427216	0.10476	0.856551	0.00351	0.592043	0.06777
RBP7	0.402663	0.10286	0.551606	0.09456	0.656504	0.0234
RCSD1	0.551012	0.01588	0.479658	0.17949	0.515825	0.02786
RDH8	1,032,490	0	1,042,418	0	1,191,678	0
RELB	0.695351	0.00134	0.484845	0.10098	0.632319	0.04211
REXO1L2P	0.405421	0.10286	0.536696	0.12084	0.473213	0.16574
REXO4	0.60534	0.00462	0.508007	0.14672	0.496195	0.13433
RFP2	0.572419	0.01588	0.517083	0.14672	0.449864	0.13502
RFX3	1,022,815	0	0.822488	0.00481	0.850619	0.00196
RGS14	0.453187	0.0798	0.459585	0.07182	0.468159	0.16574
RHEBL1	0.374937	0.11338	0.538142	0.12084	0.866717	0.00196
RHOA	0.471382	0.05942	0.601992	0.0292	0.516118	0.10837
RILP	0.354701	0.11338	0.526241	0.03091	0.456195	0.13502
RINT1	0.85798	0	0.506157	0.14672	0.632866	0.03233
RIPK5	0.551012	0.01588	0.407709	0.19063	0.703397	0.01325
RND1	0.793985	0.00044	0.48922	0.17949	0.577812	0.03751
RNF121	0.37759	0.12426	0.539301	0.12084	0.551376	0.08735
RNF138	0.735802	0.00087	0.615148	0.04899	0.576636	0.05287
RNF168	1,221,308	0	0.457514	0.07182	0.844556	0.00196
RNF170	0.917533	0	0.414719	0.19063	0.496874	0.13433
RNF175	0.560324	0.00206	0.524316	0.04338	0.581696	0.01664

RNF41	0.463158	0.0798	0.48922	0.17949	0.698189	0.01824
RNH1	0.587362	0.02024	0.514787	0.14672	0.599322	0.05287
RNPEP	0.423855	0.10476	0.455675	0.14849	0.703397	0.04366
ROBO1	0.771353	0.00044	0.409355	0.19063	0.609957	0.04211
RORC	0.423855	0.10476	0.719487	0.01656	0.375145	0.18303
RP11-138L21.1	0.60534	0.00462	0.725725	0.01656	0.590708	0.05287
RP11-139H14.4	0.990725	0	0.787936	0.00771	0.686635	0.01824
RP5-1119A7.4	0.413233	0.0798	0.443091	0.14849	0.480832	0.13433
RP5-1153D9.3	0.602069	0.01225	0.447266	0.14849	0.506836	0.10968
RPA1	0.500755	0.03147	0.598001	0.0636	0.696298	0.00711
RPIP8	0.605079	0.15642	0.789362	0.02982	0.432185	0.15516
RPL10	1,149,700	0	0.568632	0.04939	0.856422	0.00196
RPL18A	0.547852	0.02747	0.484845	0.17949	0.607999	0.05287
RPL22	0.593397	0.00745	0.647538	0.03938	0.492378	0.13433
RPL23A	1,105,834	0	0.574081	0.07797	1,176,504	0
RPL26	0.667673	0.00159	0.645842	0.03938	0.456195	0.19866
RPL3	0.983889	0	0.513053	0.12084	0.824283	0.00196
RPL35	0.626213	0.003	0.628961	0.04899	0.661593	0.01041
RPL36	0.990348	0	1,018,175	0	0.997118	0
RPL36AL	0.733052	0.00062	0.59971	0.0636	0.720673	0.01005
RPL4	0.90698	0	0.479255	0.17949	0.445826	0.13502
RPS13	0.776156	0.00049	0.612842	0.0636	0.743159	0.01005
RPS3A	0.627596	0.00462	0.425872	0.15876	0.605933	0.05287
RPS6KA1	0.529819	0.023	0.527624	0.12084	0.609611	0.0666
RRM2	0.905513	0	0.488172	0.17949	0.898666	0.00153
RTF1	0.506222	0.03147	0.479255	0.17949	0.821259	0.00287
RUSC2	0.375728	0.17587	0.628961	0.04899	0.637965	0.0152
RUTBC1	0.459025	0.05942	0.478401	0.10098	0.456195	0.19866
S100A6	0.445048	0.0798	0.671521	0.02999	0.445485	0.19866
S100PBP	0.890096	0	0.407709	0.19063	0.539271	0.08735
SALL1	0.384816	0.09315	0.69242	0.02218	0.903912	0.00153

SALL3	0.584313	0.00292	0.733445	0.01098	0.599701	0.04211
SAMM50	0.413233	0.06849	0.699617	0.0031	0.435038	0.19866
SCAND2	0.569499	0.011	0.575106	0.07797	0.469291	0.16574
SCARB2	1,008,584	0	0.449414	0.07139	0.557458	0.08735
SCD	1,114,180	0	0.808748	0.00608	1,357,616	0
SCNN1B	0.567097	0.00249	0.716297	0	0.784976	0.00471
SCRIB	0.384084	0.17587	0.609882	0.0292	0.615177	0.02429
SDHC	0.572205	0.011	0.479658	0.17949	0.539271	0.05038
SDSL	0.330827	0.17381	0.562603	0.09619	0.529661	0.10968
SEC22L1	0.551012	0.01588	0.647538	0.06484	0.609611	0.0666
SECTM1	0.47989	0.04302	0.550161	0.09619	0.696298	0.01824
SELT	0.942764	0	0.842789	0.004	0.727257	0.01005
SEMA4D	0.626213	0.00114	0.532198	0.12084	0.496195	0.13433
SENP1	0.793985	0.00044	0.48922	0.17949	0.457434	0.19866
SEPT2	0.905513	0	0.829892	0	0.685824	0.00711
SEPT9	0.563349	0.011	0.621922	0.04899	0.456195	0.19866
SEPT15	0.784132	0.00049	0.527624	0.06249	0.586165	0.02929
SERF1A	1,100,598	0	0.677283	0.02999	0.983135	0.00047
SERF1B	1,100,598	0	0.677283	0.02999	0.983135	0.00047
SERPINB6	0.503302	0.04302	0.486887	0.17949	0.664478	0.0234
SERPINE1	0.643485	0.01225	0.940005	0.00159	0.773503	0.00471
SETD1B	1,124,812	0	0.464759	0.12597	1,107,472	0
SETMAR	1,371,294	0	0.77055	0.00771	1,149,535	0
SFRP2	0.806867	0	0.674121	0	0.824069	0.00384
SFRS10	1,264,161	0	0.481594	0.17949	1,079,155	0
SFRS3	1,925,677	0	1,046,808	0	1,542,539	0
SFRS8	0.551378	0.023	0.513681	0.04162	0.698189	0.01824
SGCA	0.563349	0.00292	0.598001	0.00632	0.624267	0.00796
SGTB	0.949536	0	0.725661	0.01656	0.538383	0.08735
SH2D4A	0.640139	0.003	0.658672	0.01536	0.496874	0.08288
SH3BGRL2	0.678364	0.00232	0.705987	0.00658	0.68821	0.01824

SH3BP1	0.373878	0.13719	0.606335	0.04899	0.366348	0.18303
SH3BP5	0.792779	0.00049	0.601992	0.0636	0.469198	0.16574
SIAH1	0.405069	0.10476	0.382025	0.1565	0.523317	0.06541
SIGLEC8	0.442496	0.06849	0.678784	0.01102	0.413439	0.17011
SKP1A	0.841634	0	0.870793	0.00257	0.725647	0.01005
SLC1A1	0.60534	0.00193	0.60477	0.0636	0.56708	0.03751
SLC23A2	0.421448	0.0798	0.588507	0.0292	0.506836	0.10837
SLC24A4	0.314165	0.18102	0.551733	0.09619	0.488198	0.13433
SLC25A6	0.510978	0.03147	0.494463	0.17949	0.616711	0.05287
SLC27A2	0.485129	0.04302	0.575106	0.03811	0.703936	0.01325
SLC30A10	0.847711	0	0.74347	0.01098	0.609611	0.02429
SLC34A2	0.403433	0.12426	0.574251	0.02276	0.533221	0.06541
SLC35A2	0.404524	0.13719	0.39557	0.11173	0.737474	0.01005
SLC35B2	0.590833	0.011	0.852053	0	0.806866	0
SLC35F5	0.452757	0.0798	0.51258	0.14672	0.449333	0.19866
SLC38A1	1,036,592	0	0.684908	0.02999	1,107,472	0
SLC38A2	0.639599	0.00462	0.562603	0.09619	0.987095	0.0004
SLC39A1	0.678169	0.00159	0.431692	0.07139	0.679951	0.00711
SLC43A3	0.37759	0.12426	0.46576	0.07182	0.455485	0.13502
SLC4A8	0.595489	0.011	0.562603	0.09619	0.529661	0.10968
SLC5A11	0.364562	0.17587	0.501408	0.14672	0.451956	0.13502
SLC5A5	0.442496	0.0798	0.703026	0.02218	0.705279	0.01824
SLC8A3	0.858718	0	0.791617	0.00608	0.534693	0.08735
SLCO5A1	0.469435	0.05942	0.683067	0.02999	0.473213	0.16574
SLITRK5	0.770564	0.00062	0.640198	0.01902	0.639281	0.03233
SMAD9	0.704516	0	0.418591	0.19063	0.757666	0.00693
SMARCA2	1,315,048	0	0.508007	0.14672	0.874248	0.00193
SMARCC2	0.639599	0.00462	0.635986	0.06839	0.601887	0.05287
SMC4L1	1,071,323	0	0.698311	0.02218	0.985316	0.00047
SMC5L1	0.93932	0	0.508007	0.14672	1,063,274	0
SMYD4	0.500755	0.03147	0.598001	0.0636	0.696298	0.00711

SNAPAP	0.423855	0.08279	0.527624	0.10562	0.375145	0.18303
SNAPC1	0.963439	0	0.479768	0.13676	0.604435	0.04211
SNRP70	0.674279	0	0.53333	0.12084	0.778238	0.00693
SNX1	0.696055	0.00134	0.742845	0.01098	0.703936	0.00474
SNX25	1,053,410	0	0.449414	0.09521	0.848306	0.00287
SORT1	0.678169	0.00159	0.479658	0.17949	0.492378	0.13433
SOX5	0.705764	0.00159	0.782752	0.00771	0.674114	0.0234
SP8	0.471889	0.05942	0.506157	0.14672	0.609426	0.00796
SPAG9	0.95978	0	0.645842	0.03938	0.672288	0.0234
SPCS2	0.860065	0	0.588328	0.07797	0.791105	0.00471
SPDYC	0.440521	0.0798	0.416732	0.19063	0.455485	0.13502
SPEN	0.445048	0.0798	0.503641	0.14672	0.703397	0.01325
SPTBN1	0.689915	0.00159	0.610215	0.0636	0.378386	0.18303
SQLE	0.789505	0.00049	0.487905	0.17949	0.662499	0.00413
SRGAP1	0.441103	0.06808	0.440298	0.07139	0.457434	0.19866
SRGAP3	0.407103	0.09315	0.601992	0.0292	0.375358	0.13007
SRM	0.445048	0.0798	0.503641	0.14672	0.492378	0.08288
SSTR2	0.47989	0.04302	0.478401	0.17949	0.528226	0.10837
ST8SIA3	0.454466	0.0798	0.591488	0.0636	0.576636	0.05287
ST8SIA4	0.755312	0.00062	0.653094	0.01536	0.491567	0.13433
STAT5B	0.918051	0	0.645842	0.03938	0.744319	0.01005
STC2	0.517929	0.01404	0.604717	0.0292	0.608607	0.00842
STIM2	0.448259	0.06808	0.449414	0.15876	0.678645	0.0234
STIP1	0.629316	0.003	0.563815	0.09619	0.815078	0.00384
STK11IP	0.452757	0.0798	0.781075	0.00771	0.591228	0.05287
STK24	0.616451	0.00249	0.517083	0.14672	0.781343	0.00101
STX3A	0.461498	0.05942	0.588328	0.07797	0.719186	0.01325
SULT2B1	0.379282	0.17587	0.53333	0.12084	0.510719	0.13433
SUMO2	1,001,510	0	0.598001	0.0636	0.696298	0.00711
SUMO3	0.471278	0.04302	0.414706	0.19063	0.514622	0.06541
SUV39H2	0.835635	0	0.58818	0.07797	0.54781	0.05038

SUV420H1	0.398567	0.13719	0.490274	0.17949	0.575349	0.06777
SVEP1	0.375728	0.17587	0.483816	0.17949	0.590708	0.05287
SVOP	0.441103	0.04164	0.538142	0.06249	0.457434	0.19866
SYNE2	0.418887	0.08279	0.503757	0.14672	0.511445	0.10837
SYNGAP1	0.80966	0	0.681642	0.02999	0.735672	0.01005
SYNJ2	0.656481	0.003	0.754675	0.01098	0.617015	0.04211
SYT2	0.487434	0.04302	0.527624	0.12084	0.562718	0.03751
SYTL3	0.459537	0.0798	0.657298	0.03938	0.52209	0.06541
TANC1	0.646795	0.003	0.659032	0.03938	0.969614	0.0004
TARBP2	0.551378	0.00932	0.415837	0.19063	0.698189	0.01824
TARSL1	0.699361	0.00134	0.791435	0.00608	0.726844	0.01005
TAS2R38	0.557687	0.01588	0.409746	0.19063	0.468789	0.16574
TBC1D10B	0.344309	0.11338	0.429778	0.15876	0.618466	0.02429
TBCA	0.431607	0.10476	0.507962	0.14672	0.421343	0.16693
TBRG4	0.42899	0.10476	0.433849	0.15876	0.632866	0.03233
TBX3	0.551378	0.023	0.611525	0.0636	0.625963	0.04211
TBXAS1	0.943778	0	0.457951	0.12597	0.937579	0
TCTA	0.471382	0.05942	0.601992	0.0292	0.516118	0.10837
TDRD5	0.529819	0.023	0.719487	0.01656	0.562718	0.06777
TDRD7	0.459223	0.05942	0.58058	0.07797	0.56708	0.06777
TEX2	0.438161	0.0099	0.526241	0.12084	0.552237	0.08735
TFAP2C	0.361241	0.17587	0.77683	0.00608	0.598988	0.04211
TFDP1	0.528387	0.01404	0.443214	0.09521	0.520895	0.03168
TFRC	0.749926	0.00062	0.481594	0.17949	0.469198	0.10845
TGIF	0.908931	0	0.449531	0.12597	0.899552	0.00149
THEM5	0.508626	0.0422	0.887367	0.01128	0.492378	0.13433
THRAP2	0.72782	0	0.562603	0.04939	0.601887	0.02929
TIA1	1,164,231	0	0.683441	0.02999	1,182,456	0
TJP2	0.480097	0.04302	0.508007	0.14672	0.685221	0.01824
TK1	0.584214	0.02024	0.621922	0.04899	0.744319	0.03171
TLE2	0.484638	0.05078	0.509088	0.14672	0.607999	0.07582

TLN1	0.730582	0.00062	0.459626	0.12597	0.685221	0.01824
TLX3	0.647411	0.003	0.628906	0.01902	0.491567	0.13433
TMCC2	0.805325	0.00188	0.551606	0.09456	0.515825	0.10837
TMED1	0.379282	0.12426	0.557572	0.09456	0.656639	0.03233
TMEM1	0.471278	0.04302	0.487889	0.17949	0.467838	0.01215
TMEM129	0.470672	0.0798	0.449414	0.16507	0.508984	0.13433
TMEM138	0.461498	0.05942	0.661869	0.06484	0.455485	0.14113
TMEM20	0.514237	0.03147	0.539165	0.12084	0.523992	0.10837
TMEM63A	0.635783	0.01225	1,031,264	0	1,078,543	0
TMEM8	0.58735	0.00462	0.596914	0.0636	0.570892	0.08618
TNFAIP3	0.503302	0.01084	0.486887	0.17949	0.617015	0.00796
TNFAIP8	0.776893	0.00044	0.507962	0.14672	0.538383	0.08735
TNFRSF13B	0.500755	0.0422	0.574081	0.07797	0.648278	0.03233
TNFSF12	0.542484	0.00111	0.885042	0.00103	0.672288	0.01041
TNFSF12-TNFSF13	0.542484	0.00111	0.885042	0.00103	0.672288	0.01041
TNFSF14	0.442496	0.06849	0.509088	0.14672	0.486399	0.16574
TNFSF7	0.484638	0.04302	0.412119	0.1824	0.437759	0.15516
TOE1	0.678169	0.00159	0.575589	0.07797	0.797184	0.02105
TOM1L1	0.584214	0.00249	0.598001	0.01089	0.504216	0.13433
TOMM40L	0.339084	0.14501	0.575589	0.07797	0.515825	0.10837
TOR3A	0.911289	0	0.455675	0.12597	0.468932	0.10845
TPD52	0.682815	0.00159	0.585486	0.07797	0.638838	0.03233
TPM1	0.632777	0.003	0.43133	0.09521	0.539684	0.08735
TPM3	0.466241	0.05942	0.479658	0.10098	0.422038	0.15516
TPM4	0.442496	0.04765	0.581815	0.08746	0.437759	0.16693
TRADD	0.58735	0.00462	0.573037	0.07797	0.808763	0.00384
TRAF5	0.529819	0.023	0.503641	0.14672	0.375145	0.18703
TRFP	0.56895	0.01588	0.438199	0.16507	0.640747	0.03233
TRHDE	0.595489	0.011	0.73383	0.01656	0.625963	0.02429
TRIM41	0.733732	0.00087	0.507962	0.08005	0.538383	0.00789

TRIM52	0.388446	0.17587	0.532151	0.12084	0.514975	0.10837
TRIM72	0.384816	0.13719	0.549161	0.04939	0.523317	0.10837
TRPV5	0.42899	0.10476	0.602567	0.0636	0.468789	0.16574
TSC22D1	0.330242	0.18102	0.541706	0.12084	0.449864	0.13502
TSFM	0.573434	0.01588	0.660447	0.03938	0.794491	0.00471
TSGA14	1,244,070	0	0.482054	0.17949	0.984458	0.00047
TSHZ1	0.389542	0.17587	0.567829	0.07797	0.461309	0.06538
TSHZ3	0.484638	0.04302	0.53333	0.06249	0.559359	0.08735
TSPAN16	0.50571	0.0422	0.509088	0.12138	0.583679	0.08618
TSPY1	0.448577	0.0798	0.883318	0.00608	0.814059	0.00471
TSPY2	0.448577	0.0798	0.883318	0.00608	0.814059	0.00471
TSSC1	0.538996	0.023	0.488172	0.17949	0.449333	0.19866
TTC15	0.538996	0.023	0.488172	0.17949	0.449333	0.19866
TTC26	0.514788	0.03147	0.530259	0.12084	0.539108	0.05038
TUBA4	0.388077	0.17587	0.439355	0.16507	0.449333	0.19866
TUBB6	0.454466	0.02839	0.52051	0.06249	0.80729	0
TUG1	0.787111	0	0.489732	0.14672	0.961663	0.00047
TUSC4	0.36425	0.13555	0.481594	0.13676	0.633417	0.06151
TXLNA	0.423855	0.10476	0.479658	0.17949	0.468932	0.16574
UBC	0.86015	0	0.538142	0.03091	0.553736	0.08735
UBE2D3	0.762041	0.00087	0.574251	0.04939	0.508984	0.08288
UBE2N	0.81604	0.00049	0.709369	0.02218	0.698189	0.01824
UBE2O	0.542484	0.01588	0.574081	0.03811	0.576247	0.06777
UBE3C	0.900879	0	0.433849	0.15876	0.492229	0.03586
UBQLN4	0.61459	0.00462	0.503641	0.14672	0.726844	0.0012
UBR2	0.919073	0	0.511232	0.14672	0.87806	0
UEV3	0.587362	0.00745	0.416732	0.19063	0.647268	0.03233
UGDH	1,120,649	0	0.87386	0.004	0.605933	0.05287
ULK1	0.529323	0.03147	0.587064	0.07797	0.722265	0.01325
UNC13D	0.438161	0.04765	0.526241	0.06249	0.648278	0.03233
UPB1	0.452589	0.04302	0.606335	0.06839	0.618212	0.03233

UQCR	0.674279	0.00159	0.484845	0.17949	0.632319	0.04211
UQCRFS1	0.379282	0.04197	0.436361	0.15876	0.535039	0.03168
VAMP4	0.826518	0	0.623555	0.04899	0.750291	0.00693
VAPA	0.973855	0	0.662467	0.02999	0.645832	0.00413
VCL	0.664222	0.01019	0.465643	0.12597	0.666899	0.0234
VIL2	0.634598	0.00193	0.486887	0.17949	0.949255	0.00103
VIPR1	0.407103	0.13719	0.457514	0.07182	0.563038	0.06777
VPS13B	0.960209	0	0.487905	0.17949	0.567856	0.03751
VPS35	0.627857	0.00232	0.549161	0.09619	0.761189	0.00693
WDR45L	0.375566	0.17587	0.502321	0.14672	0.624267	0.04211
WISP2	0.361241	0.17587	0.494346	0	0.483798	0.13433
WNT10B	1,411,529	0	0.611525	0.01089	0.577812	0.01664
XRRA1	0.860065	0	0.588328	0.07797	0.791105	0.00471
YARS	0.890096	0	0.407709	0.19063	0.656504	0.0234
YTHDF1	0.461586	0.04302	0.494346	0.04162	0.46076	0.16574
ZAP70	0.431197	0.10476	0.488172	0.17949	0.496631	0.08288
ZBTB7A	0.463567	0.05768	0.509088	0.12138	0.802558	0.0269
ZBTB9	0.503302	0.04302	0.754675	0.01098	0.593284	0.05287
ZC3H11A	0.360277	0.13555	0.503641	0.14672	0.468932	0.13266
ZCCHC11	0.487434	0.04302	0.359743	0.19837	0.609611	0.04211
ZDHHC17	0.926316	0	0.415837	0.19063	0.674114	0.0234
ZFP30	0.653208	0.00232	0.509088	0.14672	0.656639	0.03233
ZHX2	1,130,913	0	0.609882	0.0636	1,183,033	0
ZIC2	0.528387	0	0.590952	0.00987	0.591927	0.05287
ZNF160	0.611066	0.00462	0.557572	0.09456	0.656639	0.03233
ZNF217	0.903103	0	0.517886	0.06249	1,082,786	0
ZNF238	0.868903	0	0.479658	0.17949	0.82063	0.00287
ZNF271	0.757443	0	0.425872	0.09521	0.830356	0.00196
ZNF414	0.442496	0.06849	0.509088	0.12138	0.535039	0.10968
ZNF447	0.400353	0.13719	0.581815	0.07797	0.583679	0.06777
ZNF471	0.50571	0.00324	0.606057	0.0636	0.875518	0.00196

ZNF498	0.493338	0.04302	0.530259	0.12084	0.398471	0.14277
ZNF555	0.484638	0.04302	0.630299	0.04899	0.535039	0.10837
ZNF566	1,053,562	0	0.75151	0.01098	0.875518	0.00196
ZNF568	0.653208	0.00232	0.436361	0.09521	0.729599	0.01325
ZNF569	0.421425	0.10476	0.509088	0.12138	0.705279	0.01824
ZNF573	0.632137	3	0.654541	0.03938	0.437759	0.16693
ZNF579	0.484638	0.04302	0.606057	0.0636	0.535039	0.06541
ZNF584	0.463567	0.05768	0.53333	0.10562	0.413439	0.17011
ZNF585B	0.568923	0.011	0.460603	0.14849	0.607999	0.05287
ZNF586	0.716422	0.00087	0.703026	0.02218	0.486399	0.16574
ZNF594	0.688538	0	0.478401	0.05974	0.696298	0.00711
ZNF606	0.653208	0.00232	0.581815	0.07797	0.656639	0.03233
ZNF608	1,294,821	0	0.725661	0.01656	1,006,543	0.00057
ZNF613	0.50571	0.01404	0.557572	0.09456	0.632319	0.02429
ZNF616	0.86392	0	0.606057	0.0636	0.802558	0.00471
ZNF670	0.720554	0.00087	0.599572	0.0292	0.703397	0.01325
ZNF691	0.529819	0.023	0.407709	0.08664	0.445485	0.19866
ZNF695	0.487434	0.04302	0.503641	0.14672	0.539271	0.08735
ZNF71	0.653208	0.00232	0.53333	0.06249	0.486399	0.10845
ZNF74	0.432911	0.05942	0.466412	0.17949	0.549522	0.06777
ZWILCH	0.90698	0	0.479255	0.17949	0.445826	0.13502

Table S3. Differentially Expressed Genes upon SOX11 silencing

Probe ID	Genes	logFC	adj.P.Val
216379_x_at	*CD24*	3,16302549	1,2728E-06
220068_at	*VPREB3*	1,67165209	0,00398443
201218_at	*CTBP2*	1,6395099	0,00014354
204915_s_at	*SOX11*	1,60850026	1,2377E-05
213371_at	*LDB3*	1,31967267	0,00024434
209789_at	*CORO2B*	1,30688531	3,1934E-05
225955_at	*METRNL*	1,28392765	0,00406165
205122_at	*TMEFF1*	1,20951192	0,00027447
205347_s_at	*TMSB15A*	1,18129656	0,00512965
206398_s_at	*CD19*	1,15036079	0,0149571
201005_at	*CD9*	1,11724892	0,00172783
225626_at	*PAG1*	1,10783574	0,0225821
1559618_at	*LOC100129447*	1,07874864	0,02033525
223500_at	*CPLX1*	1,06917592	0,00032997
227404_s_at	*EGR1*	1,05689475	0,0005994
210279_at	*GPR18*	1,05452031	0,00088345
232555_at	*CREB5*	1,03991546	0,02869173
205463_s_at	*PDGFA*	1,01291252	0,00247188
208713_at	*HNRNPUL1*	0,99582873	0,00093409
242136_x_at	*MGC70870*	0,98937117	0,00014893
206413_s_at	*TCL1B*	0,98734438	0,00541798
227336_at	*DTX1*	0,98495664	0,00072383
213436_at	*CNR1*	0,96882971	0,00080841
200644_at	*MARCKSL1*	0,89860517	0,0007729
202391_at	*BASP1*	0,87634604	0,02403768
221601_s_at	*FAIM3*	0,86299061	0,00235042
210993_s_at	*SMAD1*	0,86147304	0,00075225
226043_at	*GPSM1*	0,84500907	0,0041213
221539_at	*EIF4EBP1*	0,84284172	0,00070922
224990_at	*C4orf34*	0,84062846	0,00208088
205003_at	*DOCK4*	0,83842339	0,00347517
229487_at	*EBF1*	0,83713658	0,00047624
238480_at	*TTC39C*	0,83551438	0,00123218
206864_s_at	*HRK*	0,82272501	0,0012655
230381_at	*C1orf186*	0,81897284	0,01350178
203921_at	*CHST2*	0,81419213	0,01264445
201998_at	*ST6GAL1*	0,81096359	0,02344304
203865_s_at	*ADARB1*	0,80782815	0,01532905

1554114_s_at	*SSH2*	0,79945425	0,0052339
236918_s_at	*LRRC34*	0,79920875	0,00237934
212886_at	*CCDC69*	0,79138729	0,0227912
206140_at	*LHX2*	0,78528562	0,00068178
240633_at	*DOK7*	0,78474764	0,0014842
38340_at	*HIP1R*	0,78222454	0,0008279
1405_i_at	*CCL5*	0,77775195	0,00069417
221969_at	*PAX5*	0,77654829	0,02954662
214788_x_at	*DDN*	0,77488848	0,00155887
243313_at	*SYNPO2L*	0,77105517	0,00133474
204891_s_at	*LCK*	0,75468935	0,02108237
218974_at	*SOBP*	0,74759485	0,01510782
212737_at	*GM2A*	0,74215325	0,0069208
219745_at	*TMEM180*	0,74187555	0,00075683
211200_s_at	*EFCAB2*	0,74145775	0,00061389
204661_at	*CD52*	0,74089777	0,04640271
226548_at	*SBK1*	0,73915586	0,00221509
203119_at	*CCDC86*	0,73726628	0,04512642
37462_i_at	*SF3A2*	0,73697707	0,00250911
219232_s_at	*EGLN3*	0,73558733	0,00108642
203795_s_at	*BCL7A*	0,72888963	0,0009641
228762_at	*LFNG*	0,71205164	0,01114564
1569003_at	*VMP1*	0,71013962	0,01115874
202081_at	*IER2*	0,70587581	0,00136741
227617_at	*TMEM201*	0,70498252	0,00218308
235252_at	*KSR1*	0,70014684	0,02462122
216521_s_at	*BRCC3*	-0,70122229	0,01785683
210465_s_at	*SNAPC3*	-0,70162284	0,0068293
222061_at	*CD58*	-0,70194891	0,00169607
1552931_a_at	*PDE8A*	-0,70247917	0,02423954
201297_s_at	*MOB1A*	-0,7025069	0,02821483
1559096_x_at	*FBXO9*	-0,70291241	0,02148627
210840_s_at	*IQGAP1*	-0,70384051	0,01084815
201940_at	*CPD*	-0,70448031	0,00078786
201663_s_at	*SMC4*	-0,70528294	0,00179436
224314_s_at	*EGLN1*	-0,70531364	0,00119392
227609_at	*EPSTI1*	-0,70856678	0,00165747
220773_s_at	*GPHN*	-0,70962154	0,00427793
210568_s_at	*RECQL*	-0,70969347	0,04419921
207992_s_at	*AMPD3*	-0,70994001	0,00207243

221618_s_at	*TAF9B*	-0,71008681	0,02343905
204369_at	*PIK3CA*	-0,71257313	0,01480554
1557984_s_at	*RPAP3*	-0,71364713	0,04410941
200607_s_at	*RAD21*	-0,71364819	0,01056123
202113_s_at	*SNX2*	-0,71413215	0,00095461
203141_s_at	*AP3B1*	-0,71473019	0,04182951
1552812_a_at	*SENP1*	-0,71504193	0,01690368
209255_at	*KLHDC10*	-0,71568967	0,00486467
219499_at	*SEC61A2*	-0,71644328	0,00252194
211559_s_at	*CCNG2*	-0,71839764	0,0432253
210685_s_at	*UBE4B*	-0,71849445	0,00875966
213295_at	*CYLD*	-0,71935494	0,00105014
220220_at	*LRRC37A4P*	-0,72035629	0,02335904
1554441_a_at	*WAPAL*	-0,72048499	0,0091386
202842_s_at	*DNAJB9*	-0,72059955	0,00254491
1555797_a_at	*ARPC5*	-0,72117983	0,02504153
228032_s_at	*DENND1B*	-0,72262315	0,00168274
209508_x_at	*CFLAR*	-0,72358068	0,00116174
212482_at	*RMND5A*	-0,72455389	0,04773357
218640_s_at	*PLEKHF2*	-0,72597274	0,00245196
201681_s_at	*DLG5*	-0,72624231	0,01229776
222587_s_at	*GALNT7*	-0,72710931	0,00481315
238959_at	*LARP4*	-0,72829839	0,04401406
214729_at	*TWISTNB*	-0,72885752	0,03238764
219757_s_at	*C14orf101*	-0,73023477	0,00752213
200712_s_at	*MAPRE1*	-0,73137348	0,00738864
218446_s_at	*FAM18B1*	-0,73286114	0,0177656
210379_s_at	*TLK1*	-0,733489	0,03459952
210057_at	*SMG1*	-0,7349655	0,04493178
227835_at	*LOC389831*	-0,73535686	0,00340739
221638_s_at	*STX16*	-0,73569938	0,00715225
217894_at	*KCTD3*	-0,73580997	0,01055896
205446_s_at	*ATF2*	-0,73879766	0,00776474
238851_at	*ANKRD13A*	-0,73926005	0,00583413
219869_s_at	*SLC39A8*	-0,7408313	0,03199364
217920_at	*MAN1A2*	-0,74166664	0,01961137
228149_at	*C7orf60*	-0,74181648	0,0006982
226962_at	*ZBTB41*	-0,74385474	0,01272519
212022_s_at	*MKI67*	-0,74440574	0,00093421
222239_s_at	*INTS6*	-0,74451474	0,02106016

207164_s_at	*ZNF238*	-0,74458011	0,01165471
225246_at	*STIM2*	-0,74476408	0,0299112
1555858_at	*LOC440944*	-0,74505446	0,00773658
204128_s_at	*RFC3*	-0,74597934	0,04316096
203526_s_at	*APC*	-0,747953	0,04536741
207108_s_at	*NIPBL*	-0,75087405	0,01178125
212335_at	*GNS*	-0,75102723	0,02737561
1553219_a_at	*AMMECR1*	-0,75175538	0,01816338
207583_at	*ABCD2*	-0,75194371	0,02646719
211919_s_at	*CXCR4*	-0,75221698	0,00192983
215794_x_at	*GLUD2*	-0,75223179	0,04611787
201399_s_at	*TRAM1*	-0,75266962	0,01421525
201635_s_at	*FXR1*	-0,75352652	0,00349256
221830_at	*RAP2A*	-0,75402716	0,01827237
218782_s_at	*ATAD2*	-0,7544177	0,00232437
219262_at	*SUV39H2*	-0,75445835	0,04410101
232682_at	*MREG*	-0,75505817	0,00488514
216899_s_at	*SKAP2*	-0,75584061	0,00698143
212217_at	*PREPL*	-0,75597875	0,02123871
219209_at	*IFIH1*	-0,75793732	0,00067869
1552625_a_at	*TRNT1*	-0,75795132	0,03042563
202722_s_at	*GFPT1*	-0,75936905	0,00323192
224150_s_at	*CEP70*	-0,7606234	0,00073363
214578_s_at	*ROCK1*	-0,76185851	0,04204407
1565269_s_at	*ATF1*	-0,76276895	0,02741839
201514_s_at	*G3BP1*	-0,76670906	0,02252281
204732_s_at	*TRIM23*	-0,77013509	0,01400664
207620_s_at	*CASK*	-0,77390561	0,00345212
207616_s_at	*TANK*	-0,77505235	0,00935904
202381_at	*ADAM9*	-0,77604061	0,00072091
230226_s_at	*KDM5A*	-0,77679971	0,00780749
210895_s_at	*CD86*	-0,7774205	0,01439107
200950_at	*ARPC1A*	-0,77780931	0,00050008
218035_s_at	*RBM47*	-0,77811785	0,00060648
200008_s_at	*GDI2*	-0,77814524	0,02304105
226977_at	*IGIP*	-0,7784966	0,00068097
201300_s_at	*PRNP*	-0,77850412	0,00051007
212902_at	*SEC24A*	-0,77975646	0,00820039
201946_s_at	*CCT2*	-0,78007117	0,00078863
231975_s_at	*MIER3*	-0,78087874	0,01261663

229115_at	*DYNC1H1*	-0,78164039	0,02682036
227372_s_at	*BAIAP2L1*	-0,78221758	0,00414609
212289_at	*ANKRD12*	-0,78402065	0,00104743
232635_at	*CEP128*	-0,78496968	0,0144737
244038_at	*WDR89*	-0,78512681	0,03223115
201745_at	*TWF1*	-0,78513792	0,00876502
213501_at	*ACOX1*	-0,7867717	0,00114537
221703_at	*BRIP1*	-0,78712642	0,03904937
223352_s_at	*C17orf80*	-0,78736027	0,01781858
231918_s_at	*GFM2*	-0,78765874	0,00351532
212800_at	*STX6*	-0,7904494	0,00060407
212761_at	*TCF7L2*	-0,79068009	0,00230409
206369_s_at	*PIK3CG*	-0,79097257	0,01228021
235003_at	*UHMK1*	-0,7919374	0,01217526
212398_at	*RDX*	-0,79223141	0,00862845
203065_s_at	*CAV1*	-0,79486817	0,00061137
242900_at	*ALG10B*	-0,79767578	0,03986646
223530_at	*TDRKH*	-0,79842749	0,00047241
1552531_a_at	*NLRP11*	-0,80211324	0,00987631
242163_at	*THRAP3*	-0,80274703	0,01859601
217800_s_at	*NDFIP1*	-0,80414345	0,00256138
202932_at	*YES1*	-0,80492521	0,0033075
210007_s_at	*GPD2*	-0,80515875	0,0040925
202514_at	*DLG1*	-0,80540798	0,0189998
228367_at	*ALPK2*	-0,80563302	0,01057868
235067_at	*MKLN1*	-0,80625881	0,01617976
205809_s_at	*WASL*	-0,80683009	0,03919778
202654_x_at	*MARCH7*	-0,80686767	0,03791064
202278_s_at	*SPTLC1*	-0,80801358	0,02098948
216733_s_at	*GATM*	-0,80819928	0,03978667
200806_s_at	*HSPD1*	-0,80853066	0,00064342
214697_s_at	*PTBP3*	-0,81096496	0,01898405
200722_s_at	*CAPRIN1*	-0,81144082	0,03276273
233750_s_at	*TRMT1L*	-0,81182959	0,03734289
210538_s_at	*BIRC3*	-0,81345764	0,00407017
225238_at	*MSI2*	-0,81453184	0,0056854
211968_s_at	*HSP90AA1*	-0,81494121	0,00038149
217301_x_at	*RBBP4*	-0,81595747	0,00801843
228485_s_at	*SLC44A1*	-0,81769256	0,01354891
202874_s_at	*ATP6V1C1*	-0,82067832	0,00159101

234299_s_at	*NIN*	-0,82102032	0,0219534
212177_at	*PNISR*	-0,8237975	0,03402623
238644_at	*MYSM1*	-0,82408667	0,02623082
200778_s_at	*SEPT2*	-0,8245523	0,01284693
204147_s_at	*TFDP1*	-0,82617258	0,0082757
202784_s_at	*NNT*	-0,82801217	0,0011719
217094_s_at	*ITCH*	-0,82801743	0,04120048
1555037_a_at	*IDH1*	-0,82902631	0,00034058
214693_x_at	*NBPF10*	-0,83055668	0,02746084
224600_at	*CGGBP1*	-0,83061487	0,0223016
1554806_a_at	*FBXO8*	-0,83074806	0,00230486
212008_at	*UBXN4*	-0,83136253	0,02456603
233878_s_at	*XRN2*	-0,83334194	0,00895479
224663_s_at	*CFL2*	-0,83456413	0,00059003
1556551_s_at	*SLC39A6*	-0,83504924	0,02402523
224943_at	*BTBD7*	-0,83509337	0,01840564
212409_s_at	*TOR1AIP1*	-0,83675853	0,00054213
1556009_at	*PEX13*	-0,83706368	0,00033258
205543_at	*HSPA4L*	-0,83709277	0,00136143
211220_s_at	*HSF2*	-0,83745324	0,01518297
202058_s_at	*KPNA1*	-0,83789575	0,01512829
235103_at	*MAN2A1*	-0,83848284	0,00953402
221397_at	*TAS2R10*	-0,83868789	0,00242705
201951_at	*ALCAM*	-0,84051729	0,0012154
226897_s_at	*ZC3H7A*	-0,84158468	0,01357232
216976_s_at	*RYK*	-0,84170129	0,00059706
201641_at	*BST2*	-0,84416568	0,00565762
212595_s_at	*DAZAP2*	-0,84501036	0,00208772
222626_at	*RBM26*	-0,84563483	0,02888497
222518_at	*ARFGEF2*	-0,84653045	0,01058963
202236_s_at	*SLC16A1*	-0,84665774	0,01906774
208195_at	*TTN*	-0,84669693	0,00221043
216607_s_at	*CYP51A1*	-0,8474255	0,00249906
234975_at	*GSPT1*	-0,84861912	0,03905378
206288_at	*PGGT1B*	-0,84874582	0,0126315
243835_at	*ZDHHC21*	-0,85048647	0,03368738
218850_s_at	*LIMD1*	-0,85067085	0,00790921
205841_at	*JAK2*	-0,85188762	0,01353532
209006_s_at	*C1orf63*	-0,85448547	0,03991871
1552921_a_at	*FIGNL1*	-0,85662037	0,01516677

213016_at	*BBX*	-0,85861721	0,00503128
220285_at	*FAM108B1*	-0,85864292	0,00075237
1554277_s_at	*FANCM*	-0,85921465	0,03636956
212195_at	*IL6ST*	-0,86116139	0,00304701
1553856_s_at	*P2RY10*	-0,8626859	0,00194131
211804_s_at	*CDK2*	-0,86370863	0,00160318
222600_s_at	*UBA6*	-0,86481514	0,0050873
201831_s_at	*USO1*	-0,86746173	0,00602849
210716_s_at	*CLIP1*	-0,86814646	0,01150823
213424_at	*KIAA0895*	-0,86948217	0,00058266
233899_x_at	*ZBTB10*	-0,87129231	0,03542684
235484_at	*PTAR1*	-0,87415767	0,02557713
217881_s_at	*CDC27*	-0,87417301	0,00713169
208983_s_at	*PECAM1*	-0,87718877	0,00135395
215711_s_at	*WEE1*	-0,8788158	0,03889418
201294_s_at	*WSB1*	-0,87903951	0,02763725
219683_at	*FZD3*	-0,88190613	0,01891366
212105_s_at	*DHX9*	-0,88483946	0,01040812
209647_s_at	*SOCS5*	-0,88529833	0,00064245
202558_s_at	*HSPA13*	-0,88884462	0,02331597
212634_at	*UFL1*	-0,89011481	0,02614654
222747_s_at	*SCML1*	-0,89095859	0,00081286
219740_at	*VASH2*	-0,89172087	0,00115422
219239_s_at	*ZNF654*	-0,89425057	0,00165783
209055_s_at	*CDC5L*	-0,89427262	0,03776556
230036_at	*SAMD9L*	-0,89520461	0,0251652
210041_s_at	*PGM3*	-0,89602183	0,00633748
200641_s_at	*YWHAZ*	-0,90442396	0,00412612
201627_s_at	*INSIG1*	-0,90936634	0,0007143
203294_s_at	*LMAN1*	-0,91047534	0,02880088
228561_at	*CDC37L1*	-0,91394831	0,00298337
206383_s_at	*G3BP2*	-0,9173126	0,01414367
201971_s_at	*ATP6V1A*	-0,91784584	0,02510232
241366_at	*RBAK*	-0,92105347	0,03846773
AFFX-HUMISGF3A/M97935_MB_at	*STAT1*	-0,92377385	0,03006173
209512_at	*HSDL2*	-0,92619278	0,00639139
210432_s_at	*SCN3A*	-0,93242311	0,0012325
207983_s_at	*STAG2*	-0,94116823	0,01509963
214831_at	*MED28*	-0,94122825	0,02185035
1552660_a_at	*C5orf22*	-0,94164142	0,0172509

225386_s_at	*HNRPLL*	-0,94180343	0,00498336
212720_at	*PAPOLA*	-0,94606048	0,01933817
202382_s_at	*GNPDA1*	-0,94863343	0,00079866
206235_at	*LIG4*	-0,94887533	0,00931348
203017_s_at	*SSX2IP*	-0,95176164	0,00023555
225144_at	*BMPR2*	-0,95265321	0,00018255
224829_at	*CPEB4*	-0,95420725	0,00081121
211801_x_at	*MFN1*	-0,95474509	0,02258846
1553112_s_at	*CDK8*	-0,95533386	0,00177201
208925_at	*CLDND1*	-0,95580731	0,02413023
206667_s_at	*SCAMP1*	-0,95646947	0,03762502
211814_s_at	*CCNE2*	-0,95705094	0,04509819
201059_at	*CTTN*	-0,95935961	0,00037416
214545_s_at	*PROSC*	-0,96315727	0,00100648
201718_s_at	*EPB41L2*	-0,97200243	0,01048445
216226_at	*TAF4B*	-0,9726958	0,00082378
209392_at	*ENPP2*	-0,97819401	0,0014586
204290_s_at	*ALDH6A1*	-0,97940547	0,00016441
203158_s_at	*GLS*	-0,98292215	0,0039666
1555814_a_at	*RHOA*	-0,98760009	0,00027992
203319_s_at	*ZNF148*	-0,98805919	0,00348401
238542_at	*ULBP2*	-0,98918682	0,02526012
203810_at	*DNAJB4*	-0,98942998	0,00095307
232278_s_at	*DEPDC1*	-0,98993717	0,00260915
210284_s_at	*TAB2*	-0,9985977	0,01615238
232591_s_at	*TMEM30A*	-1,0039724	0,01005283
238490_at	*KIAA2026*	-1,00990881	0,00324407
202990_at	*PYGL*	-1,01022804	0,00024405
236621_at	*RPS27*	-1,01778265	0,00552782
1555154_a_at	*QKI*	-1,02234657	0,00566466
220477_s_at	*TMEM230*	-1,02234947	0,00094251
238468_at	*TNRC6B*	-1,02263594	0,00066416
206544_x_at	*SMARCA2*	-1,02783765	0,00014737
1560346_at	*HBS1L*	-1,03025751	0,00011433
208744_x_at	*HSPH1*	-1,03092314	0,00021481
1552760_at	*HDAC9*	-1,04114933	0,00275976
202062_s_at	*SEL1L*	-1,04132904	0,00256019
211450_s_at	*MSH6*	-1,04986983	0,01136767
241820_at	*RIF1*	-1,05044659	0,01711909
201988_s_at	*CREBL2*	-1,05874403	0,00089022

235341_at	*DNAJC3*	-1,06357276	0,0064213
216266_s_at	*ARFGEF1*	-1,06820483	0,00227049
200604_s_at	*PRKAR1A*	-1,06963139	0,0005874
209896_s_at	*PTPN11*	-1,07783791	0,0105007
1554411_at	*CTNNB1*	-1,08390066	0,00936307
206098_at	*ZBTB6*	-1,08449452	0,02423008
201742_x_at	*SRSF1*	-1,08602691	0,00570245
213470_s_at	*HNRNPH1*	-1,08725119	0,01026734
231955_s_at	*HIBADH*	-1,0953941	0,0052507
211536_x_at	*MAP3K7*	-1,10775555	0,00201342
212092_at	*PEG10*	-1,12395359	0,02273757
202213_s_at	*CUL4B*	-1,12473589	0,00703666
201646_at	*SCARB2*	-1,12625059	0,00391948
1554260_a_at	*FRYL*	-1,12864281	0,01839908
1554614_a_at	*PTBP2*	-1,13144999	0,04440203
232383_at	*TFEC*	-1,13385263	0,04645388
225912_at	*TP53INP1*	-1,15025128	9,5069E-05
223585_x_at	*KBTBD2*	-1,1511125	0,0368141
209754_s_at	*TMPO*	-1,15227638	0,01072848
205884_at	*ITGA4*	-1,15886395	0,01146328
208852_s_at	*CANX*	-1,17438201	0,00210825
1555106_a_at	*CTDSPL2*	-1,20467906	0,02584418
1554433_a_at	*ZNF146*	-1,20683428	0,02086655
204344_s_at	*SEC23A*	-1,23454384	0,02163057
218036_x_at	*NMD3*	-1,23888561	0,01822097
1553725_s_at	*ZNF644*	-1,24839378	0,01326509
206624_at	*USP9Y*	-1,26775389	0,00178565
223701_s_at	*USP47*	-1,28958393	0,01028621
214786_at	*MAP3K1*	-1,29022283	0,04440117
221428_s_at	*TBL1XR1*	-1,29640573	0,01533065
1552619_a_at	*ANLN*	-1,29690351	0,01065663
226099_at	*ELL2*	-1,30776806	8,5906E-05
1555167_s_at	*NAMPT*	-1,31177112	0,0003207
224851_at	*CDK6*	-1,31193221	0,01345065
215739_s_at	*TUBGCP3*	-1,32100283	0,02701033
211090_s_at	*PRPF4B*	-1,32701419	0,01214507
1557100_s_at	*HECTD1*	-1,34265677	0,03311674
223341_s_at	*SCOC*	-1,35488392	0,0005524
203768_s_at	*STS*	-1,3746243	3,4533E-05
218858_at	*DEPTOR*	-1,38223083	0,00017143

1553530_a_at	*ITGB1*	-1,42064396	0,00870341
214895_s_at	*ADAM10*	-1,4466992	0,00692505
211080_s_at	*NEK2*	-1,44781192	0,00206671
203357_s_at	*CAPN7*	-1,4587103	0,00148031
227337_at	*ANKRD37*	-1,54008722	0,01102987
215719_x_at	*FAS*	-1,74294792	2,1487E-05
221695_s_at	*MAP3K2*	-1,77617303	0,0077154
204427_s_at	*TMED2*	-2,06232427	0,00366088

Table S4. Significantly enriched gene signatures by GSEA analysis

MCL-SOX11+ genes							Enriched in Z138 shControl cell line			
SOX11	ZNF167	TUBB2B	DFNA5	CD24	CSNK1E	TSPAN14	KCNK9	HS3ST3B1	GAL3ST4	PHC2
ABL1	CTBP2	ZNF711	HOMER3	CDKN1C	MARCKSL1	TCL6	FADS3	ZSCAN2	SYT17	TMEFF1
DBN1	HRK	PODXL	FMNL2	CD9	JAG1	CKB	EHD1	GLUL	ZBED3	TM6SF1
PROX1	YWHAG	GPSM1	H2AFY	CNR1	PTPLAD1	TTYH3	PHC1	SERPINE2	BCR	UBE2E3
MBP	GTF2IRD1	SBK1	EGLN3	MCM7	RCC2	FLJ12334	PXDN	KHDRBS3	CENPO	MDK
SPIN1	RTN4	FARP1	SMARCA4	RGS12	PLXNB1	BDH2	RP9	TIAM1	ZNF496	DACT1
PTP4A3	PDIA5	DTNBP1	GRIP1	UCHL1	STMN1	FNBP1L	LCK	NUDT11	PHYHD1	APITD1
HES6	ZNF219	DDAH1	AMOTL1	FBXO15	MYBL2	PLXND1	KIAA1274	JAKMIP2	FBLN2	CCDC69
KCNMB4	GPC2	KCTD15	SETMAR	ARHGEF5	CARHSP1	LATS2	ZNF618	PELI2	LOC283454	CHML
RAB43	KHDRBS1	MSI2	NAV1	LDOC1L	UBE2R2	CAMSAP1	RIMS3	CAMK2N1	TACC3	CREM
APBB2	HS2ST1	PGM2L1	FADS1	MGC39372	GAS2	JUP	FGF9	CDCA7	GDF11	SATB1
DOCK6	PHGDH	MAP4K4	IGF1R	COL27A1	PDE9A	MYO6	MARK1	TJP2	PHLDB2	LTBP1
FAM125B	TCL1A	SEMA4C	HIP1	ARHGEF4	MYH10	SLFN13	PLCG1	CDK2AP1	CHI3L2	CTPS2
FCGBP	AGPAT4	MCF2L	ACVR2B	PFN2	LOC286434	FZD2	CABLES1	DLL1	TMPO	SSBP3
CDC14B	GTF2IRD2	ZBED4	SEPHS1	DNMT3A	LOC389906	AACS	EPS8L2	CYB561	HDGFRP3	KIAA1407
SUSD1	TRIM36	PTPRG	LAPTM4B	GRAMD3	PAK1	H1FX	ZNF135	AXIN2	VANGL2	CYP2R1
PARD3	DTX3	LRP6	TXNRD1	KIF26B	CIB2	IL17RB	FAM84B	ZNF22	CHL1	CRY1
LOC643529	P2RX1	CASP6	PKD2	TUBB	WWC3	CMTM3	MAP1B	FOSL2	SPTA1	FUT4
CPXM1	MIOX	ITGB8	HMGB3	SMARCA1	MIB2	MYB	DCHS1	MAGEH1	OGFRL1	FZD6
FGFR1	KIF21A	PLXNA1	PCTP	MYADM	GPR133	RAPGEF3	KIAA1958	CTTNBP2NL	SVIL	FHL1
BAIAP3	FAM69B	NSUN7	B3GALNT1	SERPINF1	GABARAPL1	CACNB3	RBMS1	CACHD1	RNF130	LDLRAD3
ATP11A	CLDN23	ARSD	SMAD2	SETD4	ZNF542	CRIM1	BTBD3	GNAS	PSD3	TNFRSF21
TMEM44	GSTP1	LUZP1	ODZ4	MEST	MYO10	MLF1IP	CECR2	NTAN1	THAP9	MBOAT2
E2F3	ZNF608	ABCA9	NBEA	LGALS3BP	UBE2F	ABCA6	TFDP2	RCN1	RUFY3	ZNF275
ZNF184	STK17A	HMG20B	PRICKLE1	MAGED1	BIK	SOCS6	CELSR1	LMO7	ULK2	SCAMP5
SRGAP3	LRRN1	AZI2	VEZT	DIP2C	SCCPDH	RRBP1	PTPRS	PNMA2	DLG5	SPATA7
PON2	N4BP2	PLCXD2	CASD1	CNN3	PLA2G2D	BAZ2B	NFE2L3	LIG4	MSR1	SMAD5
YES1	SH3BP4	TTC7B	CHMP1B	DEGS2	TIA1	RNGTT	OLFM4	WDR41	TRO	SSX2IP
SLC7A11	PACS2									

MCL-SOX11- genes							Enriched in Z138 shSOX11 cell line			
DEGS1	SLAMF1	PCSK7	SLC25A28	POU6F1	CD200	FBXW7	SYNJ2	KLF3	SLC25A37	CD82
TNFRSF1B	STAT5B	DVL1	MLLT10	MAP3K5	GPR65	SNAP23	WNT16	IDE	TFR2	ZMYM6
HVCN1	ATM	KIAA1731	PPP2R1B	EED	MXD1	MDFIC	CD48	STAMBPL1	MEF2C	DENND1B
NPAT	RHOQ	FARP2	ZNF318	POLK	MAPK14	SETDB2	PBX3	BTLA	ACAT1	DUS2L
PCYT1A	ADD3	P4HA1	PHTF2	GLS	ZBTB32	ANKRD13C	PPA1	LOC401320	PTPN22	BAG2
IFNGR1	SLC30A5	CAPN2	ACSL4	REV3L	PDE8A	CLN8	ITSN2	USP45	FAS	TMED5
PELI1	PPP3CC	AMPD3	GNRH1	PCMTD1	TMEM38B	MYC	VPS54	BLOC1S2		

B-cell vs Plasmablast							Enriched in Z138 shControl cell line and SOX11-positive MCL primary tumors				
A20	ADAM8	ALOX5AP	CBLB	CCR7	CD19	CD22	CD24	CD72	CD74	c-IAP2	COL1A1
CR1	D6S49E	DDR1	EGR1	FCGRT	FGR	GPR18	GS3686	HHEX	HLA-DOB	HLA-DQA1	HRY
HSPB1	IFITM1	IFITM2	IGFBP4	IGHD	IGKV1D-8	IGLL1	IL4R	IL8	ITGAX	JUP	KIAA0239
LGALS9	LYZ	MLP	MTAP44	MX1	MX2	MYL5	NELL2	NFKB2	PLCB2	PTGDS	PTPRK
RBMS1	RELB	RI58	RPLP0	S100A8	SATB1	SERPINB6	SKAP55	SORL1	SPIB	STAF50	SYPL
TCL1A	TGIF	TLR1									

B-cell identity							Enriched in Z138 shControl cell line				
ADAM28	ADK	AIM2	AKAP2	ARMC3	BANK1	BEND5	BIRC3	BLK	C1QTNF7	CACNA1A	CCR6
CD19	CD200	CD22	CD24	CD37	CD40	CD72	CD79A	CD79B	CNTNAP2	CORO2B	CR2
CXCR5	EBF1	EZR	FADS3	FCER2	FCRL1	FCRL2	FCRLA	GYLTL1B	HIP1R	HLA-DOB	HLA-DQA1
HRK	HVCN1	ID3	IFT57	IGHG1	IL4R	KCNG1	KIAA0040	KIAA0125	LARGE	LCN6	MAP4K2
METTL8	MGC87042	MS4A1	MTSS1	NT5E	OSBPL10	P2RX5	P2RY10	PAWR	PAX5	PCDH9	PDLIM1
PFTK1	PKHD1L1	PLA2G4C	POU2AF1	PPAPDC1B	QRSL1	RASGRP3	RP9	SCN3A	SEMA4B	STAG3	STAP1
SWAP70	SYCP3	SYT17	TNFRSF13C	TPD52	VPREB3	ZCCHC7	ZNF777	ZNF821			

PAX5 activated genes							Enriched in Z138 shControl cell line and SOX11-positive MCL primary tumors				
ALDH1B1	ALPL	ARNTL	ATP1B1	BACH2	BCAR3	BCL2L1	BFSP2	BLNK	BST1	BTG2	CCND3
CD19	CD55	CD79A	CD97	CPLX2	CRIP1	DKK3	E2F2	EBF1	EPHA2	FCRLA	ID3
IFI30	IKZF3	IRF4	IRF8	LEF1	MYH10	NEDD9	OASL1	OTUB2	PDE2A	PLEKHA2	PRKD2
RAPGEF5	SDC4	SIT1	SMARCA4	TCF7L2	TNFRSF19	TPST1	UCHL1	VPREB3			

BLIMP1 repressed genes							Enriched in Z138 shControl cell line				
AICDA	ALOX5	ARHGDIB	ATP2A3	BCL6	BLNK	BTK	CD180	CD19	CD22	CD24	CD27
CD37	CD52	CD53	CD74	CD79A	CD86	CIITA	CR2	CXCR5	DEK	EBF1	FCER1G
FCER2	FCRLA	GCET2	GPR18	HLA-DMB	HLA-DPA1	HLA-DPB1	HLA-DQA1	HLA-DRA	HLA-DRB1	IL16	INPP5D
IRF8	LRMP	LYN	MS4A1	MYBL1	MYO1E	NR1H2	PAG1	PAX5	PCDHGA8	PLEK	POU2AF1
POU2F2	RGS13	RHOH	SP110	SP140	SPIB	ST6GAL1	STAP1	STAT6	SYK	TANK	TLR10
TRAF5	VNN2	VPREB3	ZFP36L1								

Plasmacell vs B-cell							Enriched in Z138 shSOX11 cell line				
AARS	AGA	AQP3	ARF4	ARP	BCMA	C8FW	CANX	CASP10	CAV1	CCR2	CD162
CD27	CD38	CD43	CITED2	CXCR3	DCN	DDOST	DRIL1	DUSP7	ELL2	FABGL	FGL2
FKBP2	FUT8	GAS6	GGCX	GP36B	HAGH	HDLBP	HEXB	HSPA5	HU-K4	ICAM2	IGH
IGL	IL15RA	IL6R	IRF4	ITGA6	ITM1	KDELR1	KDELR2	KIAA0057	KIAA0102	KIAA0103	LGALS3
MAN1A1	NEU1	NOT56L	NUCB2	ORP150	P4HB	P5	P63	PDIR	PDK1	PDRX4	PDXK
PI12	PLOD	PM5	PPIB	PRG1	PRKCI	PYCR1	PYGB	RNASE4	RPN1	RPN2	SEC61B
SEL1L	SLC7A1	SSR1	TM9SF2	TMP21	TRA1	TRAM	UGTREL1	YIF1A			

XBP1 target genes							Enriched in Z138 shSOX11 cell line and SOX11-negative MCL primary tumors				
ACSS1	ALDH1A1	ARF3	ATF6B	ATP2A2	BMP6	CD81	CDKN3	COPE	COX15	CST3	DAD1
DDOST	DEGS1	DNAJB9	DNAJC10	DNAJC3	EDEM1	ERGIC1	FKBP14	FNBP1	FTL	FTSJ1	GLRX
GPR89B	HERPUD1	HM13	HSP90B1	HSPA5	ISG20	ITGAM	ITGB5	LIPA	LMAN1	MANF	MCFD2
MGAT2	MGC29506	MOGS	OS9	PDIA3	PDIA4	PDIA5	PLOD1	PPIB	PPP2CB	PRDX4	RABAC1
RBM7	RHOQ	RNASE4	RPN1	SEC23B	SEC24C	SEC61A1	SEC61G	SLC1A4	SLC30A5	SLC33A1	SLC3A2
SLPI	SPCS3	SPOP	SRP54	SRP9	SRPR	SSR1	SSR3	SSR4	ST6GALNA	SYVN1	TMED10
TRAM1	TXNDC5	UAP1	USO1								

IRF4 target genes							Enriched in Z138 shSOX11 cell line			
ABHD10	ACP1	ACSS2	ADAM9	AGPAT2	AHCY	ALDH1L2	ALDOC	AMPD1	ANKRD37	ANKZF1
APOBEC3B	APOBEC3D	APOBEC3H	ASB13	ATF3	ATF4	ATP5D	ATP6V1E2	ATRX	AURKA	AVPI1
AXIN1	B3GNT1	BCKDHA	BCL2	BCL2L2	BHLHB8	BMI1	BMP6	BNIP2	BSPRY	C11orf24
C12orf57	C14orf93	C16orf14	C17orf39	C1orf2	C20orf133	C22orf9	C5orf32	C9orf100	CALCOCO2	CANX
CASP3	CAV1	CCDC134	CCDC52	CCDC74B	CCL3	CCNC	CCPG1	CD38	CD97	CDK6
CDKN1B	CDT1	CEBPZ	CENPF	CFLAR	CHRAC1	CMTM8	CNOT6	CTH	CTR9	CYCS
CYP51A1	DDHD2	DDIT3	DDR2	DENND2C	DEPDC1	DIXDC1	DKFZp547E087	DNAJB5	DNAJB9	DNAJC10
DUSP5	E2F5	EIF2C2	EIF2S2	EIF3S6	EIF4A2	ELL2	ELN	EML2	ENO1	F12
FADS1	FAM100B	FBXO16	FDFT1	FHL1	FKBP11	FLJ25006	FLJ35767	FRG2	FRMD6	FYN
FZD2	FZD7	GAA	GARS	GART	GFOD1	GFPT1	GLDC	GLS	GNG10	GNG7
GNPDA1	GOLGA7	GPT2	GRB14	GRPEL2	GRSF1	GTF2IRD1	GTF3C2	HADHA	HDAC5	HIG2
HIVEP2	HK2	HMBS	HMGB1	HMGCR	HMGCS1	HMMR	HSP90AA1	HSP90B1	HSPB1	HVCN1
IDH1	IDI1	IFI16	IFNAR1	INSIG1	IRF4	ISG20	ITGA4	ITGB7	ITPKA	ITPR2
JUP	KIAA0241	KIAA0323	KLF2	KLK1	KRAS	KTN1	LDHA	LDLR	LDLRAP1	LOC157562
LOC389458	LOC442013	LOC55565	LOC728315	LOC92312	LONP1	MALAT1	MAN2A1	MARS	MDC1	ME2
MICB	MKI67	MLSTD2	MMAB	MMD	MNAT1	MOCOS	MPP1	MPZL1	MTHFD1L	MVK
MXI1	MYB	MYC	NAPSA	NAPSB	NDRG1	NFIL3	NP	NR4A1	NUP205	OSBPL8
P18SRP	P4HA1	PABPC4	PAICS	PAIP2	PALM2-AKAP2	PAM	PBEF1	PCYT1B	PDCD10	PDIA4
PDK1	PELI3	PFKFB4	PGK1	PHKA1	PIM2	PIP5K1B	PLEKHA4	PMS2L3	PPP1R2	PPP2R5C
PRDM1	PRPF40A	PRPF4B	PRR7	PTPN22	PTPN6	RAB30	RAB33A	RAD21	RIN2	RNF122
ROCK1	RPP30	SAMD8	SAV1	SC4MOL	SC5DL	SCC-112	SCD	SCYE1	SEC61A2	SERF1A
SERPINH1	SETBP1	SIRT3	SKP2	SLAMF7	SLC12A4	SLC25A37	SLC2A1	SLC31A1	SLC37A4	SLC38A2
SLC3A2	SMOC2	SNRK	SNX9	SORT1	SP3	SPATS2	SPFH1	SQLE	SREBF2	SRPK1
SSR1	ST3GAL1	ST6GAL1	STAG2	STK38L	STRBP	STS	STX18	SUB1	SUMO1	TAF9B
TAGLN2	TBC1D14	TBC1D8	TCEA1	TCERG1	TCF20	TCOF1	TDG	TERT	TIMP2	TLOC1
TM9SF4	TMEFF1	TMEM38A	TMTC4	TNFAIP3	TNFRSF12A	TNFRSF17	TNFRSF8	TNNT1	TPR	TRAM1
TUBGCP3	TUFT1	TXNDC5	UAP1	UBE2B	UBE2H	UBE2J1	UCK2	UNG	USP9X	VDAC1
VEGFA	WHSC1	WWC3	XPOT	YARS	YES1	ZC3H10	ZFP36	ZNF37A		

Plasmablast signature							Enriched in SOX11-negative MCL primary tumors			
ABLIM1	ADRBK2	AICDA	AKAP13	AKNA	ALOX5	AMIGO2	AMPD3	AMSH-LP	ANKH	ANXA4
AP1G2	APBB1IP	ARHGAP17	ARHGAP25	ARHGAP9	ARHGEF3	ARPC5	ATP2A3	BACH2	BANK1	BCL11A
BCL2	BHLHB2	BIN1	BIRC3	BIRC4BP	BLR1	BMF	BMP2K	BRDG1	BTBD15	CAPG
CARD11	CAT	CCDC6	CCNG2	CCR1	CCR6	CD19	CD1C	CD22	CD24	CD40
CD44	CD47	CD52	CD69	CD74	CD83	CDC2L6	CENTB1	CENTD1	CKIP-1	CTSS
CYBASC3	CYBB	CYSLTR1	DAAM1	DEK	DOCK10	DOK3	DTNB	DTX3L	EBF	ELF4
ELK3	ELL3	EMILIN2	FADS3	FAIM3	FAM26B	FCRH3	FCRL2	FCRL4	FCRL5	FCRLM1
FGD2	FOXP1	GBP1	GBP2	GCA	GGA2	GPR114	GPR18	GPR92	GRB2	GRN
GSN	GZMB	HCK	HHEX	HIP1R	HLA-DMA	HLA-DMB	HLA-DOA	HLA-DOB	HLA-DPB1	HLADQA2
HLA-DQB1	HLA-DRA	HLA-E	IBRDC2	ICAM3	IDH2	IFITM1	IFITM2	IFITM3	IFNGR1	IGHM
IL10RA	IL16	IL4R	ILK	INPP5A	INPP5D	IRF8	ITGB2	ITPR1	IVNS1ABP	JAK3
JAM3	JMJD2C	KMO	LACTB	LBH	LCHN	LILRB1	LMO2	LPXN	LTB	LY86
LYN	LYSMD2	MAG	MAP3K5	MAPRE2	MARCH-I	MARCKSL1	MCOLN2	MKNK2	MNDA	MPEG1
MS4A1	MS4A7	MTSS1	MX1	MX2	NAPSB	NCF4	NFKBIZ	NOD27	NOD3	NSF
NSUN6	NYREN18	OIP106	PARP12	PARP14	PARP9	PAX5	PBXIP1	PCSK7	PDCD1LG1	PDE7A
PEA15	PFKFB3	PHF11	PHF16	PIK3AP1	PIK3CD	PIP5K3	PKIG	PLAC8	PLEKHF2	PLSCR1
PLXNC1	POU2F2	PREX1	PRKX	PSCD4	PTGS1	PTK2	PTPN1	PTPN18	PTPN6	QSCN6L1
RAB31	RAB7L1	RABEP2	RABGAP1	RALGPS2	RASSF2	RBMS1	RFX5	RGL1	RHOH	RNASET2
RUNX3	S100A4	SAT	SCAP2	SEMA4D	SERPINB1	SERPINB9	SERTAD2	SESN3	SGPP1	SH3BGRL
SIDT2	SIGLEC10	SLAMF1	SLC2A3	SLC41A1	SLC7A7	SLIC1	SNN	SNX2	SOCS3	SOX5
SP110	SP140	SPIB	STAT3	STAT6	STX7	SUV420H1	SYK	SYPL1	TBC1D10C	TBC1D5
TCF4	TFEB	TGFBR2	TICAM2	TLR10	TMEM71	TMEM77	TMEPAI	TOB2	TPP1	TRAF5
TRAFD1	TRIM22	TRIM34	TRIM38	TSPAN3	TSPAN33	UBE1L	UCP2	UGCG	UNC119	UNC84B
URP2	UVRAG	VNN2	VPS13C	VRK2	WDFY4	YPEL5	ZBED2	ZBTB4	ZC3H12D	ZFP36L1
ZNF238	ZNF447									

SOX11-upregulated genes							Enriched in SOX11-positive MCL primary tumors			
ADARB1	AFF3	APOBEC3C	BASP1	C1orf186	CCDC69	CCDC86	CCL5	CD19	CD24	CD52
CD69	CD9	CDV3	CHST2	CNR1	CORO2B	CPLX1	CREB5	CTBP2	DDN	DMD
DOCK4	DOK7	DTX1	EFCAB2	EGLN3	EGR1	EIF4EBP1	FADS1	FAIM3	FOXO1	GPR18
GPSM1	HNRNPUL1	HRK	IKZF2	LCK	LDB3	LFNG	LHX2	LOC100129447	LRRC34	MARCKSL1
METRNL	MGC70870	PAG1	PAX5	PDGFA	SBK1	SF3A2	SLAIN2	SMAD1	SOBP	SOX11
SSH2	ST6GAL1	SYNPO2L	TCL1B	TMEFF1	TMEM180	TMSB15A	TTC39C	VMP1	VPREB3	

SOX11-downregulated genes							Enriched in SOX11-negative MCL primary tumors			
ABCD2	ACOX1	ADAM10	ADAM9	AKIRIN1	ALCAM	ALDH6A1	ALG10B	ALPK2	AMMECR1	AMPD3
ANKRD12	ANKRD13A	ANKRD37	ANLN	AP3B1	APC	ARFGEF1	ARFGEF2	ARHGAP5	ARPC1A	ARPC5
ASPM	ATF1	ATF2	ATL2	ATP13A3	ATP6V1A	ATRX	B3GNT2	BAIAP2L1	BBX	BCLAF1
BDP1	BIRC3	BMPR2	BST2	BTBD7	C12orf35	C14orf101	C14orf145	C16orf72	C17orf80	C1GALT1
C1orf63	C20orf30	C5orf22	C5orf24	C5orf53	C7orf60	CALU	CANX	CAPN7	CASK	CAV1
CCNE2	CCT2	CD86	CDC27	CDC37L1	CDC42SE2	CDC5L	CDK2	CDK6	CDK8	CEP290
CEP350	CEP70	CFL2	CFLAR	CGGBP1	CLDND1	CLIP1	CPEB4	CPNE3	CREBL2	CTDSPL2
CTNNB1	CTTN	CUL4B	CXCR4	CYLD	CYP51A1	DAZAP2	DBT	DCAF16	DCUN1D1	DENND1B
DEPDC1	DEPTOR	DHX9	DLG1	DLG5	DNAJB4	DNAJB9	DNAJC3	DYNC1H1	EEA1	EFHC1
EIF4A2	ELL2	ENPP2	ENPP4	EPB41L2	EPSTI1	ERLIN1	ESCO1	EXOC5	EXOC6	FAM108B1
FAM18B1	FAM98A	FANCB	FANCM	FAS	FBXO8	FGFR1OP2	FIGNL1	FRYL	FXR1	FZD3
G3BP2	GALNT7	GATM	GDI2	GFM2	GLS	GLUD2	GNPDA1	GNS	GOLIM4	GPATCH2
GPD2	GPHN	GSPT1	HAUS6	HDAC9	HEATR1	HECTD1	HERC4	HIBADH	HNRNPH1	HNRPLL
HSDL2	HSF2	HSP90AA1	HSPA13	HSPA4L	HSPD1	HSPH1	IDH1	IFIH1	IFNGR1	IKZF3
IL6ST	INSIG1	INTS6	IQGAP1	ITCH	ITGA4	ITGB1	JAK2	KBTBD2	KCTD3	KDM5A
KIAA0776	KIAA0895	KIAA2026	KLHDC10	KPNA1	LIG4	LIMD1	LMAN1	LOC389831	LOC440944	LOC642236
LRCH3	LRRC37A4	LSM11	LTN1	MAN1A1	MAN2A1	MAP3K1	MAP3K2	MAP3K7	MAPKAPK2	MAPRE1
MBNL1	MED28	MFN1	MIER3	MKI67	MLL	MPHOSPH9	MREG	MSH6	MSI2	MST4
MYSM1	NAMPT	NDFIP1	NEDD1	NEK2	NFX1	NIN	NLRP11	NMD3	NNT	NUPL1
OLFML2A	OXR1	P2RY10	PAPOLA	PECAM1	PEG10	PEX13	PGGT1B	PGM3	PHF3	PICALM
PIK3AP1	PIK3CA	PIK3CG	PLEKHF2	PLXNC1	PREPL	PRKAB2	PRKAR1A	PRNP	PROSC	PRPF4B
PSME4	PTAR1	PTBP2	PTPN11	PYGL	QKI	RAB8B	RAD21	RANBP2	RAP2A	RBAK
RBBP4	RBM26	RBM39	RBM47	RDX	RECQL	RFC3	RFX7	RHOA	RIF1	RIOK3
RNF146	RNGTT	ROCK1	ROD1	RPAP3	RPS27	RSRC1	RYK	SAMD9L	SCARB2	SCML1
SCN3A	SCOC	SEC23A	SEC24A	SEC61A2	SEL1L	SELPLG	SENP1	SEPT2	SGPP1	SKAP2
SLC39A6	SLC39A8	SLC44A1	SLFN13	SMARCA2	SMCHD1	SMG1	SNX2	SOCS5	SPTLC1	SRSF1
SS18	SSR1	SSX2IP	STAG2	STIM2	STS	STX16	STX6	SUV39H2	TAB2	TAF4B
TANK	TAS2R10	TBL1XR1	TCF7L2	TDRKH	TFAM	THRAP3	TLK1	TMED2	TMEM30A	TMPO
TNKS2	TNRC6B	TOR1AIP1	TP53INP1	TPR	TRAM1	TRIM23	TRMT1L	TTN	TUBGCP3	TWF1
TWISTNB	UBA6	UBE4B	UBXN4	ULBP2	UQCRC2	USO1	USP47	USP9Y	VASH2	WAPAL
WASL	WDR89	WEE1	WSB1	XRN2	YES1	YWHAZ	ZBTB10	ZBTB41	ZBTB6	ZC3H7A
ZMYM6	ZNF146	ZNF148	ZNF238	ZNF644	ZNF654	ZNF655	ZNF678	ZNF800		

Table S5. B-cell differentiation gene signatures in Z138shControl and Z138shSOX11 cell lines.

	Enrichment in			
	Z138shControl		Z138shSOX11	
Gene signature	NES	FDR	NES	FDR
B-cell vs plasmablast [1]	2.09	$<10^{-4}$		
B-cell identity [2]	1.88	$<10^{-4}$		
PAX5 activated genes [3]	1.81	0.001		
BLIMP-1 repressed genes [2]	2.19	$<10^{-4}$		
Plasma cell vs B-cell [1]			-2.28	$<10^{-4}$
IRF4 target genes [2]			-2.15	$<10^{-4}$
XBP1 target genes [2]			-2.03	$<10^{-4}$

GSEA was used to test for significant enrichment of defined gene signatures related to different steps of the mature B-cell and plasma cell differentiation programs. NES and FDR *P*-val are shown. Significance is considered when FDR<0.05. Gene signatures of B-cell differentiation (**1**) were extracted from data of [7] and (**3**) of [8] or downloaded (**2**) from http://lymphochip.nhi.gov/signauredb/index.html.[9]

Table S6. SOX11-bound genes that overlap with differential expression data upon SOX11 silencing

Statistical criteria	ChIP-chip	**FDR<0.1 and peak score>0.5**	**FDR<0.1 and peak score>0.5**
	expression array	***P*-val<0.05**	***P*-val<0.05 and logFC>0.7**
		147 overlapping genes	**18 overlapping genes**
		CDK6	*PAX5*
		SCARB2	*MSI2*
		SMARCA2	*HSPD1*
		RHOA	*SUV39H2*
		CDC37L1	*SEPT2*
		TFDP1	*EGLN1*
		MSI2	*SENP1*
		HSPD1	*ZNF238*
		CD86	*STIM2*
		SUV39H2	*CXCR4*
		CXCR4	*CD86*
		STIM2	*TFDP1*
		ZNF238	*CDC37L1*
		SENP1	*RHOA*
		EGLN1	*SMARCA2*
		ZC3H11A	*SCARB2*
		OGT	*CDK6*
		LIN9	*LHX2*
		RANBP9	
		EDEM3	
		SELT	
		RFX3	
		CNOT6L	
		ZNF217	
		MYCBP2	
		ONECUT2	
		SPAG9	
		CCDC47	
		SMAD9	
		ZNF160	
		STIP1	
		VAPA	
		PURB	
		TUG1	
		CD46	
		CD1D	
		MAPK1	
		PSEN1	
		CDC6	
		NFATC3	
		PXMP4	

ZWILCH
MPZL1
SLC38A2
HIPK1
TFRC
DNM1L
PIGN
MGC24125
CLYBL
GAB1
PPP1R10
HOOK3
FAM54B
CDK5RAP2
DNAJC7
ODF2L
SUV420H1
FLII
HMGCR
SQLE
DDX42
AHNAK
PRUNE
LRRFIP1
CD37
UBR2
ARID5B
GOLPH3
BRP44
SLC35F5
PRDM8
MKL1
IRF2BP2
MX1
PCF11
TPD52
TDRD7
IGF2BP1
ATXN2L
MAP1LC3A
SVEP1
CANT1
ARHGEF18
GNB2L1
CDC42SE1
YARS

SSTR2
H6PD
MCM10
ZNF579
CRH
PPP2CA
CEP68
RNF41
PTGER4
NTRK2
MYCL1
RHEBL1
CHD9
GNA12
DLG4
ATP12A
UBQLN4
NIPSNAP1
DENND2A
COL1A2
ULK1
MTG1
HOXA4
ALK
GLDC
CPNE2
IRF5
FGFR1
NOX5
MYO9B
AUTS2
NCOR2
CMTM1
PRIC285
ENAH
ARHGAP17
AP1M2
MLLT6
PLAUR
KCNN4
EP400NL
PRR5
DPEP2
PRLR
MTA1
LMO3

IRF8
ZHX2
GPSM3
DNAJC6
FLJ39739
CABP1
MLLT11
MAP3K12
FOXC1
ZNF606
PAX5
LHX2
SEPT2
SEPT9

IV. SUPPLEMENTAL REFERENCES:

1. Swerdlow S, Campo E, Harris N et al. (Eds.):WHO Classification of Tumours of Haematopoietic and Lymphoid Tissues. AIRC: Lyon; 2008.

2. Fernandez V, Salamero O, Espinet B et al. Genomic and gene expression profiling defines indolent forms of mantle cell lymphoma. *Cancer Res.* 2010;**70**(4):1408-1418.

3. Royo C, Navarro A, Clot G et al. Non-nodal type of mantle cell lymphoma is a specific biological and clinical subgroup of the disease. *Leukemia* 2012; **26**(8):1895-1898.

4. Vegliante MC, Royo C, Palomero J et al. Epigenetic activation of SOX11 in lymphoid neoplasms by histone modifications. *PLoS.One.* 2011;**6**(6):e21382.

5. Smyth GK. Linear models and empirical bayes methods for assessing differential expression in microarray experiments. *Stat.Appl.Genet.Mol.Biol*. 2004;3:Article3.

6. Brennan SK, Meade B, Wang Q et al. Mantle cell lymphoma activation enhances bortezomib sensitivity. *Blood* 2010;**116**(20):4185-4191.

7. Tarte K, Zhan F, De VJ, Klein B, Shaughnessy J, Jr. Gene expression profiling of plasma cells and plasmablasts: toward a better understanding of the late stages of B-cell differentiation. *Blood* 2003;**102**(2):592-600.

8. McManus S, Ebert A, Salvagiotto G et al. The transcription factor Pax5 regulates its target genes by recruiting chromatin-modifying proteins in committed B cells. *EMBO J.* 2011;**30**(12):2388-2404.

9. Shaffer AL, Wright G, Yang L et al. A library of gene expression signatures to illuminate normal and pathological lymphoid biology. *Immunol.Rev.* 2006;**210**:67-85.

Paper II

SOX11 promotes tumor angiogenesis through transcriptional regulation of PDGFA in mantle cell lymphoma.

Abstract

SOX11 is overexpressed in several solid tumors and in the vast majority of aggressive mantle cell lymphomas (MCL). We have recently proven that SOX11-silencing reduces tumor growth in a MCL xenograft model, consistent with the indolent clinical course of the human SOX11-negative MCL. However, the direct oncogenic mechanisms and downstream effector pathways implicated in SOX11 driven transformation remain poorly understood. Here, we observed that SOX11-positive xenograft and human primary MCL tumors overexpressed angiogenic gene signatures and had a higher microvascular density compared to their SOX11-negative counterparts. Conditioned media of SOX11-positive MCL cell lines induced *in vitro* endothelial cell proliferation, migration, tube formation and activation of downstream angiogenic pathways. We identified *PDGFA* as a SOX11 direct target gene upregulated in MCL cells whose inhibition impaired SOX11-enhanced *in vitro* angiogenic effects on endothelial cells. In addition, PDGFA was overexpressed in SOX11-positive but not in negative MCL. *In vivo*, imatinib impaired tumor angiogenesis and lymphoma growth in SOX11-positive MCL xenograft tumors. Overall our results demonstrate a prominent role for SOX11 as a driver of pro-angiogenic signals in MCL, and highlight the SOX11-PDGFA axis as a potential therapeutic target for the treatment of this aggressive disease.

Regular Article

LYMPHOID NEOPLASIA

SOX11 promotes tumor angiogenesis through transcriptional regulation of PDGFA in mantle cell lymphoma

Jara Palomero,[1] Maria Carmela Vegliante,[1] Marta Leonor Rodríguez,[1] Álvaro Eguileor,[1] Giancarlo Castellano,[1] Ester Planas-Rigol,[2] Pedro Jares,[1] Inmaculada Ribera-Cortada,[3] Maria C. Cid,[2] Elias Campo,[1,3] and Virginia Amador[1]

[1]Hematopathology Unit, Pathology Department, and [2]Vasculitis Research Unit, Department of Autoimmune Diseases, Institut d'Investigacions Biomèdiques August Pi i Sunyer, and [3]Department of Anatomic Pathology, Pharmacology and Microbiology, Hospital Clínic, University of Barcelona, Barcelona, Spain

Key Points

- SOX11 mediates regulation of angiogenesis via the PDGFA signaling pathway in MCL.
- SOX11-dependent increased angiogenesis contributes to a more aggressive MCL phenotype.

SOX11 is overexpressed in several solid tumors and in the vast majority of aggressive mantle cell lymphomas (MCLs). We have recently proven that SOX11 silencing reduces tumor growth in a MCL xenograft model, consistent with the indolent clinical course of the human SOX11-negative mantle cell lymphoma (MCL). However, the direct oncogenic mechanisms and downstream effector pathways implicated in SOX11-driven transformation remain poorly understood. Here, we observed that SOX11-positive xenograft and human primary MCL tumors overexpressed angiogenic gene signatures and had a higher microvascular density compared with their SOX11-negative counterparts. Conditioned media of SOX11-positive MCL cell lines induced in vitro endothelial cell proliferation, migration, tube formation, and activation of downstream angiogenic pathways. We identified *PDGFA* as a SOX11 direct target gene upregulated in MCL cells whose inhibition impaired SOX11-enhanced in vitro angiogenic effects on endothelial cells. In addition, platelet-derived growth factor A (PDGFA) was overexpressed in SOX11-positive but not in SOX11-negative MCL. In vivo, imatinib impaired tumor angiogenesis and lymphoma growth in SOX11-positive MCL xenograft tumors. Overall, our results demonstrate a prominent role for SOX11 as a driver of proangiogenic signals in MCL, and highlight the SOX11-PDGFA axis as a potential therapeutic target for the treatment of this aggressive disease. (*Blood*. 2014;124(14):2235-2247)

Introduction

Mantle cell lymphoma (MCL) is an aggressive lymphoid neoplasia derived from mature B cells genetically characterized by the presence of the t(11;14)(q13;q32) translocation causing cyclin D1 overexpression.[1] Furthermore, other secondary genetic alterations also contribute to the development and aggressiveness of MCL.[2] However, recent studies have identified a subset of MCL with indolent clinical behavior that tends to present with leukemic disease instead of extensive nodal infiltration and patients may not need chemotherapy for long periods.[3-5] Recently, molecular studies have identified *SOX11* (SRY [*sex determining region-Y*]-*box11*), as one of the best characterized discriminatory genes between these 2 clinical subtypes of MCL tumors.[6]

SOX11, together with *SOX4* and *SOX12*, belongs to the subgroup C of the *SOX* gene family encoding for transcription factors which play a critical role in embryonic development and cell differentiation.[7,8] SOX11 plays an important role in the regulation of neuronal cell survival and neurite growth, and is highly expressed in different central nervous system malignancies, solid tumors, aggressive MCL, and at lower levels in a subgroup of Burkitt and lymphoblastic lymphomas.[9-14] However, the oncogenic mechanisms of SOX11 contributing to the development and progression of these tumors are largely unknown.

We have recently demonstrated the in vivo tumorigenic potential of SOX11 in a MCL xenograft model. SOX11 blocks the terminal B-cell differentiation through direct positive regulation of PAX5[15] but the specific mechanisms regulated by SOX11 promoting the oncogenic and rapid tumor growth of aggressive MCL still remain to be elucidated.

To further characterize the potential oncogenic mechanisms regulated by SOX11 in MCL, we have investigated the gene and protein expression profiling of SOX11-positive and -knockdown MCL xenograft tumors, cell lines, and primary SOX11-positive and SOX11-negative MCL. We have identified that SOX11 modulates angiogenesis in MCL, and this mechanism is mediated by the upregulation of several proangiogencic factors, principally platelet-derived growth factor A (PDGFA). The inhibition of the PDGFA pathway not only impairs angiogenic development both in vitro and in vivo but also MCL tumor growth in vivo, offering a promising novel therapeutic strategy for the treatment of aggressive MCL.

Submitted April 16, 2014; accepted July 19, 2014. Prepublished online as *Blood* First Edition paper, August 4, 2014; DOI 10.1182/blood-2014-04-569566.

The microarray data reported in this article have been deposited in the Gene Expression Omnibus database (accession numbers GSE52892, for the xenograft tumor gene expression arrays).

The online version of this article contains a data supplement.

There is an Inside *Blood* Commentary on this article in this issue.

The publication costs of this article were defrayed in part by page charge payment. Therefore, and solely to indicate this fact, this article is hereby marked "advertisement" in accordance with 18 USC section 1734.

Methods

Cell lines and primary tumors

Three well-characterized SOX11-expressing MCL cell lines (Z138, GRANTA519, and JEKO1) were used for SOX11 silencing, xenograft experiments, western blot (WB), chromatin immunoprecipitation–quantitative polymerase chain reaction (ChIP-qPCR), in vitro experiments, and immunohistochemical studies. These 3 cell lines carry the t(11;14) and cyclin D1 overexpression.[16] Human umbilical vein endothelial cells (HUVECs) were used for in vitro angiogenesis experimental studies.

Microarray gene expression profiling (GEP) data from 38 primary MCL tumors, 16 SOX11-expressing, and 22 SOX11-negative were used for gene set enrichment analyses (GSEAs) (GSE36000).[17] In addition, 17 splenic MCL, 8 SOX11-expressing, and 9 SOX11-negative, were also investigated for the expression of PDGFA, CD31, CD34 by immunohistochemistry. Details on cell culture and human primary tumor information are provided in supplemental Methods (available on the *Blood* Web site).

Xenograft mouse model

With the use of a protocol approved by the animal testing ethical committee of the University of Barcelona, CB17-severe combined immunodeficient (CB17-SCID) mice (Charles River Laboratories) were subcutaneously inoculated into their lower dorsum with Z138, JEKO1, and GRANTA519 shControl, shSOX11.1, and shSOX11.3 cells as previously described,[15] generating SOX11-positive and -knockdown xenograft tumors (shControl, shSOX11.1, and shSOX11.3, respectively).

When tumor volumes reached 75 to 100 mm^3, mice were randomized to receive imatinib (LC Laboratories) dissolved in phosphate-buffered saline (PBS; Roche Applied Science) at 45 mg/kg or vehicle PBS twice daily by intraperitoneal (IP) injections for 2 weeks. Animals were euthanized according to institutional guidelines, and tumor xenografts were paraffin embedded on saline-coated slides in a fully automated immunostainer (Bond Max; Vision Biosystems) for immunohistochemical analysis and on Tissue-Tek OCT (Sakura) frozen in dry ice and stored at −80°C for RNA and protein extraction.

GEP and GSEA analyses

To identify oncogenic pathways related to SOX11 high expression in MCL, we performed GSEA[18] on expression data sets derived from MCL primary tumors (GSE36000),[17] in vitro SOX11 silencing experiments (GSE34763),[15] and MCL xenografts (GEP derived from Z138 shControl, n = 4; shSOX11.1, n = 5; and shSOX11.3, n = 5). Experimental details on RNA extraction and GEP from xenograft tumors and GSEA are provided in supplemental Methods.

Angiogenesis proteome profiler antibody array

Total protein extracts from in vitro and xenograft SOX11-positive and SOX11-negative cells were used to study the human angiogenesis proteome profiler antibody array (R&D Systems) following the manufacturer's protocol. Experimental details on protein extraction and proteome array are provided in supplemental Methods.

HUVECs in vitro angiogenesis studies

HUVECs were resuspended in RPMI + 10% fetal bovine serum (FBS) or SOX11-positive or SOX11-negative conditioned media (CM) and after the corresponding incubation time, their tube formation, proliferation, and migration were analyzed. Experimental details are provided in supplemental Methods.

HUVEC WB and PDGF pathway phosphospecific antibody array experiments

HUVECs were incubated in RPMI + 10% FBS or SOX11-positive or SOX11-negative CM for 3 hours, and WB experiments[19] and PDGF pathway phosphospecific antibody array were performed. Experimental details are provided in supplemental Methods.

Custom human quantibody array

SOX11-positive and SOX11-negative CM were incubated in the protein arrays for the quantification of the secreted levels of 8 proangiogenic factors (ANG, ANGPT1, ANGPT2, FGF1, FGF2, PDGFA, PDGFB, and VEGF) according to the manufacturer's protocol (RayBiotech). Experimental details are provided in supplemental Methods.

ChIP and ChIP-qPCR experiments

ChIP was carried out using the HighCell #ChIP kit (Diagenode). Briefly, Z138 and JEKO1 MCL cell lines were fixed and then sonicated with Bioruptor sonicator (Diagenode). SOX11 antibody was used to immunoprecipitate protein-DNA complexes, and after immunoprecipitation, DNA was purified and quantified.

Primers for ChIP-qPCR were designed for SOX11 ChIP-enriched genomic DNA, and SOX11-ChIP DNA and 1:100 diluted input samples were analyzed in duplicate by qRT-PCR regions. Experimental details on ChIP, primers for ChIP-qPCR, and ChIP gene ontology (GO) categories analysis are provided in supplemental Methods.

Reporter plasmid constructs and luciferase assay

The SOX11-binding site to the regulatory region of *PDGFA* gene was amplified, cloned in front of a minimal promoter luciferase reporter vector pGL4.23[*luc2*/minP] (Promega), and used for transient cotransfection experiments and luciferase activity assays in HEK293 cells. Experimental details are provided in supplemental Methods.

In vitro PDGFA inhibition experiments

HUVECs were treated with 1μM imatinib or 10 μg/mL neutralizing antibody against human PDGFR-α (MAB322; R&D Systems) for 1 hour, and resuspended in RPMI + 10% FBS or SOX11-positive or SOX11-negative CM. HUVEC tube formation and migration were studied as previously described. Experimental details are provided in supplemental Methods.

Immunohistochemical staining and MVD quantification

Immunohistochemical staining studies were performed as previously described.[14,20] CD31 or CD34-positive microvessel density (MVD) areas were calculated as the sum of areas of MVD (μm^2) evaluated divided by the total area of the core analyzed (μm^2) as previously described.[21] Experimental details on immunohistochemical staining, antibodies used, and MVD quantification are provided in supplemental Methods.

Statistical analysis

Data are represented as mean ± standard deviation (SD) of 3 independent experiments. Statistical tests were performed using SPSS, v16.0 software (SPSS). Comparison between 2 groups of samples was evaluated by independent sample Student *t* test, and results were considered statistically significant when $P < .05$.

Results

SOX11 induces the expression of proangiogenic factors and promotes angiogenesis in MCL xenograft tumors

To investigate the mechanisms regulated by SOX11 promoting MCL tumor growth, we first compared the GEPs of SOX11-positive and SOX11-knockdown xenograft tumors.[15] GSEA showed that SOX11-positive xenografts were significantly enriched in gene signatures related to tumor angiogenesis among other tumor microenvironment prosurvival signals, including phosphatidylinositol 3-kinase cascade (Figure 1A, Table 1). At the protein level, SOX11-positive xenografts had a significantly increased expression of

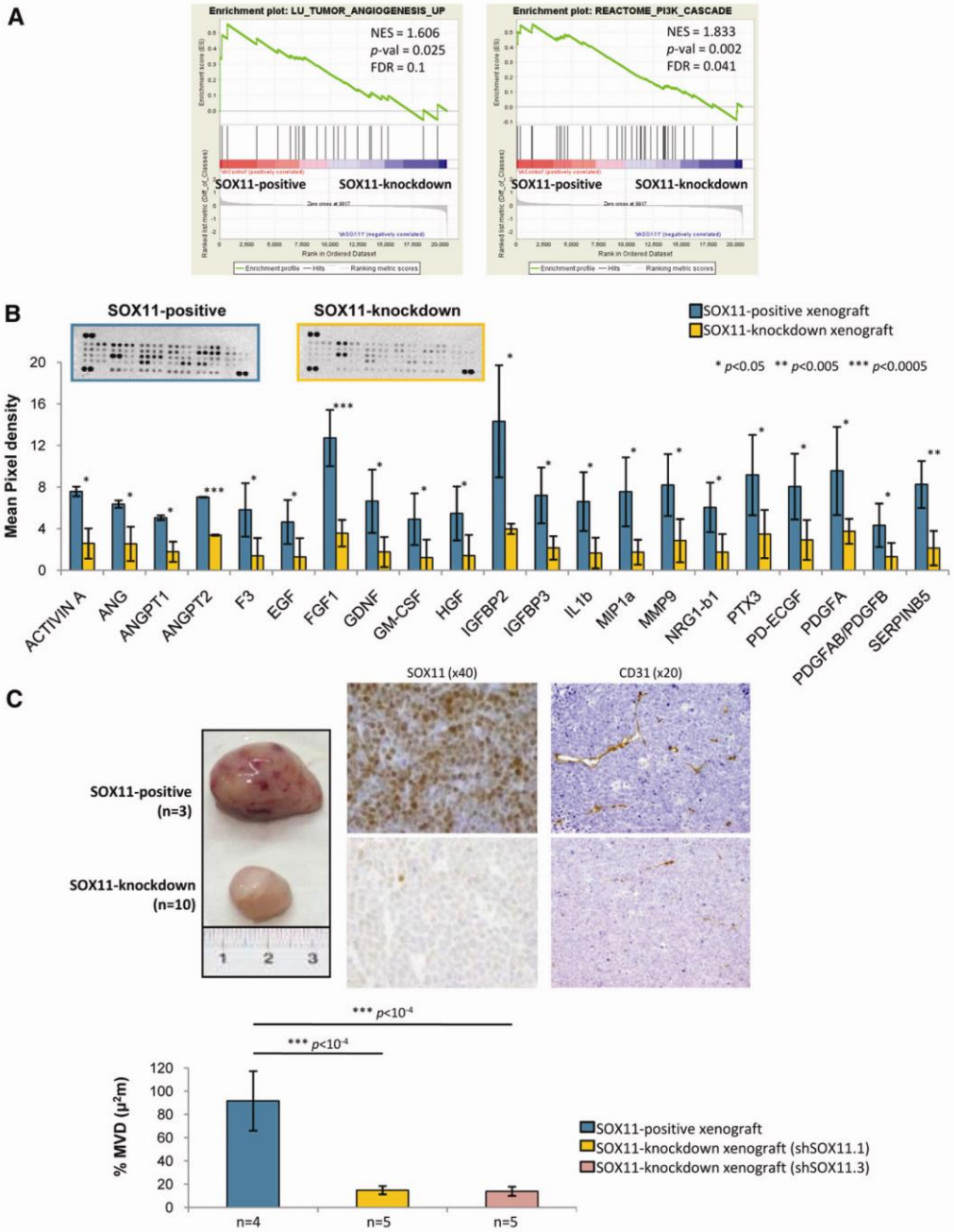

Figure 1. SOX11 induces the expression of proangiogenic factors and promotes angiogenesis in xenograft MCL-derived tumors. (A) GSEA analysis on expression data set from SOX11-positive and SOX11-knockdown xenograft tumors showing enriched gene sets related to angiogenesis pathways. NES, *P*-val, and FDR are represented. Statistical significance is considered when FDR <0.2. (B) Top panel, Representative images showing human-specific angiogenesis antibody array membranes incubated with protein extracts from SOX11-positive (n = 2) and SOX11-knockdown (n = 2) xenograft tissue lysates. Bottom panel, Quantification of the mean pixel densities showing 21 angiogenic proteins significantly upregulated in SOX11-positive compared with SOX11-knockdown xenografts. (C) Top panel, Macroscopic appearance and consecutive histological sections from representative SOX11-positive and SOX11-knockdown xenografts (Z138 shControl, n = 3; shSOX11.1, n = 5; and shSOX11.3, n = 5) stained with a specific antibody anti-human SOX11 (×40) and a specific antibody anti-mouse CD31 (×20). Bottom panel, Density (% of CD31-positive microvessel areas) of CD31-positive MVD areas in SOX11-positive and SOX11-knockdown tumors delineated by the presence of CD31-positive staining. Bar plot represents the mean percentage ± SD. *P*-val are shown. The significance of difference was determined by the independent samples Student *t* test. FDR, false discovery rate; NES, normalized enrichment score; *P*-val, *P* value.

Table 1. Angiogenic gene signatures

Gene set	*P* value		FDR *q* value	Upregulated in class
	NES	Nominal		
Enriched in SOX11-positive (n = 4) vs SOX11-knockdown (n = 10) xenograft tumors				
LU_TUMOR_ANGIOGENESIS_UP	1.606	.025	0.1	Z138 SOX11-positive xenograft tumors
REACTOME_PI_3K_CASCADE	1.833	.002	0.04	Z138 SOX11-positive xenograft tumors
Enriched in leukemic SOX11-expressing (n = 16) vs SOX11-negative (n = 22) MCL primary tumors				
LU_TUMOR_VASCULATURE_UP	1.51	.03	0.12	SOX11-expressing leukemic MCL primary tumors
ANGIOGENESIS	1.51	.02	0.1	SOX11-expressing leukemic MCL primary tumors
VASCULATURE_DEVELOPMENT	1.44	.04	0.18	SOX11-expressing leukemic MCL primary tumors
REGULATION_OF_ANGIOGENESIS	1.44	.04	0.14	SOX11-expressing leukemic MCL primary tumors
LU_TUMOR_ENDOTHELIAL_MARKERS_UP	1.60	.02	0.11	SOX11-expressing leukemic MCL primary tumors
Enriched in SOX11-positive (n = 2) vs SOX11-silenced (n = 4) MCL cell lines				
LU_TUMOR_ANGIOGENESIS_UP	1.646	.01	0.06	Z138 SOX11-positive MCL cell line

GSEA was used to test for significant enrichment of defined gene signatures related to angiogenesis. NES and FDR *P* values are shown and significance is considered when FDR <0.2. Gene signatures were downloaded from the MSigDB, Molecular Signature Database of Broad Institute.

FDR, false discovery rate; NES, normalized enrichment score.

21 proangiogenic factors compared with SOX11-knockdown xenografts including ANG, MMP9, PDGFA, and PDGFAB/PDGFB (Figure 1B). Moreover, SOX11-positive xenografts displayed higher CD31-positive MVD areas than SOX11-knockdown ones (90% ± μm^2 vs 15% ± μm^2, respectively, $P < 1 \times 10^{-4}$) (Figure 1C). Together, these results suggest that SOX11 may facilitate tumor growth by upregulating different proangiogenic factors and enhancing MCL tumor angiogenesis in vivo.

Conditioned media from SOX11-positive cell lines promote in vitro angiogenesis

We next analyzed the effects of the CM derived from SOX11-positive and -silenced MCL cell lines on several angiogenic responses of endothelial cells in vitro. We first performed tube formation assays using cultured HUVECs on Matrigel matrix.[22] As shown in Figure 2A, SOX11-positive CM significantly promoted a prominent increase in tube formation compared with CM from SOX11-negative cells and RPMI + 10% FBS. Conversely, SOX11-negative CM did not have an effect on tube formation compared with RPMI + 10% FBS. Concordantly, HUVECs displayed significantly increased proliferation (Figure 2B) and migration (Figure 2C) toward SOX11-positive CM of the 3 cell lines compared with SOX11-negative CM. We next confirmed that SOX11-positive CM media induced phosphorylation of Akt, FAK, and Erk1/2 compared with SOX11-negative CM or RPMI + 10% FBS whereas basal levels of these proteins did not change (Figure 2D). These results suggest that SOX11-positive CM may contain soluble factors that promote endothelial tube formation, proliferation, migration, and activation of signaling pathways required for angiogenesis.

SOX11 drives transcriptional activation of *PDGFA*

To identify the angiogenic factors expressed and secreted by SOX11-positive cells, we first performed a GSEA of the differential gene expression data sets of our MCL cell lines[15] and observed that, similarly to the xenograft tumors, SOX11-positive cell lines were also enriched in gene signatures related to tumor angiogenesis (Figure 3A, Table 1). We next investigated the expression levels of several angiogenic factors in the protein extracts of SOX11-positive and SOX11-silenced cells. Although the number of proangiogenic proteins differentially expressed between SOX11-positive and SOX11-silenced cell lines was much lower than in the tumor xenograft lysates, SOX11-positive cells still expressed significantly higher levels of the proangiogenic factors Activin A, ANGPT2, PDGFA, and VEGF compared with SOX11-silenced ones (Figure 3B).

To determine whether MCL cells secreted these factors in vitro, we analyzed SOX11-CM using a quantibody angiogenesis array and observed that SOX11-positive CM had significantly increased levels of PDGFA secretion compared with SOX11-negative CM (Figure 3C). No other proangiogenic factors analyzed (PDGFB, ANG, ANGPT1, ANGPT2, VEGF, FGF1, or FGF2) were detected in any MCL CM.

We performed a GO term analysis of our previous genome-wide promoter ChIP-chip study,[15] which showed that blood vessel development was one of the most significant biological processes overrepresented among the SOX11-bound genes (Figure 3D). However, among the proangiogenic factors overexpressed in the SOX11-positive cell lines (Figure 3B), *PDGFA* was the only one identified as a SOX11-bound gene by ChIP experiments, with no significant binding to *Activin A*, *ANGPT2*, or *VEGF* regulatory regions. Following on these results, we validated the specific binding of SOX11 to the regulatory region of *PDGFA* by ChIP-qPCR experiments. We observed a ±twofold and ±fourfold enrichment for *PDGFA* in Z138 and JEKO1, respectively, demonstrating that SOX11 directly binds to regulatory regions of *PDGFA* (Figure 3E).

Luciferase reporter assays with a *PDGFA* regulatory construct encompassing the SOX11 binding site showed a significant threefold induction ($P < 1 \times 10^{-4}$) in luciferase activity upon coexpression of SOX11 but not with an inactive truncated SOX11 protein lacking the High Mobility Group (HMG) domain (ΔHMGSOX11). Similar results were obtained with a *PAX5*-enhancer-luciferase reporter vector,[15] used as a positive control (Figure 3F).

Together, these findings verify the positive transcriptional effect of SOX11 on the *PDGFA* regulatory region and suggest that PDGFA may be the major mediator of angiogenic in SOX11-positive MCLs.

Inhibition of the PDGFA signaling pathway on endothelial cells impairs SOX11-enforced angiogenesis in MCL

To validate the involvement of PDGFA in promoting angiogenesis in MCL, we analyzed the phosphorylation level of endogenous PDGFR-α in HUVECs upon incubation with Z138 SOX11-positive

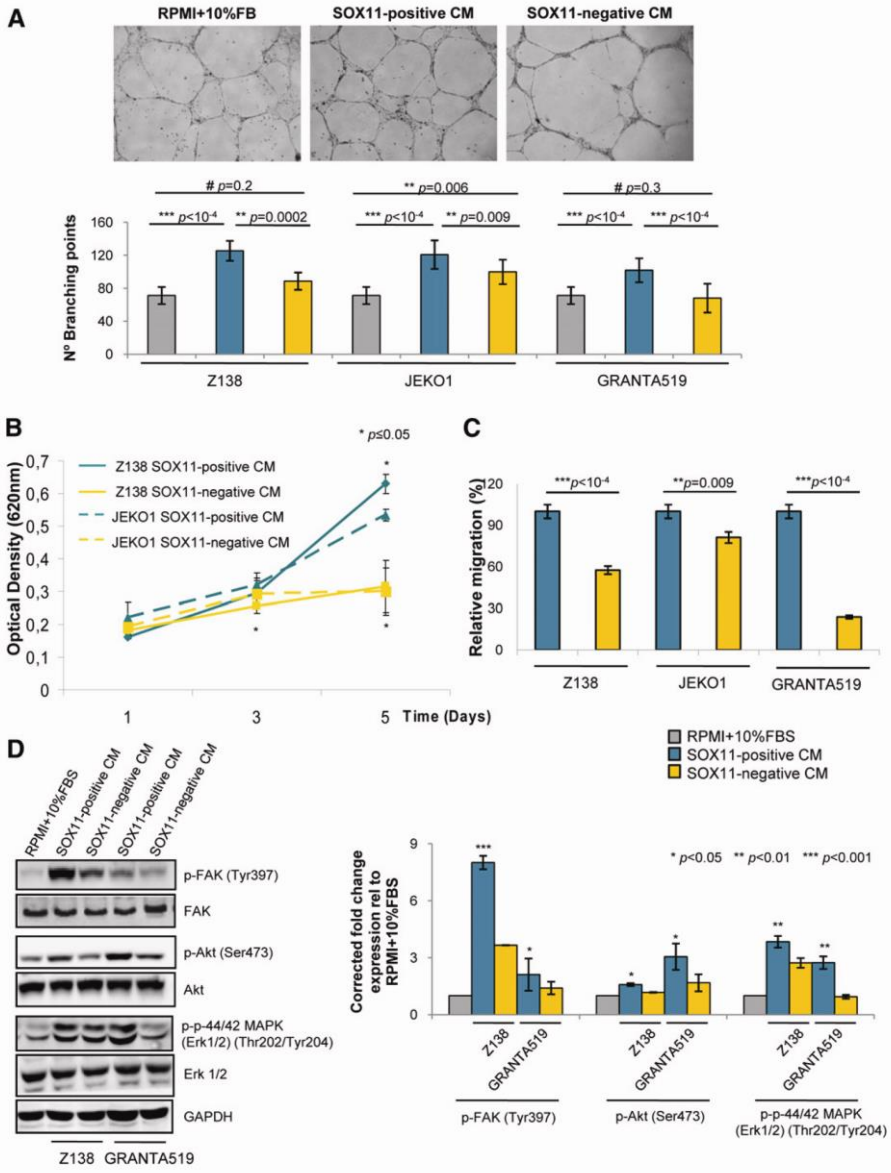

Figure 2. SOX11 promotes endothelial tube formation, cell proliferation and migration, and activation of angiogenic signaling cascades in vitro. (A) Top panel, Representative images showing the capillary tube formation by HUVECs growing on Matrigel matrix for 6 hours in the presence of control RPMI + 10% FBS, SOX11-positive or SOX11-negative CM on Matrigel matrix. Bottom panel, Quantification of the number of branching points representing tube formation by HUVECs cultured for 6 hours in RPMI + 10% FBS or SOX11-positive and SOX11-negative CM from Z138, JEKO1, and GRANTA519 MCL cell lines. SOX11-positive CM significantly promoted a prominent increase in tube formation compared with CM from SOX11-negative cells (126 vs 89 branching points, $P = .0002$, 121 vs 100 branching points, $P = .009$, and 102 vs 70 branching points, $P < 1 \times 10^{-4}$ in Z138, JEKO1, and GRANTA519) and RPMI + 10% FBS (126 vs 76 branching points, $P < 1 \times 10^{-4}$, 121 vs 76 branching points, $P < 1 \times 10^{-4}$, and 102 vs 76 branching points, $P < 1 \times 10^{-4}$ in Z138, JEKO1, and GRANTA519). Conversely, SOX11-negative CM did not have an effect on tube formation compared with RPMI + 10% FBS (89 vs 76 branching points, $P = .2$, 70 vs 76 branching points, $P = .3$ in Z138 and GRANTA519). (B) Kinetics of HUVEC growth in SOX11-positive CM (blue) or SOX11-negative CM (yellow) derived from SOX11-positive and SOX11-silenced Z138 (solid line) and JEKO1 (dashed line) MCL cell lines. Graph showing the optical density (620 nm) after staining the HUVECs with 0.2% crystal violet and measured at 620-nm wavelengths at the indicated time points (1, 3, and 5 days). (C) Graph displaying the percentage of migratory HUVEC cells toward SOX11-positive and SOX11-negative CM from Z138, JEKO1, and GRANTA519 MCL cell lines, relative to the percentage of migratory HUVEC cells toward RPMI + 10% FBS. HUVECs displayed significantly increased migration toward SOX11-positive CM cell lines (±90% migration) compared with SOX11-negative CM (±30%-70% migration, in Z138 and GRANTA519 [$P < 1 \times 10^{-4}$] and JEKO1 [$P = .009$]). (D) Left panel, WB experiments showing expression levels of basal and phosphorylated forms of FAK, Akt, and Erk1/2 proteins in HUVECs cultured in RPMI + 10% FBS or SOX11-positive and SOX11-negative CM from Z138 and GRANTA519 MCL cell lines for 3 hours. GAPDH was used as a loading control. Right panel, Fold change differences of phosphorylated forms of FAK, Akt, and Erk1/2 proteins in HUVECs cultured in RPMI + 10% FBS or SOX11-positive and SOX11-negative CM from Z138 and GRANTA519 MCL cell lines for 3 hours, correlated by quantification of GAPDH expression levels. Bar plot represents the mean percentage ± SD, n = 3. *P*-val is shown. The significance of difference was determined by independent samples Student *t* test. GAPDH, glyceraldehyde-3-phosphate dehydrogenase.

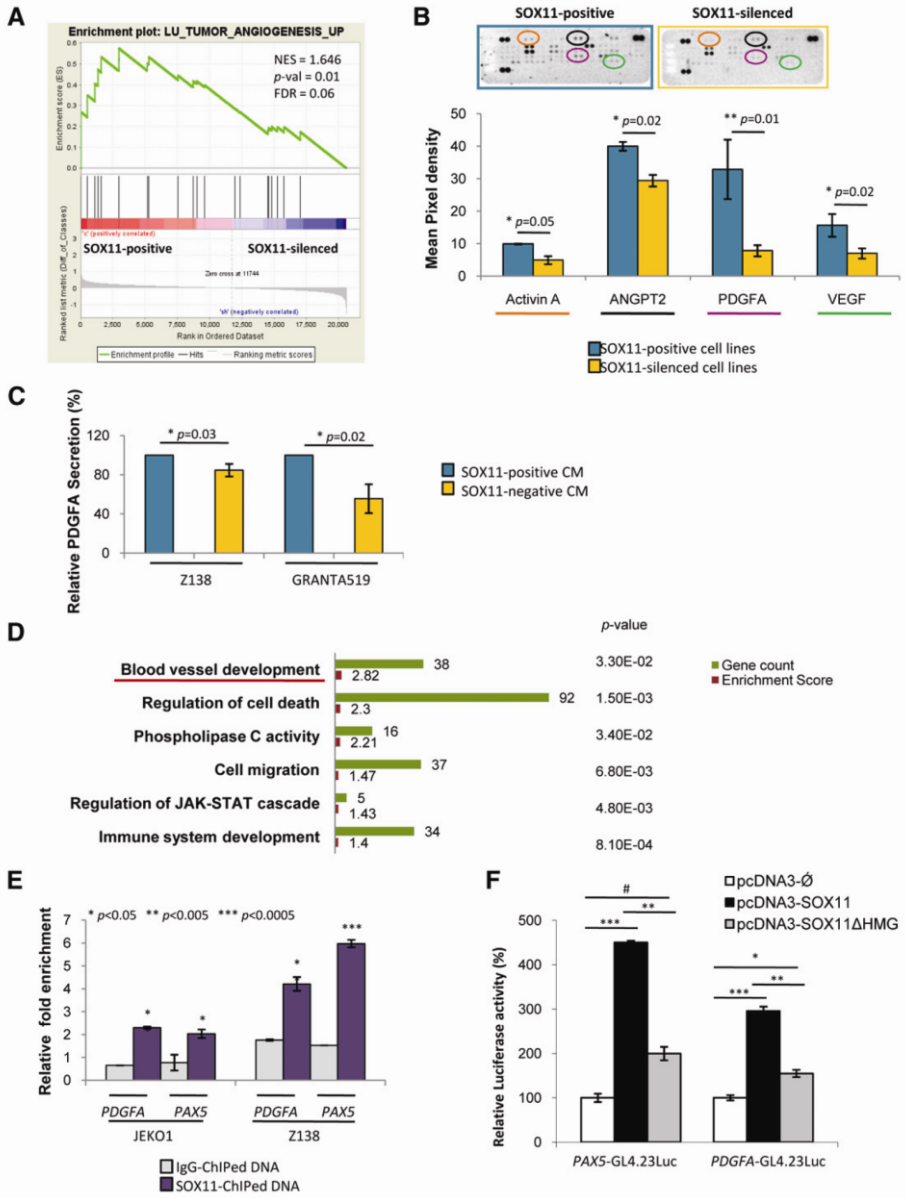

Figure 3. SOX11 binds to regulatory regions of *PDGFA* and positively regulates its transcription. (A) GSEA analysis on expression data set from SOX11-positive and SOX11-silenced MCL cell lines showing enriched gene sets related to angiogenesis pathways. NES, *P*-val, and FDR are represented. Statistical significance is considered when FDR < 0.2. (B) Top panel, Image showing human-specific angiogenesis antibody array membranes incubated with protein lysates from Z138 SOX11-positive (n = 2) and SOX11-silenced (n = 2) MCL cell lines. Bottom panel, Quantification of mean pixel density of the proangiogenic factors Activin A, ANGPT2, PDGFA, and VEGF comparing SOX11-positive and SOX11-silenced MCL cell lines. (C) Graph displaying the relative levels of PDGFA secreted by SOX11-positive and SOX11-silenced CM derived from Z138 and GRANTA519 MCL cell lines. Concentration was analyzed by a quantibody human angiogenesis array. Results are shown as relative percentage of PDGFA secretion compared with SOX11-positive CM. (D) Graph displaying the GO term results obtained from DAVID functional annotation tool of the high confidence SOX11-bound genes identified by ChIP-chip experiments (GSE3502).[15] The 6 most significant biological process GO terms and their gene count, enrichment score, and *P*-val are shown. Underlined is the blood vessel development GO biological term. (E) ChIP-qPCR analysis of specific binding of SOX11 to the regulatory regions of *PDGFA* in JEKO1 and Z138 MCL cell lines. Binding to *PAX5* was used as a positive internal control.[15] Relative DNA enrichment was measured by qPCR using specific primers for the respective regulatory regions (see "Methods"), and is displayed as fold enrichment relative to their respective input chromatin. Purple bars represent ChIP-qPCR enrichment of the SOX11 pull-down (SOX11-ChIPed DNA) while gray bars represent the negative control (IgG-ChIPed DNA). (F) Luciferase assays in transient cotransfections of *PAX5*-GL4.23 Luc and *PDGFA*-GL4.23 Luc with SOX11 full-length (pcDNA3-SOX11) and the truncated SOX11 proteins (pcDNA3-SOX11ΔHMG) expression vectors in HEK293 cells. Results are shown as the percentage of fold induction relative to luciferase activity in cotransfection with the empty vector (pcDNA3-Ø). Bar plot represents the mean percentage ± SD of 3 independent experiments. *P*-val are shown. The significance of difference was determined by independent samples Student *t* test.

RESULTS

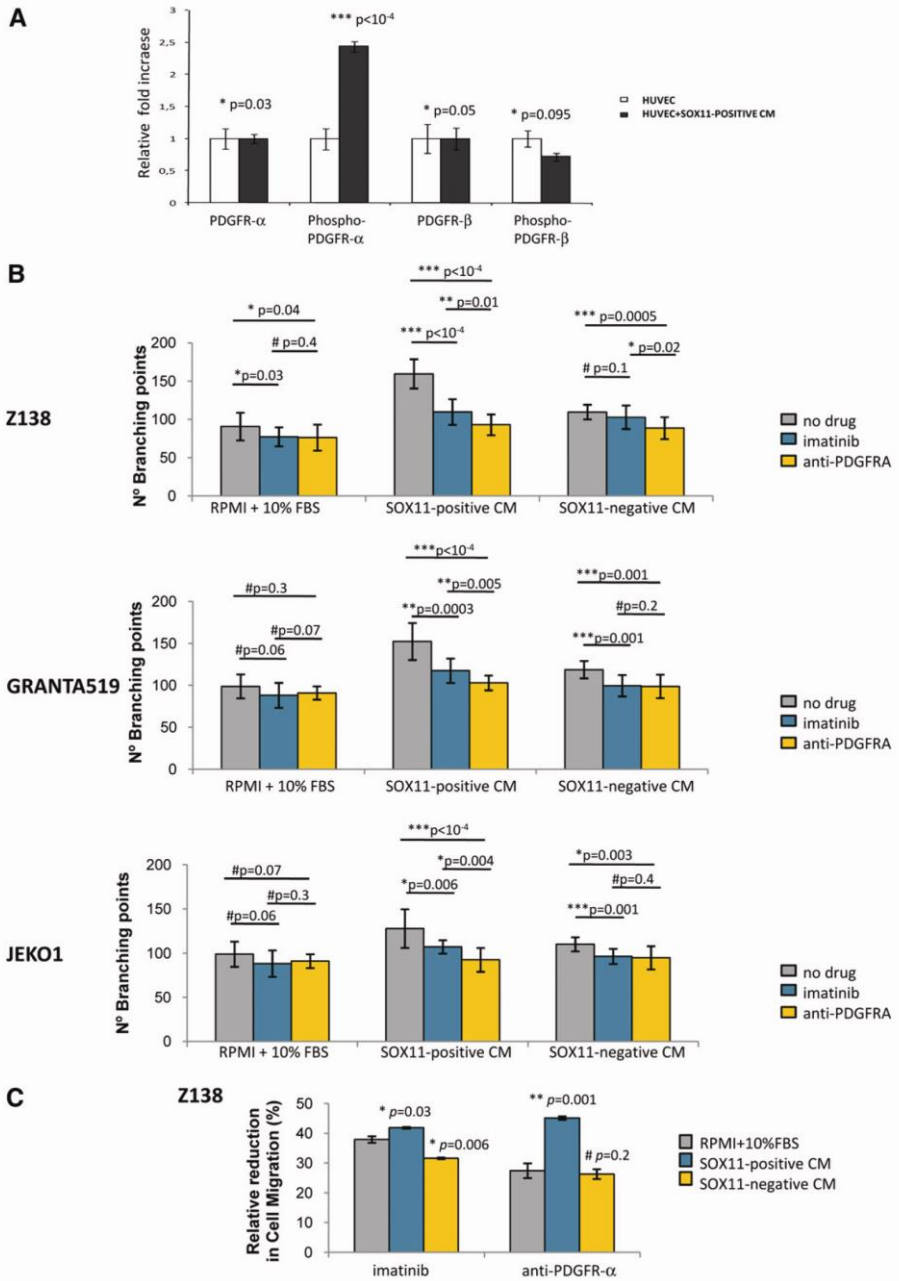

Figure 4. PDGFA inhibition on endothelial cells impairs SOX11-enforced angiogenesis in MCL. (A) Graph showing the relative fold change expression levels of the basal and phosphorylated forms of PDGFRα and PDGFRβ by HUVEC cells upon 3-hour incubation with RPMI + 10% FBS (HUVEC) or Z138 SOX11-positive CM (HUVEC+ SOX11-positive CM). Results are shown as fold increase relative to the corresponding expression levels by the HUVECs incubated with RPMI + 10% FBS. (B) Graphs showing number of branching points representing tube formation by HUVECs. HUVECs were pretreated with control PBS (gray), imatinib (blue), or a neutralizing antibody anti-PDGFRα (yellow) for 1 hour, and then incubated for 6 hours with RPMI + 10% FBS, SOX11-positive or SOX11-negative CM from Z138, GRANTA519, and JEKO1 MCL cell lines. (C) Graph displaying the relative perctage reduction in migration of HUVECs. HUVECs were pretreated with control PBS, imatinib, or a neutralizing antibody anti-PDGFRα for 1 hour, and then allowed to migrate toward RPMI + 10% FBS (gray), SOX11-positive CM (blue) or SOX11-negative CM (yellow) from Z138 MCL cell line. Upon overnight incubation, migratory cells were quantified and represented as the percentage of migration HUVECs compared with no drug (control PBS) treatment. Bar plot represents the mean percentage ± SD of 3 independent experiments. *P*-val are shown. The significance of difference was determined by independent samples Student *t* test.

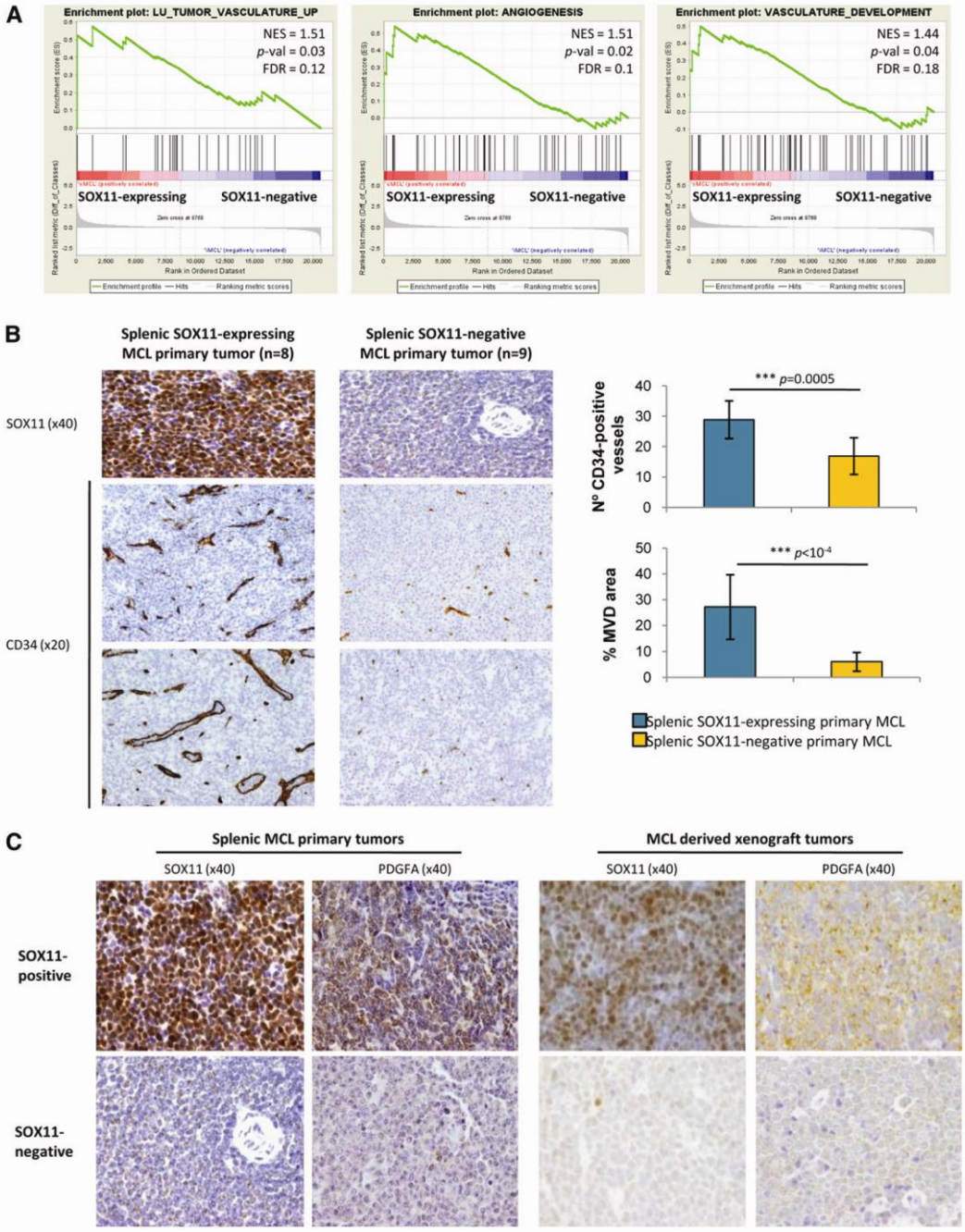

Figure 5. SOX11-positive MCL tumors have increased tumor angiogenesis network and PDGFA overexpression. (A) GSEA analysis on expression data sets from leukemic MCL primary tumors (16 SOX11-expressing and 22 SOX11-negative (GSE36000)[17] showing enriched gene sets related to angiogenesis pathways. NES, *P*-val, and FDR are shown. Statistical significance is considered when FDR < 0.2. (B) Left panel, Histological sections from representative SOX11-expresing (n = 8) and SOX11-negative (n = 9) splenic MCL primary tumors stained with specific antibodies against human SOX11 (×40) and CD34 (×20). Right panel, Graph showing quantification of number of CD34-positive vessels and percentage of CD34-positive MVD areas of the splenic MCL primary tumors. Bar plot represents the mean percentage ± SD. *P*-val are shown. The significance of difference was determined by independent samples *t* test. (C) Representative histological sections from SOX11-positive and SOX11-negative tumors from splenic MCL primary samples (n = 8 and n = 9, respectively) and MCL xenograft tumors (n = 3 and n = 10, respectively) stained with a specific antibody anti-human SOX11 (×40) and PDGFA (×40).

Table 2. Clinical and pathological characteristics of MCL with splenic involvement

	SOX11-negative MCL	SOX11-positive MCL
Patients		
No.	9	8
Median age, y (range)	70 (62-75)	65 (42-89)
Sex		
Male (%)	6 (67)	6 (75)
Female (%)	3 (33)	2 (25)
Histology		
Small cell (%)	4/9 (44)	1/8 (13)
Classic (%)	5/9 (56)	7/8 (87)
Ki67 index, mean ± SD	12.1 ± 9.83	28.63 ± 16.21
Ann Arbor stage		
I/II (%)	0/5 (0)	0/5 (0)
III/IV (%)	5/5 (100)	5/5 (100)
LDH level > normal (%)	2/5 (40)	0/2 (0)
Nodal involvement (%)	2/9 (22)	3/8 (38)
Leukemic involvement (%)	7/7 (100)	4/4 (100)
BM involvement (%)	5/5 (100)	5/5 (100)
Therapy		
Chemotherapy (%)	2/8 (25)	5/6 (83)
Only splenectomy (%)	6/8 (75)	1/6 (17)
Mean survival, mo (range)	96 (76-116)	49 (31-67)

BM, bone marrow; LDH, L-lactate dehydrogenase.

CM. We observed a significant 2.4-fold increase ($P < 1 \times 10^{-4}$) in PDGFR-α but not in PDGFR-β phosphorylation when HUVECs were cultured in Z138 SOX11-positive CM compared with RPMI + 10% FBS (Figure 4A), demonstrating the paracrine activation of the PDGFA/PDGFR-α angiogenic pathway on endothelial cells in MCL. Furthermore, we treated HUVECs with imatinib, a tyrosine kinase inhibitor of PDGFR, or a neutralizing antibody against human PDGFR-α, and then performed tube formation and migration assays in the presence of RPMI + 10% FBS or SOX11-positive CM. The tube formation induced by SOX11-positive CM of Z138, GRANTA519, and JEKO1 was significantly decreased when HUVECs were pretreated with imatinib or the neutralizing PDGFR-α antibody (Figure 4B). Both pretreatments also caused a significant reduction on HUVEC migration toward SOX11-positive CM when compared with no drug treatment (Figure 4C).

To determine whether PDGFR-α was expressed in MCL cells lines and primary tumors, we analyzed its messenger RNA (mRNA) levels in the GEP microarray data of our primary MCL tumors and MCL cell lines using as positive and negative references the previously published data of peripheral T-cell lymphoma (PTCL), a tumor known to express high levels of PDGFR-α, and the GEP of normal mature T cells, a subset of cells known to be negative for this receptor.[23] We confirmed the high levels of PDGFR-α in the PTCL whereas all our primary MCL and MCL cell lines had undetectable levels similarly to normal T lymphocytes (supplemental Figure 1). These findings indicate the lack of expression of PDGFR-α in MCL cells and support the idea that the secreted PDGFA must have a paracrine effect on the endothelial cells rather than an autocrine action on the MCL cells. Altogether, these results demonstrate that the enhanced angiogenic activity of the SOX11-positive CM is mediated by PDGFA expression, and its inhibition impairs SOX11-promoted angiogenic effects on endothelial cells.

Human SOX11-positive primary MCL overexpress PDGFA and have increased angiogenesis

To determine whether SOX11 could be regulating angiogenesis in vivo, we analyzed gene expression signatures of primary human MCL samples. GSEA revealed that SOX11-expressing human primary tumors were also significantly enriched in signatures related to angiogenesis such as tumor vasculature, angiogenesis, vasculature development, regulation of angiogenesis, and tumor endothelial markers (Figure 5A, Table 1). We then analyzed the MVD in an independent series of human MCL primary tumors (Table 2) by staining splenic tissue sections of 8 SOX11-expressing and 9 SOX11-negative tumors for CD31 and CD34. Both antibodies provided similar results with SOX11-positive tumors showing a significantly higher number of vessels than SOX11-negative MCL (±30 microvessels per μm^2 vs ±15 per μm^2, respectively, $P = .0005$) and larger vascular areas (30% ± μm^2 vs 5% ± μm^2, $P < 1 \times 10^{-4}$) (Figure 5B). These results confirm that SOX11 may also promote angiogenesis in primary human MCL.

We next investigated whether PDGFA mRNA was also overexpressed in human primary SOX11-positive MCL using the data of our microarray GEP of 38 primary MCL tumors, 16 SOX11-expressing, and 22 SOX11-negative and found a significant 1.6-fold increased level in SOX11-positive tumors ($P = .0303$) (supplemental Figure 2). Concordantly, high PDGFA expression was immunohistochemically demonstrated on the tumor cells of 8 SOX11-expressing MCL whereas it was not detected in the tumor cells of 9 SOX11-negative tumors. These results were also confirmed in the SOX11-positive and SOX11-negative xenograft tumors (Figure 5C). Therefore, these findings indicate that SOX11 upregulates PDGFA expression in MCL both in vitro and in vivo, mediating the SOX11-enforced angiogenesis that may contribute to the aggressiveness of these tumors.

Imatinib reduces tumor growth and angiogenesis of SOX11-positive MCL xenograft tumors

To demonstrate whether the in vitro inhibitory effect of imatinib on the SOX11-induced angiogenesis may also occur in vivo and, consequently, have an effect on tumor growth, we treated SOX11-positive and SOX11-negative MCL xenografts with imatinib or vehicle PBS and followed tumor growth up. In these experiments, imatinib treatment significantly suppressed tumor growth of the SOX11-positive xenografts compared with vehicle-treated controls (Figure 6A-B) bringing down the growth of SOX11-positive MCL xenograft to that of SOX11-knockdown tumors (Figure 6B).

To determine whether tumor growth reduction upon imatinib treatment was associated with impaired angiogenesis, tumor microvasculature was visualized by histologically staining imatinib- or PBS-treated xenografts with CD31. Compared with PBS treatment, administration of imatinib was strongly associated with a loss of microvasculature in the SOX11-positive xenografts, equaling the number of CD31-positive vessels and MVD areas to those observed in the SOX11-knockdown tumors (Figure 6C), suggesting that the abolishment in MVD was responsible for the tumor reduction observed in the imatinib-treated xenografts. Altogether, these results indicate that PDGFA inhibition could be effective to improve disease outcome of SOX11-positive MCL.

Discussion

Our study shows that increased tumor angiogenesis is a prominent feature of SOX11-positive MCL required for effective tumor growth, and provides evidences to support the inhibition of this mechanism as a new strategy for the management of aggressive MCL patients.

Angiogenesis deregulation is one of the hallmarks of cancer widely investigated in solid malignancies where it has been

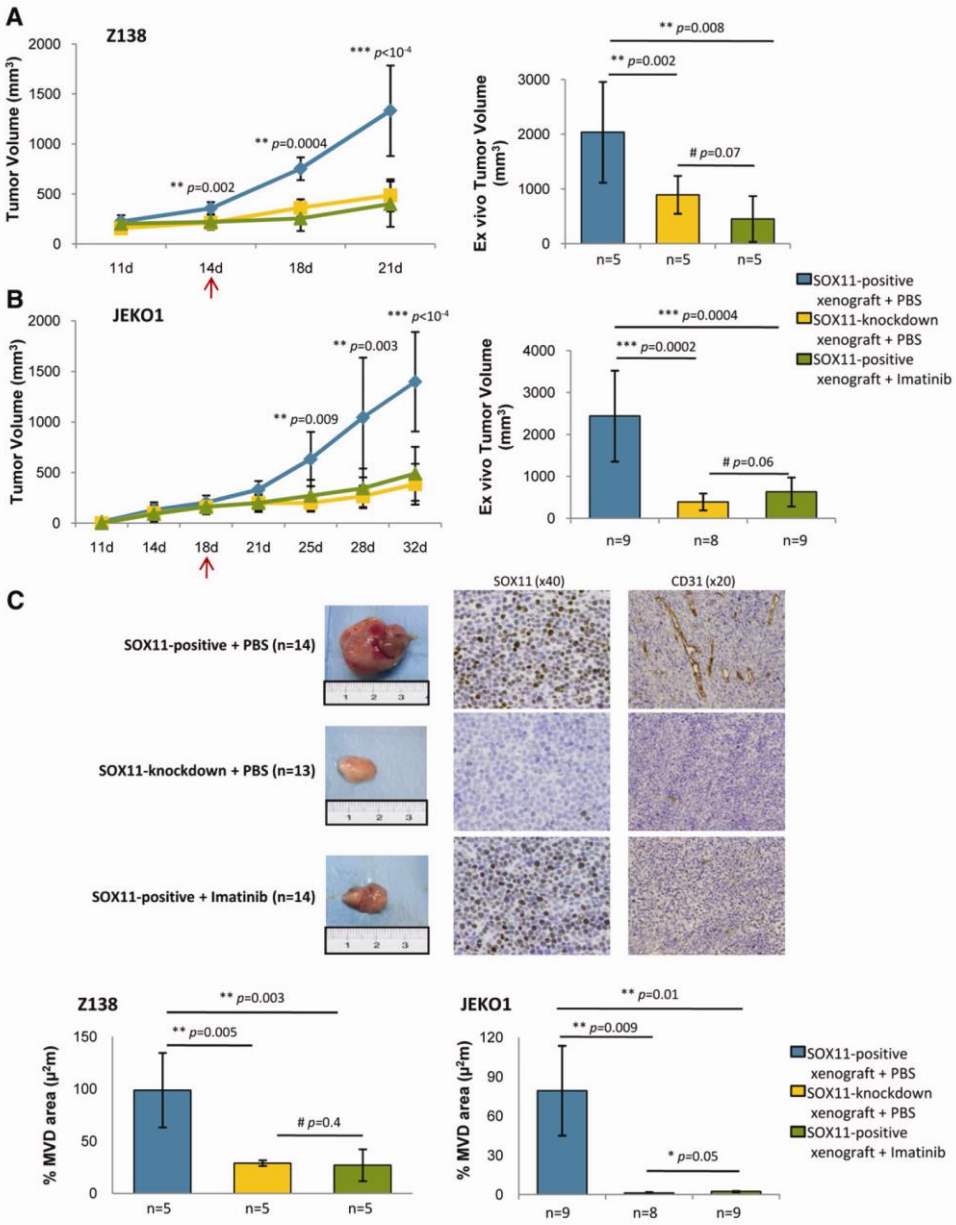

Figure 6. Imatinib reduces MCL tumor growth and angiogenesis of SOX11-positive MCL xenograft tumors. (A-B) Left panel, Tumor growth represented by tumor volumes (mm^3) at the indicated days PI of Z138 and JEKO1 SOX11-positive xenografts treated with IP injections of imatinib (n = 5, n = 9) (green) or vehicle PBS (n = 5, n = 9) (blue) and SOX11-knockdown xenografts treated with IP of vehicle PBS (n = 5, n = 8) (yellow). Right panel, Graph displaying tumor volumes (mm^3) at the time of tissue harvest, comparing imatinib (green) vs vehicle PBS (blue) treated SOX11-positive xenografts and (yellow) vehicle PBS-treated SOX11-knockdown xenografts. Compared with vehicle PBS, imatinib treatment significantly suppressed tumor growth of the SOX11-positive xenografts observed during follow-up (400 mm^3 vs 1330 mm^3, $P < 1 \times 10^{-4}$, and 490 mm^3 vs 1400 mm^3, $P < 1 \times 10^{-4}$ in Z138 and JEKO1, respectively) and ex vivo measurements (450 mm^3 vs 2000 mm^3, $P = .008$, and 630 mm^3 vs 2400 mm^3, $P = .0004$ in Z138 and JEKO1, respectively). (C) Top panel, Macroscopic appearance and consecutive histological sections from representative SOX11-positive (n = 14) and SOX11-knockdown xenograft tumors (n = 13) upon imatinib or vehicle PBS treatment. Immunohistochemical stainings were performed with a specific antibody anti-human SOX11 (×40) and an anti-mouse CD31 (×20). Bottom panel, Graph displaying the percentage of density of CD31-positive MVD areas in Z138 and JEKO1 xenograft tumors in (green) imatinib or (blue) vehicle PBS-treated SOX11-positive xenografts and (yellow) vehicle PBS-treated SOX11-knockdown xenografts, delineated by the presence of CD31-positive staining. Bar plot represents the mean percentage ± SD. *P*-val are shown. The significance of difference was determined by independent sample Student *t* test. PI, postinoculation.

associated with neoplastic growth and progression.[24-26] Recent studies have also revealed the pathogenic relevance and clinical impact of the "angiogenic switch" in lymphoid neoplasms but the mechanisms regulating this phenomenon are not well known.[26,27] In this study, we have shown that the more aggressive SOX11-positive MCL xenografts were enriched in angiogenic gene signatures and displayed much larger microvascular density areas than their SOX11-negative counterparts, concurring with other observations that an increased MVD correlates with disease progression in lymphoid neoplasms.[28,29] We therefore postulated that SOX11-positive MCL cells could promote a pronounced vasculature development and obtain an increased and deregulated blood supply that may contribute to their aggressive progression.

Interestingly, SOX11-positive CM promoted vascular tube formation, endothelial cell proliferation, and migration, and activation of relative angiogenic downstream pathways in HUVECs, indicating that SOX11-positive MCL cells secrete soluble factors that enhance signaling pathways related to cell migration and survival which are known to be activated by PDGFs in other cell types.[30] Concordant with our results, a recent study in zebrafish has reported the involvement of SOX11b, the human ortholog of SOX11, in promoting sprouting angiogenesis of caudal vein plexus.[31]

The gene transcriptional profile of SOX11-positive MCL cell lines was enriched in signatures related to angiogenesis and expressed higher levels of several proangiogenic factors than SOX11-negative ones. On the other hand, the number of proangiogenic factors upregulated in SOX11-positive tumor xenografts was much larger than in the respective cell lines, highlighting the cross-talk between tumor and accessory cells of the microenvironment in the regulation of angiogenesis. Among the proangiogenic factors overexpressed by SOX11-positive MCL cell lines in vitro, we could only detect secreted PDGFA at high levels in their corresponding CM, and *PDGFA* was the only gene directly bound by SOX11 in our ChIP-chip study, strongly supporting the idea that this gene could be one of the main SOX11-dependent factors regulating angiogenesis in MCL.

PDGFA is a member of the PDGF family of proangiogenic factors which may participate in the development of a vascular tumor microenvironment through a direct effect on the endothelium but also indirectly by recruiting mesenchymal stromal cells that release additional angiogenic elements.[32-35] The PDGF family consists of 5 isoforms that exert their cellular effects by binding to PDGFR-α or PDGFR-β with different affinities. PDGFA only binds to PDGFR-α, activating their downstream pathways involved in several oncogenic mechanisms including angiogenesis.[36,37] Several studies have demonstrated that PDGFR-α is expressed by HUVECs and solid tumor endothelial cells,[38,39] and here we demonstrated an increased phosphorylation of PDGFR-α but not PDGFR-β in HUVECs upon SOX11-positive CM incubation. Furthermore, we have demonstrated the activation of AKT, ERK, and FAK upon SOX11-positive CM incubation. The activation of these signaling pathways mediates proliferation, survival, and migration of endothelial responses required by the complex and multistep process of angiogenesis.

Pretreatment of HUVECs with imatinib or a specific neutralizing antibody against PDGFR-α inhibited their tube formation and migration promoted by the SOX11-positive CM. Although imatinib does not specifically target PDGFR kinases,[40-42] the lack of expression of PDGFR-α and the 2 other target kinases c-KIT and BCR-ABL in MCL cell lines and primary tumors indicates that its inhibitory effects on HUVEC angiogenic capacities are due to a blockade of the PDGFA/PDGFR-α angiogenic pathway cascade. The similar inhibitory effects obtained using the specific neutralizing antibody against PDGFR-α corroborate the blockade of the PDGFA/PDGFR-α axis by imatinib impairing HUVEC angiogenic abilities and support the idea that PDGFA promotes angiogenesis in MCL by a direct paracrine effect on endothelial cells.

SOX11-positive primary MCL showed a significant enrichment in angiogenic-related expression signatures and higher MVD than negative tumors. In addition, PDGFA was strongly expressed in SOX11-positive MCL but not detected in negative tumors, strongly supporting that the SOX11-PDGFA–related angiogenic development identified in the experimental models also plays a role in human tumors. SOX11-negative MCL usually present clinically with non-nodal leukemic disease whereas SOX11-positive tumors involve lymph nodes and have extensive extranodal infiltration.[4,5] The SOX11-dependent "angiogenic switch" discovered in this study may explain MCL clinical heterogeneity because the low angiogenic potential of SOX11-negative cells may impair their tissue infiltration and retain them in the bloodstream whereas SOX11-induced angiogenesis facilitates tissue infiltration and growth of the SOX11-expressing MCL cells.

The importance of tumor angiogenesis in the development and clinical progression of lymphoid neoplasias has suggested that these mechanisms may be potential targets for new therapies.[43] Imatinib has proven antiangiogenic effects in a DLBCL xenograft model targeting pericytes via PDGFR-β,[44] and lenalidomide impairs lymphangiogenesis in MCL preclinical models.[45] The striking growth impairment of the SOX11-positive xenografts due to a significant reduction in MVD and an impaired angiogenesis, together with the direct endothelial inhibitory effect of imatinib similar to the anti-PDGFR-α in the in vitro experiments, suggest that angiogenic pathway may represent a novel therapeutic strategy for the treatment of aggressive MCL. However, imatinib treatment may have some limitations in the clinical context since the development of MCL has been observed in 2 patients during treatment of chronic myelogenous leukemia (CML) with this tyrosine kinase inhibitor.[46,47] These 2 MCL cases were "blastoid" variants that had accumulated complex karyotypes including deletions of chromosome 9 (*INK4a*) and *ATM* and *TP53* mutations. These genetic alterations are associated with an angiogenic switch through different mechanisms such as induction of VEGF, HIF-1, and downregulation of thrombospondin-1, respectively.[48-50] Therefore, blastoid tumors may develop angiogenic stimuli alternative to the PDGFA–PDGFR-α axis.

In conclusion, we provide unique evidences on the SOX11-mediatied regulation of angiogenesis via the PDGFA pathway in MCL that in turn facilitates tumor growth. These findings in experimental models and primary human tumors support the oncogenic role of SOX11 in the aggressive behavior of MCL. Targeting the SOX11-PDGFA axis, which regulates the maintenance, migration, and proliferation of vascular endothelial cells, represents an attractive strategy to dismantle the lymphoma vasculature and therefore the growth and progression of this tumor. Modulation of this angiogenic pathway may therefore constitute a potential novel therapeutic strategy for the treatment of aggressive MCL.

Acknowledgments

This work was supported by the Ministerio de Economía y Competitividad (BFU2009-09235, BFU2012-30857, and RYC-2006-002110 [V.A.]), the Fundació La Marató de TV3 (TV3-Cancer-I3/20130110 [V.A.]), and the Instituto de Salud Carlos III (SAF2012-38432 and PIE13/00033 [E.C.] and SAF11/30073 [M.C.C.]). Fondo Europeo de Desarrollo Regional. Unión Europea. Una manera de hacer Europa.

Authorship

Contribution: J.P. performed all of the in vitro and in vivo experiments, and quantified MVD in both xenograft and MCL primary tumors; M.C.V. performed ChIP experiments; M.L.R. performed WB experiments; A.E. performed luciferase assays; G.C. performed statistical analysis; E.P.-R. performed angiogenic experiments in vitro; P.J. performed GEP analysis; I.R.-C. performed immunohistochemistry experiments and quantified MVD in MCL primary tumors; M.C.C. supervised the angiogenic experiments in vitro; E.C. identified morphologically MCL tumors, analyzed data, and supervised experiments; V.A. designed, performed, and supervised experiments, analyzed data, and wrote the manuscript; and all authors discussed the results and commented on the manuscript.

Conflict-of-interest disclosure: The authors declare no competing financial interests.

Correspondence: Virginia Amador, Centre Esther Koplowitz (CEK), C/Rosselló 153, Barcelona-08036, Spain; e-mail: vamador@clinic.ub.es.

References

1. Swerdlow SH, Campo E, Harris NL, et al. *WHO Classification of Tumours of Haematopoietic and Lymphoid Tissues.* Lyon, France: AIRC Press; 2008.
2. Jares P, Colomer D, Campo E. Molecular pathogenesis of mantle cell lymphoma. *J Clin Invest.* 2012;122(10):3416-3423.
3. Orchard J, Garand R, Davis Z, et al. A subset of t(11;14) lymphoma with mantle cell features displays mutated IgVH genes and includes patients with good prognosis, nonnodal disease. *Blood.* 2003;101(12):4975-4981.
4. Fernàndez V, Salamero O, Espinet B, et al. Genomic and gene expression profiling defines indolent forms of mantle cell lymphoma. *Cancer Res.* 2010;70(4):1408-1418.
5. Espinet B, Ferrer A, Bellosillo B, et al. Distinction between asymptomatic monoclonal B-cell lymphocytosis with cyclin D1 overexpression and mantle cell lymphoma: from molecular profiling to flow cytometry. *Clin Cancer Res.* 2014;20(4):1007-1019.
6. Royo C, Navarro A, Clot G, et al. Non-nodal type of mantle cell lymphoma is a specific biological and clinical subgroup of the disease. *Leukemia.* 2012;26(8):1895-1898.
7. Sock E, Rettig SD, Enderich J, Bösl MR, Tamm ER, Wegner M. Gene targeting reveals a widespread role for the high-mobility-group transcription factor Sox11 in tissue remodeling. *Mol Cell Biol.* 2004;24(15):6635-6644.
8. Haslinger A, Schwarz TJ, Covic M, Lie DC. Expression of Sox11 in adult neurogenic niches suggests a stage-specific role in adult neurogenesis. *Eur J Neurosci.* 2009;29(11):2103-2114.
9. Mu L, Berti L, Masserdotti G, et al. SoxC transcription factors are required for neuronal differentiation in adult hippocampal neurogenesis. *J Neurosci.* 2012;32(9):3067-3080.
10. Lin L, Lee VM, Wang Y, et al. Sox11 regulates survival and axonal growth of embryonic sensory neurons. *Dev Dyn.* 2011;240(1):52-64.
11. Weigle B, Ebner R, Temme A, et al. Highly specific overexpression of the transcription factor SOX11 in human malignant gliomas. *Oncol Rep.* 2005;13(1):139-144.
12. de Bont JM, Kros JM, Passier MM, et al. Differential expression and prognostic significance of SOX genes in pediatric medulloblastoma and ependymoma identified by microarray analysis. *Neuro-oncol.* 2008;10(5):648-660.
13. Dictor M, Ek S, Sundberg M, et al. Strong lymphoid nuclear expression of SOX11 transcription factor defines lymphoblastic neoplasms, mantle cell lymphoma and Burkitt's lymphoma. *Haematologica.* 2009;94(11):1563-1568.
14. Mozos A, Royo C, Hartmann E, et al. SOX11 expression is highly specific for mantle cell lymphoma and identifies the cyclin D1-negative subtype. *Haematologica.* 2009;94(11):1555-1562.
15. Vegliante MC, Palomero J, Pérez-Galán P, et al. SOX11 regulates PAX5 expression and blocks terminal B-cell differentiation in aggressive mantle cell lymphoma. *Blood.* 2013;121(12):2175-2185.
16. Salaverria I, Perez-Galan P, Colomer D, Campo E. Mantle cell lymphoma: from pathology and molecular pathogenesis to new therapeutic perspectives. *Haematologica.* 2006;91(1):11-16.
17. Navarro A, Clot G, Royo C, et al. Molecular subsets of mantle cell lymphoma defined by the IGHV mutational status and SOX11 expression have distinct biologic and clinical features. *Cancer Res.* 2012;72(20):5307-5316.
18. Subramanian A, Tamayo P, Mootha VK, et al. Gene set enrichment analysis: a knowledge-based approach for interpreting genome-wide expression profiles. *Proc Natl Acad Sci USA.* 2005;102(43):15545-15550.
19. Vegliante MC, Royo C, Palomero J, et al. Epigenetic activation of SOX11 in lymphoid neoplasms by histone modifications. *PLoS ONE.* 2011;6(6):e21382.
20. Roué G, Pérez-Galán P, Mozos A, et al. The Hsp90 inhibitor IPI-504 overcomes bortezomib resistance in mantle cell lymphoma in vitro and in vivo by down-regulation of the prosurvival ER chaperone BiP/Grp78. *Blood.* 2011;117(4):1270-1279.
21. Cardesa-Salzmann TM, Colomo L, Gutierrez G, et al. High microvessel density determines a poor outcome in patients with diffuse large B-cell lymphoma treated with rituximab plus chemotherapy. *Haematologica.* 2011;96(7):996-1001.
22. Kubota Y, Kleinman HK, Martin GR, Lawley TJ. Role of laminin and basement membrane in the morphological differentiation of human endothelial cells into capillary-like structures. *J Cell Biol.* 1988;107(4):1589-1598.
23. Piccaluga PP, Agostinelli C, Zinzani PL, Baccarani M, Dalla Favera R, Pileri SA. Expression of platelet-derived growth factor receptor alpha in peripheral T-cell lymphoma not otherwise specified. *Lancet Oncol.* 2005;6(6):440.
24. Yancopoulos GD, Davis S, Gale NW, Rudge JS, Wiegand SJ, Holash J. Vascular-specific growth factors and blood vessel formation. *Nature.* 2000;407(6801):242-248.
25. Hanahan D, Weinberg RA. Hallmarks of cancer: the next generation. *Cell.* 2011;144(5):646-674.
26. Baeriswyl V, Christofori G. The angiogenic switch in carcinogenesis. *Semin Cancer Biol.* 2009;19(5):329-337.
27. Lenz G, Wright G, Dave SS, et al; Lymphoma/Leukemia Molecular Profiling Project. Stromal gene signatures in large-B-cell lymphomas. *N Engl J Med.* 2008;359(22):2313-2323.
28. Perry AM, Cardesa-Salzmann TM, Meyer PN, et al. A new biologic prognostic model based on immunohistochemistry predicts survival in patients with diffuse large B-cell lymphoma. *Blood.* 2012;120(11):2290-2296.
29. Korkolopoulou P, Thymara I, Kavantzas N, et al. Angiogenesis in Hodgkin's lymphoma: a morphometric approach in 286 patients with prognostic implications. *Leukemia.* 2005;19(6):894-900.
30. Lozano E, Segarra M, García-Martínez A, Hernández-Rodríguez J, Cid MC. Imatinib mesylate inhibits in vitro and ex vivo biological responses related to vascular occlusion in giant cell arteritis. *Ann Rheum Dis.* 2008;67(11):1581-1588.
31. Schmitt CE, Woolls MJ, Jin SW. Mutant-specific gene expression profiling identifies SRY-related HMG box 11b (SOX11b) as a novel regulator of vascular development in zebrafish. *Mol Cells.* 2013;35(2):166-172.
32. Risau W, Drexler H, Mironov V, et al. Platelet-derived growth factor is angiogenic in vivo. *Growth Factors.* 1992;7(4):261-266.
33. Dong J, Grunstein J, Tejada M, et al. VEGF-null cells require PDGFR alpha signaling-mediated stromal fibroblast recruitment for tumorigenesis. *EMBO J.* 2004;23(14):2800-2810.
34. Ferrara N, Kerbel RS. Angiogenesis as a therapeutic target. *Nature.* 2005;438(7070):967-974.
35. Ding W, Knox TR, Tschumper RC, et al. Platelet-derived growth factor (PDGF)-PDGF receptor interaction activates bone marrow-derived mesenchymal stromal cells derived from chronic lymphocytic leukemia: implications for an angiogenic switch. *Blood.* 2010;116(16):2984-2993.
36. Heldin CH. Targeting the PDGF signaling pathway in tumor treatment. *Cell Commun Signal.* 2013;11:97.
37. Andrae J, Gallini R, Betsholtz C. Role of platelet-derived growth factors in physiology and medicine. *Genes Dev.* 2008;22(10):1276-1312.
38. Gerber DE, Gupta P, Dellinger MT, et al. Stromal platelet-derived growth factor receptor α (PDGFRα) provides a therapeutic target independent of tumor cell PDGFRα expression in lung cancer xenografts. *Mol Cancer Ther.* 2012;11(11):2473-2482.
39. Zhu K, Pan Q, Zhang X, et al. MiR-146a enhances angiogenic activity of endothelial cells in hepatocellular carcinoma by promoting PDGFRA expression. *Carcinogenesis.* 2013;34(9):2071-2079.
40. Goldman JM, Melo JV. Chronic myeloid leukemia—advances in biology and new approaches to treatment. *N Engl J Med.* 2003;349(15):1451-1464.
41. Milojkovic D, Apperley J. Mechanisms of resistance to imatinib and second-generation tyrosine inhibitors in chronic myeloid leukemia. *Clin Cancer Res.* 2009;15(24):7519-7527.

42. Tauchi T, Ohyashiki K. Molecular mechanisms of resistance of leukemia to imatinib mesylate. *Leuk Res.* 2004;28(suppl 1):S39-S45.

43. Ruan J, Hajjar K, Rafii S, Leonard JP. Angiogenesis and antiangiogenic therapy in non-Hodgkin's lymphoma. *Ann Oncol.* 2009;20(3): 413-424.

44. Ruan J, Luo M, Wang C, et al. Imatinib disrupts lymphoma angiogenesis by targeting vascular pericytes. *Blood.* 2013;121(26):5192-5202.

45. Song K, Herzog BH, Sheng M, et al. Lenalidomide inhibits lymphangiogenesis in preclinical models of mantle cell lymphoma [published correction appears in *Cancer Res.* 2014;74(4):1284]. *Cancer Res.* 2013;73(24):7254-7264.

46. Garzia M, Sora F, Teofili L, et al. Blastoid mantle cell lymphoma occurring in a patient in complete remission of chronic myelogenous leukemia. *Lab Hematol.* 2007;13(1):30-33.

47. Rodler E, Welborn J, Hatcher S, et al. Blastic mantle cell lymphoma developing concurrently in a patient with chronic myelogenous leukemia and a review of the literature. *Am J Hematol.* 2004; 75(4):231-238.

48. Zhang J, Lu A, Li L, Yue J, Lu Y. p16 Modulates VEGF expression via its interaction with HIF-1alpha in breast cancer cells. *Cancer Invest.* 2010;28(6): 588-597.

49. Ousset M, Bouquet F, Fallone F, et al. Loss of ATM positively regulates the expression of hypoxia inducible factor 1 (HIF-1) through oxidative stress: Role in the physiopathology of the disease. *Cell Cycle.* 2010;9(14): 2814-2822.

50. Grossfeld GD, Ginsberg DA, Stein JP, et al. Thrombospondin-1 expression in bladder cancer: association with p53 alterations, tumor angiogenesis, and tumor progression. *J Natl Cancer Inst.* 1997;89(3):219-227.

SUPPLEMENTAL INFORMANTION

SOX11 PROMOTES TUMOR ANGIOGENESIS THROUGH TRANSCRIPTIONAL REGULATION OF PDGFA IN MANTLE CELL LYMPHOMA

Jara Palomero *et al.*

SUPPLEMENTAL METHODS

Cell culture

MCL cell lines Z138 (CRL-3001, ATCC) and JEKO1 (CRL-3006, ATCC) were cultured in RPMI 1640 medium (Sigma-Aldrich, St Louis, MO), supplemented with 10% fetal bovine serum (FBS; Sigma-Aldrich,), 2µM L-glutamine (Lonza, Allendale, NJ), 100U/mL penicillin, and 100µg/mL streptomycin (Gibco, Life Technologies, Carlsbad, CA). GRANTA519 MCL cell line (ACC-342, DSMZ) was cultured in DMEM medium (Sigma-Aldrich), supplemented with 10% FBS, 2µM L-glutamine, 100U/mL penicillin, and 100µg/mL streptomycin.

HUVEC were obtained from freshly delivered umbilical cords as previously described[1] and were grown in HUVEC medium containing RPMI 1640 medium, supplemented with 20% defined bovine calf serum (BCS; Thermo Scientific, Waltham, MA), 100mg endothelial cell growth supplement (ECGS; BD Biosciences, Franklin Lakes, NJ), 2500U sodium heparin (Fisher BioReagents, Waltham, MA), 2mM glutamine, 100U/mL penicillin/streptomycin, 500µg/mL gentamicin (Invitrogen, Life Technologies) and 2.5µg/mL Fungizone (amphotericin B) (Sigma-Aldrich).

All human leukemic primary tumors were highly purified MCL cells (>95% as determined by flow cytometry) and carried the t(11;14) and/or expressed cyclin D1. All these cases together with the splenic primary tumors were diagnosed according to previous defined criteria;[2,3] and their SOX11 expression levels were quantified by qRT-PCR.[4]

All samples were obtained from the Hospital Clínic Biobank-tumor Bank (Barcelona, Spain). The study was approved by the Institutional Review Board of the Hospital Clínic, Barcelona, Spain (Hospital Clínic de Barcelona Ethics Institutional

Review Board). Written informed consent was obtained from all participants and the Ethics Committee approved this consent procedure.

SOX11 silencing by lentiviral infection

SOX11 knockdown stable MCL cell lines were generated by lentiviral transduction of PLKO1-puro-shSOX11 and PLKO1-puro-scramble constructs in Z138, JEKO1 and GRANTA519 as previously described,[5] generating SOX11-positive and -silenced MCL cell lines (shControl, shSOX11.1 and shSOX11.3, respectively).

RNA extraction and Gene Expression Profiling (GEP)

20 Tissue-Tek OCT (Sakura, Torrance, CA) frozen 15µm-cryostat xenograft tissue sections were obtained for RNA extraction. Total RNA of SOX11-positive and -knockdown derived xenograft tumors (Z138 shControl (n=4), shSOX11.1 (n=5) and shSOX11.3 (n=5)) was extracted with the TRIzol reagent following the manufacturer's recommendations (Invitrogen, Life Technologies). RNA integrity was examined with the Agilent 2100 Bioanalyser (Agilent Technologies, Palo Alto, CA) and hybridized to HG-U133plus2.0 GeneChips (Affymetrix, Santa Clara, CA) according to Affymetrix standard protocols. The hybridized arrays were scanned. The analysis of the scanned images and the determination of the signal value for each probe set of the array were obtained with GeneChip® Command Console® Software (AGCC) (Affymetrix). Raw data were imported to R Statistical Package (http://www.r-project.org/) for analysis and data were normalized using the Robust Multichip Analysis (RMA) algorithm of the BioConductor affy Package and genes with p-val>0.01 were excluded. Differential gene expression between SOX11-positive and -knockdown derived xenograft tumors was determined using moderated t-statistics with empirical Bayes shrinkage of the standard

errors implemented in the BioConductor limma Package.[6] The FDR controlling method of Benjamini and Hochberg was used to adjust the *p*-val for each gene based on a significance level of 0.01 and log2 FC>1.3.

Gene Set Enrichment Analysis (GSEA)

To identify oncogenic pathways related to SOX11 high expression in MCL, we also performed GSEA on expression datasets derived from MCL primary tumors, *in vitro* SOX11 silencing experiments and xenograft MCL tumors. To assess statistical significance, we randomized our expression datasets, previously normalized with RMA, by permuting gene sets 1000 times and considered only gene sets with a *p*-value<0.05. We investigated enrichment of gene sets related to angiogenesis (downloaded from the MSigDB, Molecular Signature Database of Broad Institute) in two phenotype labels according to SOX11 expression (SOX11-expressing or -negative leukemic MCL primary tumors, SOX11-positive and -silenced Z138 MCL cell line and SOX11-positive and -knockdown derived xenograft tumors). Data were analyzed using GSEA across the complete list of genes ranked by Diff_of_classes.

Protein extraction

Total protein lysate from Z138 SOX11-positive and -silenced MCL cell lines was extracted with RIPA buffer (Sigma-Aldrich) as previously described.[5]

Total protein lysate from Z138 SOX11-positive and -knockdown xenograft tumors was obtained using T-PER tissue protein extraction reagent (Thermo Fisher Scientific). Briefly, 20 OCT frozen 15µm-cryostat xenograft tissue sections were resuspended in T-PER buffer and incubated on ice for 5min. After vortexing, samples

were incubated on ice for 1h. Tubes were then centrifuged at 12000rpm for 15 min, and total protein from tissue sections was quantified as previously described.[5]

Both total protein lysates derived from MCL cell lines and xenograft tumors were used for angiogenesis proteome profiler antibody array experiments.

Angiogenesis proteome profiler antibody array

100µg of total protein extract from SOX11-positive and -silenced MCL cell lines (Z138shControl and Z138shSOX11, respectively) and from tissue lysates derived from SOX11-positive and -knockdown derived xenograft tumors (Z138shControl and Z138shSOX11, respectively) were used to study the human angiogenesis proteome profiler antibody array (R&D Systems, Minneapolis, MN) following manufacturer's protocol. Membranes were exposed 1-10min, and mean pixel density images were obtained with ImageQuant LAS4000 (Fujifilm, Tokyo, Japan) and quantified with MultiGauge Software (Fujifilm).

HUVEC tube formation assay on Matrigel matrix

300µL of Matrigel basement membrane matrix (Becton Dickinson, San Jose, CA) were added to 24-well plate and were incubated for 45min at 37ºC. 500µL of RPMI+10%FBS or SOX11-positive or -negative conditioned media (CM) obtained from the supernatants derived from SOX11-positive and -silenced MCL cell lines growing *in vitro* (Z138, JEKO1 and GRANTA519 shControl and shSOX11, respectively) were added on top of the polymerized Matrigel matrix. After O/N serum starvation, $6x10^4$ HUVEC were resuspended and plated on top of the corresponding medium of the 24-well plate. Plates were incubated at 37ºC and 5%CO_2 and after 6h, images were acquired using Leica DFC 295 (LEICA, Solms, Germany). Number of

tubes were analyzed with LAS V3.7 software (LEICA) for each of the different media tested counting the number of branching points.

HUVEC proliferation assay

Confluent HUVECs were plated in flat-bottom 96-well plates at 10000 cells/well and incubated at 37° C in 5% CO_2 for 1 to 5 days with 1:2 diluted HUVEC complete growth medium supplemented with SOX11-positive or -negative CM derived from SOX11-positive and -silenced MCL cell lines growing *in vitro* (Z138 and JEKO1 shControl and shSOX11, respectively). At several time-points, cells were fixed and stained with 0.2% crystal violet (Sigma-Aldrich, Madrid, Spain) in 20% methanol for 20 min. Wells were washed, air-dried, and solubilized in 1% sodium dodecyl sulfate (SDS). Optical density was measured with a plate reader (Multiskan Ascent, Thermo Scientific) at 620 nm wavelength. Quadruplicates of each conditioned was performed and statistical analysis was done using Mann Whitney test.

HUVEC migration assay

0.5-1x10^6 cells/mL HUVEC were serum starved O/N, and 300µL of the cell suspension solution was added to the inside of each insert. 500µL of RPMI+10%FBS or SOX11-positive or -negative CM obtained from the supernatants derived from SOX11-positive and -silenced MCL cell lines growing *in vitro* (Z138shControl and shSOX11, respectively) were added to the lower well of the Cytoselect™ 24-well cell migration plate (Cell Biolabs, San Diego, CA). Upon O/N incubation, migratory cells were analyzed following manufacturer's recommendations and quantified measuring the OD at 560nm using Gen5 1.10 software, Synergy HT (BioTeK).

HUVEC WB experiments

After O/N serum starvation, HUVEC were incubated for 3h in RPMI+10%FBS or SOX11-positive or -negative CM obtained from the supernatants derived from SOX11-positive and -silenced MCL cell lines growing *in vitro* (Z138 and GRANTA519 shControl and shSOX11, respectively). HUVEC were then lysed and protein extraction and WB experiments were performed as previously described[7] using antibodies against human ERK1/2 (Cell Signaling Technology, Danvers, MA; 9102), Akt (Santa Cruz Biotechnology, Santa Cruz, CA; C20), FAK (Santa Cruz Biotechnology, C20), p-Akt (Ser473) (D9E), p-FAK (Tyr397) (D20B1), p-p38 MAPK (Thr180/Tyr182) (D3F9), p-p44/42 MAPK (Erk1/2) (Thr202/Tyr204) (D13.14.4E) and p-PLCγ1 (Ser1248) (D49G4) all from Cell Signaling Technology. GAPDH (Santa Cruz Biotechnology, A-3) and α-tubulin (Oncogene, Uniondale, NY; CP06-100UG) were used as loading control. Membranes were developed with chemiluminescence substrate Pierce® ELC Western blotting substrate (Thermo Fisher Scientific) and visualized on a LAS4000 device. Protein quantification was done with Image Gauge software (Fujifilm).

Custom human quantibody array

SOX11-positive and -negative CM derived from the supernatants of SOX11-positive and -silenced MCL cell lines (Z138 and GRANTA519 shControl and shSOX11, respectively) were harvested and incubated in the protein arrays for the quantification of the secreted levels of eight pro-angiogenic factors according to manufacturer's protocol (RayBiotech, Norcoss, GA). Custom human quantibody array was designed for the quantitative measurement of the secreted levels of the pro-angiogenic factors ANG, Ang1, Ang2, aFGF, bFGF, PDGFA, PDGFB and VEGF. Manufacturer's protocol was carried out, glass chip arrays were analyzed and data

extracted using the microarray software GenePix4000B (Molecular Devices, Sunnyvale, CA). The quantitative analysis of the eight pro-angiogenic factors secreted in the SOX11-positive and -negative conditioned media was done using the Quantibody® Q-Analyzer software (RayBiotech).

Chromatin Immunoprecipitation (ChIP) and ChIP-quantitative-PCR (ChIP-qPCR)

ChIP was carried out using HighCell #ChIP kit (Diagenode, Liège, Belguim). Briefly, $80x10^6$ fixed Z138 and JEKO1 MCL cell lines were lysed with Shearing Buffer S1 and sonicated on ice with Biorupter™ sonicator from Diagenode (3 cycles of 10min [40 seconds "ON"/ 20 seconds "OFF"]). Sonicated chromatin was incubated overnight (O/N) with 10µg of SOX11 antibody (sc-17347; Santa Cruz Biotechnology) and then with Protein G-coated magnetic beads for 6h. After immunoprecipitation, beads were washed and DNA was eluted and decrosslinked O/N at 65ºC. DNA was eluted and purified with IPure kit (Diagenode) and quantified with Qubit ® 2.0 Fluorometer (Invitrogen Life technologies).

Primers for ChIP-qPCR were designed for SOX11 ChIP-enriched genomic DNA regions using Primer3 (http://frodo.wi.mit.edu/) (**PDGFA:** Forward 5'-GGACAGTGCGACGGTATTTT-3' and Reverse 5'-GGGAGAAACACAAAGCCAGA-3') and (**PAX5** Forward 5'-TAATCCTCTGCCCTTCATGG-3' and Reverse 5'-TGTTGCCTTAGGGAATTTCG-3'). SOX11-ChIP DNA and 1:100 diluted input samples were analyzed in duplicate by qRT-PCR using Fast SYBR ®Green Master Mix in a StepOnePlus PCR detection system (Applied Biosystems, Foster City, CA).

We used DAVID (The Database for Annotation, Visualization and Integrated Discovery) Bioinformatic Resources (http://david.abcc.ncifcrf.gov/) to determine the statistically overrepresented GO categories within the identified SOX11 target genes by ChIP-chip across three replicates of Z138 MCL cell line.[5] This analysis yielded 1909 high confidence genes bound by SOX11.

Reporter plasmid constructs and luciferase assay

The SOX11-binding site from the regulatory region of *PDGFA* gene was amplified by PCR using GRANTA519 genomic DNA and primers (F 5'-CCGCTCGAGGTGCGGTCTTTGTTCTCCTC-3' and R 5'-GAAGATCTGGCACACCAACAACACAGAC-3'). Subsequently, the PCR fragment was cloned in front of a minimal promoter luciferase reporter vector pGL4.23[*luc2*/minP] (Promega, Leiden, The Netherlands). Constructs were sequenced using internal primers prior to use. *PAX5 enhancer*-PGL4.23[*luc2*/minP] luciferase reporter vector[5] was used as a positive control for SOX11-dependent activation of the luciferase activity.

Lipofectamine 2000 system (Invitrogen Life Technologies) was used for transient cotransfection experiments in HEK293 cells, following the manufacturer's instructions. Co-transfected HEK293 cells were harvested and luciferase activity was measured 24h after transfection with Dual-Glo® Luciferase Assay System (Promega) and a Modulus microplate luminometer (Turner BioSystems, Promega). All assays were performed in triplicate on separated days.

PDGF Pathway Phospho-Specific Antibody Array

After O/N serum starvation, HUVEC were incubated for 3h in Z138 SOX11-positive CM or RPMI+10%FBS. HUVEC were then lysed and protein extraction and PDGF pathway phospho-specific antibody microarray were carried out following manufacturer's protocol (Full Moon Biosystems, Sunnyvale, CA). Arrays were analyzed and data extracted using the microarray software GenePix4000B (Molecular Devices). The quantitative analysis of the basal and phosphorylated forms of PDGFR-α and PDGFR-β by HUVEC cells upon 3h incubation with RPMI+10%FBS or Z138 SOX11-positive CM was done using the Quantibody® Q-Analyzer software (RayBiotech). The levels of basal and phosphorylated forms in each condition were corrected by the corresponding expression levels of the array's positive control and represented as fold induction relative to the corresponding expression levels by HUVEC incubated with RPMI+10%FBS.

***In vitro* PDGFA inhibition experiments**

After O/N serum starvation, HUVEC were treated with 1μM imatinib (LC Laboratories, Woburn, MA) or 10μg/mL neutralizing antibody against human PDGFRα (R&D Systems, MAB322) at 37ºC and 5%CO_2 for 1h. After this incubation, cells were washed and resuspended in RPMI+10%FBS or SOX11-positive or -negative CM derived from SOX11-positive and -silenced MCL cell lines growing *in vitro* (Z138, JEKO1 and GRANTA519 shControl and shSOX11, respectively). HUVEC were then used for tube formation assays on Matrigel matrix after 6h of incubation, and for migration assays after O/N incubation in the corresponding media as previously described.

Immunohistochemical staining and MVD quantification

Immunohistochemical staining studies were performed with the use of antibodies against human anti SOX11 (Atlas Antibodies, Stockholm, Sweden; HPA000536), PDGFA (Santa Cruz Biotechnology, N-30), mouse and human anti CD31 (Santa Cruz Biotechnology, M20) and CD34 (DAKO, Glostrup, Denmark; QBEnd 10). Preparations were evaluated with an Olympus BX51 microscope by means of a 20×/0.75 NA objective and DPManager software v2.1.1 (Olympus, Tokyo, Japan). Three representative fields from each staining were counted for the presence of positive cells.

MVD areas were quantified using the digitalized images of CD31 or CD34-positive microvessel immunohistochemical staining, acquired with an Olympus BX51 microscope at x20 magnification, and analyzed with an Olympus Cell B Basic Imaging Software (Olympus). MVD areas were delineated by CD31 or CD34-positive vessels, and calculated as the sum of number of microvessels or areas of microvessel density (μm^2) evaluated divided by the total area of the core analyzed (μm^2).

SUPPLEMENTAL FIGURES

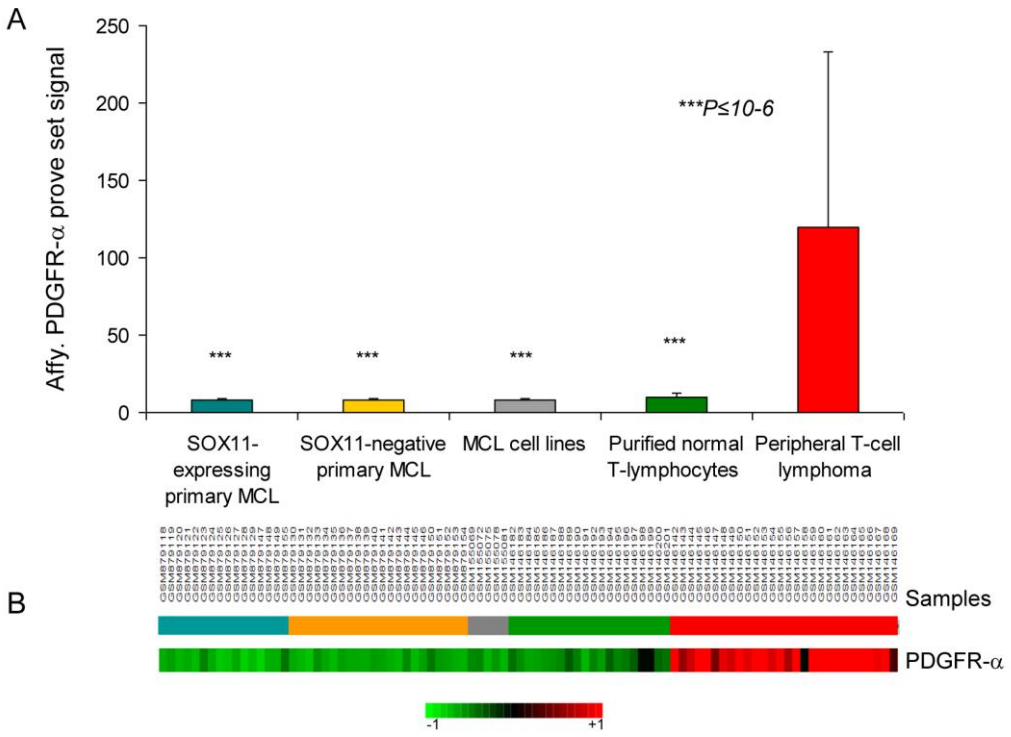

Supplemental Figure S1. PDGFR-α is not expressed in MCL cells.

A) Average levels of the PDGFR-α prove set signals obtained from the analysis of Affymetrix HG-U133 2.0 plus microarrays from our 38 primary MCL tumors (16 SOX11-expressing and 22 SOX11-negative) (GSE36000)[8] and five well defined MCL cell lines (GRANTA519, REC1, UPN1, HBL2 and JEKO1) (GSE6728).[9] We have used as positive and negative control the published gene expression profiling (GEP) of 28 peripheral T-cell lymphoma (PTCL), a tumor known to express high levels of PDGFR-α, and the GEP of normal mature T-cells, a subset of cells previously shown to be negative for this receptor (GSE6338).[10,11]

Both our MCL GEP and Piccaluga GE studies were obtained with the same platform (Affymetrix HG-U133 2.0 plus microarrays) and after normalizing all data, we

confirmed the high levels of PDGFR-α in the PTCL whereas all our primary MCL and MCL cell lines had undetectable levels similarly to normal T-lymphocytes (fold change around -16 and -14; respectively, $p \leq 10^{-6}$). These findings support the lack of expression of PDGFR-α in MCL cells.

B) Heat map illustrating PDGFR-α expression in primary MCL tumors, MCL cell lines, purified T-cell lymphocytes and primary PTCL tumors.

Red indicates increased expression and green decreased expression relative to the median expression levels accordingly to the color scale shown.

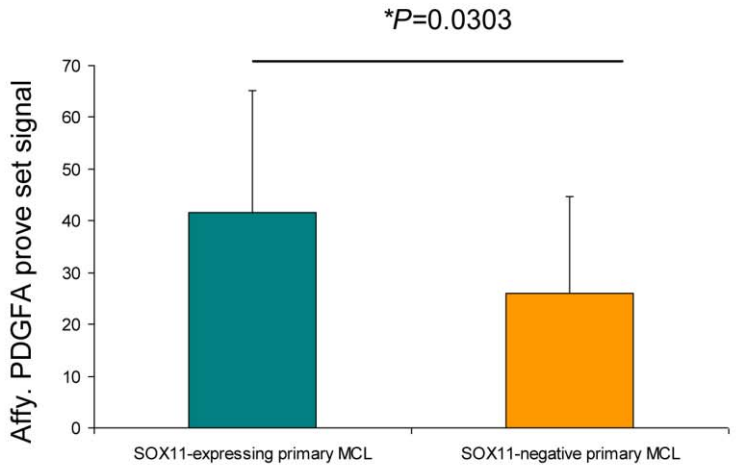

Supplemental Figure S2. SOX11-expressing MCL significantly express higher levels of PDGFA than SOX11-negative MCL primary tumors. Average levels of PDGFA prove set signals obtained from the analysis of Affymetrix HG-U133 2.0 plus microarrays from our 38 primary MCL tumors (16 SOX11-expressing and 22 SOX11-negative) (GSE36000).[8] We found a significant 1.6 fold increased level of PDGFA in SOX11-expressing MCL primary cases compared to SOX11-negative MCL ones (p=0.0303).

SUPPLEMENTAL REFERENCES

1. Kleinman HK, Cid MC. Preparation of endothelial cells. *Curr Protoc Cell Biol* 2001;Chapter 2,Unit 2.3.
2. Swerdlow SH, Campo E, Harris NL, et al. WHO Classification of Tumours of Haematopoietic and Lymphoid Tissues. *AIRC Press*, *Lyon France.* 2008.
3. Fernàndez V, Salamero O, Espinet B, et al. Genomic and gene expression profiling defines indolent forms of mantle cell lymphoma. *Cancer Res* 2010;**70**(4):1408-18.
4. Royo C, Navarro A, Clot G, et al. Non-nodal type of mantle cell lymphoma is a specific biological and clinical subgroup of the disease. *Leukemia* 2012;**26**(8):1895-8.
5. Vegliante MC, Palomero J, Pérez-Galán P, et al. SOX11 regulates PAX5 expression and blocks terminal B-cell differentiation in aggressive mantle cell lymphoma. *Blood* 2013;**121**(12):2175-85.
6. Smyth, G.K. Linear models and empirical bayes methods for assessing differential expression in microarray experiments. *Stat Appl Genet Mol Bio.* 2004;3,Article3.
7. Vegliante MC, Royo C, Palomero J. Epigenetic activation of SOX11 in lymphoid neoplasms by histone modifications. *PLoS One* 2011;**6**(6):e21382.
8. Navarro A, Clot G, Royo C, et al. Molecular subsets of mantle cell lymphoma defined by the IGHV mutational status and SOX11 expression have distinct biological and clinical features. *Cancer Res* 2012;**72**(20):5307-16.
9. Pinyol M, Bea S, Plà L, Ribrag V, Bosq J, Rosenwald A, Campo E, Jares P. Inactivation of RB1 in mantle-cell lymphoma detected by nonsense-mediated mRNA decay pathway inhibition and microarray analysis. *Blood* 2007;**109**(12):5422-9.

10. Piccaluga PP, Agostinelli C, Califano A, Carbone A, Fantoni L, Ferrari S, Gazzola A, Gloghini A, Righi S, Rossi M, Tagliafico E, Zinzani PL, Zupo S, Baccarani M, Pileri SA. Gene expression analysis of angioimmunoblastic lymphoma indicates derivation from T follicular helper cells and vascular endothelial growth factor deregulation. *Cancer Res* 2007;**67**(22):10703-10.

11. Piccaluga PP, Agostinelli C, Zinzani PL, Baccarani M, Dalla Favera R, Pileri SA. Expression of platelet-derived growth factor receptor alpha in peripheral T-cell lymphoma not otherwise specified. *Lancet Oncol* 2005;**6**(6):440.

DISCUSSION

This PhD project has aimed to study and decipher the molecular mechanisms involved in the pathogenesis of an aggressive lymphoid neoplasm. Particularly, it has comprised the analysis of the transcriptional program regulated by SOX11 in MCL, a NHL derived from mature B cells genetically characterized by the presence of the t(11;14)(q13;q32) translocation causing cyclin D1 overexpression and additional secondary genetic alterations (Jares et al., 2012; Swerdlow, 2008). Recent studies have recognized a subset of MCL with indolent clinical behavior even without chemotherapy that tend to present with leukemic non-nodal disease instead of extensive nodal infiltration (Espinet et al., 2005; Fernandez et al., 2010; Orchard et al., 2003). Several reports have identified the neuronal TF SOX11 as a reliable and specific biomarker of MCL as it is expressed in virtually all MCLs and at lower levels in a subgroup of BLs and ALLs but not in other lymphoid neoplasms (Dictor et al., 2009; Mozos et al., 2009). Moreover, recent molecular studies have identified *SOX11* as one of the best characterized discriminatory genes between the aggressive and indolent clinical subtypes of MCL (Fernandez et al., 2010; Royo et al., 2012), being exclusively overexpressed in the aggressive presentation of the disease. Therefore, SOX11 might play an important role in the aggressive development of MCL although its regulated oncogenic mechanisms contributing to the development and progression of the disease are largely unknown.

With such a starting hypothesis, in paper I we initiated the molecular characterization and elucidation of the SOX11-regulated transcriptional program in MCL. To do so, we performed an integrative analysis coupling data from human genome-wide promoter analysis by SOX11 ChIP-chip experiments and GEP upon SOX11 silencing in MCL cell lines. Since SOX11 and SOX4 are very homologous to each other, we first fulfilled a thorough and meticulous identification of a specific antibody against SOX11 protein expression to ensure that none of the subsequently identified targets and pathways was common to SOX4.

Our ChIP-chip approach revealed the first human genome wide-promoter analysis of SOX11 and uncovered 1133 unique target genes in MCL that were involved in different biological pathways including transcription, embryonic and neuronal development, cell growth and proliferation, cell death and apoptosis, cell cycle, hematopoiesis and hematological system development and function. Likewise, GEP before and after SOX11 silencing showed that the transcriptional program regulated by SOX11

comprised lymphocyte activation and differentiation, phosphorylation, cell cycle, immune system development and hematopoiesis.

Of note, our study approach combining ChIP-chip and GEP data showed to be very tissue-specific as we could detect binding of SOX11 to regulatory regions of genes involved in neuronal development (*BTG2, MEIS1* and *NR2E1*) but their expression was not observed in our lymphoid model. The direct regulation of early neural lineage development by the different members of the *Sox* gene family, including *Sox11*, has been recently recognized in a mouse model (Bergsland et al., 2011). However, in our study, the main target genes modulated by SOX11 were involved in immune system development and hematopoiesis, as evidenced by the regulation of the top SOX11 direct target genes *PAX5, MSI2* and *HSPD1*.

Taking into account that both GEP and GSEA showed that SOX11-positive MCL cell lines were enriched in genes and pathways involved in maintaining the mature B cell program whereas SOX11-silenced cells in those related to PC differentiation program, we hypothesized that SOX11 silencing triggers a shift from the mature B cell to a plasmacytic GEP in MCL cells. Therefore, we focused our subsequent investigations on PAX5, as it is the master regulator of B cell identity while preventing PC differentiation. Furthermore, *PAX5* stood out as one of SOX11 major direct and transcriptional target genes in our ChIP-chip and SOX11 silencing combined approach.

We validated SOX11 direct binding to regulatory regions of *PAX5* by ChIP-qPCR and verified the transcriptional effect of SOX11 on *PAX5* promoter using a luciferase assay. SOX11 specifically regulated PAX5 transcription since luciferase activity was only induced with SOX11 but not with SOX4 or truncated SOX11 proteins lacking the HMG domain or the C-terminal TAD domain, both of which are required for its transcriptional activity (Dy et al., 2008; Wiebe et al., 2003). Consistent with PAX5 function in maintaining B cell identity, SOX11 silencing downregulated several B cell specific genes that comprise direct targets of PAX5 while upregulating the master regulator of plasmacytic differentiation BLIMP1, which is directly repressed by PAX5-binding to its promoter (Mora-Lopez et al., 2007). Additionally, the slight upregulation of the unspliced variant of *XBP1* but not the spliced form responsible for Ig secretion together with downregulation of B cell specific immunophenotypic B cell markers

indicated that SOX11 downregulation is able to initiate the terminal B cell differentiation but not sufficient to drive the full PC phenotype.

In order to ensure that our observed results and phenotype were reflective of the *in vivo* situation and could thus be translated into human primary MCL tumors, we compared the GEP derived from our *in vitro* SOX11 silencing model with the one observed between primary SOX11-positive and negative human MCL primary tumors, and found that they were indeed very similar, confirming the validity of our approach. Moreover, SOX11 major target genes were modulated in microarray data from SOX11-positive cells, both from MCL cell lines and human primary samples, strengthening the significance of the SOX11-regulated biological phenotype in human MCL. Strikingly, and concordant with the *in vitro* situation, human SOX11-positive primary tumors where enriched in B cell specific and PAX5 regulated gene signatures and upregulated expression of B cell surface immunophenotypic markers. Contrarily, SOX11-negative tumors were enriched in plasmablast and XBP1 signatures, and some of them presented plasmacytic differentiation and expressed BLIMP1. Thus, these results confirmed that the SOX11 modulation of B cell and plasmacytic differentiation programs also occurs in MCL primary tumors.

The progress to plasmacytic differentiation is a feature of many B cell lymphomas, particularly lymphoplasmacytic lymphoma and MZL, but it can also be observed in FL, DLBCL and CLL (Gradowski et al., 2010; Martinez et al., 2013; Montes-Moreno et al., 2010; Montes-Moreno et al., 2012). However, plasmacytic differentiation is usually absent or present in extremely low numbers in MCL. Although primary MCLs have a monotonous cell morphology lacking the modulation towards plasmacytic differentiation observed in other types of B cell lymphomas (Swerdlow, 2008), our results may explain some intriguingly rare cases of MCL that have been reported showing clonal plasmacytic differentiation (Naushad et al., 2009; Visco et al., 2011; Young et al., 2006a).

SOX11 is a HMG TF characterized by its critical involvement in embryonic development and cell differentiation (Haslinger et al., 2009; Lin et al., 2011; Sock et al., 2004). However, it has no described function in lymphoid progenitors or in mature normal B cells, it is not apparently expressed in any normal cell subtype of the lymphoid system but is implicated in tumor development of several solid tumors (de

Bont et al., 2008; Weigle et al., 2005). To interrogate the potential tumorigenic ability of SOX11 in MCL *in vivo*, we inoculated SOX11-positive and silenced MCL cell lines in immunodeficient mice. Remarkably, SOX11-silenced cells presented reduced tumor growth and burden compared to mice bearing SOX11-positive control cells. Moreover, and concordant with the *in vitro* results, SOX11-silenced xenografts showed PAX5 downregulation and BLIMP1 upregulation compared to SOX11-positive tumors. Although proliferation rates between SOX11-positive and negative xenografts were the same, SOX11-negative tumors had large necrotic areas with high levels of activated caspase 3 that were minimal or not observed in SOX11-positive tumors, suggesting that SOX11 sustains B cell differentiation program and tumor cell survival *in vivo.*

Despite the fact that the block of the B cell program does not represent an oncogenic mechanism *per se* accounting for the malignant cellular transformation and subsequent tumor progression, the significance of blocking PC differentiation program as a relevant oncogenic mechanism in lymphoid neoplasias has been previously observed. The impairment of terminal B cell differentiation caused by SOX11 overexpression in MCL may parallel the forced expression of PAX5 by the t(9;14)(p13;q32) translocation identified in some B cell lymphomas (Busslinger et al., 1996; Iida et al., 1996; Morrison et al., 1998), and the inactivating mutations of *PRDM1* in DLBCLs (Mandelbaum et al., 2010; Pasqualucci et al., 2006; Tam et al., 2006). Recent studies demonstrate the oncogenic role of PAX5 by mutations or alterations in the expression of *PAX5* gene (Mullighan et al., 2007; Sadakane et al., 2007; Souabni et al., 2007). PAX5 deregulation is associated with certain types of acute leukemias, particularly B cell-precursor acute lymphoblastic leukemia (B-ALL). *PAX5* monoallelic deletions, fusion translocations, or point mutations that disrupt *PAX5* DNA-binding or transcriptional regulatory functions occur in approximately one-third of B-ALLs (Kuiper et al., 2007; Mullighan et al., 2007). Moreover, germline mutations in *PAX5* have recently been associated with B-ALL susceptibility (Shah et al., 2013). .

The role of SOX11 in MCL has been controversial during the last years because some groups have associated SOX11 negativity with a better OS of the patients (Fernandez et al., 2010; Navarro et al., 2012; Ondrejka et al., 2011) while others did it with a worse OS (Nygren et al., 2012). However, detailed and thorough studies on additional secondary alterations have started to shed light on such discrepancy. Royo and colleagues identified that *TP53* and 17p alterations likely contributed to disease

progression in SOX11-negative MCLs further stratifying outcome in MCL subsets independently of SOX11 expression levels (Royo et al., 2012). In a subsequent and very recent study, Nordstrom and colleagues found that SOX11-negative patients with aggressive presentation of the disease had mutations in *TP53*, corroborating previous results (Nordstrom et al., 2014). Therefore, some non-nodal SOX11-negative patients might have an aggressive clinical presentation because of *TP53* or 17p alterations. In fact, most of the SOX11 negative MCLs in the Nygren study had alterations of *TP53*.

This has been very recently supported by NGS results from Beà and co-workers showing that whereas mutations in *ATM* were only seen in SOX11-positive human tumors, mutations in *TP53* were equally distributed among SOX11-positive and negative MCL tumors (Bea et al., 2013). Additionally, in two SOX11-negative/*IGHV*-mutated MCLs, Beà and colleagues also found mutations in *TLR2* associated with increased tumor cell production of IL1RA and IL6. High levels of IL1RA have been associated with aggressive behavior in some lymphomas (Charbonneau et al., 2012), and IL6 sustains growth and survival of MCL cells (Zhang et al., 2012), suggesting that *TLR2* mutations may contribute to the pathogenesis of a subset of SOX11-negative/*IGHV*-mutated MCLs by modulating TME responses. Thus, SOX11 is important to recognize two subtypes of MCL but not a prognostic factor *per se*.

Despite some controversial results and still ongoing investigations, a MCL development model can be constructed using all the results obtained until date. An initiating t(11;14) translocation occurs in an early precursor B lymphocyte that matures into a naïve B cell representing the initial *in situ* MCL-like-B cell. The cells that maintain a naïve B cell like phenotype and overexpress SOX11 upregulate PAX5 and prevent BLIMP1 expression. Therefore, they cannot go into the GC reaction, do not undergo considerable somatic *IGVH* mutation, and their further progress into differentiation is blocked in a mature B cell stage. Lymphoma would develop upon genetic progression and occurrence of secondary genetic alterations involving genes and pathways targeted by recurrent secondary abnormalities (Figure 30).

Alternatively, some t(11;14) harboring cells may proceed into the GC reaction, present hypermutated *IGHV* and a leukemic, non-nodal and splenic involvement. These cells lack SOX11 expression, allowing their progression into the plasmacytic differentiation process. Some of these variants remain genetically stable without progression events

and have an indolent clinical course. However, progression to aggressive MCL may occur by the presence of *TP53/TLR2* gene alterations, 17p deletions or other secondary genetic alterations (Figure 30).

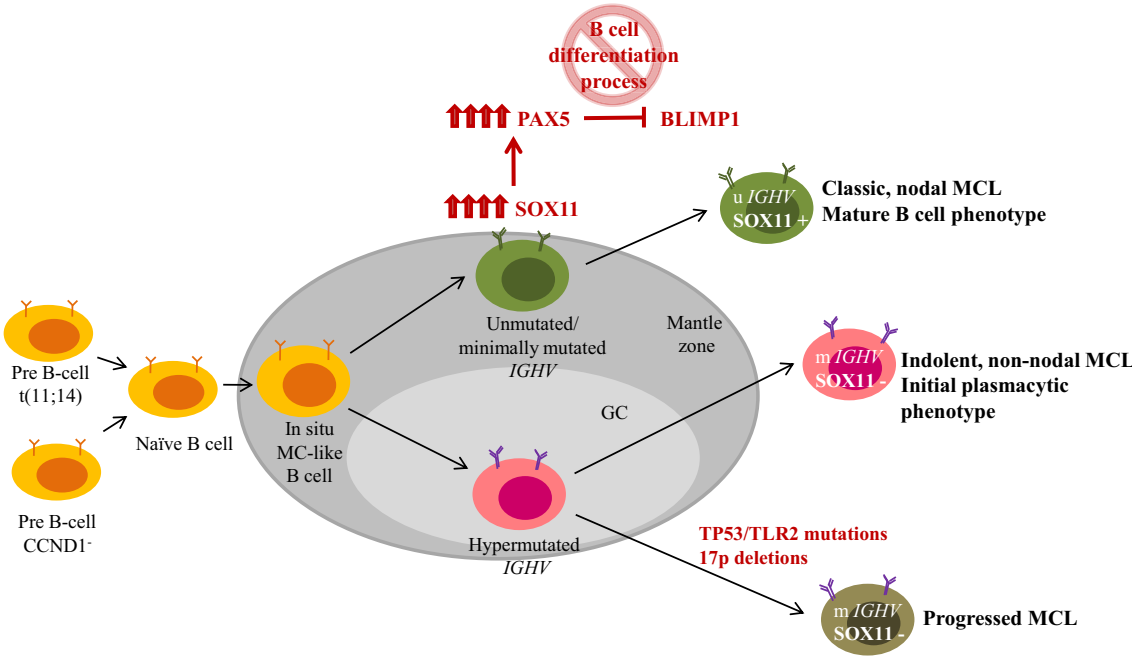

Figure 30. Hypothetical model of the different MCL subtypes development. *SOX11 is overexpressed in some MCL tumors and promotes an enhanced upregulation of PAX5. These cells are blocked in the B cell differentiation process and do not enter the GC. These MCL tumors represent the classical and aggressive phenotype of the disease. On the contrary, MCL tumors that do not express SOX11 can proceed into the GC reaction, present hypermutated IGHV genes and can progress into the first steps of the plasmacytic differentiation process. These tumors have a non-nodal, leukemic presentation of the disease with very long survival of the patients. Some SOX11-negative MCLs develop TP53/TLR2 mutations or 17p deletions, and thus progress into an aggressive, progressed clinical presentation.*

Overall, in paper I we have identified target genes and transcriptional programs biologically and clinically relevant regulated by SOX11 including the block of mature B cell differentiation, modulation of cell cycle, apoptosis, and stem cell development. *PAX5* stands out as a major target gene of SOX11, and SOX11 silencing downregulates its expression, induces BLIMP1 expression, and promotes the shift from a mature B cell into the initial plasmacytic differentiation phenotype *in vitro* and *in vivo* in both human primary and xenograft MCL tumor cells. We have also demonstrated the oncogenic implication of SOX11 expression in the aggressive behavior of MCL as SOX11-silenced derived tumors display a significant reduction on tumor growth compared to SOX11-control tumors in subcutaneous MCL xenografts.

However, the specific SOX11-regulated mechanisms promoting the oncogenic and rapid tumor growth of aggressive MCL still remained to be elucidated. There are no *in vitro* differences in cell cycle, proliferation and viability between SOX11-positive and negative cells. However, the presence of caspase 3-positive areas and the enrichment of these cells in apoptotic and caspase gene signatures in the SOX11-silenced xenografts suggest that SOX11 may be regulating pro-survival signals from the TME contributing to the more pronounced growth of the SOX11-positive xenografts. Consequently, in paper II, we further characterized the potential SOX11-regulated oncogenic mechanisms by integrating our ChIP-chip data with further analyses including GEP derived from the xenograft SOX11-positive and silenced tumors.

A thorough investigation both from a transcriptional and protein perspective revealed that SOX11-positive xenograft tumors were enriched in angiogenic gene signatures and upregulated several pro-angiogenic factors compared to SOX11-silenced tumors. Moreover, IHC analyses of the tumors displayed higher MVD areas in the SOX11-positive xenograft samples. Importantly, human primary SOX11-positive MCL tumors were also enriched in angiogenic signatures and their IHC analyses revealed better developed microvasculature networks compared to SOX11-negative tumors.

The growth of solid tumors requires the development of microvessels, therefore tumor expansion correlates with the extent of angiogenesis (Folkman, 1985). Although many evidences suggest that increased MVD in many carcinoma types correlates with the increased risk of metastatic spread and subsequently a poor prognosis, there is much less information available regarding the significance of MVD in malignant lymphomas. However, some studies have been performed showing increased MVD in NHL (Negaard et al., 2009). Several studies are concurrent with our results as it has been described that an increased MVD correlates with disease progression in lymphoid neoplasms (Cardesa-Salzmann et al., 2011; Korkolopoulou et al., 2005; Perry et al., 2012). Concordant with these studies, our initial findings in the xenotrasplant tumors suggested that angiogenesis could be the mechanism deregulated in our MCL xenograft model and that SOX11 could facilitate their tumor growth by enhancing pro-angiogenic factors *in vivo*.

Although no angiogenic function has been previously elucidated for human SOX11, a recent study in Zebrafish has reported the involvement of sox11b, the human ortholog

of SOX11, in promoting sprouting angiogenesis of caudal vein plexus (Schmitt et al., 2013). Furthermore, other members of the SOX family are also involved in angiogenesis, as specific gene-based studies recently described that the SOXF members *SOX7*, *17* and *18* are implicated in lymphangiogenesis (Clasper et al., 2008; Francois et al., 2010). SOX18 is transiently expressed in ECs of all developing blood vessels and plays a key role in both vascular development and postnatal neovascularization (Francois et al., 2010; Matsui et al., 2006; Sakamoto et al., 2007). Moreover, its expression is reactivated during adult neovascularization when it is associated with wound healing and tumorigenesis (Darby et al., 2001; Young et al., 2006b). *SOX7* and *SOX17* genes are also known to have compensatory roles during angiogenesis and lymphangiogenesis (Cermenati et al., 2008; Matsui et al., 2006; Sakamoto et al., 2007). All these observations supported the hypothesis that SOX11 could also be involved in angiogenesis.

The importance of the TME in B cell lymphomas is exponentially growing in the last years as evidenced by a compelling body of literature interrogating the cross-talk between tumor and their accompanying stromal cells, as well as therapies targeting such interactions (Scott and Gascoyne, 2014). Angiogenesis is one of the multiple mechanisms involved in TME and it represents one of the hallmarks of cancer allowing cancer cells to survive, proliferate, and disseminate.

In order to study a putative regulation of angiogenesis by SOX11 we generated an *in vitro* model that would mimic EC responses to external stimuli. Therefore, we derived SOX11-positive and negative conditioned media (CM) from the corresponding cells growing in culture, and used them as incubating media for human umbilical vein endothelial cells (HUVECs). Confirming our initial hypothesis, SOX11-positive CM produced a prominent increase in *in vitro* tube formation, proliferation and migration of HUVECs as well as induction of higher phosphorylation levels of Akt, FAK and Erk1/2, downstream signaling proteins involved in these processes.

We then proceeded to explore putative SOX11-regulated pro-angiogenic factors that could be responsible for such enhanced angiogenesis in ECs. Concordant with xenograft results, SOX11-positive MCL cell lines were enriched in angiogenic gene signatures and expressed higher levels of pro-angiogenic factors compared to SOX11-silenced cells. However, the number of pro-angiogenic factors overexpressed in cell lines was

much lower than in xenograft tumors, suggesting that TME is indeed playing a major role in the regulation of angiogenesis and MCL growth *in vivo*.

To determine how SOX11 was regulating pro-angiogenic responses in xenograft tumors and ECs *in vitro*, we analyzed the soluble factors secreted by MCL cell lines in their corresponding CM. We found that PDGFA was the only pro-angiogenic factor both expressed and secreted by SOX11-positive MCL cells. Moreover, *PDGFA* was identified as a SOX11-bound gene by ChIP experiments, and the specific binding of SOX11 to its regulatory region was verified by ChIP-chip and luciferase induction activity assays. Supporting the positive transcriptional effect of SOX11 on *PDGFA* regulatory region and the hypothesis that PDGFA might be the major mediator of angiogenesis in MCL, SOX11-positive xenografts and human primary samples expressed higher levels of PDGFA than their SOX11-negative cellular counterparts.

Although not many studies investigate the involvement of the SOX family members in angiogenesis, some similar studies have been done deciphering the regulation of some genes involved in angiogenesis by different SOX proteins. Samant and colleagues described that Sox17 and 18 are putative regulators of *robo4* gene expression, a gene that participates in sprouting angiogenesis in zebrafish *in vivo*. Both Sox family members co-localized with robo4 transcripts, and Sox18 bound to a region in *robo4* promoter responsible for *robo4* promoter activity in ECs (Samant et al., 2011). Other studies by Hosking and colleagues have also shown that SOX18 mediates its functions in ECs by interacting with the TF MEF2C and by directly activating *VCAM1*, a gene involved in vascular development (Hosking et al., 2001; Hosking et al., 2004).

Members of the PDGF family and their receptors have been shown to influence tumor growth and invasion through effects on tumor cells and their surrounding microenvironment. Persistent high levels of PDGFs and PDGFRs in malignant cells have been detected in various cancers including glioma, Kaposi's sarcoma, prostate cancer, pancreatic cancer and PTCLs (Heinrich et al., 2003; Hermanson et al., 1992; McCarty et al., 2007; Piccaluga et al., 2007; Sitaras et al., 1988). Depending on the expression of both the ligand and the receptor in malignant and stromal cells, PDGF members can act via paracrine or autocrine ways. In particular, PDGFA may participate in the development of a vascular TME through a direct effect on the endothelium but also indirectly by recruiting MSCs that release additional angiogenic elements (Ding et

al., 2010; Dong et al., 2004b; Ferrara and Kerbel, 2005; Risau et al., 1992). PDGFA only binds to PDGFRα, activating its downstream pathway involved in several oncogenic mechanisms including angiogenesis (Andrae et al., 2008; Heldin, 2013).

In our study, PDGFA exerted its effect in a paracrine way on ECs, as HUVECs expressed PDGFRα but not MCL cell lines or human primary tumors. Moreover, incubation of HUVECs with SOX11-positive CM promoted an increased phosphorylation of PDGFRα that was downregulated upon treatment with two blocking PDGFRα agents, imatinib, a tyrosine kinase inhibitor of PDGFR, and a specific neutralizing antibody against the receptor. Additionally, PDGFRα inhibition also decreased the induction in tube formation and migration when HUVECs were incubated in the presence of SOX11-positive CM.

Our results are very similar to those described by Ding and colleagues showing that CLL leukemic cells secreted PDGF which mainly functioned in a paracrine fashion towards MSCs. This was achieved through a PDGF-PDGFR-PI-3-K-Akt pathway that modified MSCs function and in particular their pro-angiogenic factor production. Moreover, blocking PDGFR activation by a specific inhibitor abrogated the CLL-CM-driven MSC proliferation, indicating the key role of PDGFR activation in CLL-CM-mediated MSC proliferation and Akt activation (Ding et al., 2010). In support of the role of PDGF-PDGFR signaling in hematological malignancies, PDGF has also been reported to be important in the prosurvival pathway in large granular lymphocytic (LGL) leukemia (Yang et al., 2010; Zhang et al., 2008).

In order to verify whether PDGFA upregulation by SOX11 mediated the SOX11-enforced angiogenesis in MCL contributing to the aggressiveness of the tumors, we treated SOX11-positive and negative xenografts with imatinib and observed that such treatment significantly suppressed the growth and progression of SOX11-positive tumors. Importantly, such reduction was accompanied by a decline in the number and percentage of MVD areas in the corresponding samples. The striking growth impairment of the SOX11-positive xenografts due to an impaired angiogenesis together with the direct endothelial inhibitory effect of imatinib in *in vitro* experiments suggest that the PDGFA-PDGFRα pathway may represent a novel therapeutic strategy for the treatment of aggressive MCL.

The importance of tumor angiogenesis in the development and clinical progression of lymphoid neoplasias has suggested that these mechanisms may be potential targets for new therapies (Ruan et al., 2009). Imatinib has proven anti-angiogenic effects in a DLBCL xenograft model targeting pericytes via PDGFRβ (Ruan et al., 2013), and lenalidomide impairs lymphangiogenesis in MCL preclinical models (Song et al., 2013). Lenalidomide has been recently shown to produce rapid and durable responses in heavily pretreated patients with aggressive, relapsed or refractory MCL, including patients who had failed bortezomib therapy (Goy et al., 2013; Vose et al., 2013; Witzig et al., 2011; Zinzani et al., 2013). Although brtezomib induces response rates in patients with relapsed disease (Fisher et al., 2006; Goy et al., 2009; O'Connor et al., 2009), more than half of MCL patients are resistant or develop resistance to this drug (Perez-Galan et al., 2011b). The molecular bases underlying this resistance have not been totally defined but some studies pointed to oxidative and endoplasmic reticulum stress, activation of the cytoprotective arm of the unfolded protein response, and a cellular phenotype characteristic of partial plasmacytic differentiation (Perez-Galan et al., 2011b; Roue et al., 2011; Weniger et al., 2011). Thus, inhibition of the PDGFA pathway with imatinib might confer a promising novel therapeutic strategy for the treatment of aggressive MCL. Future treatment strategies must take into account the interactions of the lymphoma microenvironment with the neoplastic cells, rather than only concentrating on the latter cells.

Nowadays, reliable markers that identify those patients with aggressive disease who might benefit from novel treatment approaches and, alternatively, patients with indolent disease who might be best initially observed without intervention are still lacking. Therefore, our results may be of clinical importance since they represent an accurate characterization of SOX11 as a biomarker of the aggressive behavior of MCL. SOX11-negative MCLs usually present clinically with non-nodal leukemic disease whereas SOX11-positive tumors involve lymph nodes and have extensive extranodal infiltration (Espinet et al., 2014; Fernandez et al., 2010). The SOX11-PDGFA-dependent angiogenic switch discovered in this study may explain MCL clinical heterogeneity because the low angiogenic potential of SOX11-negative cells may impair their tissue infiltration and retain them in the blood stream whereas SOX11-PAX5-induced angiogenesis facilitates tissue infiltration and growth of the SOX11-expressing MCL cells (Figure 31).

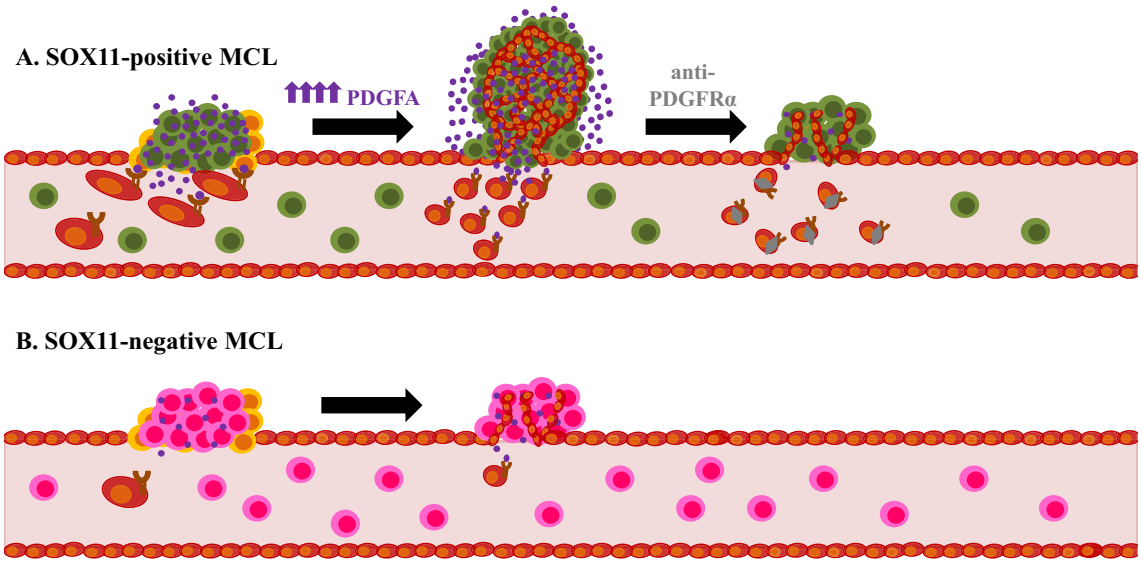

Figure 31. Hypothetical model of oncogenic growth of MCL tumors. *(A) SOX11-positive tumors (green) secrete the pro-angiogenic factor PDGFA (purple), which binds to its specific receptor PDFGRα on ECs (red). ECs proliferate and migrate towards the PDGFA-tumor mass and start forming new blood vessels. Thus, SOX11-positive tumors are extremely nurtured and tumor growth and progression is enhanced. The high pro-angiogenic potential of SOX11-positive MCL cells may facilitate their tissue infiltration and growth. Inactivation of PDGFA-PDFGRα signaling pathway with a blocking agent (grey) inhibits EC migration and tube formation, and MCL growth is strikingly diminished. (B) SOX11-negative tumors (pink) secrete low levels of PDGFA and thus, microvasculature networks are not well developed. Therefore, their growth is not promoted and the clinical presentation of the disease is non-nodal, leukemic and indolent.*

Similar observations were presented in a study by Eom and colleagues, showing that SOX18 was associated with the presence of lymphovascular invasion, advanced stage disease and poor overall and recurrence-free survivals in gastric cancer. The frequencies of both lymphovascular invasion and lymph node metastasis were significantly increased in the SOX18-positive patients, suggesting that SOX18 participates in both lymphangiogenesis and lymphatic metastasis during gastric cancer progression (Eom et al., 2012). Ding and colleagues also observed a positive correlation between PDGF and VEGF levels in CLL plasma, especially evident in CLL patients with progressive disease requiring therapy, patients with late stage, or those who were ZAP-70 or CD38 positive (Ding et al., 2010).

Our results demonstrate, for the first time, that SOX11 regulates PDGFA expression and its upregulation promotes the malignant and rapid growth of MCL tumors *in vivo*. However, the observation that more pro-angiogenic factors are upregulated in the xenograft tumors indicates that cells from the TME are also involved in angiogenic

functions in MCL. It would be very interesting to study how the different stromal cells such as fibroblasts or macrophages are contributing to the angiogenic switch in the SOX11-positive xenograft samples. Also, xenograft derived tumor cells or human primary MCL tumors could be grown *in vitro* to analyze a clearer picture of the *in vivo* situation. Co-culture of our stably silenced MCL cell lines as well as MCL xenograft and human primary-derived cultures with different stromal cell populations (T cells, TAMs, fibroblasts, DCs) would represent a possible model to analyze the contribution of the TME milieu to the growth of MCL.

Overall, the work derived from this PhD project has led to the understanding of the deregulated oncogenic mechanisms mediated by SOX11 in MCL, defining this TF as a biomarker of the aggressive presentation of MCL and a putative master regulator of the disease. This is the first characterization of SOX11 as a regulator of B cell development and angiogenesis in MCL. Despite being possible that SOX11 has different effects on tumor cells depending on the context and primary transformation mechanism, a deeper and scrupulous exploration of its functional role in MCL and additional functional studies of the disease needs to be done. It looks as if the contribution of the different deregulated mechanisms will hint to the pathogenesis of the disease rather than a single gene or pathway. Our results are or may be of clinical importance as they provide molecular clues for the understanding of a distinct progression for MCL development. Not only have we characterized the transcriptional program regulated by SOX11 in MCL cells and its oncogenic role in the pathogenesis of the disease but we also provided evidence for attractive therapeutic strategies for such an aggressive and incurable disease.

The development of MCL mouse models that reflect the human pathophysiology of the disease has been a longstanding challenge. Overexpression of cyclin D1 alone failed to produce lymphoproliferative disease, and resulted in little or no alteration in B cell development (Bodrug et al., 1994; Lovec et al., 1994). Combination with transgenic overexpression of n-MYC or c-MYC, overexpression of a constitutively mutant cyclin D1 or overexpression of MYC and IL14α accelerated the formation of B cell lymphomas and recapitulated many features of MCL. However, most of these lymphomas represented the blastoid or pleomorphic variants of the disease and the underlying genetic lesions bearded little resemblance to human MCL (Beltran et al., 2011; Bodrug et al., 1994; Ford et al., 2007; Gladden et al., 2006; Hao et al., 2002;

Lovec et al., 1994). A recent study by Katz and colleagues reported the generation and characterization of a genetically-engineered mouse model of MCL development in the context of cyclin D1 overexpression and deletion of pro-apoptotic *Bim* in B lymphocytes, recapitulating two common cytogenetic abnormalities in human MCL (Katz et al., 2014).

Our studies point out to a role of SOX11 as a master regulator of MCL aggressive development. Thus, the generation of SOX11 inducible transgenic mouse models in B lymphocytes would help to define whether SOX11 could be a sole driver of MCL initiation or it may need the cooperation with other molecular mechanisms such as cyclin D1 overexpression to trigger MCL initiation. Furthermore, it would represent an invaluable tool to study SOX11 oncogenic role in MCL as the human situation is much more similarly represented. Very importantly as well, it would provide an extraordinary model to study the intriguing SOX11 expression in MCL B cells as it is still unknown how SOX11 gets activated in human MCL. Although a study in our laboratory showed that SOX11 expression in aggressive lymphoid malignancies is associated with a change from inactivating to activating histone marks, no more insights are known on that respect (Vegliante et al., 2011).

As a whole, we have provided new molecular clues on the transcriptional program regulated by SOX11 in MCL and have described its involvement in malignant B lymphocytes. This PhD project has unraveled and characterized the oncogenic role of SOX11 and the tumorigenic pathways it governs in MCL. Importantly, it has shed light on SOX11 target genes involved in B cell differentiation and angiogenesis. The elucidation of molecular mechanisms that are deregulated by SOX11 in MCL will aid the management and stratification of MCL patients and lead to the development of new therapeutic strategies for this aggressive disease.

CONCLUSIONS

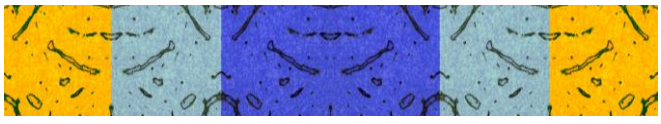

1. Our tissue-specific approach combining *SOX11*-ChIP-chip and GEP upon SOX11 silencing in MCL cell lines revealed SOX11 direct target genes and transcriptional pathways. The main regulated mechanism was the blockade of mature B cell development.

2. The main target genes modulated by SOX11 were involved in immune system development and hematopoiesis as evidenced by *PAX5, MSI2* and *HSPD1*.

3. SOX11 bound to regulatory regions of *PAX5* and directly regulated its transcriptional activity. Moreover, SOX11 silencing promoted the initial steps into the plasmacytic differentiation in MCL cell lines by the downregulation of PAX5 expression and increasing levels of BLIMP1. In human primary MCL, SOX11-positive tumors were enriched in B cell specific and PAX5 regulated gene signatures whereas SOX11-negative tumors were enriched in plasmablastic signatures, and some of them presented plasmacytic differentiation.

4. Human SOX11-positive and -negative primary MCLs were enriched in SOX11-upregulated and -downregulated genes, respectively. Thus, our *in vitro* model reflected the *in vivo* human situation.

5. The strong expression of SOX11 in conventional MCLs may block the cells in a mature B-cell stage preventing their further progress into differentiation. However, SOX11-negative MCLs may modulate the mature B cell phenotype and progress into the initial steps of the plasmacytic differentiation program.

6. The significant reduction in tumor growth of the SOX11-knockdown xenograft tumors highlights that SOX11 sustains tumor cell survival *in vivo* and supports the implication of SOX11 expression in the aggressive behavior of these tumors.

7. SOX11-positive xenografts are enriched in apoptotic pathways whereas no differences in cell viability were observed *in vitro*. Thus, SOX11 may be regulating pro-survival signals from the TME contributing to the more pronounced growth of the SOX11-positive xenografts.

8. The combination of *SOX11*-ChIP-chip and MCL-xenograft derived GEP showed that angiogenesis was the main mechanism regulated by SOX11 *in vivo*. SOX11-positive MCL cells were enriched in angiogenic gene signatures, overexpressed pro-

angiogenic factors, induced enhanced angiogenic responses in EC and presented better developed microvasculature netwoks than SOX11-negative cells both *in vitro* and *in vivo*.

9. The SOX11-mediated angiogenesis was controlled by the direct and transcriptional regulation of the pro-angiogenic factor PDGFA *in vitro* and *in vivo*.

10. PDGFA exerted its effect in a paracrine way on ECs, and inhibition of the downstream PDGFA-PDGFRα activation blocked the SOX11-enhanced angiogenic axis.

11. Treatment of SOX11-positive xenografts with imatinib reduced their tumor growth and progression by diminishing tumor microvasculature formation, suggesting that the PDGFA pro-angiogenic pathway may represent a novel therapeutic strategy for the treatment of aggressive MCL.

12. Our results describe *SOX11* as a new oncogene in MCL and may explain the clinical heterogeneity of this disease. The low angiogenic potential of the human SOX11-negative cells may impair their tissue infiltration and retain them in the blood stream. On the other hand, human SOX11-positive primary MCLs have enhanced angiogenic potential by the SOX11-induced upregulation of PDGFA, facilitating their tissue infiltration and tumor aggressive growth and progression.

REFERENCES

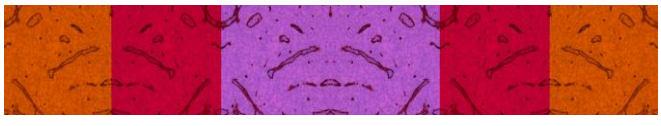

- Aaboe, M., Birkenkamp-Demtroder, K., Wiuf, C., Sorensen, F.B., Thykjaer, T., Sauter, G., Jensen, K.M., Dyrskjot, L., and Orntoft, T. (2006). SOX4 expression in bladder carcinoma: clinical aspects and in vitro functional characterization. Cancer Res *66*, 3434-3442.
- Adam, P., Schiefer, A.I., Prill, S., Henopp, T., Quintanilla-Martinez, L., Bosmuller, H.C., Chott, A., and Fend, F. (2012). Incidence of preclinical manifestations of mantle cell lymphoma and mantle cell lymphoma in situ in reactive lymphoid tissues. Mod Pathol *25*, 1629-1636.
- Adolfsson, J., Mansson, R., Buza-Vidas, N., Hultquist, A., Liuba, K., Jensen, C.T., Bryder, D., Yang, L., Borge, O.J., Thoren, L.A.*, et al.* (2005). Identification of Flt3+ lympho-myeloid stem cells lacking erythro-megakaryocytic potential a revised road map for adult blood lineage commitment. Cell *121*, 295-306.
- Aldinucci, D., Gloghini, A., Pinto, A., De Filippi, R., and Carbone, A. (2010). The classical Hodgkin's lymphoma microenvironment and its role in promoting tumour growth and immune escape. J Pathol *221*, 248-263.
- Alt, J.R., Cleveland, J.L., Hannink, M., and Diehl, J.A. (2000). Phosphorylation-dependent regulation of cyclin D1 nuclear export and cyclin D1-dependent cellular transformation. Genes Dev *14*, 3102-3114.
- Allman, D., Jain, A., Dent, A., Maile, R.R., Selvaggi, T., Kehry, M.R., and Staudt, L.M. (1996). BCL-6 expression during B-cell activation. Blood *87*, 5257-5268.
- Andersen, C.L., Christensen, L.L., Thorsen, K., Schepeler, T., Sorensen, F.B., Verspaget, H.W., Simon, R., Kruhoffer, M., Aaltonen, L.A., Laurberg, S.*, et al.* (2009). Dysregulation of the transcription factors SOX4, CBFB and SMARCC1 correlates with outcome of colorectal cancer. Br J Cancer *100*, 511-523.
- Andrae, J., Gallini, R., and Betsholtz, C. (2008). Role of platelet-derived growth factors in physiology and medicine. Genes Dev *22*, 1276-1312.
- Angelin-Duclos, C., Cattoretti, G., Chang, D.H., Lin, K.I., Lin, Y., Yu, J., and Calame, K. (1999). Role of B-lymphocyte-induced maturation protein-1 in terminal differentiation of B cells and other cell lineages. Cold Spring Harb Symp Quant Biol *64*, 61-70.
- Angelopoulou, M.K., Siakantariz, M.P., Vassilakopoulos, T.P., Kontopidou, F.N., Rassidakis, G.Z., Dimopoulou, M.N., Kittas, C., and Pangalis, G.A. (2002). The splenic form of mantle cell lymphoma. Eur J Haematol *68*, 12-21.
- Augustin, H.G., Koh, G.Y., Thurston, G., and Alitalo, K. (2009). Control of vascular morphogenesis and homeostasis through the angiopoietin-Tie system. Nat Rev Mol Cell Biol *10*, 165-177.

- Baeriswyl, V., and Christofori, G. (2009). The angiogenic switch in carcinogenesis. Semin Cancer Biol *19*, 329-337.
- Bain, G., Maandag, E.C., Izon, D.J., Amsen, D., Kruisbeek, A.M., Weintraub, B.C., Krop, I., Schlissel, M.S., Feeney, A.J., van Roon, M.*, et al.* (1994). E2A proteins are required for proper B cell development and initiation of immunoglobulin gene rearrangements. Cell *79*, 885-892.
- Balciunaite, G., Ceredig, R., Massa, S., and Rolink, A.G. (2005). A B220+ CD117+ CD19- hematopoietic progenitor with potent lymphoid and myeloid developmental potential. Eur J Immunol *35*, 2019-2030.
- Balkwill, F.R., Capasso, M., and Hagemann, T. (2012). The tumor microenvironment at a glance. J Cell Sci *125*, 5591-5596.
- Bassarova, A., Tierens, A., Lauritzsen, G.F., Fossa, A., and Delabie, J. (2008). Mantle cell lymphoma with partial involvement of the mantle zone: an early infiltration pattern of mantle cell lymphoma? Virchows Arch *453*, 407-411.
- Bauman, J.E., Eaton, K.D., and Martins, R.G. (2007). Antagonism of platelet-derived growth factor receptor in non small cell lung cancer: rationale and investigations. Clin Cancer Res *13*, s4632-4636.
- Bea, S., Salaverria, I., Armengol, L., Pinyol, M., Fernandez, V., Hartmann, E.M., Jares, P., Amador, V., Hernandez, L., Navarro, A.*, et al.* (2009). Uniparental disomies, homozygous deletions, amplifications, and target genes in mantle cell lymphoma revealed by integrative high-resolution whole-genome profiling. Blood *113*, 3059-3069.
- Bea, S., Tort, F., Pinyol, M., Puig, X., Hernandez, L., Hernandez, S., Fernandez, P.L., van Lohuizen, M., Colomer, D., and Campo, E. (2001). BMI-1 gene amplification and overexpression in hematological malignancies occur mainly in mantle cell lymphomas. Cancer Res *61*, 2409-2412.
- Bea, S., Valdes-Mas, R., Navarro, A., Salaverria, I., Martin-Garcia, D., Jares, P., Gine, E., Pinyol, M., Royo, C., Nadeu, F.*, et al.* (2013). Landscape of somatic mutations and clonal evolution in mantle cell lymphoma. Proc Natl Acad Sci U S A *110*, 18250-18255.
- Beenken, A., and Mohammadi, M. (2009). The FGF family: biology, pathophysiology and therapy. Nat Rev Drug Discov *8*, 235-253.
- Beltran, E., Fresquet, V., Martinez-Useros, J., Richter-Larrea, J.A., Sagardoy, A., Sesma, I., Almada, L.L., Montes-Moreno, S., Siebert, R., Gesk, S.*, et al.* (2011). A cyclin-D1 interaction with BAX underlies its oncogenic role and potential as a therapeutic target in mantle cell lymphoma. Proc Natl Acad Sci U S A *108*, 12461-12466.

- Bereshchenko, O.R., Gu, W., and Dalla-Favera, R. (2002). Acetylation inactivates the transcriptional repressor BCL6. Nat Genet *32*, 606-613.
- Bergers, G., and Benjamin, L.E. (2003). Tumorigenesis and the angiogenic switch. Nat Rev Cancer *3*, 401-410.
- Bergers, G., and Hanahan, D. (2008). Modes of resistance to anti-angiogenic therapy. Nat Rev Cancer *8*, 592-603.
- Bergsland, M., Ramskold, D., Zaouter, C., Klum, S., Sandberg, R., and Muhr, J. (2011). Sequentially acting Sox transcription factors in neural lineage development. Genes Dev *25*, 2453-2464.
- Bewley, C.A., Gronenborn, A.M., and Clore, G.M. (1998). Minor groove-binding architectural proteins: structure, function, and DNA recognition. Annu Rev Biophys Biomol Struct *27*, 105-131.
- Bi, W., Deng, J.M., Zhang, Z., Behringer, R.R., and de Crombrugghe, B. (1999). Sox9 is required for cartilage formation. Nat Genet *22*, 85-89.
- Bisping, G., Leo, R., Wenning, D., Dankbar, B., Padro, T., Kropff, M., Scheffold, C., Kroger, M., Mesters, R.M., Berdel, W.E.*, et al.* (2003). Paracrine interactions of basic fibroblast growth factor and interleukin-6 in multiple myeloma. Blood *101*, 2775-2783.
- Blobe, G.C., Schiemann, W.P., and Lodish, H.F. (2000). Role of transforming growth factor beta in human disease. N Engl J Med *342*, 1350-1358.
- Bodrug, S.E., Warner, B.J., Bath, M.L., Lindeman, G.J., Harris, A.W., and Adams, J.M. (1994). Cyclin D1 transgene impedes lymphocyte maturation and collaborates in lymphomagenesis with the myc gene. EMBO J *13*, 2124-2130.
- Bondurand, N., Pingault, V., Goerich, D.E., Lemort, N., Sock, E., Le Caignec, C., Wegner, M., and Goossens, M. (2000). Interaction among SOX10, PAX3 and MITF, three genes altered in Waardenburg syndrome. Hum Mol Genet *9*, 1907-1917.
- Bosch, F., Jares, P., Campo, E., Lopez-Guillermo, A., Piris, M.A., Villamor, N., Tassies, D., Jaffe, E.S., Montserrat, E., Rozman, C.*, et al.* (1994). PRAD-1/cyclin D1 gene overexpression in chronic lymphoproliferative disorders: a highly specific marker of mantle cell lymphoma. Blood *84*, 2726-2732.
- Boxer, L.M., and Dang, C.V. (2001). Translocations involving c-myc and c-myc function. Oncogene *20*, 5595-5610.
- Brennan, D.J., Ek, S., Doyle, E., Drew, T., Foley, M., Flannelly, G., O'Connor, D.P., Gallagher, W.M., Kilpinen, S., Kallioniemi, O.P.*, et al.* (2009). The transcription factor Sox11 is a prognostic factor for improved recurrence-free survival in epithelial ovarian cancer. Eur J Cancer *45*, 1510-1517.

- Brown, J.L., Cao, Z.A., Pinzon-Ortiz, M., Kendrew, J., Reimer, C., Wen, S., Zhou, J.Q., Tabrizi, M., Emery, S., McDermott, B.*, et al.* (2010). A human monoclonal anti-ANG2 antibody leads to broad antitumor activity in combination with VEGF inhibitors and chemotherapy agents in preclinical models. Mol Cancer Ther *9*, 145-156.
- Burger, J.A., and Ford, R.J. (2011). The microenvironment in mantle cell lymphoma: cellular and molecular pathways and emerging targeted therapies. Semin Cancer Biol *21*, 308-312.
- Burger, J.A., Ghia, P., Rosenwald, A., and Caligaris-Cappio, F. (2009). The microenvironment in mature B-cell malignancies: a target for new treatment strategies. Blood *114*, 3367-3375.
- Burger, J.A., and Kipps, T.J. (2002). Chemokine receptors and stromal cells in the homing and homeostasis of chronic lymphocytic leukemia B cells. Leuk Lymphoma *43*, 461-466.
- Burger, J.A., Tsukada, N., Burger, M., Zvaifler, N.J., Dell'Aquila, M., and Kipps, T.J. (2000). Blood-derived nurse-like cells protect chronic lymphocytic leukemia B cells from spontaneous apoptosis through stromal cell-derived factor-1. Blood *96*, 2655-2663.
- Busslinger, M. (2004). Transcriptional control of early B cell development. Annu Rev Immunol *22*, 55-79.
- Busslinger, M., Klix, N., Pfeffer, P., Graninger, P.G., and Kozmik, Z. (1996). Deregulation of PAX-5 by translocation of the Emu enhancer of the IgH locus adjacent to two alternative PAX-5 promoters in a diffuse large-cell lymphoma. Proc Natl Acad Sci U S A *93*, 6129-6134.
- Calame, K. (2001). Immunology. End game for B cells. Nature *412*, 289-290.
- Calvo, K.R., Dabir, B., Kovach, A., Devor, C., Bandle, R., Bond, A., Shih, J.H., and Jaffe, E.S. (2008). IL-4 protein expression and basal activation of Erk in vivo in follicular lymphoma. Blood *112*, 3818-3826.
- Camacho, E., Hernandez, L., Hernandez, S., Tort, F., Bellosillo, B., Bea, S., Bosch, F., Montserrat, E., Cardesa, A., Fernandez, P.L.*, et al.* (2002). ATM gene inactivation in mantle cell lymphoma mainly occurs by truncating mutations and missense mutations involving the phosphatidylinositol-3 kinase domain and is associated with increasing numbers of chromosomal imbalances. Blood *99*, 238-244.
- Camacho, F.I., Algara, P., Rodriguez, A., Ruiz-Ballesteros, E., Mollejo, M., Martinez, N., Martinez-Climent, J.A., Gonzalez, M., Mateo, M., Caleo, A.*, et al.* (2003). Molecular heterogeneity in MCL defined by the use of specific VH genes and the frequency of somatic mutations. Blood *101*, 4042-4046.

- Camacho, F.I., Garcia, J.F., Cigudosa, J.C., Mollejo, M., Algara, P., Ruiz-Ballesteros, E., Gonzalvo, P., Martin, P., Perez-Seoane, C., Sanchez-Garcia, J.*, et al.* (2004). Aberrant Bcl6 protein expression in mantle cell lymphoma. Am J Surg Pathol *28*, 1051-1056.
- Cao, R., Brakenhielm, E., Pawliuk, R., Wariaro, D., Post, M.J., Wahlberg, E., Leboulch, P., and Cao, Y. (2003). Angiogenic synergism, vascular stability and improvement of hind-limb ischemia by a combination of PDGF-BB and FGF-2. Nat Med *9*, 604-613.
- Cao, Y. (2013). Multifarious functions of PDGFs and PDGFRs in tumor growth and metastasis. Trends Mol Med *19*, 460-473.
- Cao, Y., Cao, R., and Hedlund, E.M. (2008). R Regulation of tumor angiogenesis and metastasis by FGF and PDGF signaling pathways. J Mol Med (Berl) *86*, 785-789.
- Cardesa-Salzmann, T.M., Colomo, L., Gutierrez, G., Chan, W.C., Weisenburger, D., Climent, F., Gonzalez-Barca, E., Mercadal, S., Arenillas, L., Serrano, S.*, et al.* (2011). High microvessel density determines a poor outcome in patients with diffuse large B-cell lymphoma treated with rituximab plus chemotherapy. Haematologica *96*, 996-1001.
- Cariappa, A., Liou, H.C., Horwitz, B.H., and Pillai, S. (2000). Nuclear factor kappa B is required for the development of marginal zone B lymphocytes. J Exp Med *192*, 1175-1182.
- Carmeliet, P. (2003). Angiogenesis in health and disease. Nat Med *9*, 653-660.
- Carmeliet, P., and Jain, R.K. (2011). Molecular mechanisms and clinical applications of angiogenesis. Nature *473*, 298-307.
- Carvajal-Cuenca, A., Sua, L.F., Silva, N.M., Pittaluga, S., Royo, C., Song, J.Y., Sargent, R.L., Espinet, B., Climent, F., Jacobs, S.A.*, et al.* (2012). In situ mantle cell lymphoma: clinical implications of an incidental finding with indolent clinical behavior. Haematologica *97*, 270-278.
- Casimiro, M.C., Crosariol, M., Loro, E., Ertel, A., Yu, Z., Dampier, W., Saria, E.A., Papanikolaou, A., Stanek, T.J., Li, Z.*, et al.* (2012). ChIP sequencing of cyclin D1 reveals a transcriptional role in chromosomal instability in mice. J Clin Invest *122*, 833-843.
- Cermenati, S., Moleri, S., Cimbro, S., Corti, P., Del Giacco, L., Amodeo, R., Dejana, E., Koopman, P., Cotelli, F., and Beltrame, M. (2008). Sox18 and Sox7 play redundant roles in vascular development. Blood *111*, 2657-2666.
- Cerutti, A., Cols, M., and Puga, I. (2013). Marginal zone B cells: virtues of innate-like antibody-producing lymphocytes. Nat Rev Immunol *13*, 118-132.

- Clasper, S., Royston, D., Baban, D., Cao, Y., Ewers, S., Butz, S., Vestweber, D., and Jackson, D.G. (2008). A novel gene expression profile in lymphatics associated with tumor growth and nodal metastasis. Cancer Res *68*, 7293-7303.
- Cobaleda, C., Jochum, W., and Busslinger, M. (2007a). Conversion of mature B cells into T cells by dedifferentiation to uncommitted progenitors. Nature *449*, 473-477.
- Cobaleda, C., Schebesta, A., Delogu, A., and Busslinger, M. (2007b). Pax5: the guardian of B cell identity and function. Nat Immunol *8*, 463-470.
- Coupland, S.E. (2011). The challenge of the microenvironment in B-cell lymphomas. Histopathology *58*, 69-80.
- Chang, C.P., de Vivo, I., and Cleary, M.L. (1997). The Hox cooperativity motif of the chimeric oncoprotein E2a-Pbx1 is necessary and sufficient for oncogenesis. Mol Cell Biol *17*, 81-88.
- Charbonneau, B., Maurer, M.J., Ansell, S.M., Slager, S.L., Fredericksen, Z.S., Ziesmer, S.C., Macon, W.R., Habermann, T.M., Witzig, T.E., Link, B.K.*, et al.* (2012). Pretreatment circulating serum cytokines associated with follicular and diffuse large B-cell lymphoma: a clinic-based case-control study. Cytokine *60*, 882-889.
- Chen, R.W., Bemis, L.T., Amato, C.M., Myint, H., Tran, H., Birks, D.K., Eckhardt, S.G., and Robinson, W.A. (2008). Truncation in CCND1 mRNA alters miR-16-1 regulation in mantle cell lymphoma. Blood *112*, 822-829.
- Cheng, Y.C., Lee, C.J., Badge, R.M., Orme, A.T., and Scotting, P.J. (2001). Sox8 gene expression identifies immature glial cells in developing cerebellum and cerebellar tumours. Brain Res Mol Brain Res *92*, 193-200.
- Chiarle, R., Budel, L.M., Skolnik, J., Frizzera, G., Chilosi, M., Corato, A., Pizzolo, G., Magidson, J., Montagnoli, A., Pagano, M.*, et al.* (2000). Increased proteasome degradation of cyclin-dependent kinase inhibitor p27 is associated with a decreased overall survival in mantle cell lymphoma. Blood *95*, 619-626.
- Damiano, J.S., Cress, A.E., Hazlehurst, L.A., Shtil, A.A., and Dalton, W.S. (1999). Cell adhesion mediated drug resistance (CAM-DR): role of integrins and resistance to apoptosis in human myeloma cell lines. Blood *93*, 1658-1667.
- Darby, I.A., Bisucci, T., Raghoenath, S., Olsson, J., Muscat, G.E., and Koopman, P. (2001). Sox18 is transiently expressed during angiogenesis in granulation tissue of skin wounds with an identical expression pattern to Flk-1 mRNA. Lab Invest *81*, 937-943.
- de Boer, C.J., Vaandrager, J.W., van Krieken, J.H., Holmes, Z., Kluin, P.M., and Schuuring, E. (1997). Visualization of mono-allelic chromosomal aberrations 3' and 5' of the cyclin D1 gene in mantle cell lymphoma using DNA fiber fluorescence in situ hybridization. Oncogene *15*, 1599-1603.

- de Bont, J.M., Kros, J.M., Passier, M.M., Reddingius, R.E., Sillevis Smitt, P.A., Luider, T.M., den Boer, M.L., and Pieters, R. (2008). Differential expression and prognostic significance of SOX genes in pediatric medulloblastoma and ependymoma identified by microarray analysis. Neuro Oncol *10*, 648-660.
- de Martino, S., Yan, Y.L., Jowett, T., Postlethwait, J.H., Varga, Z.M., Ashworth, A., and Austin, C.A. (2000). Expression of sox11 gene duplicates in zebrafish suggests the reciprocal loss of ancestral gene expression patterns in development. Dev Dyn *217*, 279-292.
- De Palma, M., Venneri, M.A., Roca, C., and Naldini, L. (2003). Targeting exogenous genes to tumor angiogenesis by transplantation of genetically modified hematopoietic stem cells. Nat Med *9*, 789-795.
- De, S., and Barnes, B.J. (2014). B cell transcription factors: Potential new therapeutic targets for SLE. Clin Immunol *152*, 140-151.
- DeNardo, D.G., Barreto, J.B., Andreu, P., Vasquez, L., Tawfik, D., Kolhatkar, N., and Coussens, L.M. (2009). CD4(+) T cells regulate pulmonary metastasis of mammary carcinomas by enhancing protumor properties of macrophages. Cancer Cell *16*, 91-102.
- Dias, S., Mansson, R., Gurbuxani, S., Sigvardsson, M., and Kee, B.L. (2008). E2A proteins promote development of lymphoid-primed multipotent progenitors. Immunity *29*, 217-227.
- Dictor, M., Ek, S., Sundberg, M., Warenholt, J., Gyorgy, C., Sernbo, S., Gustavsson, E., Abu-Alsoud, W., Wadstrom, T., and Borrebaeck, C. (2009). Strong lymphoid nuclear expression of SOX11 transcription factor defines lymphoblastic neoplasms, mantle cell lymphoma and Burkitt's lymphoma. Haematologica *94*, 1563-1568.
- Ding, W., Knox, T.R., Tschumper, R.C., Wu, W., Schwager, S.M., Boysen, J.C., Jelinek, D.F., and Kay, N.E. (2010). Platelet-derived growth factor (PDGF)-PDGF receptor interaction activates bone marrow-derived mesenchymal stromal cells derived from chronic lymphocytic leukemia: implications for an angiogenic switch. Blood *116*, 2984-2993.
- Dong, C., Wilhelm, D., and Koopman, P. (2004a). Sox genes and cancer. Cytogenet Genome Res *105*, 442-447.
- Dong, J., Grunstein, J., Tejada, M., Peale, F., Frantz, G., Liang, W.C., Bai, W., Yu, L., Kowalski, J., Liang, X.*, et al.* (2004b). VEGF-null cells require PDGFR alpha signaling-mediated stromal fibroblast recruitment for tumorigenesis. EMBO J *23*, 2800-2810.

- Donnem, T., Al-Saad, S., Al-Shibli, K., Andersen, S., Busund, L.T., and Bremnes, R.M. (2008). Prognostic impact of platelet-derived growth factors in non-small cell lung cancer tumor and stromal cells. J Thorac Oncol *3*, 963-970.
- Dy, P., Penzo-Mendez, A., Wang, H., Pedraza, C.E., Macklin, W.B., and Lefebvre, V. (2008). The three SoxC proteins--Sox4, Sox11 and Sox12--exhibit overlapping expression patterns and molecular properties. Nucleic Acids Res *36*, 3101-3117.
- Ek, S., Andreasson, U., Hober, S., Kampf, C., Ponten, F., Uhlen, M., Merz, H., and Borrebaeck, C.A. (2006). From gene expression analysis to tissue microarrays: a rational approach to identify therapeutic and diagnostic targets in lymphoid malignancies. Mol Cell Proteomics *5*, 1072-1081.
- Ek, S., Dictor, M., Jerkeman, M., Jirstrom, K., and Borrebaeck, C.A. (2008). Nuclear expression of the non B-cell lineage Sox11 transcription factor identifies mantle cell lymphoma. Blood *111*, 800-805.
- Eom, B.W., Jo, M.J., Kook, M.C., Ryu, K.W., Choi, I.J., Nam, B.H., Kim, Y.W., and Lee, J.H. (2012). The lymphangiogenic factor SOX 18: a key indicator to stage gastric tumor progression. Int J Cancer *131*, 41-48.
- Espinet, B., Ferrer, A., Bellosillo, B., Nonell, L., Salar, A., Fernandez-Rodriguez, C., Puigdecanet, E., Gimeno, J., Garcia-Garcia, M., Vela, M.C*., et al.* (2014). Distinction between asymptomatic monoclonal B-cell lymphocytosis with cyclin D1 overexpression and mantle cell lymphoma: from molecular profiling to flow cytometry. Clin Cancer Res *20*, 1007-1019.
- Espinet, B., Sole, F., Pedro, C., Garcia, M., Bellosillo, B., Salido, M., Florensa, L., Camacho, F.I., Baro, T., Lloreta, J*., et al.* (2005). Clonal proliferation of cyclin D1-positive mantle lymphocytes in an asymptomatic patient: an early-stage event in the development or an indolent form of a mantle cell lymphoma? Hum Pathol *36*, 1232-1237.
- Farinha, P., Kyle, A.H., Minchinton, A.I., Connors, J.M., Karsan, A., and Gascoyne, R.D. (2010). Vascularization predicts overall survival and risk of transformation in follicular lymphoma. Haematologica *95*, 2157-2160.
- Fernandez, V., Salamero, O., Espinet, B., Sole, F., Royo, C., Navarro, A., Camacho, F., Bea, S., Hartmann, E., Amador, V*., et al.* (2010). Genomic and gene expression profiling defines indolent forms of mantle cell lymphoma. Cancer Res *70*, 1408-1418.
- Ferrara, N. (2009). Vascular endothelial growth factor. Arterioscler Thromb Vasc Biol *29*, 789-791.
- Ferrara, N., Gerber, H.P., and LeCouter, J. (2003). The biology of VEGF and its receptors. Nat Med *9*, 669-676.

- Ferrara, N., and Kerbel, R.S. (2005). Angiogenesis as a therapeutic target. Nature *438*, 967-974.
- Ferreiros-Vidal, I., Carroll, T., Taylor, B., Terry, A., Liang, Z., Bruno, L., Dharmalingam, G., Khadayate, S., Cobb, B.S., Smale, S.T.*, et al.* (2013). Genome-wide identification of Ikaros targets elucidates its contribution to mouse B-cell lineage specification and pre-B-cell differentiation. Blood *121*, 1769-1782.
- Ferrer, A., Bosch, F., Villamor, N., Rozman, M., Graus, F., Gutierrez, G., Mercadal, S., Campo, E., Rozman, C., Lopez-Guillermo, A.*, et al.* (2008). Central nervous system involvement in mantle cell lymphoma. Ann Oncol *19*, 135-141.
- Fisher, R.I., Bernstein, S.H., Kahl, B.S., Djulbegovic, B., Robertson, M.J., de Vos, S., Epner, E., Krishnan, A., Leonard, J.P., Lonial, S.*, et al.* (2006). Multicenter phase II study of bortezomib in patients with relapsed or refractory mantle cell lymphoma. J Clin Oncol *24*, 4867-4874.
- Fitzgibbon, J., Smith, L.L., Raghavan, M., Smith, M.L., Debernardi, S., Skoulakis, S., Lillington, D., Lister, T.A., and Young, B.D. (2005). Association between acquired uniparental disomy and homozygous gene mutation in acute myeloid leukemias. Cancer Res *65*, 9152-9154.
- Folberg, R., Hendrix, M.J., and Maniotis, A.J. (2000). Vasculogenic mimicry and tumor angiogenesis. Am J Pathol *156*, 361-381.
- Folkman, J. (1985). Tumor angiogenesis. Adv Cancer Res *43*, 175-203.
- Ford, R.J., Shen, L., Lin-Lee, Y.C., Pham, L.V., Multani, A., Zhou, H.J., Tamayo, A.T., Zhang, C., Hawthorn, L., Cowell, J.K.*, et al.* (2007). Development of a murine model for blastoid variant mantle-cell lymphoma. Blood *109*, 4899-4906.
- Fortney, J.E., Hall, B.M., Bartrug, L., and Gibson, L.F. (2002). Chemotherapy induces bcl-2 cleavage in lymphoid leukemic cell lines. Leuk Lymphoma *43*, 2171-2178.
- Francois, M., Koopman, P., and Beltrame, M. (2010). SoxF genes: Key players in the development of the cardio-vascular system. Int J Biochem Cell Biol *42*, 445-448.
- Frierson, H.F., Jr., El-Naggar, A.K., Welsh, J.B., Sapinoso, L.M., Su, A.I., Cheng, J., Saku, T., Moskaluk, C.A., and Hampton, G.M. (2002). Large scale molecular analysis identifies genes with altered expression in salivary adenoid cystic carcinoma. Am J Pathol *161*, 1315-1323.
- Fu, K., Weisenburger, D.D., Greiner, T.C., Dave, S., Wright, G., Rosenwald, A., Chiorazzi, M., Iqbal, J., Gesk, S., Siebert, R.*, et al.* (2005). Cyclin D1-negative mantle cell lymphoma: a clinicopathologic study based on gene expression profiling. Blood *106*, 4315-4321.

- Fu, M., Wang, C., Li, Z., Sakamaki, T., and Pestell, R.G. (2004). Minireview: Cyclin D1: normal and abnormal functions. Endocrinology *145*, 5439-5447.
- Fuxa, M., and Busslinger, M. (2007). Reporter gene insertions reveal a strictly B lymphoid-specific expression pattern of Pax5 in support of its B cell identity function. J Immunol *178*, 8222-8228.
- Ganjoo, K.N., Moore, A.M., Orazi, A., Sen, J.A., Johnson, C.S., and An, C.S. (2008). The importance of angiogenesis markers in the outcome of patients with diffuse large B cell lymphoma: a retrospective study of 97 patients. J Cancer Res Clin Oncol *134*, 381-387.
- Gascoyne, R.D., Rosenwald, A., Poppema, S., and Lenz, G. (2010). Prognostic biomarkers in malignant lymphomas. Leuk Lymphoma *51 Suppl 1*, 11-19.
- Georgopoulos, K., Bigby, M., Wang, J.H., Molnar, A., Wu, P., Winandy, S., and Sharpe, A. (1994). The Ikaros gene is required for the development of all lymphoid lineages. Cell *79*, 143-156.
- Gesk, S., Klapper, W., Martin-Subero, J.I., Nagel, I., Harder, L., Fu, K., Bernd, H.W., Weisenburger, D.D., Parwaresch, R., and Siebert, R. (2006). A chromosomal translocation in cyclin D1-negative/cyclin D2-positive mantle cell lymphoma fuses the CCND2 gene to the IGK locus. Blood *108*, 1109-1110.
- Giltiay, N.V., Chappell, C.P., and Clark, E.A. (2012). B-cell selection and the development of autoantibodies. Arthritis Res Ther *14 Suppl 4*, S1.
- Gladden, A.B., Woolery, R., Aggarwal, P., Wasik, M.A., and Diehl, J.A. (2006). Expression of constitutively nuclear cyclin D1 in murine lymphocytes induces B-cell lymphoma. Oncogene *25*, 998-1007.
- Gnessi, L., Basciani, S., Mariani, S., Arizzi, M., Spera, G., Wang, C., Bondjers, C., Karlsson, L., and Betsholtz, C. (2000). Leydig cell loss and spermatogenic arrest in platelet-derived growth factor (PDGF)-A-deficient mice. J Cell Biol *149*, 1019-1026.
- Goetz, C.A., and Baldwin, A.S. (2008). NF-kappaB pathways in the immune system: control of the germinal center reaction. Immunol Res *41*, 233-247.
- Gong, J.Z., Lagoo, A.S., Peters, D., Horvatinovich, J., Benz, P., and Buckley, P.J. (2001). Value of CD23 determination by flow cytometry in differentiating mantle cell lymphoma from chronic lymphocytic leukemia/small lymphocytic lymphoma. Am J Clin Pathol *116*, 893-897.
- Gounari, F., Aifantis, I., Martin, C., Fehling, H.J., Hoeflinger, S., Leder, P., von Boehmer, H., and Reizis, B. (2002). Tracing lymphopoiesis with the aid of a pTalpha-controlled reporter gene. Nat Immunol *3*, 489-496.

- Goy, A., Bernstein, S.H., Kahl, B.S., Djulbegovic, B., Robertson, M.J., de Vos, S., Epner, E., Krishnan, A., Leonard, J.P., Lonial, S., *et al.* (2009). Bortezomib in patients with relapsed or refractory mantle cell lymphoma: updated time-to-event analyses of the multicenter phase 2 PINNACLE study. Ann Oncol *20*, 520-525.
- Goy, A., Sinha, R., Williams, M.E., Kalayoglu Besisik, S., Drach, J., Ramchandren, R., Zhang, L., Cicero, S., Fu, T., and Witzig, T.E. (2013). Single-agent lenalidomide in patients with mantle-cell lymphoma who relapsed or progressed after or were refractory to bortezomib: phase II MCL-001 (EMERGE) study. J Clin Oncol *31*, 3688-3695.
- Gradowski, J.F., Jaffe, E.S., Warnke, R.A., Pittaluga, S., Surti, U., Gole, L.A., and Swerdlow, S.H. (2010). Follicular lymphomas with plasmacytic differentiation include two subtypes. Mod Pathol *23*, 71-79.
- Graham, J.D., Hunt, S.M., Tran, N., and Clarke, C.L. (1999). Regulation of the expression and activity by progestins of a member of the SOX gene family of transcriptional modulators. J Mol Endocrinol *22*, 295-304.
- Greiner, T.C., Moynihan, M.J., Chan, W.C., Lytle, D.M., Pedersen, A., Anderson, J.R., and Weisenburger, D.D. (1996). p53 mutations in mantle cell lymphoma are associated with variant cytology and predict a poor prognosis. Blood *87*, 4302-4310.
- Grothey, A., and Galanis, E. (2009). Targeting angiogenesis: progress with anti-VEGF treatment with large molecules. Nat Rev Clin Oncol *6*, 507-518.
- Guo, P., Hu, B., Gu, W., Xu, L., Wang, D., Huang, H.J., Cavenee, W.K., and Cheng, S.Y. (2003). Platelet-derived growth factor-B enhances glioma angiogenesis by stimulating vascular endothelial growth factor expression in tumor endothelia and by promoting pericyte recruitment. Am J Pathol *162*, 1083-1093.
- Gure, A.O., Stockert, E., Scanlan, M.J., Keresztes, R.S., Jager, D., Altorki, N.K., Old, L.J., and Chen, Y.T. (2000). Serological identification of embryonic neural proteins as highly immunogenic tumor antigens in small cell lung cancer. Proc Natl Acad Sci U S A *97*, 4198-4203.
- Gustavsson, E., Sernbo, S., Andersson, E., Brennan, D.J., Dictor, M., Jerkeman, M., Borrebaeck, C.A., and Ek, S. (2010). SOX11 expression correlates to promoter methylation and regulates tumor growth in hematopoietic malignancies. Mol Cancer *9*, 187.
- Gyory, I., Boller, S., Nechanitzky, R., Mandel, E., Pott, S., Liu, E., and Grosschedl, R. (2012). Transcription factor Ebf1 regulates differentiation stage-specific signaling, proliferation, and survival of B cells. Genes Dev *26*, 668-682.
- Hadzidimitriou, A., Agathangelidis, A., Darzentas, N., Murray, F., Delfau-Larue, M.H., Pedersen, L.B., Lopez, A.N., Dagklis, A., Rombout, P., Beldjord, K., *et al.* (2011). Is

there a role for antigen selection in mantle cell lymphoma? Immunogenetic support from a series of 807 cases. Blood *118*, 3088-3095.

- Hanahan, D., and Coussens, L.M. (2012). Accessories to the crime: functions of cells recruited to the tumor microenvironment. Cancer Cell *21*, 309-322.
- Hanahan, D., and Folkman, J. (1996). Patterns and emerging mechanisms of the angiogenic switch during tumorigenesis. Cell *86*, 353-364.
- Hanahan, D., and Weinberg, R.A. (2011). Hallmarks of cancer: the next generation. Cell *144*, 646-674.
- Hao, S., Sanger, W., Onciu, M., Lai, R., Schlette, E.J., and Medeiros, L.J. (2002). Mantle cell lymphoma with 8q24 chromosomal abnormalities: a report of 5 cases with blastoid features. Mod Pathol *15*, 1266-1272.
- Harbour, J.W., and Dean, D.C. (2000). The Rb/E2F pathway: expanding roles and emerging paradigms. Genes Dev *14*, 2393-2409.
- Hargrave, M., Wright, E., Kun, J., Emery, J., Cooper, L., and Koopman, P. (1997). Expression of the Sox11 gene in mouse embryos suggests roles in neuronal maturation and epithelio-mesenchymal induction. Dev Dyn *210*, 79-86.
- Harwood, N.E., and Batista, F.D. (2010). Early events in B cell activation. Annu Rev Immunol *28*, 185-210.
- Hashizume, H., Falcon, B.L., Kuroda, T., Baluk, P., Coxon, A., Yu, D., Bready, J.V., Oliner, J.D., and McDonald, D.M. (2010). Complementary actions of inhibitors of angiopoietin-2 and VEGF on tumor angiogenesis and growth. Cancer Res *70*, 2213-2223.
- Haslinger, A., Schwarz, T.J., Covic, M., and Lie, D.C. (2009). Expression of Sox11 in adult neurogenic niches suggests a stage-specific role in adult neurogenesis. Eur J Neurosci *29*, 2103-2114.
- Hattori, K., Dias, S., Heissig, B., Hackett, N.R., Lyden, D., Tateno, M., Hicklin, D.J., Zhu, Z., Witte, L., Crystal, R.G.*, et al.* (2001). Vascular endothelial growth factor and angiopoietin-1 stimulate postnatal hematopoiesis by recruitment of vasculogenic and hematopoietic stem cells. J Exp Med *193*, 1005-1014.
- Hattori, K., Heissig, B., Wu, Y., Dias, S., Tejada, R., Ferris, B., Hicklin, D.J., Zhu, Z., Bohlen, P., Witte, L.*, et al.* (2002). Placental growth factor reconstitutes hematopoiesis by recruiting VEGFR1(+) stem cells from bone-marrow microenvironment. Nat Med *8*, 841-849.
- Heinrich, M.C., Corless, C.L., Duensing, A., McGreevey, L., Chen, C.J., Joseph, N., Singer, S., Griffith, D.J., Haley, A., Town, A.*, et al.* (2003). PDGFRA activating mutations in gastrointestinal stromal tumors. Science *299*, 708-710.

- Heldin, C.H. (2013). Targeting the PDGF signaling pathway in tumor treatment. Cell Commun Signal *11*, 97.
- Heldin, C.H., and Westermark, B. (1999). Mechanism of action and in vivo role of platelet-derived growth factor. Physiol Rev *79*, 1283-1316.
- Hellberg, C., Ostman, A., and Heldin, C.H. (2010). PDGF and vessel maturation. Recent Results Cancer Res *180*, 103-114.
- Hellstrom, M., Kalen, M., Lindahl, P., Abramsson, A., and Betsholtz, C. (1999). Role of PDGF-B and PDGFR-beta in recruitment of vascular smooth muscle cells and pericytes during embryonic blood vessel formation in the mouse. Development *126*, 3047-3055.
- Herblot, S., Aplan, P.D., and Hoang, T. (2002). Gradient of E2A activity in B-cell development. Mol Cell Biol *22*, 886-900.
- Herens, C., Lambert, F., Quintanilla-Martinez, L., Bisig, B., Deusings, C., and de Leval, L. (2008). Cyclin D1-negative mantle cell lymphoma with cryptic t(12;14)(p13;q32) and cyclin D2 overexpression. Blood *111*, 1745-1746.
- Hermanson, M., Funa, K., Hartman, M., Claesson-Welsh, L., Heldin, C.H., Westermark, B., and Nister, M. (1992). Platelet-derived growth factor and its receptors in human glioma tissue: expression of messenger RNA and protein suggests the presence of autocrine and paracrine loops. Cancer Res *52*, 3213-3219.
- Hernandez, L., Bea, S., Pinyol, M., Ott, G., Katzenberger, T., Rosenwald, A., Bosch, F., Lopez-Guillermo, A., Delabie, J., Colomer, D.*, et al.* (2005). CDK4 and MDM2 gene alterations mainly occur in highly proliferative and aggressive mantle cell lymphomas with wild-type INK4a/ARF locus. Cancer Res *65*, 2199-2206.
- Hernandez, L., Fest, T., Cazorla, M., Teruya-Feldstein, J., Bosch, F., Peinado, M.A., Piris, M.A., Montserrat, E., Cardesa, A., Jaffe, E.S.*, et al.* (1996). p53 gene mutations and protein overexpression are associated with aggressive variants of mantle cell lymphomas. Blood *87*, 3351-3359.
- Hesslein, D.G., Pflugh, D.L., Chowdhury, D., Bothwell, A.L., Sen, R., and Schatz, D.G. (2003). Pax5 is required for recombination of transcribed, acetylated, 5' IgH V gene segments. Genes Dev *17*, 37-42.
- Hirt, C., Schuler, F., Dolken, L., Schmidt, C.A., and Dolken, G. (2004). Low prevalence of circulating t(11;14)(q13;q32)-positive cells in the peripheral blood of healthy individuals as detected by real-time quantitative PCR. Blood *104*, 904-905.
- Ho, C.L., Sheu, L.F., and Li, C.Y. (2002). Immunohistochemical expression of basic fibroblast growth factor, vascular endothelial growth factor, and their receptors in stage IV non-Hodgkin lymphoma. Appl Immunohistochem Mol Morphol *10*, 316-321.

- Hoffman, D.G., Tucker, S.J., Emmanoulides, C., Rosen, P.A., and Naeim, F. (1998). CD8-positive mantle cell lymphoma: a report of two cases. Am J Clin Pathol *109*, 689-694.
- Hofmann, W.K., de Vos, S., Tsukasaki, K., Wachsman, W., Pinkus, G.S., Said, J.W., and Koeffler, H.P. (2001). Altered apoptosis pathways in mantle cell lymphoma detected by oligonucleotide microarray. Blood *98*, 787-794.
- Horcher, M., Souabni, A., and Busslinger, M. (2001). Pax5/BSAP maintains the identity of B cells in late B lymphopoiesis. Immunity *14*, 779-790.
- Hoser, M., Potzner, M.R., Koch, J.M., Bosl, M.R., Wegner, M., and Sock, E. (2008). Sox12 deletion in the mouse reveals nonreciprocal redundancy with the related Sox4 and Sox11 transcription factors. Mol Cell Biol *28*, 4675-4687.
- Hosking, B.M., Wang, S.C., Chen, S.L., Penning, S., Koopman, P., and Muscat, G.E. (2001). SOX18 directly interacts with MEF2C in endothelial cells. Biochem Biophys Res Commun *287*, 493-500.
- Hosking, B.M., Wang, S.C., Downes, M., Koopman, P., and Muscat, G.E. (2004). The VCAM-1 gene that encodes the vascular cell adhesion molecule is a target of the Sry-related high mobility group box gene, Sox18. J Biol Chem *279*, 5314-5322.
- Hsi, E.D., and Martin, P. (2014). Indolent mantle cell lymphoma. Leuk Lymphoma *55*, 761-767.
- Hudson, C., Clements, D., Friday, R.V., Stott, D., and Woodland, H.R. (1997). Xsox17alpha and -beta mediate endoderm formation in Xenopus. Cell *91*, 397-405.
- Iida, S., Rao, P.H., Nallasivam, P., Hibshoosh, H., Butler, M., Louie, D.C., Dyomin, V., Ohno, H., Chaganti, R.S., and Dalla-Favera, R. (1996). The t(9;14)(p13;q32) chromosomal translocation associated with lymphoplasmacytoid lymphoma involves the PAX-5 gene. Blood *88*, 4110-4117.
- Jain, R.K. (2003). Molecular regulation of vessel maturation. Nat Med *9*, 685-693.
- Jankowski, M.P., Cornuet, P.K., McIlwrath, S., Koerber, H.R., and Albers, K.M. (2006). SRY-box containing gene 11 (Sox11) transcription factor is required for neuron survival and neurite growth. Neuroscience *143*, 501-514.
- Jares, P., and Campo, E. (2008). Advances in the understanding of mantle cell lymphoma. Br J Haematol *142*, 149-165.
- Jares, P., Campo, E., Pinyol, M., Bosch, F., Miquel, R., Fernandez, P.L., Sanchez-Beato, M., Soler, F., Perez-Losada, A., Nayach, I.*, et al.* (1996). Expression of retinoblastoma gene product (pRb) in mantle cell lymphomas. Correlation with cyclin D1 (PRAD1/CCND1) mRNA levels and proliferative activity. Am J Pathol *148*, 1591-1600.

- Jares, P., Colomer, D., and Campo, E. (2007). Genetic and molecular pathogenesis of mantle cell lymphoma: perspectives for new targeted therapeutics. Nat Rev Cancer *7*, 750-762.
- Jares, P., Colomer, D., and Campo, E. (2012). Molecular pathogenesis of mantle cell lymphoma. J Clin Invest *122*, 3416-3423.
- Jiang, Q., Feng, M.G., and Mo, Y.Y. (2009). Systematic validation of predicted microRNAs for cyclin D1. BMC Cancer *9*, 194.
- Jirawatnotai, S., Hu, Y., Michowski, W., Elias, J.E., Becks, L., Bienvenu, F., Zagozdzon, A., Goswami, T., Wang, Y.E., Clark, A.B.*, et al.* (2011). A function for cyclin D1 in DNA repair uncovered by protein interactome analyses in human cancers. Nature *474*, 230-234.
- Kallies, A., and Nutt, S.L. (2007). Terminal differentiation of lymphocytes depends on Blimp-1. Curr Opin Immunol *19*, 156-162.
- Karlsson, L., Lindahl, P., Heath, J.K., and Betsholtz, C. (2000). Abnormal gastrointestinal development in PDGF-A and PDGFR-(alpha) deficient mice implicates a novel mesenchymal structure with putative instructive properties in villus morphogenesis. Development *127*, 3457-3466.
- Katz, S.G., Labelle, J.L., Meng, H., Valeriano, R.P., Fisher, J.K., Sun, H., Rodig, S.J., Kleinstein, S.H., and Walensky, L.D. (2014). Mantle cell lymphoma in cyclin D1 transgenic mice with Bim-deficient B cells. Blood *123*, 884-893.
- Kerbel, R.S. (2008). Tumor angiogenesis. N Engl J Med *358*, 2039-2049.
- Khong, H.T., and Rosenberg, S.A. (2002). The Waardenburg syndrome type 4 gene, SOX10, is a novel tumor-associated antigen identified in a patient with a dramatic response to immunotherapy. Cancer Res *62*, 3020-3023.
- Kikuchi, M., Miki, T., Kumagai, T., Fukuda, T., Kamiyama, R., Miyasaka, N., and Hirosawa, S. (2000). Identification of negative regulatory regions within the first exon and intron of the BCL6 gene. Oncogene *19*, 4941-4945.
- Kim, R., Trubetskoy, A., Suzuki, T., Jenkins, N.A., Copeland, N.G., and Lenz, J. (2003). Genome-based identification of cancer genes by proviral tagging in mouse retrovirus-induced T-cell lymphomas. J Virol *77*, 2056-2062.
- Klein, U., Casola, S., Cattoretti, G., Shen, Q., Lia, M., Mo, T., Ludwig, T., Rajewsky, K., and Dalla-Favera, R. (2006). Transcription factor IRF4 controls plasma cell differentiation and class-switch recombination. Nat Immunol *7*, 773-782.
- Knodel, M., Kuss, A.W., Lindemann, D., Berberich, I., and Schimpl, A. (1999). Reversal of Blimp-1-mediated apoptosis by A1, a member of the Bcl-2 family. Eur J Immunol *29*, 2988-2998.

- Korc, M., and Friesel, R.E. (2009). The role of fibroblast growth factors in tumor growth. Curr Cancer Drug Targets *9*, 639-651.
- Korkolopoulou, P., Thymara, I., Kavantzas, N., Vassilakopoulos, T.P., Angelopoulou, M.K., Kokoris, S.I., Dimitriadou, E.M., Siakantaris, M.P., Anargyrou, K., Panayiotidis, P.*, et al.* (2005). Angiogenesis in Hodgkin's lymphoma: a morphometric approach in 286 patients with prognostic implications. Leukemia *19*, 894-900.
- Koster, A., and Raemaekers, J.M. (2005). Angiogenesis in malignant lymphoma. Curr Opin Oncol *17*, 611-616.
- Kridel, R., Meissner, B., Rogic, S., Boyle, M., Telenius, A., Woolcock, B., Gunawardana, J., Jenkins, C., Cochrane, C., Ben-Neriah, S.*, et al.* (2012). Whole transcriptome sequencing reveals recurrent NOTCH1 mutations in mantle cell lymphoma. Blood *119*, 1963-1971.
- Kuhlbrodt, K., Herbarth, B., Sock, E., Enderich, J., Hermans-Borgmeyer, I., and Wegner, M. (1998a). Cooperative function of POU proteins and SOX proteins in glial cells. J Biol Chem *273*, 16050-16057.
- Kuhlbrodt, K., Herbarth, B., Sock, E., Hermans-Borgmeyer, I., and Wegner, M. (1998b). Sox10, a novel transcriptional modulator in glial cells. J Neurosci *18*, 237-250.
- Kuiper, R.P., Schoenmakers, E.F., van Reijmersdal, S.V., Hehir-Kwa, J.Y., van Kessel, A.G., van Leeuwen, F.N., and Hoogerbrugge, P.M. (2007). High-resolution genomic profiling of childhood ALL reveals novel recurrent genetic lesions affecting pathways involved in lymphocyte differentiation and cell cycle progression. Leukemia *21*, 1258-1266.
- Kuramoto, K., Sakai, A., Shigemasa, K., Takimoto, Y., Asaoku, H., Tsujimoto, T., Oda, K., Kimura, A., Uesaka, T., Watanabe, H.*, et al.* (2002). High expression of MCL1 gene related to vascular endothelial growth factor is associated with poor outcome in non-Hodgkin's lymphoma. Br J Haematol *116*, 158-161.
- Kurtova, A.V., Tamayo, A.T., Ford, R.J., and Burger, J.A. (2009). Mantle cell lymphoma cells express high levels of CXCR4, CXCR5, and VLA-4 (CD49d): importance for interactions with the stromal microenvironment and specific targeting. Blood *113*, 4604-4613.
- Kwon, K., Hutter, C., Sun, Q., Bilic, I., Cobaleda, C., Malin, S., and Busslinger, M. (2008). Instructive role of the transcription factor E2A in early B lymphopoiesis and germinal center B cell development. Immunity *28*, 751-762.
- LeBien, T.W. (2000). Fates of human B-cell precursors. Blood *96*, 9-23.
- LeBien, T.W., and Tedder, T.F. (2008). B lymphocytes: how they develop and function. Blood *112*, 1570-1580.

- Lee, C.J., Appleby, V.J., Orme, A.T., Chan, W.I., and Scotting, P.J. (2002). Differential expression of SOX4 and SOX11 in medulloblastoma. J Neurooncol *57*, 201-214.
- Lee, S., Chen, T.T., Barber, C.L., Jordan, M.C., Murdock, J., Desai, S., Ferrara, N., Nagy, A., Roos, K.P., and Iruela-Arispe, M.L. (2007). Autocrine VEGF signaling is required for vascular homeostasis. Cell *130*, 691-703.
- Lefebvre, V., Dumitriu, B., Penzo-Mendez, A., Han, Y., and Pallavi, B. (2007). Control of cell fate and differentiation by Sry-related high-mobility-group box (Sox) transcription factors. Int J Biochem Cell Biol *39*, 2195-2214.
- Leich, E., Hartmann, E.M., Burek, C., Ott, G., and Rosenwald, A. (2007). Diagnostic and prognostic significance of gene expression profiling in lymphomas. APMIS *115*, 1135-1146.
- Li, X., Tjwa, M., Moons, L., Fons, P., Noel, A., Ny, A., Zhou, J.M., Lennartsson, J., Li, H., Luttun, A.*, et al.* (2005). Revascularization of ischemic tissues by PDGF-CC via effects on endothelial cells and their progenitors. J Clin Invest *115*, 118-127.
- Lin, K.I., Angelin-Duclos, C., Kuo, T.C., and Calame, K. (2002). Blimp-1-dependent repression of Pax-5 is required for differentiation of B cells to immunoglobulin M-secreting plasma cells. Mol Cell Biol *22*, 4771-4780.
- Lin, L., Lee, V.M., Wang, Y., Lin, J.S., Sock, E., Wegner, M., and Lei, L. (2011). Sox11 regulates survival and axonal growth of embryonic sensory neurons. Dev Dyn *240*, 52-64.
- Lin, Y.C., Jhunjhunwala, S., Benner, C., Heinz, S., Welinder, E., Mansson, R., Sigvardsson, M., Hagman, J., Espinoza, C.A., Dutkowski, J.*, et al.* (2010). A global network of transcription factors, involving E2A, EBF1 and Foxo1, that orchestrates B cell fate. Nat Immunol *11*, 635-643.
- Lindner, V., Majack, R.A., and Reidy, M.A. (1990). Basic fibroblast growth factor stimulates endothelial regrowth and proliferation in denuded arteries. J Clin Invest *85*, 2004-2008.
- Linterman, M.A., Rigby, R.J., Wong, R.K., Yu, D., Brink, R., Cannons, J.L., Schwartzberg, P.L., Cook, M.C., Walters, G.D., and Vinuesa, C.G. (2009). Follicular helper T cells are required for systemic autoimmunity. J Exp Med *206*, 561-576.
- Liu, P., Ramachandran, S., Ali Seyed, M., Scharer, C.D., Laycock, N., Dalton, W.B., Williams, H., Karanam, S., Datta, M.W., Jaye, D.L.*, et al.* (2006). Sex-determining region Y box 4 is a transforming oncogene in human prostate cancer cells. Cancer Res *66*, 4011-4019.

- Lopez, F.J., Cuadros, M., Cano, C., Concha, A., and Blanco, A. (2012). Biomedical application of fuzzy association rules for identifying breast cancer biomarkers. Med Biol Eng Comput *50*, 981-990.
- Lovec, H., Grzeschiczek, A., Kowalski, M.B., and Moroy, T. (1994). Cyclin D1/bcl-1 cooperates with myc genes in the generation of B-cell lymphoma in transgenic mice. EMBO J *13*, 3487-3495.
- Lu, R. (2008). Interferon regulatory factor 4 and 8 in B-cell development. Trends Immunol *29*, 487-492.
- Lyden, D., Hattori, K., Dias, S., Costa, C., Blaikie, P., Butros, L., Chadburn, A., Heissig, B., Marks, W., Witte, L.*, et al.* (2001). Impaired recruitment of bone-marrow-derived endothelial and hematopoietic precursor cells blocks tumor angiogenesis and growth. Nat Med *7*, 1194-1201.
- Mancuso, P., Burlini, A., Pruneri, G., Goldhirsch, A., Martinelli, G., and Bertolini, F. (2001). Resting and activated endothelial cells are increased in the peripheral blood of cancer patients. Blood *97*, 3658-3661.
- Mandel, E.M., and Grosschedl, R. (2010). Transcription control of early B cell differentiation. Curr Opin Immunol *22*, 161-167.
- Mandelbaum, J., Bhagat, G., Tang, H., Mo, T., Brahmachary, M., Shen, Q., Chadburn, A., Rajewsky, K., Tarakhovsky, A., Pasqualucci, L.*, et al.* (2010). BLIMP1 is a tumor suppressor gene frequently disrupted in activated B cell-like diffuse large B cell lymphoma. Cancer Cell *18*, 568-579.
- Martin, P., Chadburn, A., Christos, P., Weil, K., Furman, R.R., Ruan, J., Elstrom, R., Niesvizky, R., Ely, S., Diliberto, M.*, et al.* (2009). Outcome of deferred initial therapy in mantle-cell lymphoma. J Clin Oncol *27*, 1209-1213.
- Martinez, D., Valera, A., Perez, N.S., Sua Villegas, L.F., Gonzalez-Farre, B., Sole, C., Gine, E., Lopez-Guillermo, A., Roue, G., Martinez, S.*, et al.* (2013). Plasmablastic transformation of low-grade B-cell lymphomas: report on 6 cases. Am J Surg Pathol *37*, 272-281.
- Martinez, N., Camacho, F.I., Algara, P., Rodriguez, A., Dopazo, A., Ruiz-Ballesteros, E., Martin, P., Martinez-Climent, J.A., Garcia-Conde, J., Menarguez, J.*, et al.* (2003). The molecular signature of mantle cell lymphoma reveals multiple signals favoring cell survival. Cancer Res *63*, 8226-8232.
- Marzec, M., Kasprzycka, M., Lai, R., Gladden, A.B., Wlodarski, P., Tomczak, E., Nowell, P., Deprimo, S.E., Sadis, S., Eck, S.*, et al.* (2006). Mantle cell lymphoma cells express predominantly cyclin D1a isoform and are highly sensitive to selective inhibition of CDK4 kinase activity. Blood *108*, 1744-1750.

- Maschhoff, K.L., Anziano, P.Q., Ward, P., and Baldwin, H.S. (2003). Conservation of Sox4 gene structure and expression during chicken embryogenesis. Gene *320*, 23-30.
- Matsui, T., Kanai-Azuma, M., Hara, K., Matoba, S., Hiramatsu, R., Kawakami, H., Kurohmaru, M., Koopman, P., and Kanai, Y. (2006). Redundant roles of Sox17 and Sox18 in postnatal angiogenesis in mice. J Cell Sci *119*, 3513-3526.
- Matthias, P., and Rolink, A.G. (2005). Transcriptional networks in developing and mature B cells. Nat Rev Immunol *5*, 497-508.
- Mavropoulos, A., Devos, N., Biemar, F., Zecchin, E., Argenton, F., Edlund, H., Motte, P., Martial, J.A., and Peers, B. (2005). sox4b is a key player of pancreatic alpha cell differentiation in zebrafish. Dev Biol *285*, 211-223.
- McCarty, M.F., Somcio, R.J., Stoeltzing, O., Wey, J., Fan, F., Liu, W., Bucana, C., and Ellis, L.M. (2007). Overexpression of PDGF-BB decreases colorectal and pancreatic cancer growth by increasing tumor pericyte content. J Clin Invest *117*, 2114-2122.
- McDonald, D.M., Munn, L., and Jain, R.K. (2000). Vasculogenic mimicry: how convincing, how novel, and how significant? Am J Pathol *156*, 383-388.
- McKercher, S.R., Torbett, B.E., Anderson, K.L., Henkel, G.W., Vestal, D.J., Baribault, H., Klemsz, M., Feeney, A.J., Wu, G.E., Paige, C.J.*, et al.* (1996). Targeted disruption of the PU.1 gene results in multiple hematopoietic abnormalities. EMBO J *15*, 5647-5658.
- Medina, P.P., Castillo, S.D., Blanco, S., Sanz-Garcia, M., Largo, C., Alvarez, S., Yokota, J., Gonzalez-Neira, A., Benitez, J., Clevers, H.C.*, et al.* (2009). The SRY-HMG box gene, SOX4, is a target of gene amplification at chromosome 6p in lung cancer. Hum Mol Genet *18*, 1343-1352.
- Medvedovic, J., Ebert, A., Tagoh, H., and Busslinger, M. (2011). Pax5: a master regulator of B cell development and leukemogenesis. Adv Immunol *111*, 179-206.
- Mezei, T., Horvath, E., Turcu, M., Gurzu, S., Raica, M., and Jung, I. (2012). Microvascular density in non-Hodgkin B-cell lymphomas measured using digital morphometry. Rom J Morphol Embryol *53*, 67-71.
- Monestiroli, S., Mancuso, P., Burlini, A., Pruneri, G., Dell'Agnola, C., Gobbi, A., Martinelli, G., and Bertolini, F. (2001). Kinetics and viability of circulating endothelial cells as surrogate angiogenesis marker in an animal model of human lymphoma. Cancer Res *61*, 4341-4344.
- Montes-Moreno, S., Gonzalez-Medina, A.R., Rodriguez-Pinilla, S.M., Maestre, L., Sanchez-Verde, L., Roncador, G., Mollejo, M., Garcia, J.F., Menarguez, J., Montalban, C.*, et al.* (2010). Aggressive large B-cell lymphoma with plasma cell differentiation:

immunohistochemical characterization of plasmablastic lymphoma and diffuse large B-cell lymphoma with partial plasmablastic phenotype. Haematologica *95*, 1342-1349.

- Montes-Moreno, S., Montalban, C., and Piris, M.A. (2012). Large B-cell lymphomas with plasmablastic differentiation: a biological and therapeutic challenge. Leuk Lymphoma *53*, 185-194.
- Montserrat, E., Bosch, F., Lopez-Guillermo, A., Graus, F., Terol, M.J., Campo, E., and Rozman, C. (1996). CNS involvement in mantle-cell lymphoma. J Clin Oncol *14*, 941-944.
- Mora-Lopez, F., Reales, E., Brieva, J.A., and Campos-Caro, A. (2007). Human BSAP and BLIMP1 conform an autoregulatory feedback loop. Blood *110*, 3150-3157.
- Morrison, A.M., Jager, U., Chott, A., Schebesta, M., Haas, O.A., and Busslinger, M. (1998). Deregulated PAX-5 transcription from a translocated IgH promoter in marginal zone lymphoma. Blood *92*, 3865-3878.
- Mozos, A., Royo, C., Hartmann, E., De Jong, D., Baro, C., Valera, A., Fu, K., Weisenburger, D.D., Delabie, J., Chuang, S.S.*, et al.* (2009). SOX11 expression is highly specific for mantle cell lymphoma and identifies the cyclin D1-negative subtype. Haematologica *94*, 1555-1562.
- Mullighan, C.G., Goorha, S., Radtke, I., Miller, C.B., Coustan-Smith, E., Dalton, J.D., Girtman, K., Mathew, S., Ma, J., Pounds, S.B.*, et al.* (2007). Genome-wide analysis of genetic alterations in acute lymphoblastic leukaemia. Nature *446*, 758-764.
- Murakami, M., Nguyen, L.T., Zhuang, Z.W., Moodie, K.L., Carmeliet, P., Stan, R.V., and Simons, M. (2008). The FGF system has a key role in regulating vascular integrity. J Clin Invest *118*, 3355-3366.
- Muramatsu, M., Kinoshita, K., Fagarasan, S., Yamada, S., Shinkai, Y., and Honjo, T. (2000). Class switch recombination and hypermutation require activation-induced cytidine deaminase (AID), a potential RNA editing enzyme. Cell *102*, 553-563.
- Nagy, J.A., Dvorak, A.M., and Dvorak, H.F. (2007). VEGF-A and the induction of pathological angiogenesis. Annu Rev Pathol *2*, 251-275.
- Nakamura, N., Hase, H., Sakurai, D., Yoshida, S., Abe, M., Tsukada, N., Takizawa, J., Aoki, S., Kojima, M., Nakamura, S.*, et al.* (2005). Expression of BAFF-R (BR 3) in normal and neoplastic lymphoid tissues characterized with a newly developed monoclonal antibody. Virchows Arch *447*, 53-60.
- Naushad, H., Choi, W.W., Page, C.J., Sanger, W.G., Weisenburger, D.D., and Aoun, P. (2009). Mantle cell lymphoma with flow cytometric evidence of clonal plasmacytic differentiation: a case report. Cytometry B Clin Cytom *76*, 218-224.

- Navarro, A., Clot, G., Royo, C., Jares, P., Hadzidimitriou, A., Agathangelidis, A., Bikos, V., Darzentas, N., Papadaki, T., Salaverria, I.*, et al.* (2012). Molecular subsets of mantle cell lymphoma defined by the IGHV mutational status and SOX11 expression have distinct biologic and clinical features. Cancer Res *72*, 5307-5316.
- Negaard, H.F., Iversen, N., Bowitz-Lothe, I.M., Sandset, P.M., Steinsvik, B., Ostenstad, B., and Iversen, P.O. (2009). Increased bone marrow microvascular density in haematological malignancies is associated with differential regulation of angiogenic factors. Leukemia *23*, 162-169.
- Nera, K.P., Kohonen, P., Narvi, E., Peippo, A., Mustonen, L., Terho, P., Koskela, K., Buerstedde, J.M., and Lassila, O. (2006). Loss of Pax5 promotes plasma cell differentiation. Immunity *24*, 283-293.
- Nescakova, Z., and Bystricky, S. (2011). B cells - ontogenesis and immune memory development. Gen Physiol Biophys *30*, 1-10.
- Niitsu, N., Okamato, M., Nakamine, H., Yoshino, T., Tamaru, J., Nakamura, S., Higashihara, M., and Hirano, M. (2002). Simultaneous elevation of the serum concentrations of vascular endothelial growth factor and interleukin-6 as independent predictors of prognosis in aggressive non-Hodgkin's lymphoma. Eur J Haematol *68*, 91-100.
- Nishishita, T., and Lin, P.C. (2004). Angiopoietin 1, PDGF-B, and TGF-beta gene regulation in endothelial cell and smooth muscle cell interaction. J Cell Biochem *91*, 584-593.
- Nissen-Meyer, L.S., Jemtland, R., Gautvik, V.T., Pedersen, M.E., Paro, R., Fortunati, D., Pierroz, D.D., Stadelmann, V.A., Reppe, S., Reinholt, F.P.*, et al.* (2007). Osteopenia, decreased bone formation and impaired osteoblast development in Sox4 heterozygous mice. J Cell Sci *120*, 2785-2795.
- Nissen, L.J., Cao, R., Hedlund, E.M., Wang, Z., Zhao, X., Wetterskog, D., Funa, K., Brakenhielm, E., and Cao, Y. (2007). Angiogenic factors FGF2 and PDGF-BB synergistically promote murine tumor neovascularization and metastasis. J Clin Invest *117*, 2766-2777.
- Niu, H., Ye, B.H., and Dalla-Favera, R. (1998). Antigen receptor signaling induces MAP kinase-mediated phosphorylation and degradation of the BCL-6 transcription factor. Genes Dev *12*, 1953-1961.
- Nodit, L., Bahler, D.W., Jacobs, S.A., Locker, J., and Swerdlow, S.H. (2003). Indolent mantle cell lymphoma with nodal involvement and mutated immunoglobulin heavy chain genes. Hum Pathol *34*, 1030-1034.

- Nordstrom, L., Sernbo, S., Eden, P., Gronbaek, K., Kolstad, A., Raty, R., Karjalainen, M.L., Geisler, C., Ralfkiaer, E., Sundstrom, C.*, et al.* (2014). SOX11 and TP53 add prognostic information to MIPI in a homogenously treated cohort of mantle cell lymphoma--a Nordic Lymphoma Group study. Br J Haematol *166*, 98-108.
- Nurieva, R.I., Chung, Y., Hwang, D., Yang, X.O., Kang, H.S., Ma, L., Wang, Y.H., Watowich, S.S., Jetten, A.M., Tian, Q.*, et al.* (2008). Generation of T follicular helper cells is mediated by interleukin-21 but independent of T helper 1, 2, or 17 cell lineages. Immunity *29*, 138-149.
- Nutt, S.L., Heavey, B., Rolink, A.G., and Busslinger, M. (1999). Commitment to the B-lymphoid lineage depends on the transcription factor Pax5. Nature *401*, 556-562.
- Nutt, S.L., and Kee, B.L. (2007). The transcriptional regulation of B cell lineage commitment. Immunity *26*, 715-725.
- Nutt, S.L., Morrison, A.M., Dorfler, P., Rolink, A., and Busslinger, M. (1998). Identification of BSAP (Pax-5) target genes in early B-cell development by loss- and gain-of-function experiments. EMBO J *17*, 2319-2333.
- Nygren, L., Baumgartner Wennerholm, S., Klimkowska, M., Christensson, B., Kimby, E., and Sander, B. (2012). Prognostic role of SOX11 in a population-based cohort of mantle cell lymphoma. Blood *119*, 4215-4223.
- O'Connor, B.P., Gleeson, M.W., Noelle, R.J., and Erickson, L.D. (2003). The rise and fall of long-lived humoral immunity: terminal differentiation of plasma cells in health and disease. Immunol Rev *194*, 61-76.
- O'Connor, O.A., Moskowitz, C., Portlock, C., Hamlin, P., Straus, D., Dumitrescu, O., Sarasohn, D., Gonen, M., Butos, J., Neylon, E.*, et al.* (2009). Patients with chemotherapy-refractory mantle cell lymphoma experience high response rates and identical progression-free survivals compared with patients with relapsed disease following treatment with single agent bortezomib: results of a multicentre Phase 2 clinical trial. Br J Haematol *145*, 34-39.
- O'Riordan, M., and Grosschedl, R. (1999). Coordinate regulation of B cell differentiation by the transcription factors EBF and E2A. Immunity *11*, 21-31.
- Ochiai, K., Maienschein-Cline, M., Simonetti, G., Chen, J., Rosenthal, R., Brink, R., Chong, A.S., Klein, U., Dinner, A.R., Singh, H.*, et al.* (2013). Transcriptional regulation of germinal center B and plasma cell fates by dynamical control of IRF4. Immunity *38*, 918-929.
- Oliner, J., Min, H., Leal, J., Yu, D., Rao, S., You, E., Tang, X., Kim, H., Meyer, S., Han, S.J.*, et al.* (2004). Suppression of angiogenesis and tumor growth by selective inhibition of angiopoietin-2. Cancer Cell *6*, 507-516.

- Ondrejka, S.L., Lai, R., Smith, S.D., and Hsi, E.D. (2011). Indolent mantle cell leukemia: a clinicopathological variant characterized by isolated lymphocytosis, interstitial bone marrow involvement, kappa light chain restriction, and good prognosis. Haematologica *96*, 1121-1127.
- Orchard, J., Garand, R., Davis, Z., Babbage, G., Sahota, S., Matutes, E., Catovsky, D., Thomas, P.W., Avet-Loiseau, H., and Oscier, D. (2003). A subset of t(11;14) lymphoma with mantle cell features displays mutated IgVH genes and includes patients with good prognosis, nonnodal disease. Blood *101*, 4975-4981.
- Ostman, A. (2004). PDGF receptors-mediators of autocrine tumor growth and regulators of tumor vasculature and stroma. Cytokine Growth Factor Rev *15*, 275-286.
- Ostman, A., and Heldin, C.H. (2001). Involvement of platelet-derived growth factor in disease: development of specific antagonists. Adv Cancer Res *80*, 1-38.
- Ott, G., Kalla, J., Ott, M.M., Schryen, B., Katzenberger, T., Muller, J.G., and Muller-Hermelink, H.K. (1997). Blastoid variants of mantle cell lymphoma: frequent bcl-1 rearrangements at the major translocation cluster region and tetraploid chromosome clones. Blood *89*, 1421-1429.
- Pan, X., Zhao, J., Zhang, W.N., Li, H.Y., Mu, R., Zhou, T., Zhang, H.Y., Gong, W.L., Yu, M., Man, J.H.*, et al.* (2009). Induction of SOX4 by DNA damage is critical for p53 stabilization and function. Proc Natl Acad Sci U S A *106*, 3788-3793.
- Pardali, E., and ten Dijke, P. (2009). Transforming growth factor-beta signaling and tumor angiogenesis. Front Biosci (Landmark Ed) *14*, 4848-4861.
- Pasqualucci, L., Compagno, M., Houldsworth, J., Monti, S., Grunn, A., Nandula, S.V., Aster, J.C., Murty, V.V., Shipp, M.A., and Dalla-Favera, R. (2006). Inactivation of the PRDM1/BLIMP1 gene in diffuse large B cell lymphoma. J Exp Med *203*, 311-317.
- Pazgal, I., Zimra, Y., Tzabar, C., Okon, E., Rabizadeh, E., Shaklai, M., and Bairey, O. (2002). Expression of basic fibroblast growth factor is associated with poor outcome in non-Hodgkin's lymphoma. Br J Cancer *86*, 1770-1775.
- Pearse, R.N., Sordillo, E.M., Yaccoby, S., Wong, B.R., Liau, D.F., Colman, N., Michaeli, J., Epstein, J., and Choi, Y. (2001). Multiple myeloma disrupts the TRANCE/ osteoprotegerin cytokine axis to trigger bone destruction and promote tumor progression. Proc Natl Acad Sci U S A *98*, 11581-11586.
- Pennisi, D., Gardner, J., Chambers, D., Hosking, B., Peters, J., Muscat, G., Abbott, C., and Koopman, P. (2000). Mutations in Sox18 underlie cardiovascular and hair follicle defects in ragged mice. Nat Genet *24*, 434-437.
- Penzo-Mendez, A.I. (2010). Critical roles for SoxC transcription factors in development and cancer. Int J Biochem Cell Biol *42*, 425-428.

- Perez-Galan, P., Dreyling, M., and Wiestner, A. (2011a). Mantle cell lymphoma: biology, pathogenesis, and the molecular basis of treatment in the genomic era. Blood *117*, 26-38.
- Perez-Galan, P., Mora-Jensen, H., Weniger, M.A., Shaffer, A.L., 3rd, Rizzatti, E.G., Chapman, C.M., Mo, C.C., Stennett, L.S., Rader, C., Liu, P.*, et al.* (2011b). Bortezomib resistance in mantle cell lymphoma is associated with plasmacytic differentiation. Blood *117*, 542-552.
- Perry, A.M., Cardesa-Salzmann, T.M., Meyer, P.N., Colomo, L., Smith, L.M., Fu, K., Greiner, T.C., Delabie, J., Gascoyne, R.D., Rimsza, L.*, et al.* (2012). A new biologic prognostic model based on immunohistochemistry predicts survival in patients with diffuse large B-cell lymphoma. Blood *120*, 2290-2296.
- Piccaluga, P.P., Agostinelli, C., Califano, A., Rossi, M., Basso, K., Zupo, S., Went, P., Klein, U., Zinzani, P.L., Baccarani, M.*, et al.* (2007). Gene expression analysis of peripheral T cell lymphoma, unspecified, reveals distinct profiles and new potential therapeutic targets. J Clin Invest *117*, 823-834.
- Piccaluga, P.P., Agostinelli, C., Zinzani, P.L., Baccarani, M., Dalla Favera, R., and Pileri, S.A. (2005). Expression of platelet-derived growth factor receptor alpha in peripheral T-cell lymphoma not otherwise specified. Lancet Oncol *6*, 440.
- Pietras, K., Sjoblom, T., Rubin, K., Heldin, C.H., and Ostman, A. (2003). PDGF receptors as cancer drug targets. Cancer Cell *3*, 439-443.
- Pighi, C., Gu, T.L., Dalai, I., Barbi, S., Parolini, C., Bertolaso, A., Pedron, S., Parisi, A., Ren, J., Cecconi, D.*, et al.* (2011). Phospho-proteomic analysis of mantle cell lymphoma cells suggests a pro-survival role of B-cell receptor signaling. Cell Oncol (Dordr) *34*, 141-153.
- Pinyol, M., Bea, S., Pla, L., Ribrag, V., Bosq, J., Rosenwald, A., Campo, E., and Jares, P. (2007). Inactivation of RB1 in mantle-cell lymphoma detected by nonsense-mediated mRNA decay pathway inhibition and microarray analysis. Blood *109*, 5422-5429.
- Pinyol, M., Cobo, F., Bea, S., Jares, P., Nayach, I., Fernandez, P.L., Montserrat, E., Cardesa, A., and Campo, E. (1998). p16(INK4a) gene inactivation by deletions, mutations, and hypermethylation is associated with transformed and aggressive variants of non-Hodgkin's lymphomas. Blood *91*, 2977-2984.
- Potzner, M.R., Griffel, C., Lutjen-Drecoll, E., Bosl, M.R., Wegner, M., and Sock, E. (2007). Prolonged Sox4 expression in oligodendrocytes interferes with normal myelination in the central nervous system. Mol Cell Biol *27*, 5316-5326.
- Quintanilla-Martinez, L., Slotta-Huspenina, J., Koch, I., Klier, M., Hsi, E.D., de Leval, L., Klapper, W., Gesk, S., Siebert, R., and Fend, F. (2009). Differential diagnosis of

cyclin D2+ mantle cell lymphoma based on fluorescence in situ hybridization and quantitative real-time-PCR. Haematologica *94*, 1595-1598.

- Ramirez, J., Lukin, K., and Hagman, J. (2010). From hematopoietic progenitors to B cells: mechanisms of lineage restriction and commitment. Curr Opin Immunol *22*, 177-184.
- Ramos, A.H., Dutt, A., Mermel, C., Perner, S., Cho, J., Lafargue, C.J., Johnson, L.A., Stiedl, A.C., Tanaka, K.E., Bass, A.J., *et al.* (2009). Amplification of chromosomal segment 4q12 in non-small cell lung cancer. Cancer Biol Ther *8*, 2042-2050.
- Reimold, A.M., Etkin, A., Clauss, I., Perkins, A., Friend, D.S., Zhang, J., Horton, H.F., Scott, A., Orkin, S.H., Byrne, M.C., *et al.* (2000). An essential role in liver development for transcription factor XBP-1. Genes Dev *14*, 152-157.
- Reimold, A.M., Iwakoshi, N.N., Manis, J., Vallabhajosyula, P., Szomolanyi-Tsuda, E., Gravallese, E.M., Friend, D., Grusby, M.J., Alt, F., and Glimcher, L.H. (2001). Plasma cell differentiation requires the transcription factor XBP-1. Nature *412*, 300-307.
- Reimold, A.M., Ponath, P.D., Li, Y.S., Hardy, R.R., David, C.S., Strominger, J.L., and Glimcher, L.H. (1996). Transcription factor B cell lineage-specific activator protein regulates the gene for human X-box binding protein 1. J Exp Med *183*, 393-401.
- Reljic, R., Wagner, S.D., Peakman, L.J., and Fearon, D.T. (2000). Suppression of signal transducer and activator of transcription 3-dependent B lymphocyte terminal differentiation by BCL-6. J Exp Med *192*, 1841-1848.
- Revilla, I.D.R., Bilic, I., Vilagos, B., Tagoh, H., Ebert, A., Tamir, I.M., Smeenk, L., Trupke, J., Sommer, A., Jaritz, M., *et al.* (2012). The B-cell identity factor Pax5 regulates distinct transcriptional programmes in early and late B lymphopoiesis. EMBO J *31*, 3130-3146.
- Reynaud, D., Demarco, I.A., Reddy, K.L., Schjerven, H., Bertolino, E., Chen, Z., Smale, S.T., Winandy, S., and Singh, H. (2008). Regulation of B cell fate commitment and immunoglobulin heavy-chain gene rearrangements by Ikaros. Nat Immunol *9*, 927-936.
- Ria, R., Roccaro, A.M., Merchionne, F., Vacca, A., Dammacco, F., and Ribatti, D. (2003). Vascular endothelial growth factor and its receptors in multiple myeloma. Leukemia *17*, 1961-1966.
- Ribatti, D. (2007). The discovery of endothelial progenitor cells. An historical review. Leuk Res *31*, 439-444.
- Ribatti, D., Nico, B., Ranieri, G., Specchia, G., and Vacca, A. (2013). The role of angiogenesis in human non-Hodgkin lymphomas. Neoplasia *15*, 231-238.

- Richard, P., Vassallo, J., Valmary, S., Missoury, R., Delsol, G., and Brousset, P. (2006). "In situ-like" mantle cell lymphoma: a report of two cases. J Clin Pathol *59*, 995-996.
- Rinaldi, A., Kwee, I., Taborelli, M., Largo, C., Uccella, S., Martin, V., Poretti, G., Gaidano, G., Calabrese, G., Martinelli, G.*, et al.* (2006). Genomic and expression profiling identifies the B-cell associated tyrosine kinase Syk as a possible therapeutic target in mantle cell lymphoma. Br J Haematol *132*, 303-316.
- Risau, W., Drexler, H., Mironov, V., Smits, A., Siegbahn, A., Funa, K., and Heldin, C.H. (1992). Platelet-derived growth factor is angiogenic in vivo. Growth Factors *7*, 261-266.
- Rizzatti, E.G., Falcao, R.P., Panepucci, R.A., Proto-Siqueira, R., Anselmo-Lima, W.T., Okamoto, O.K., and Zago, M.A. (2005). Gene expression profiling of mantle cell lymphoma cells reveals aberrant expression of genes from the PI3K-AKT, WNT and TGFbeta signalling pathways. Br J Haematol *130*, 516-526.
- Rodig, S.J., Shahsafaei, A., Li, B., Mackay, C.R., and Dorfman, D.M. (2005). BAFF-R, the major B cell-activating factor receptor, is expressed on most mature B cells and B-cell lymphoproliferative disorders. Hum Pathol *36*, 1113-1119.
- Roessler, S., Gyory, I., Imhof, S., Spivakov, M., Williams, R.R., Busslinger, M., Fisher, A.G., and Grosschedl, R. (2007). Distinct promoters mediate the regulation of Ebf1 gene expression by interleukin-7 and Pax5. Mol Cell Biol *27*, 579-594.
- Rosenwald, A., Wright, G., Wiestner, A., Chan, W.C., Connors, J.M., Campo, E., Gascoyne, R.D., Grogan, T.M., Muller-Hermelink, H.K., Smeland, E.B.*, et al.* (2003). The proliferation gene expression signature is a quantitative integrator of oncogenic events that predicts survival in mantle cell lymphoma. Cancer Cell *3*, 185-197.
- Roue, G., Perez-Galan, P., Mozos, A., Lopez-Guerra, M., Xargay-Torrent, S., Rosich, L., Saborit-Villarroya, I., Normant, E., Campo, E., and Colomer, D. (2011). The Hsp90 inhibitor IPI-504 overcomes bortezomib resistance in mantle cell lymphoma in vitro and in vivo by down-regulation of the prosurvival ER chaperone BiP/Grp78. Blood *117*, 1270-1279.
- Royo, C., Navarro, A., Clot, G., Salaverria, I., Gine, E., Jares, P., Colomer, D., Wiestner, A., Wilson, W.H., Vegliante, M.C.*, et al.* (2012). Non-nodal type of mantle cell lymphoma is a specific biological and clinical subgroup of the disease. Leukemia *26*, 1895-1898.
- Royo, C., Salaverria, I., Hartmann, E.M., Rosenwald, A., Campo, E., and Bea, S. (2011). The complex landscape of genetic alterations in mantle cell lymphoma. Semin Cancer Biol *21*, 322-334.

- Ruan, J., Hajjar, K., Rafii, S., and Leonard, J.P. (2009). Angiogenesis and antiangiogenic therapy in non-Hodgkin's lymphoma. Ann Oncol *20*, 413-424.
- Ruan, J., Luo, M., Wang, C., Fan, L., Yang, S.N., Cardenas, M., Geng, H., Leonard, J.P., Melnick, A., Cerchietti, L.*, et al.* (2013). Imatinib disrupts lymphoma angiogenesis by targeting vascular pericytes. Blood *121*, 5192-5202.
- Rudelius, M., Pittaluga, S., Nishizuka, S., Pham, T.H., Fend, F., Jaffe, E.S., Quintanilla-Martinez, L., and Raffeld, M. (2006). Constitutive activation of Akt contributes to the pathogenesis and survival of mantle cell lymphoma. Blood *108*, 1668-1676.
- Rumfelt, L.L., Zhou, Y., Rowley, B.M., Shinton, S.A., and Hardy, R.R. (2006). Lineage specification and plasticity in CD19- early B cell precursors. J Exp Med *203*, 675-687.
- Sadakane, Y., Zaitsu, M., Nishi, M., Sugita, K., Mizutani, S., Matsuzaki, A., Sueoka, E., Hamasaki, Y., and Ishii, E. (2007). Expression and production of aberrant PAX5 with deletion of exon 8 in B-lineage acute lymphoblastic leukaemia of children. Br J Haematol *136*, 297-300.
- Saharinen, P., Eklund, L., Pulkki, K., Bono, P., Alitalo, K. (2010). VEGF and angiopoietin signaling in tumor angiogenesis and metastasis. Trends Mol Med *17*, 347-62.
- Saitoh, T., and Katoh, M. (2002). Expression of human SOX18 in normal tissues and tumors. Int J Mol Med *10*, 339-344.
- Sakamoto, Y., Hara, K., Kanai-Azuma, M., Matsui, T., Miura, Y., Tsunekawa, N., Kurohmaru, M., Saijoh, Y., Koopman, P., and Kanai, Y. (2007). Redundant roles of Sox17 and Sox18 in early cardiovascular development of mouse embryos. Biochem Biophys Res Commun *360*, 539-544.
- Sakurai, T., and Kudo, M. (2011). Signaling pathways governing tumor angiogenesis. Oncology *81 Suppl 1*, 24-29.
- Salaverria, I., Royo, C., Carvajal-Cuenca, A., Clot, G., Navarro, A., Valera, A., Song, J.Y., Woroniecka, R., Rymkiewicz, G., Klapper, W.*, et al.* (2013). CCND2 rearrangements are the most frequent genetic events in cyclin D1(-) mantle cell lymphoma. Blood *121*, 1394-1402.
- Salaverria, I., Zettl, A., Bea, S., Moreno, V., Valls, J., Hartmann, E., Ott, G., Wright, G., Lopez-Guillermo, A., Chan, W.C.*, et al.* (2007). Specific secondary genetic alterations in mantle cell lymphoma provide prognostic information independent of the gene expression-based proliferation signature. J Clin Oncol *25*, 1216-1222.
- Salven, P., Orpana, A., Teerenhovi, L., and Joensuu, H. (2000). Simultaneous elevation in the serum concentrations of the angiogenic growth factors VEGF and bFGF is an

independent predictor of poor prognosis in non-Hodgkin lymphoma: a single-institution study of 200 patients. Blood *96*, 3712-3718.

- Samant, G.V., Schupp, M.O., Francois, M., Moleri, S., Kothinti, R.K., Chun, C.Z., Sinha, I., Sellars, S., Leigh, N., Pramanik, K.*, et al.* (2011). Sox factors transcriptionally regulate ROBO4 gene expression in developing vasculature in zebrafish. J Biol Chem *286*, 30740-30747.
- Sander, B., Flygare, J., Porwit-Macdonald, A., Smith, C.I., Emanuelsson, E., Kimby, E., Liden, J., and Christensson, B. (2005). Mantle cell lymphomas with low levels of cyclin D1 long mRNA transcripts are highly proliferative and can be discriminated by elevated cyclin A2 and cyclin B1. Int J Cancer *117*, 418-430.
- Sasaki, Y., Derudder, E., Hobeika, E., Pelanda, R., Reth, M., Rajewsky, K., and Schmidt-Supprian, M. (2006). Canonical NF-kappaB activity, dispensable for B cell development, replaces BAFF-receptor signals and promotes B cell proliferation upon activation. Immunity *24*, 729-739.
- Scott, D.W., and Gascoyne, R.D. (2014). The tumour microenvironment in B cell lymphomas. Nat Rev Cancer *14*, 517-534.
- Schebesta, M., Pfeffer, P.L., and Busslinger, M. (2002). Control of pre-BCR signaling by Pax5-dependent activation of the BLNK gene. Immunity *17*, 473-485.
- Schilham, M.W., Moerer, P., Cumano, A., and Clevers, H.C. (1997). Sox-4 facilitates thymocyte differentiation. Eur J Immunol *27*, 1292-1295.
- Schilham, M.W., Oosterwegel, M.A., Moerer, P., Ya, J., de Boer, P.A., van de Wetering, M., Verbeek, S., Lamers, W.H., Kruisbeek, A.M., Cumano, A.*, et al.* (1996). Defects in cardiac outflow tract formation and pro-B-lymphocyte expansion in mice lacking Sox-4. Nature *380*, 711-714.
- Schmitt, C.E., Woolls, M.J., and Jin, S.W. (2013). Mutant-specific gene expression profiling identifies SRY-related HMG box 11b (SOX11b) as a novel regulator of vascular development in zebrafish. Mol Cells *35*, 166-172.
- Schwartz, J.D., Rowinsky, E.K., Youssoufian, H., Pytowski, B., and Wu, Y. (2010). Vascular endothelial growth factor receptor-1 in human cancer: concise review and rationale for development of IMC-18F1 (Human antibody targeting vascular endothelial growth factor receptor-1). Cancer *116*, 1027-1032.
- Sernbo, S., Gustavsson, E., Brennan, D.J., Gallagher, W.M., Rexhepaj, E., Rydnert, F., Jirstrom, K., Borrebaeck, C.A., and Ek, S. (2011). The tumour suppressor SOX11 is associated with improved survival among high grade epithelial ovarian cancers and is regulated by reversible promoter methylation. BMC Cancer *11*, 405.

- Shaffer, A.L., 3rd, Young, R.M., and Staudt, L.M. (2012). Pathogenesis of human B cell lymphomas. Annu Rev Immunol *30*, 565-610.
- Shaffer, A.L., Lin, K.I., Kuo, T.C., Yu, X., Hurt, E.M., Rosenwald, A., Giltnane, J.M., Yang, L., Zhao, H., Calame, K.*, et al.* (2002). Blimp-1 orchestrates plasma cell differentiation by extinguishing the mature B cell gene expression program. Immunity *17*, 51-62.
- Shaffer, A.L., Rosenwald, A., Hurt, E.M., Giltnane, J.M., Lam, L.T., Pickeral, O.K., and Staudt, L.M. (2001). Signatures of the immune response. Immunity *15*, 375-385.
- Shaffer, A.L., Yu, X., He, Y., Boldrick, J., Chan, E.P., and Staudt, L.M. (2000). BCL-6 represses genes that function in lymphocyte differentiation, inflammation, and cell cycle control. Immunity *13*, 199-212.
- Shah, S., Schrader, K.A., Waanders, E., Timms, A.E., Vijai, J., Miething, C., Wechsler, J., Yang, J., Hayes, J., Klein, R.J.*, et al.* (2013). A recurrent germline PAX5 mutation confers susceptibility to pre-B cell acute lymphoblastic leukemia. Nat Genet *45*, 1226-1231.
- Shapiro-Shelef, M., Lin, K.I., Savitsky, D., Liao, J., and Calame, K. (2005). Blimp-1 is required for maintenance of long-lived plasma cells in the bone marrow. J Exp Med *202*, 1471-1476.
- Shiller, S.M., Zieske, A., Holmes, H., 3rd, Feldman, A.L., Law, M.E., and Saad, R. (2011). CD5-positive, cyclinD1-negative mantle cell lymphoma with a translocation involving the CCND2 gene and the IGL locus. Cancer Genet *204*, 162-164.
- Shlomchik, M.J., and Weisel, F. (2012). Germinal centers. Immunol Rev *247*, 5-10.
- Sitaras, N.M., Sariban, E., Bravo, M., Pantazis, P., and Antoniades, H.N. (1988). Constitutive production of platelet-derived growth factor-like proteins by human prostate carcinoma cell lines. Cancer Res *48*, 1930-1935.
- Sock, E., Rettig, S.D., Enderich, J., Bosl, M.R., Tamm, E.R., and Wegner, M. (2004). Gene targeting reveals a widespread role for the high-mobility-group transcription factor Sox11 in tissue remodeling. Mol Cell Biol *24*, 6635-6644.
- Solomon, D.A., Wang, Y., Fox, S.R., Lambeck, T.C., Giesting, S., Lan, Z., Senderowicz, A.M., Conti, C.J., and Knudsen, E.S. (2003). Cyclin D1 splice variants. Differential effects on localization, RB phosphorylation, and cellular transformation. J Biol Chem *278*, 30339-30347.
- Song, K., Herzog, B.H., Sheng, M., Fu, J., McDaniel, J.M., Chen, H., Ruan, J., and Xia, L. (2013). Lenalidomide inhibits lymphangiogenesis in preclinical models of mantle cell lymphoma. Cancer Res *73*, 7254-7264.

- Souabni, A., Jochum, W., and Busslinger, M. (2007). Oncogenic role of Pax5 in the T-lymphoid lineage upon ectopic expression from the immunoglobulin heavy-chain locus. Blood *109*, 281-289.
- Stockmann, C., Doedens, A., Weidemann, A., Zhang, N., Takeda, N., Greenberg, J.I., Cheresh, D.A., and Johnson, R.S. (2008). Deletion of vascular endothelial growth factor in myeloid cells accelerates tumorigenesis. Nature *456*, 814-818.
- Swerdlow, S.H. (2008). WHO classification of tumours of haematopoietic and lymphoid tissues (Lyon, International Agency for Research on Cancer).
- Tam, W., Gomez, M., Chadburn, A., Lee, J.W., Chan, W.C., and Knowles, D.M. (2006). Mutational analysis of PRDM1 indicates a tumor-suppressor role in diffuse large B-cell lymphomas. Blood *107*, 4090-4100.
- Tammela, T., and Alitalo, K. (2010). Lymphangiogenesis: Molecular mechanisms and future promise. Cell *140*, 460-476.
- Tangye, S.G., and Tarlinton, D.M. (2009). Memory B cells: effectors of long-lived immune responses. Eur J Immunol *39*, 2065-2075.
- Thelander, E.F., Walsh, S.H., Thorselius, M., Laurell, A., Landgren, O., Larsson, C., Rosenquist, R., and Lagercrantz, S. (2005). Mantle cell lymphomas with clonal immunoglobulin V(H)3-21 gene rearrangements exhibit fewer genomic imbalances than mantle cell lymphomas utilizing other immunoglobulin V(H) genes. Mod Pathol *18*, 331-339.
- Thompson, E.C., Cobb, B.S., Sabbattini, P., Meixlsperger, S., Parelho, V., Liberg, D., Taylor, B., Dillon, N., Georgopoulos, K., Jumaa, H.*, et al.* (2007). Ikaros DNA-binding proteins as integral components of B cell developmental-stage-specific regulatory circuits. Immunity *26*, 335-344.
- Thorselius, M., Walsh, S., Eriksson, I., Thunberg, U., Johnson, A., Backlin, C., Enblad, G., Sundstrom, C., Roos, G., and Rosenquist, R. (2002). Somatic hypermutation and V(H) gene usage in mantle cell lymphoma. Eur J Haematol *68*, 217-224.
- Tian, J., Okabe, T., Miyazaki, T., Takeshita, S., and Kudo, A. (1997). Pax-5 is identical to EBB-1/KLP and binds to the VpreB and lambda5 promoters as well as the KI and KII sites upstream of the Jkappa genes. Eur J Immunol *27*, 750-755.
- Tourigny, M.R., Ursini-Siegel, J., Lee, H., Toellner, K.M., Cunningham, A.F., Franklin, D.S., Ely, S., Chen, M., Qin, X.F., Xiong, Y.*, et al.* (2002). CDK inhibitor p18(INK4c) is required for the generation of functional plasma cells. Immunity *17*, 179-189.
- Usui, T., Wakatsuki, Y., Matsunaga, Y., Kaneko, S., Koseki, H., and Kita, T. (1997). Overexpression of B cell-specific activator protein (BSAP/Pax-5) in a late B cell is

sufficient to suppress differentiation to an Ig high producer cell with plasma cell phenotype. J Immunol *158*, 3197-3204.

- Vacca, A., Ribatti, D., Ruco, L., Giacchetta, F., Nico, B., Quondamatteo, F., Ria, R., Iurlaro, M., and Dammacco, F. (1999). Angiogenesis extent and macrophage density increase simultaneously with pathological progression in B-cell non-Hodgkin's lymphomas. Br J Cancer *79*, 965-970.
- van de Wetering, M., Oosterwegel, M., van Norren, K., and Clevers, H. (1993). Sox-4, an Sry-like HMG box protein, is a transcriptional activator in lymphocytes. EMBO J *12*, 3847-3854.
- Vasanwala, F.H., Kusam, S., Toney, L.M., and Dent, A.L. (2002). Repression of AP-1 function: a mechanism for the regulation of Blimp-1 expression and B lymphocyte differentiation by the B cell lymphoma-6 protooncogene. J Immunol *169*, 1922-1929.
- Vegliante, M.C., Royo, C., Palomero, J., Salaverria, I., Balint, B., Martin-Guerrero, I., Agirre, X., Lujambio, A., Richter, J., Xargay-Torrent, S.*, et al.* (2011). Epigenetic activation of SOX11 in lymphoid neoplasms by histone modifications. PLoS One *6*, e21382.
- Victora, G.D., and Nussenzweig, M.C. (2012). Germinal centers. Annu Rev Immunol *30*, 429-457.
- Visco, C., Hoeller, S., Malik, J.T., Xu-Monette, Z.Y., Wiggins, M.L., Liu, J., Sanger, W.G., Liu, Z., Chang, J., Ranheim, E.A.*, et al.* (2011). Molecular characteristics of mantle cell lymphoma presenting with clonal plasma cell component. Am J Surg Pathol *35*, 177-189.
- Vizcarra, E., Martinez-Climent, J.A., Benet, I., Marugan, I., Terol, M.J., Prosper, F., Marco, J., Sanchez, D., Ferrandez, A., Tormo, M.*, et al.* (2001). Identification of two subgroups of mantle cell leukemia with distinct clinical and biological features. Hematol J *2*, 234-241.
- Vose, J.M., Habermann, T.M., Czuczman, M.S., Zinzani, P.L., Reeder, C.B., Tuscano, J.M., Lossos, I.S., Li, J., Pietronigro, D., and Witzig, T.E. (2013). Single-agent lenalidomide is active in patients with relapsed or refractory aggressive non-Hodgkin lymphoma who received prior stem cell transplantation. Br J Haematol *162*, 639-647.
- Wakatsuki, Y., Neurath, M.F., Max, E.E., and Strober, W. (1994). The B cell-specific transcription factor BSAP regulates B cell proliferation. J Exp Med *179*, 1099-1108.
- Walsh, S.H., Thorselius, M., Johnson, A., Soderberg, O., Jerkeman, M., Bjorck, E., Eriksson, I., Thunberg, U., Landgren, O., Ehinger, M.*, et al.* (2003). Mutated VH genes and preferential VH3-21 use define new subsets of mantle cell lymphoma. Blood *101*, 4047-4054.

- Wang, D., Huang, H.J., Kazlauskas, A., and Cavenee, W.K. (1999). Induction of vascular endothelial growth factor expression in endothelial cells by platelet-derived growth factor through the activation of phosphatidylinositol 3-kinase. Cancer Res *59*, 1464-1472.
- Wang, J.H., Nichogiannopoulou, A., Wu, L., Sun, L., Sharpe, A.H., Bigby, M., and Georgopoulos, K. (1996). Selective defects in the development of the fetal and adult lymphoid system in mice with an Ikaros null mutation. Immunity *5*, 537-549.
- Wang, L., Fortney, J.E., and Gibson, L.F. (2004). Stromal cell protection of B-lineage acute lymphoblastic leukemic cells during chemotherapy requires active Akt. Leuk Res *28*, 733-742.
- Wang, X., Asplund, A.C., Porwit, A., Flygare, J., Smith, C.I., Christensson, B., and Sander, B. (2008). The subcellular Sox11 distribution pattern identifies subsets of mantle cell lymphoma: correlation to overall survival. Br J Haematol *143*, 248-252.
- Wasik, A.M., Lord, M., Wang, X., Zong, F., Andersson, P., Kimby, E., Christensson, B., Karimi, M., and Sander, B. (2013). SOXC transcription factors in mantle cell lymphoma: the role of promoter methylation in SOX11 expression. Sci Rep *3*, 1400.
- Wegner, M. (1999). From head to toes: the multiple facets of Sox proteins. Nucleic Acids Res *27*, 1409-1420.
- Wehrli, B.M., Huang, W., De Crombrugghe, B., Ayala, A.G., and Czerniak, B. (2003). Sox9, a master regulator of chondrogenesis, distinguishes mesenchymal chondrosarcoma from other small blue round cell tumors. Hum Pathol *34*, 263-269.
- Weigle, B., Ebner, R., Temme, A., Schwind, S., Schmitz, M., Kiessling, A., Rieger, M.A., Schackert, G., Schackert, H.K., and Rieber, E.P. (2005). Highly specific overexpression of the transcription factor SOX11 in human malignant gliomas. Oncol Rep *13*, 139-144.
- Welzel, N., Le, T., Marculescu, R., Mitterbauer, G., Chott, A., Pott, C., Kneba, M., Du, M.Q., Kusec, R., Drach, J.*, et al.* (2001). Templated nucleotide addition and immunoglobulin JH-gene utilization in t(11;14) junctions: implications for the mechanism of translocation and the origin of mantle cell lymphoma. Cancer Res *61*, 1629-1636.
- Weniger, M.A., Rizzatti, E.G., Perez-Galan, P., Liu, D., Wang, Q., Munson, P.J., Raghavachari, N., White, T., Tweito, M.M., Dunleavy, K.*, et al.* (2011). Treatment-induced oxidative stress and cellular antioxidant capacity determine response to bortezomib in mantle cell lymphoma. Clin Cancer Res *17*, 5101-5112.

- Werner, M.H., Huth, J.R., Gronenborn, A.M., and Clore, G.M. (1995). Molecular basis of human 46X,Y sex reversal revealed from the three-dimensional solution structure of the human SRY-DNA complex. Cell *81*, 705-714.
- Wiebe, M.S., Nowling, T.K., and Rizzino, A. (2003). Identification of novel domains within Sox-2 and Sox-11 involved in autoinhibition of DNA binding and partnership specificity. J Biol Chem *278*, 17901-17911.
- Wiestner, A., Tehrani, M., Chiorazzi, M., Wright, G., Gibellini, F., Nakayama, K., Liu, H., Rosenwald, A., Muller-Hermelink, H.K., Ott, G.*, et al.* (2007). Point mutations and genomic deletions in CCND1 create stable truncated cyclin D1 mRNAs that are associated with increased proliferation rate and shorter survival. Blood *109*, 4599-4606.
- Wilson, M., and Koopman, P. (2002). Matching SOX: partner proteins and co-factors of the SOX family of transcriptional regulators. Curr Opin Genet Dev *12*, 441-446.
- Wilson, M.E., Yang, K.Y., Kalousova, A., Lau, J., Kosaka, Y., Lynn, F.C., Wang, J., Mrejen, C., Episkopou, V., Clevers, H.C.*, et al.* (2005). The HMG box transcription factor Sox4 contributes to the development of the endocrine pancreas. Diabetes *54*, 3402-3409.
- Witzig, T.E., Vose, J.M., Zinzani, P.L., Reeder, C.B., Buckstein, R., Polikoff, J.A., Bouabdallah, R., Haioun, C., Tilly, H., Guo, P.*, et al.* (2011). An international phase II trial of single-agent lenalidomide for relapsed or refractory aggressive B-cell non-Hodgkin's lymphoma. Ann Oncol *22*, 1622-1627.
- Wlodarska, I., Dierickx, D., Vanhentenrijk, V., Van Roosbroeck, K., Pospisilova, H., Minnei, F., Verhoef, G., Thomas, J., Vandenberghe, P., and De Wolf-Peeters, C. (2008). Translocations targeting CCND2, CCND3, and MYCN do occur in t(11;14)-negative mantle cell lymphomas. Blood *111*, 5683-5690.
- Xia, Y., Papalopulu, N., Vogt, P.K., and Li, J. (2000). The oncogenic potential of the high mobility group box protein Sox3. Cancer Res *60*, 6303-6306.
- Yang, J., Liu, X., Nyland, S.B., Zhang, R., Ryland, L.K., Broeg, K., Baab, K.T., Jarbadan, N.R., Irby, R., and Loughran, T.P., Jr. (2010). Platelet-derived growth factor mediates survival of leukemic large granular lymphocytes via an autocrine regulatory pathway. Blood *115*, 51-60.
- Yin, C.C., Medeiros, L.J., Cromwell, C.C., Mehta, A.P., Lin, P., Luthra, R., and Abruzzo, L.V. (2007). Sequence analysis proves clonal identity in five patients with typical and blastoid mantle cell lymphoma. Mod Pathol *20*, 1-7.
- Yoshida, H., Matsui, T., Yamamoto, A., Okada, T., and Mori, K. (2001). XBP1 mRNA is induced by ATF6 and spliced by IRE1 in response to ER stress to produce a highly active transcription factor. Cell *107*, 881-891.

- Yoshida, T., Mei, H., Dorner, T., Hiepe, F., Radbruch, A., Fillatreau, S., and Hoyer, B.F. (2010). Memory B and memory plasma cells. Immunol Rev *237*, 117-139.
- Young, K.H., Chan, W.C., Fu, K., Iqbal, J., Sanger, W.G., Ratashak, A., Greiner, T.C., and Weisenburger, D.D. (2006a). Mantle cell lymphoma with plasma cell differentiation. Am J Surg Pathol *30*, 954-961.
- Young, N., Hahn, C.N., Poh, A., Dong, C., Wilhelm, D., Olsson, J., Muscat, G.E., Parsons, P., Gamble, J.R., and Koopman, P. (2006b). Effect of disrupted SOX18 transcription factor function on tumor growth, vascularization, and endothelial development. J Natl Cancer Inst *98*, 1060-1067.
- Zhang, L., Yang, J., Qian, J., Li, H., Romaguera, J.E., Kwak, L.W., Wang, M., and Yi, Q. (2012). Role of the microenvironment in mantle cell lymphoma: IL-6 is an important survival factor for the tumor cells. Blood *120*, 3783-3792.
- Zhang, R., Shah, M.V., Yang, J., Nyland, S.B., Liu, X., Yun, J.K., Albert, R., and Loughran, T.P., Jr. (2008). Network model of survival signaling in large granular lymphocyte leukemia. Proc Natl Acad Sci U S A *105*, 16308-16313.
- Zinzani, P.L., Vose, J.M., Czuczman, M.S., Reeder, C.B., Haioun, C., Polikoff, J., Tilly, H., Zhang, L., Prandi, K., Li, J.*, et al.* (2013). Long-term follow-up of lenalidomide in relapsed/refractory mantle cell lymphoma: subset analysis of the NHL-003 study. Ann Oncol *24*, 2892-2897.
- Zvelebil, M., Oliemuller, E., Gao, Q., Wansbury, O., Mackay, A., Kendrick, H., Smalley, M.J., Reis-Filho, J.S., and Howard, B.A. (2013). Embryonic mammary signature subsets are activated in Brca1-/- and basal-like breast cancers. Breast Cancer Res *15*, R25.

APPENDIX

Appendix I

PLoS ONE. 2011;6(6):e21382.

Epigenetic activation of SOX11 in lymphoid neoplasms by histone modifications.

Vegliante MC, Royo C, Palomero J, Salaverria I, Balint B, Martín-Guerrero I, Agirre X, Lujambio A, Richter J, Xargay-Torrent S, Bea S, Hernandez L, Enjuanes A, Calasanz MJ, Rosenwald A, Ott G, Roman-Gomez J, Prosper F, Esteller M, Jares P, Siebert R, Campo E, Martín-Subero JI, Amador V.

Recent studies have shown aberrant expression of SOX11 in various types of aggressive B-cell neoplasms. To elucidate the molecular mechanisms leading to such deregulation, we performed a comprehensive SOX11 gene expression and epigenetic study in stem cells, normal hematopoietic cells and different lymphoid neoplasms. We observed that SOX11 expression is associated with unmethylated DNA and presence of activating histone marks (H3K9/14Ac and H3K4me3) in embryonic stem cells and some aggressive B-cell neoplasms. In contrast, adult stem cells, normal hematopoietic cells and other lymphoid neoplasms do not express SOX11. Such repression was associated with silencing histone marks H3K9me2 and H3K27me3. The SOX11 promoter of non-malignant cells was consistently unmethylated whereas lymphoid neoplasms with silenced SOX11 tended to acquire DNA hypermethylation. SOX11 silencing in cell lines was reversed by the histone deacetylase inhibitor SAHA but not by the DNA methyltransferase inhibitor AZA. These data indicate that, although DNA hypermethylation of SOX11 is frequent in lymphoid neoplasms, it seems to be functionally inert, as SOX11 is already silenced in the hematopoietic system. In contrast, the pathogenic role of SOX11 is associated with its de novo expression in some aggressive lymphoid malignancies, which is mediated by a shift from inactivating to activating histone modifications.

Appendix II

Cancer Res. 2012;72(20):5307-16.

Molecular subsets of mantle cell lymphoma defined by the IGHV mutational status and SOX11 expression have distinct biologic and clinical features.

Navarro A, Clot G, Royo C, Jares P, Hadzidimitriou A, Agathangelidis A, Bikos V, Darzentas N, Papadaki T, Salaverria I, Pinyol M, Puig X, Palomero J, Vegliante MC, Amador V, Martinez-Trillos A, Stefancikova L, Wiestner A, Wilson W, Pott C, Calasanz MJ, Trim N, Erber W, Sander B, Ott G, Rosenwald A, Colomer D, Giné E, Siebert R, Lopez-Guillermo A, Stamatopoulos K, Beà S, Campo E.

Mantle cell lymphoma (MCL) is a heterogeneous disease with most patients following an aggressive clinical course, whereas others having an indolent behavior. We conducted an integrative and multidisciplinary analysis of 177 MCL to determine whether the immunogenetic features of the clonotypic B-cell receptors (BcR) may identify different subsets of tumors. Truly unmutated (100% identity) IGHV genes were found in 24% cases, 40% were minimally/borderline mutated (99.9%-97%), 19% significantly mutated (96.9%-95%), and 17% hypermutated (<95%). Tumors with high or low mutational load used different IGHV genes, and their gene expression profiles were also different for several gene pathways. A gene set enrichment analysis showed that MCL with high and low IGHV mutations were enriched in memory and naive B-cell signatures, respectively. Furthermore, the highly mutated tumors had less genomic complexity, were preferentially SOX11-negative, and showed more frequent nonnodal disease. The best cut-off of germline identity of IGHV genes to predict survival was 97%. Patients with high and low mutational load had significant different outcome with 5-year overall survival (OS) of 59% and 40%, respectively (P = 0.004). Nodal presentation and SOX11 expression also predicted for poor OS. In a multivariate analysis, IGHV gene status and SOX11 expression were independent risk factors. In conclusion, these observations suggest the idea that MCL with mutated IGHV, SOX11-negativity, and nonnodal presentation correspond to a subtype of the disease with more indolent behavior.